THESIS FOR THE DEGREE OF DOCTOR OF PHILOSOPHY

Design and Operation of a Chemical-Looping Reformer for Catalytic Upgrading of Biomass-Derived Gas

Fredrik Lind

Department of Energy and Environment

CHALMERS UNIVERSITY OF TECHNOLOGY

Göteborg, Sweden 2013

Design and Operation of a Chemical-Looping Reformer for Catalytic Upgrading of Biomass-Derived Gas
Fredrik Lind
ISBN 978-91-7385-823-6

Doktorsavhandling vid Chalmers tekniska högskola
Ny serie nr 3504
ISSN 0346-718X

Department of Energy and Environment
Division of Energy Technology
Chalmers University of Technology
SE-412 96 Gothenburg
Sweden
Telephone + 46 (0)31-772 1000

Chalmers Reproservice
Göteborg 2013

Design and Operation of a Chemical-Looping reformer for Catalytic Upgrading of Biomass-Derived Gas

Fredrik Lind
Department of Energy Technology
Chalmers University of Technology
SE-412 96 Gothenburg (Sweden)

Abstract

The removal of tar from the raw gas produced during biomass gasification is necessary before the gas can be used as a feedstock for synthetic fuels. The currently commercially available technologies for gas cleaning, i.e., scrubber systems, have various disadvantages, such as heat penalties and loss of the energy that is chemically stored within the tars. In addressing these problems in this work, a novel method for secondary tar cleaning is proposed and experimentally validated. This method combines tar cleaning with catalyst regeneration in a system of dual fluidized beds, which is experimentally explored in two reactors systems of identical size: a cold Perspex unit; and a high-temperature steel unit. Fluid dynamics and operation controllability were evaluated in the cold system; the results indicate that solid circulation is controllable and that adequate gas tightness of the loop-seals can be achieved. The knowledge gained from operating the cold system was subsequently used to demonstrate the tar-cleaning method in the hot reactor system. This was done using the raw gas from the Chalmers biomass gasifier, which contained 20–30 g_{tar}/Nm^3_{tar}. The tar-reforming activity, catalyst regeneration, and potential for catalytically adjusting the raw gas were investigated. The results of these experiments indicate that almost all tars can be reformed using a catalyst that consists of nickel oxide supported on an α-Al_2O_3 matrix (NiO/Al_2O_3). Promising tar-reforming properties were also observed when the naturally occurring ore ilmenite ($FeTiO_3$, in its most reduced form) was used; in this set-up, approximately 60% of the tar fraction was reduced. A clear trend towards enhanced hydrogen production was seen in the reactor system, and this was enhanced with increases in the operating temperature. The accumulation of coke on the catalyst was minimized, as the transported carbon was continuously oxidized to CO_2 in the regenerator, even though as much as 30 g_{tar}/Nm^3_{gas} were feed into the reformer reactor. Deactivation of the catalysts was not detected during the experiments.

A method for the online determination of the moisture content of gas, which was originally developed for measuring the moisture content of the raw gas from a gasifier, was experimentally evaluated using flue gases from biomass combustion in a grate furnace and in a CFB boiler. In the CFB experiments, the moisture-measuring unit was operated in series with an FT-IR cell, to enable comparison with a well-established technique. The proposed method gave highly accurate measurements and a response time that was in seconds, in the absence of significant hysteresis.

Possibilities to increase the oxygen distribution and even out both the temperature and the profile of unburned species in a CFB furnace were investigated by the incorporation of a metal oxide (ilmenite) into the bed material. The investigation was conducted in the Chalmers 12-MW$_{th}$ boiler/gasifier system, and up to 40 wt.% of the ordinary used silica-sand bed material was replaced with ilmenite. Experiments, which initially involved the boiler only and that subsequently also included the gasifier, showed that the amount of unburned spices was lowered when ilmenite was mixed in with the bed material. In addition, the study revealed that more of the combustion reactions were allocated to the furnace when ilmenite was used, in comparison with using silica-sand only, in which case part of the combustion occurred in the cyclone. Given the similarities in process layout between the boiler/gasifier system and the proposed tar-cleaning reactor system, operation with metal oxides in boiler/gasifier system can provide important information related to the scale-up of the tar-cleaning method.

Keywords: Tar cleaning, Catalytic gas cleaning, Biomass gasification, Biomass combustion, Oxygen carriers, Moisture measurements, Ilmenite, CFB

List of Publications

I. Fredrik Lind, Martin Seemann, Henrik Thunman. Evaluation of fluid dynamics in a hot and a cold system of interconnecting fluidized beds. In: International Conference on Fluidization, Fluidization XIII, Gyeong-ju Korea, 2010; pp 869–876.

II. Fredrik Lind, Martin Seemann, Henrik Thunman. Continuous catalytic tar reforming of biomass derived raw gas with simultaneous catalyst regeneration. Ind. Eng. Chem. Res., 2011, 50 (20), pp 11553–11562

III. Fredrik Lind, Mikael Israelsson, Martin Seemann, Henrik Thunman. Manganese oxide as catalyst for tar cleaning of biomass derived gas. Journal of Biomass and Biorefinery, 2012, 2, (2), pp 133–140.

IV. Nicolas Berguerand, Fredrik Lind, Martin Seemann and Henrik Thunman. Use of nickel as tar catalyst for tar elimination in a chemical looping reformer operated with biomass producer gas. Ind. Eng. Chem. Res., 2012, 51 (51), pp 16610–16616

V. Fredrik Lind, Nicolas Berguerand, Henrik Thunman, Martin Seemann. Ilmenite and nickel as catalysts for upgrading of raw gas derived from biomass gasification. Accepted for publication in Energy & Fuels, 2013

VI. Sven Hermansson, Fredrik Lind, Henrik Thunman. On-line Monitoring of Fuel Moisture-Content in Biomass-Fired Furnaces by Measuring Relative Humidity of the Flue Gases. Chem. Eng. Res. Des., 2011, 89, (11), pp 2470–2476

VII. Henrik Thunman, Fredrik Lind, Claes Breitholtz, Nicolas Berguerand, Martin Seemann. Investigation of using an oxygen-carrier as bed material for combustion of biomass in a 12 MW_{th} CFB-boiler. Sent for publication February 2013.

Author details

Professor Henrik Thunman, who is the principal academic supervisor of this work, contributed with ideas, discussion, and editing of **Papers I–VII** and was responsible for securing financial support for the projects. Dr. Martin Seemann is the assistant academic supervisor and he organized and participated in the experimental work, as well as contributed to the discussion and editing of **Papers I, II, III, IV, V** and **VII**.

Papers I, II, III and V: Fredrik Lind is the principal author and was responsible for conducting the experiments and evaluating the results. Mikael Israelsson contributed to the evaluation of the results presented in **Paper III** and was responsible for the tar analyses in **Papers IV** and **V**. Dr. Nicolas Berguerand was involved in the experiments presented in **Paper V** and contributed with discussions and editing of this paper**.**

Paper IV: Dr. Nicolas Berguerand is the principal author of this paper. Fredrik Lind was responsible for the experiments and contributed with discussions and editing of this paper**.**

Paper VI: Dr. Sven Hermansson is the principal author of this paper and Fredrik Lind made contributions to the design and construction of the measurement equipment, as well as to the experimental work.

Paper VII: Professor Henrik Thunman is the principal author of this paper. Fredrik Lind contributed with experimental evaluation, editing, and writing. Dr. Nicolas Berguerand contributed with experimental evaluation, editing, and writing. Dr. Claes Breitholtz performed the experiments together with Dr. Martin Seemann.

Acknowledgments

First of all, I would like to express the greatest gratitude to my main supervisor and mentor Henrik Thunman. Thank you for giving me encouragement, dedicating time for supervision and bringing enthusiasm to our group. Martin Seemann, thanks for all your support in research, for that you are sharing your skills and for being a good listener and friend.

Nicolas Berguerand thanks for your first class co-operation in experiments and writing and not least for supporting me and being a good friend. Mr. Larsson, Mikael Israelsson and Jelena Marinkovic thank you for your help with the experiments and for good friendship, special thanks to Mikael for his work on the tar analysis. Sven Hermansson, thanks for excellent work cooperation as co-author and for all the great visits at Holmesberg.

I would like to acknowledge Jessica Bohwalli, Rustan Marberg and Johannes Öhlin for their outstanding work in the KC and for the cheerful mind which always surrounds them. Extra thanks are also directed to Rustan for his patience, working-skills and for being a sounding board when designing and building the CLR-system. The boiler operating staff at Akademiska Hus: Per, Mikael, Raymond, Robert and Malin are acknowledged for their fingertip control when running the boiler and gasifier.
Thanks all colleagues at the division of Energy Technology for creating the best working environment and special thanks are directed to Inger Hessel for always taking her time and helping with everyday issues at the division.

Thank you Eva and Lasse for that you are being supportive and always putting family first! Last but not least, Lotta, my best Friend and Love thank you for all your support, encouragement and for that you once introduced me to the world of science. Finally, Oskar, Gustav and Astrid thank you for giving me perspective on life!

This project was supported financially by E.On, the Swedish Gasification Centre (Svenskt Förgasningscentrum; SFC) and the ERA-Net program. The operation of the gasifier was facilitated by Göteborg Energi, Metso, Akademiska Hus, and the Swedish Energy Agency.
Fredrik Lind, Göteborg 2013

Table of Contents

Till min morfar

Tack för allt det stöd du gav

”Hårt arbete lönar sig”

1 - Introduction

Historically, the use of biomass as a fuel is probably occurred around the time man mastered fire, and for a long time biomass constituted an essential fuel for domestic heating and for cooking purposes. The importance of biomass decreased with increasing energy demands during the industrial revolution in the early 19th-century, at which point energy-dense coal outcompeted biomass as a fuel. Thereafter, the utilization of fuels based on fossil feedstock, such as coal, oil, and natural gas, has increased and are currently the primary energy sources worldwide[1]. However, fossil-based energy is a finite resource and once the energy from these sources is expended, the process releases carbon dioxide (CO_2) to the atmosphere. It is currently believed that the intensification of CO_2 emissions as a result of fossil energy use has a negative impact on the environment, as for example in Global Warming.

Potential routes to deal with CO_2 emissions and to reduce the dependency on fossil energy are frequently discussed among policymakers[2]. Increased usage of alternative fuels or so-called CO_2-neutral fuels from renewable energy sources has been proposed as one possible solution. This is also the reason why there is renewed interest in biomass as a fuel, with a preference for lignocelluloses, as these can be cultivated without interfering with the farming of crops for food production.

The conversion of biomass *via* combustion or gasification, followed by gas cleaning and fuel synthesis, is considered in this thesis. These processes can be used for converting native biomass into high-value energy carriers, i.e., electricity in the case of combustion, and various combinations of vehicle fuels and electricity in the case of gasification. In the parts of this thesis concerning gasification, key issues associated with the gas-cleaning procedure upstream of fuel synthesis are addressed, and a proposal for a novel reactor design that can resolve these issues is investigated. For the parts of the thesis concerned with combustion, a proposal for improving the distribution of oxygen in the furnace of a circulating fluidized bed (CFB) boiler through the addition of metal oxides to the bed is studied. Finally, to increase the possibilities for process control and process evaluation, a method for online determination of the moisture content in the effluents from a boiler, gasifier or gas-cleaning unit is designed and demonstrated to be operational.

1.1 Biomass gasification, gas upgrading and fuel synthesis

Direct usage of the energy stored in native lignocelluloses that have approximately 50wt-% moisture content is restricted primarily to heat and power production. However, with additional processing steps, this biomass can be refined further into, for example, high-quality fuels for transportation. These processes are needed if biomass is to be competitive with the wide range of final products available from fossil feedstocks. At present, some of these green techniques are moving from the developmental stages into the industrial scale. However, process maturity, in terms of the achievement of diverse fuel production and economic viability, is essential if these processes are to receive commercial acceptance.

One technique that could meet these demands is the gasification path, which involves the thermochemical conversion of biomass *via* gasification, followed by gas cleaning and fuel synthesis (**Fig. 1)**. The gasifier constitutes the first step, which in this instance is illustrated by the Chalmers indirect gasifier[3, 4] (**Fig. 2)**. The indirect gasifier is operated as a bubbling fluidized bed (BFB) (4) and is coupled to a 12-MW_{th} biomass-fired CFB boiler (1), which produces hot water for district heating. The hot sand from the boiler is separated from the flue gases in the water-cooled cyclone (2) and is transported to a particle distributor (3), while the flue gases are used for heat and steam production in the convection path of the boiler. The particle distributer can be fluidized in two ways: 1) all the bed material is returned to the boiler (without entering the gasifier); or 2) a proportion of the bed material is recirculated back to the boiler *via* the gasifier. In the gasifier, the hot bed material is mixed with biomass and steam, and a raw gas is produced. Approximately 3 tons of silica sand is circulated within the boiler/gasifier loop. Char from the gasifier and supplementary wood chips are used as the fuel in the boiler. The additional fuel is needed in this application as heat is not only used for the endothermic gasification reactions but it is also extracted for the district heating system.

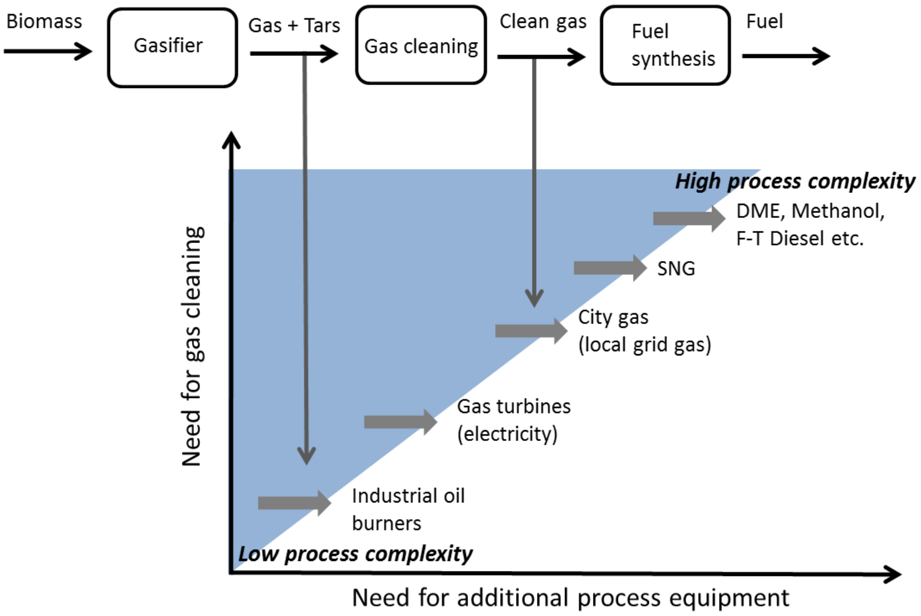

Figure 1. Conversion pathways from lignocelluloses to gaseous fuels *via* gasification

The biomass gasification operation itself is a process that is approaching the level of maturity needed for commercialization. In this process, the presence of an oxidizing agent at high temperature decomposes the large biomass polymers, initially into lighter molecules and eventually into permanent gases (H_2, CO, CO_2, CH_4, and light hydrocarbons), ash, char, tars, and minor contaminants according to reaction (**1**):

$$\begin{aligned}\text{Biomass} + O_2 \text{ or } H_2O &\rightarrow CO, CO_2, H_2O\, H_2, CH_4 + \text{other hydrocarbons}\\ &\rightarrow \text{char} + \text{tar} + \text{ash}\\ &\rightarrow HCN + NH_3 + HCl + H_2S + \text{other sulfur gases}\end{aligned} \qquad (\mathbf{1})$$

The permanent gases (the desired product) constitute the molecular building blocks for downstream fuel synthesis. In contrast, the “tar” fraction is an undesirable byproduct. These tars are condensable hydrocarbons that are often referred to as ‘aromatic compounds’, consisting mainly of 1- to 5-ring aromatic compounds together with oxygenates and sulfur-containing hydrocarbons[5-11]. The presence of these hydrocarbons is a consequence of incomplete conversion of the biomass[12]. The energy stored in this fraction may be up to 5% of the total energy content of the fed biomass. If unconverted, these species start to condense at temperatures of ≥350°C[13], causing severe fouling of downstream equipment and potentially deactivating the fuel synthesis catalysts.

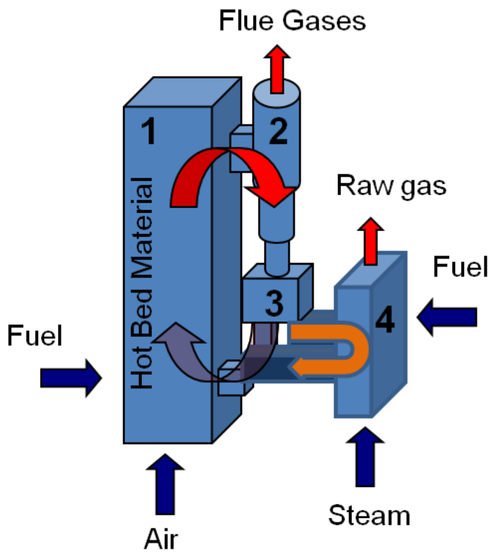

1. Biomass-fired CFB boiler
2. Cyclone
3. Particle distributor
4. Biomass gasifier

Figure 2. Schematic of the Chalmers boiler and gasifier system

Industrial implementation of the gasification path is at present largely dependent upon its potential to produce tar-free gas with simultaneous valorization of the tar energy. The possibilities regarding direct use of the raw gas from the gasifier are therefore rather limited. However, if the gas is maintained at a temperature >350°C, the gas can be used directly or after the removal of particles to substitute for fossil gas and oil in industrial burners (**Fig 1). Figure 1** illustrates how the demands for gas cleaning and process equipment increase as the raw gas is refined from a low- to a high-grade fuel. If the gas cleaning is further upgraded to also remove tars, the gas can be used as a fuel for modified internal combustion engines and gas turbines or even in the local gas grid. Additional process steps are required if the gas is to be used as a feedstock for synthetic fuel production. For synthesis into Substitute Natural Gas (SNG), the H_2/CO ratio needs to be controlled, and the gas needs to be cleaned of sulfur (to protect the catalyst from deactivation). If additional downstream processes are available, the gas can be further refined to liquid fuels, such as dimethyl ether (DME)[14], methanol[15], and Fisher-Tropsch diesel (F-T Diesel)[5].

The tar issue is addressed in the present work, and a method that combines catalytic gas upgrading with continuous regeneration of coke deposits is proposed and investigated. A bench-scale gas-upgrading system based on the Chemical-Looping Reforming (CLR) concept, which was originally presented by Mattisson et al.[16] as a spin-off technology from Chemical-Looping Combustion (CLC), was designed and operated. The CLR concept was initially applied as a method for the partial oxidation of methane into CO and H_2. The system, which consists of two interconnected fluidized beds, was in the present work studied both under cold conditions in a Perspex reactor system and under hot conditions in a high-temperature-resistant steel unit. The overall goal in applying the CLR concept in the present work was to investigate experimentally the possibility of applying an inexpensive and non-toxic ore (in this case, ilmenite) to secondary gas upgrading. For ilmenite, once it has been mined, grinding is essentially the only refining process, which means that the cost of producing this catalyst is low compared with the cost of manufactured catalysts.

To date, only a few investigations have been published on the use of ilmenite as a tar-reforming catalyst, and none of those studies involved fluidized beds. Therefore, to evaluate the tar-cleaning performance of the reactor system and the ilmenite catalyst, a reference catalyst based on nickel oxide (NiO/Al_2O_3) was chosen. The choice of NiO was motivated by previous findings that: 1) Ni-based catalysts show very high activity with respect to tar reformation; and 2) many tar-cleaning studies using Ni-based catalysts have been performed. Therefore, in the present study, it was possible to quantify the tar-reducing efficiencies of the two catalysts by comparisons with similar investigations reported in the literature.

1.2 Catalytic tar cleaning using the CLR concept

The CLR system is fed with tar-rich raw gas from biomass gasification. The idea behind the tar-cleaning method is to reform the unwanted tar components (C_nH_m) into useful gaseous molecules. The reactor system consists of the following reactors: 1) a regenerator reactor, also termed the Air Reactor (AR); and 2) a reformer reactor, also referred to as the Fuel Reactor (FR), which is fed with the raw gas (**Fig. 3)**. Two loop seals (LS), the superior (SLS) and inferior (ILS), which are fluidized with inert gas or steam, prevent gas cross-contamination of the effluents from the respective reactors, while enabling overall catalyst circulation. In this bench-scale system, the oxidized metal oxide Me_xO_y exits the SLS and descends through the gas phase for about 15 cm before reaching the bubbling bed, which creates an oxygen-rich zone. During its descent, a part or all of the Me_xO_y is reduced to Me_xO_{y-1}, as hydrocarbons (C_iH_j), H_2, and CO are available for combustion according to reaction **2a**:

$$\begin{aligned} &C_iH_j + nH_2 + zCO + [2i + 0.5\,(j+z) + n]Me_xO_y \rightarrow \\ &[i+z]CO_2 + [j/2 + n]H_2O + [2i + 0.5\,(j+z) + n]Me_xO_{y-1} \end{aligned} \qquad \textbf{(2a)}$$

The reduced metal oxide Me_xO_{y-1} in the bed acts as a catalyst for reforming the tars (C_nH_m) in the presence of reforming media*, such as steam or CO_2 in the raw gas, according to the simplified reaction **2b**. In addition to the desired tar-reforming reaction, additional carbon-forming reactions cause carbon to be deposited on the catalysts.

$$C_nH_m + Me_xO_{y-1} + H_2O^* + CO_2{}^* \rightarrow C_iH_j + H_2 + CO + Me_xO_{y-1} + C \qquad \textbf{(2b)}$$

While the Me_xO_{y-1} is re-oxidized to Me_xO_y in a strongly exothermic reaction in the AR, the carbon deposits on the catalytic surfaces are oxidized to CO_2 according to reaction **2c**. The oxidation of coke deposits contributes to maintaining the heat balance, as the formed heat is transported *via* the catalyst back to the FR, and subsequently used in the endothermic tar reactions.

$$\begin{aligned} & n_1 Me_xO_{y-1} + n_2C + [n_1/2 + n_2](O_2 + 3.77N_2) \rightarrow \\ & n_1 Me_xO_y + n_2CO_2 + [n_1/2 + n_2]3.77N_2 \end{aligned} \tag{2c}$$

The production of heat from the regeneration of coke in a catalytic twin-bed system is a well-known concept and is the driving force behind the commercially applied process of Fluid Catalytic Cracking (FCC), which is used to boost the yield of gasoline from heavy crude distillates in oil refineries[17]. It should be noted that the oxygen transport affects the composition of the permanent gases, given that a minor fraction of the hydrocarbons and/or H_2 and CO is either partly or fully oxidized. These reactions may also be essential if the heat contribution from the oxidation of coke deposits is insufficient to sustain the heat balance. Depending on process integration, the heat balance in the CLR can be achieved by combusting in the regenerator the tail and purge gases from potential downstream fuel synthesis, as indicated in **Figure 3**. This concept in combination with downstream ethanol synthesis was proposed by Dutta et al.[18]. However, in the present study, tar removal rather than heat integration is the main consideration.

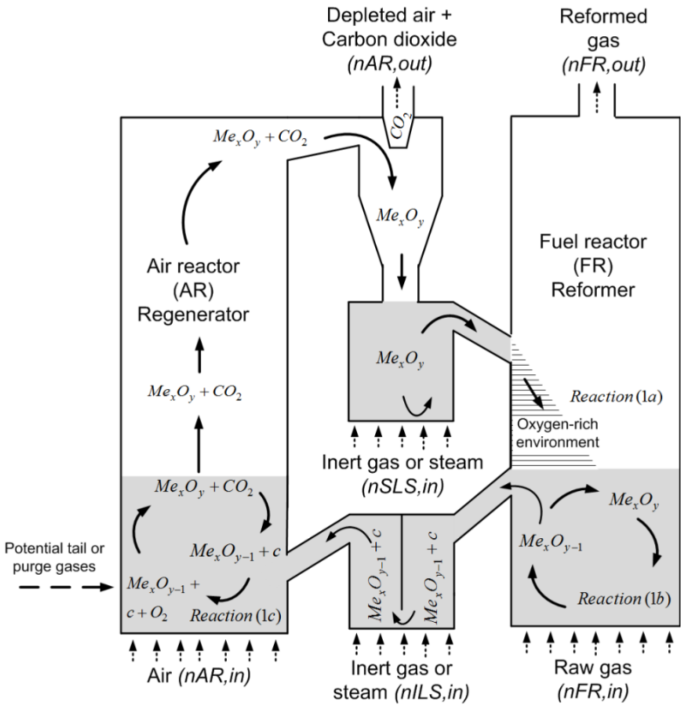

Figure 3. CLR concept for secondary upgrading of biomass producer gas

1.3 Moisture measurements in gasification and combustion processes

The moisture content of the gasification reactor is an important operating parameter, as water is involved in both the gasification reactions and tar-reforming reactions. As water is both consumed and produced during gasification, to be able to close the mass balance in a gasification unit, knowledge of the moisture content is needed. A common way to determine the water content of a gas is to weigh the condensed water fraction as a function of gas volume flow. However, measuring the moisture content in a tar-rich gas is more complex, as the condensate includes condensable hydrocarbons. In the present study, this issue was addressed and a unit for online measurements of moisture content was developed. The idea is that the moisture measuring unit is placed downstream of a combustion reactor in which all the combustibles in a slipstream of the raw gas are oxidized by air. The temperature of the flue gases is reduced to around 90°C inside the unit, and the relative humidity of the gas is measured and converted to moisture content (vol.%) Detailed descriptions of the experimental setup and the mass balance during moisture measurements of the raw gas produced in the Chalmers gasifier are presented elsewhere[19].

The water content is also important when combustion of biomass is considered, as the water content of the biomass is essentially a measure of the heating value of the fuel. In all combustion applications, control of the combustion temperature is vital to achieving sufficient fuel conversion. For biomass-fired boilers, this temperature is closely related to the fuel moisture content and the amount of air fed to the furnace. This is exemplified by a situation in which there is a sudden drop in combustion temperature, which usually is compensated by automatically increasing the air feed to the furnace, so as to increase the combustion reactions. However, if the temperature drop is coupled to an increase in fuel moisture, the surplus air fed to the furnace will instead lower the temperature even more. If this amount of fuel-related moisture could be monitored online, then the combustion temperature could be controlled in a more efficient manner, leading to more stable operation. This is especially important in boilers that are supplied with a variety of fuels, wherein the moisture content can vary from a few wt.% for wood pellets to 35–50 wt.% for wood chips and up to 60 wt.% for wet sawdust. The above-described method was initially evaluated experimentally for measuring the moisture content of flue gases from biomass combustion.

1.4 Oxygen carriers in a biomass-fired CFB boiler

The heterogeneous nature of biomass, together with its moisture content and in some extreme cases ash contents of as much as 6 wt.%[20] complicate the combustion operation and the final burn-out of the fuel. To ensure complete conversion of the fuel and to minimize emissions of harmful species, it is crucial to have proper mixing of the fuel and oxygen in space and over time[21]. In combustion units, a commonly applied measure to control the oxygen level in relation to the specific properties of the fuel is to adjust the level of excess air. However, increasing the oxygen supply to the furnace usually requires that an excess of air be fed to the combustion unit, which results in a loss of boiler efficiency. This can also create a situation in which there is irregular heat release inside the combustion chamber, resulting from the uneven distribution of oxygen and fuel both spatially and temporally. The resulting aberrant distribution can in turn induce a number of emission-related issues, e.g., involving NOx and the slippage of unreacted hydrocarbons (HC) and CO into the flue gases, and extensive efforts have been made to address this problem. Furthermore, an effect of the uneven heat release is that high-temperatures zones can be formed as small volumes inside the furnace. These temperature gradients are likely to induce melting of ash components, which promotes the formation of sticky ash that can be deposited onto cooling surfaces. The condensation of ash onto a super-heater is a common feature of biomass combustion, and this eventually leads to degraded heat transfer and corrosion problems for heat exchangers[22-24].

The issues related to the mixing of the fuel and oxidizer in a CFB furnace are addressed in this work, and a solution is proposed whereby the whole or a fraction of the ordinary used bed material is replaced with an oxygen-carrying metal oxide (**Fig. 4)**. The metal-oxide, which has the ability to absorb and release oxygen during redox-reactions at the temperatures present in the furnace, will theoretically, based on the reactions with gaseous HC and the fluid dynamics present in the riser furnace, enable simultaneous oxygen supply throughout the furnace geometry. When the oxidized metal oxide (*MeO*) is conveyed upwards throughout the furnace geometry, the bound oxygen is consumed as it reacts with the volatiles (C_iH_j) to generate carbon dioxide and water, and the metal oxide is reduced to (*Me*). The reduced (*Me*) is then separated from the flue gases in the cyclone and transferred back to the bottom bed. The feed of air to the furnace can then be balanced in relation to the oxygen consumption needed for converting the char fraction (*nChar*) to CO_2, together with the oxygen demand for re-oxidizing the reduced metal oxide (*Me*), so as to complete the redox cycle. This idea was experimentally investigated in the present work using ilmenite as the oxygen carrier in the 12-MW_{th} CFB boiler at Chalmers University of Technology.

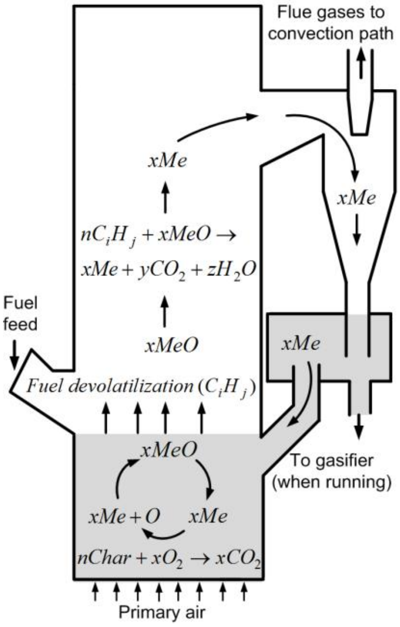

Figure 4. Reactions involving fuel and oxygen carriers in the boiler.

1.5 Outline, further developments, and contribution of the thesis

The major part of this thesis comprises a summation of the work conducted on catalytic upgrading of biomass-derived gas in the CLR system. The blue field in **Figure 5** depicts an outline of this work and the progression of the CLR system, initially with fluid dynamic experiments conducted at ambient conditions in the Perspex system, to subsequent raw gas experiments in the first hot system. In parallel with these CLR experiments, two other studies are presented in the blue field (**Fig. 5)**. The first one deals with the concept of online monitoring of moisture content in a gas stream. This method was originally developed with the aim of determining the moisture content of the raw gas from biomass gasification, so as to enable an appropriate mass balance across the gasifier. However, the method was first evaluated with flue gases from a boiler, as presented in the present work. The second study involves an idea based on experiences with the operation of the CLR system. This work is an investigation of the use of an oxygen-carrying material to increase the oxygen distribution in biomass-fired CFB boilers (**Fig 5)**. The work is also interesting from a CLR point-of-view, as the reactor configuration in the boiler/gasifier system is essentially the same, which means that the system can be used to study scale-up effects. Finally, the two panels in the figure outside the blue shading reflect the current status of the work on the CLR system and projections regarding further work. The first of these panels, term 'Hot system 2.0', represents a development of the CLR concept based on the present work. The experiences gained from using Hot system 1.0 have suggested a different design for the reactor system. A major goal of the later-generation reactor is to increase the gas-solid contacts between the catalysts and the raw gas by decreasing particle size and by turning the reactor configuration around, so that the reformer reactor is operated as a

CFB rather than as a BFB. This system has recently been put into operation. The last panel, termed ‘Industrial scale’, represents a newly started project in which the CLR system together with the gasifier is modeled in ASPEN + on an industrial scale. The CLR part of this project is based on the experimental data generated in the present work. Furthermore, the experimental work on using ilmenite in the boiler/gasifier system is a valuable first step towards an industrial-scale process.

In this thesis, the following contributions are presented to improve the understanding, operation, and analysis of secondary catalytic gas upgrading using the CLR system and to improve the combustion of biomass using metal oxides as bed material in a CFB boiler. The design, operational controllability, and the possibilities to transfer data and operating knowledge from the cold Perspex CLR system to the hot CLR system are investigated in **Paper I**. The initial operating experiences, experimental setup, and proof of the CLR concept using the natural occurring ore ilmenite are presented in **Paper II**. The effects of using different catalysts on tar cleaning efficiency, gas compositions, and the possibilities to minimize coke deposition onto the catalyst are investigated using as the catalyst: ilmenite (**Papers II and V)**; manganese oxide supported on zirconia oxide (**Paper III),** and NiO supported on an α-Al_2O_3 matrix (**Papers IV and V**). A system-wide molar balance for the CLR system and how to validate the efficiency of tar reduction by the catalysts in the upgraded gas are addressed and discussed in **Paper V**. The difficulties associated with measuring the water content of flue gases with a rapid response time are addressed in **Paper VI,** together with a development of an online moisture measurement unit, which is experimentally evaluated with flue gases from a grate furnace and from a CFB boiler. The remaining part of the thesis considers the use of a metal oxide as bed material in a CFB-boiler (**Paper VII**). The possibilities to even out the temperature profile and to increase the distribution of oxygen in the system, and thereby reduce the amount of excess air needed to reach complete combustion of the fuel are investigated.

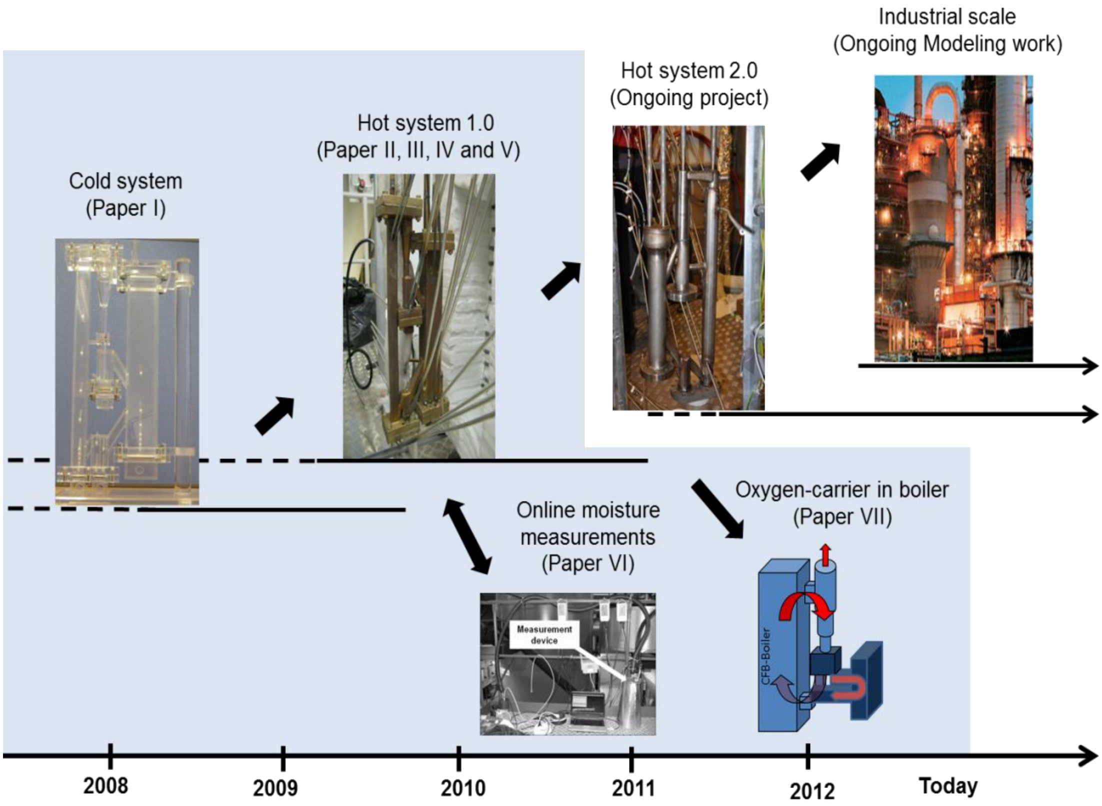

Figure 5. Evolution of the CLR concept for gas upgrading.

2 - Theory

In this chapter, theoretical considerations regarding tar formation during thermochemical conversion of biomass, tar-cleaning techniques, catalysts for tar reforming, and possibilities for integrating the CLR system with an indirect gasifier are discussed.

2.1 Thermal conversion of biomass and tar formation

A biomass particle is converted by a complex pattern of chemical reactions. However, the general path can be explained as a three-stage process of: drying, pyrolysis/devolatilization, and char conversion (**Fig. 6**). The first two stages in the conversion process behave similarly during combustion and gasification. When a fuel particle is surrounded by a hot gas, heat is transferred from the gas to the surface of the particle. The particle is heated together with its water content until the evaporation temperature is reached. This stage is called drying and it is highly endothermic, with the water leaving the particle in the form of steam.

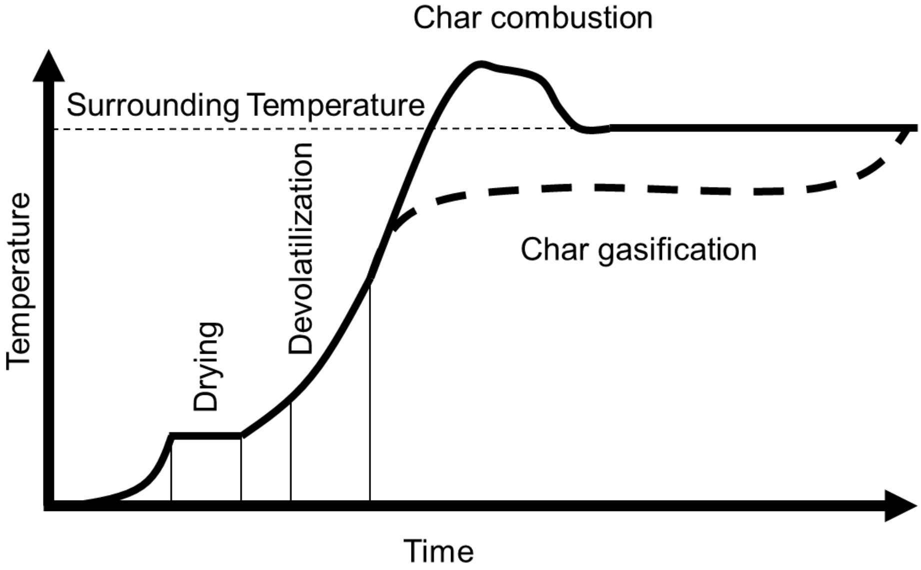

Figure 6. Conversion stages for a solid fuel particle

As the surface temperature of the particle is increased, heat is propagated towards the center of the particle and the fuel starts to decompose, releasing volatiles. This step is termed pyrolysis if no oxygen is present and devolatilization if oxygen is present, hereinafter referred to collectively as pyrolysis. The pyrolysis process as a whole is an endothermic process. For wood, the hemicellulose undergoes pyrolysis at temperatures in the range of 225°–325°C, the cellulose at 325°–375°C, and lignin at 300°–500°C. Tars are mainly formed during this pyrolysis step. These tars are called primary tars, and they can further react to generate secondary and tertiary tar compounds in the gas phase. After the pyrolysis step, only the char fraction remains. The conversion process for the char fraction differs between gasification and combustion. Steam and/or sub-stoichiometric amounts of oxygen are used as oxidizing agents during gasification, whereas for combustion stoichiometric amounts (or more usually a surplus) of oxygen are supplied to the char combustion reactions. As a consequence, the gasification operation as a whole is endothermic, in contrast to the exothermic combustion operation (**Fig. 6).** The result is that the energy from the biomass is stored chemically and as latent heat in the gases leaving the gasifier, whereas in the case of combustion, the energy in the biomass is utilized for heat production.

Several studies have been conducted on tar formation during thermal conversion of biomass. In the 1980s, Evans and Milne conducted a series of pyrolysis experiments in a reactor with two different temperature zones and measured the tar components using molecular-beam mass spectroscopy[25, 26]. In these studies, they mapped numerous different tar species, which they categorized into primary, secondary, and tertiary tars as a function of temperature. The effects of temperature on the chemical compositions of the biomass tars were also investigated by Elliot[27], who defined the transition from primary tars to phenolic compounds to aromatic compounds as a function of process temperature. These studies show that the process temperature in a gasifier strongly influences the distribution of tar products. **Figure 7** depicts a simplified classification system for the transition from primary to secondary tars and from secondary to tertiary tar compounds as a function of process temperature. As shown in **Figure 7**, at low temperatures for pyrolysis (around 400°C), mostly primary tars are formed, which are commonly referred to as bio-oils. These tars are characterized by low condensation temperatures and they often have branches, and since they contain high levels of oxygen they are very reactive. When the operating temperature is increased to 600°–700°C, more secondary tars are formed; at these temperatures, phenolic, branched, and non-branched aromatic compounds tend to form. At higher temperatures of 800°–900°C, tertiary tars are formed. These species are represented by aromatic rings without branches, and different types of polycyclic aromatic hydrocarbons (PAH) are commonly seen as products. Overall, regarding tar formation, higher process temperatures during biomass conversion *via* gasification tend to favor the formation of more stable aromatic compounds, which contain less oxygen and fewer branches.

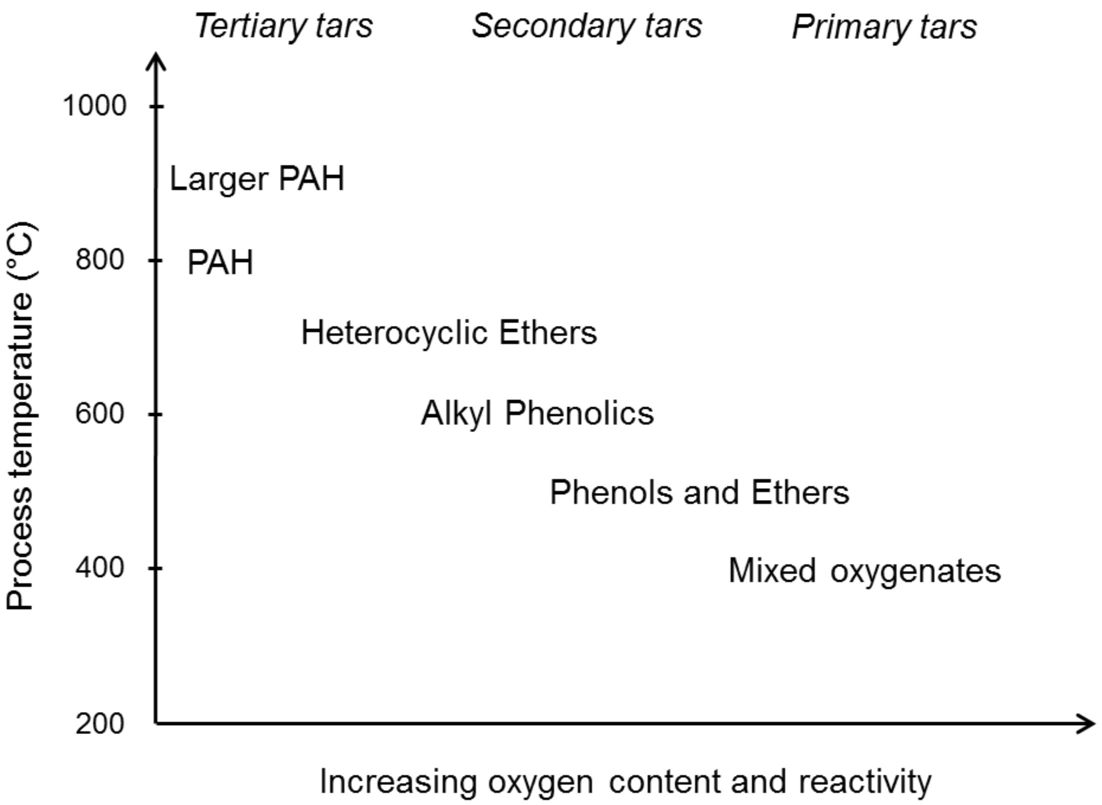

Figure 7. Simplified classification system for the formation of primary, secondary, and tertiary tar compounds as a function of process temperature.

2.2 Tar-cleaning techniques

Extensive work has been performed on tar cleaning in connection with gas conditioning, and several approaches suitable for gas cleaning have been reported in the primary literature[6, 28-31] and in review papers[7, 9]. Tar cleaning of biomass producer gas can be divided into two main categories: wet cleaning and dry cleaning. Wet cleaning is usually performed in scrubber units, where the tar is condensed onto water or oil droplets during rapid cooling of the gas. The wet cleaning techniques are commercialized and represent state-of-the-art technology. Dry cleaning is mostly referred to as ‘catalytic’ or ‘high-temperature’ cleaning (thermal cracking of tars). Catalytic cleaning can be integrated with the gasifier outlet temperature, whereas high-temperature cleaning needs to be performed at temperatures >1100°C, to achieve high conversion efficiencies[9]. Some of the product gas needs to be consumed to increase the exit temperature of the gasifier (from around 800°C to 1100°C); this can be accomplished by adding high-value oxygen to the product gas[9].

The path from native biomass to SNG (**Fig. 1**) was selected as a reference process to compare the three techniques. **Figure 8** illustrates the operating temperatures for the three process steps. The gas cleaning step in **Figure 8** is divided into high-temperature cleaning, catalytic cleaning, and cleaning by scrubbers. The reactions (**Table 1, reactions 3 and 4**) that occur during high-temperature cleaning are endothermic and all the hydrocarbons, including tars, are theoretically broken down to CO and H_2. As the production of SNG is the eventual target, the methane already formed in the gasification operation is cracked down during the high-temperature cleaning.

Table 1 Reactions for tar cleaning and methanation

Operation	Chemical reaction	No.	Heat of reaction
High-temperature cleaning	$C_xH_y + H_2O \rightarrow nCO + (1+m/2)H_2$	(3)	Endothermic
	$CH_4 + H_2O \rightarrow CO + 3H_2$	(4)	Endothermic
Catalytic cleaning	$C_nH_m + H_2O \rightarrow C_iH_j + pCO + qH_2$	(5)	Endothermic
	$CO + H_2O \rightarrow H_2 + CO_2$	(6)	Exothermic
Methanation	$CO + 3H_2 \rightarrow CH_4 + H_2O$	(7)	Exothermic

Gas cleaning using a scrubber technology is a well-known method that can be applied to tar cleaning of biomass producer gas. However, there is a large thermodynamic penalty, as the gas is rapidly cooled from approximately 400°C to ambient temperature or even lower[29] (**Fig. 8)**. Furthermore, the chemically bounded energy within the tars is lost. After the tars have been removed, the gas needs to be reheated to allow SNG synthesis (**Table 1, reaction 7**), which typically is performed at 200°–450°C [32]. Significant expenses related to the scrubber technology are for fresh scrubber fluid and for managing the spent fluid.

Catalytic tar cleaning is regarded as the most promising of the three techniques, as it shows the highest potentials for heat integration with the gasifier and for recovery of the chemically stored energy within the tars. The technique can be conducted as either primary or secondary cleaning. Primary cleaning involves catalysts that are already in the gasification step itself, in order to promote cracking of the tars [7]. Thus, the tar cleaning and gasification reactions take place at the same temperature. Therefore, this method is less flexible in terms of optimization of the tar cleaning, in comparison to secondary tar cleaning, which can be optimized independently of the gasifier operating properties[9] (**Fig. 8)**. Secondary tar cleaning has three features: 1) catalyst reactor temperatures are thermally integrated with the gasifier outlet; 2) steam can be added to ensure complete reformation of the tars (**Table 3, reaction 5**); and 3) the composition of the product gas can be catalytically adjusted[9] (**Table 1, reaction 6**). This means that it is possible to control the ratio of hydrogen to carbon monoxide for methanation already in the tar cleaning step and as a result, the gas conditioning step in the SNG synthesis can be simplified or even becomes redundant.

It has been shown that a high tar content of biomass producer gas initiates carbon formation on the catalytic surfaces, causing severe deactivation of the catalyst[7, 9, 29].

Several approaches to minimize the formation of carbon deposits on the surface of the catalyst have been reported in the literature. For example, catalyst deactivation as a result of carbon deposits was compared for fixed and fluidized beds used for secondary tar cleaning by Baker et al.[33]. They found that carbon deposits on the catalysts and catalyst deactivation were significantly lower in the fluidized bed. In parallel with secondary catalytic tar cleaning, Seemann et al.[32] reported that the internal catalyst circulation in a fluidized bed for methanation contributed to keeping the catalyst free of carbon deposits. The methanation experiments showed that carbon deposits were formed on the catalyst in the bottom zone of the bed, and as the catalyst was transported upwards in the bed, the carbon deposits were removed by hydrogenation and gasification reactions with water steam. Miyazawa et al.[34] reported a lower carbon yield on various nickel catalysts during partial oxidation than during steam reforming. This phenomenon can be explained by carbon combustion in the presence of O_2 during catalyst fluidization.

The problems associated with carbon formation on catalysts during the reformation of hydrocarbons are well-known from the oil industry. A process that deals with the twin problems of conversion of hydrocarbons and formation of carbon on active surfaces is FCC, which is performed in a dual fluidized bed to increase petrol yield in the petroleum refining industry[17] (**Fig. 9**). In FCC reactors, the problem of carbon formation *via* the cracking of higher hydrocarbons is tackled by continuous regeneration of the catalyst surfaces, which in this case is a zeolite. Catalyst regeneration is performed in an air-fed reactor, where the heat released from oxidation of the carbon deposits is transferred to the endothermic cracking reactor (**Fig. 9**). The CLR method shares several features with the FCC system, such as: catalytic treatment of hydrocarbons by a circulating catalyst; regeneration of spent catalysts in air; and heat from the regenerator can be transferred to the hydrocarbon reactions. However, the major difference these systems is the opportunity for active molecule transport offered by the method proposed in this thesis. The tar-cleaning method has therefore been named Chemical Looping Reforming.

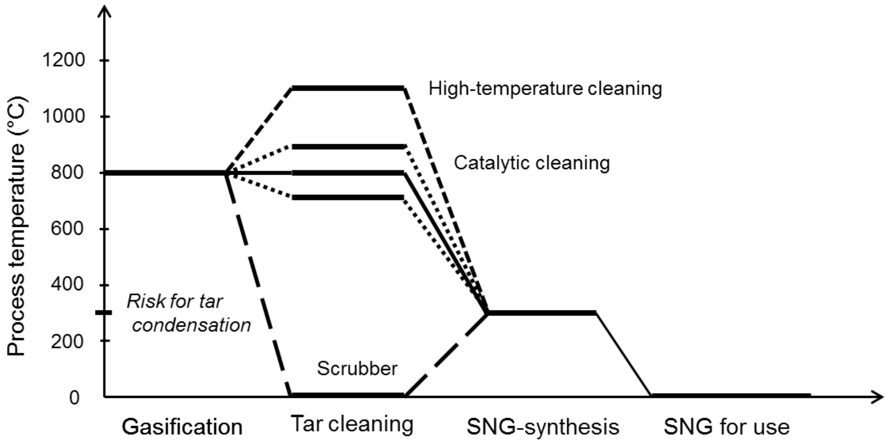

Figure 8. Heat losses from tar cleaning in SNG production.

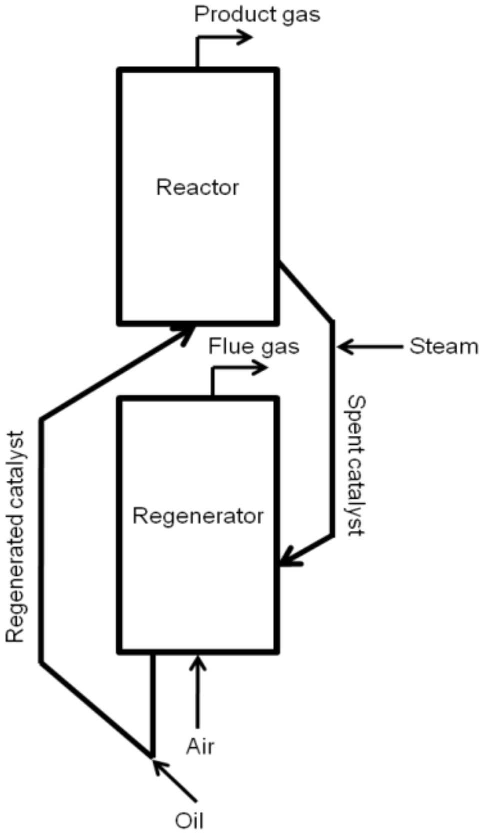

Figure 9. Schematic of an FCC unit[17].

2.3 Catalysts

Studies have shown that metal oxides, such as NiO[9, 29, 35-37], Fe_2O_3[9, 35, 38], and Mn_3O_4[39-41] supported on various inert materials have characteristics that are suitable for use as oxygen carriers and tar-reforming catalysts. In the present work, ilmenite ($FeTiO_3$ in its most reduced form), which is a naturally occurring mineral with a bulk price that is only slightly higher than that of hard coal, is investigated as a tar-reforming catalyst. Ilmenite has also been applied as a tar-reforming catalyst. Min et al.[42] conducted experiments in a fixed bed using ilmenite as a steam-reforming catalyst for the conversion of tars that were formed during the pyrolysis of Australian Mallee wood. They observed that although ilmenite exhibited good activity for tar decomposition, it also generated high levels of coke deposits, which in the case of fixed beds would clearly be detrimental. Mendiara et al.[41] showed that the activity of ilmenite for tar reformation was increased with repeated redox cycles in TGA experiments using toluene as the tar component.

The activity of ilmenite has also been studied in CLC experiments, and ilmenite is been commonly used as an oxygen carrier in CLC operations [43-45]. CLC operations have demonstrated that ilmenite particles are not fully oxidized in their crude state. Leion et al.[43] found that the degree of oxidation increased with repeated cycles of CLC. During the cyclic periods of oxidation and reduction, the porosity of the particles increased and so did their reactivity. Cuadrat et al.[46] also observed an increase in ilmenite particle porosity during repeated redox cycles, and they noted that an external Fe-rich shell was formed on the particle. A 3-day CLC experiment carried out by Leion et al.[43] showed that the ilmenite particle area increased from 0.11 m^2/g to 0.28 m^2/g; the authors concluded that ilmenite is an attractive oxygen carrier in CLC processes, with no evidence of decreases in reactivity towards pure methane and syngas (50% CO and 50% H_2).

Manganese oxide has properties that make it suitable as an oxygen carrier in CLC. Johansson et al.[39] investigated the potential of a manufactured oxygen carrier that consisted of 40% manganese oxide (Mn_3O_4) supported on 60% magnesium-zirconium oxide (M4MgZ1150). They confirmed that the material was suitable for CLC operation as it could handle continuous redox reactions while retaining high-level reactivity. This implies that this material is suitable even for a CLR system in which the catalyst is continuously exposed to reduction and oxidation reactions. Mendiara et al.[47] investigated the tar-reforming activity of M4MgZ1150, which was from the same batch as that used by Johansson used, in TGA experiments at 600°C and 800°C with toluene as the tar component. They found that the material had high reactivity for toluene and showed reforming activity at both temperatures. The same catalyst is used in CLR experiments to study the tar-decomposing activity of the manganese oxide itself, whereas the long-term goal is to use naturally occurring ores that contain manganese.

NiO-based materials have shown high activities both as oxygen carriers and for tar reformation, and have therefore been investigated as oxygen carriers in CLC and as catalysts for biomass gas upgrading. Several studies using Ni-based catalysts have been conducted. For instance, Corella et al.[36] reported biomass tar conversion rates of 99.5% with commercial Ni-based steam-reforming catalysts, while Aznar et al.[48] showed that tar conversion at >98% efficiency could be achieved in the temperature range of 650°–820°C. Bangala et al.[28] used a Ni-based catalyst to study its use in the steam reformation of naphthalene, which is one of the major biomass tar components, and they showed that complete conversion of naphthalene could be achieved at 750°C. Rownaghi and Huhnke[49] conducted experiments in a fixed bed with toluene and steam over a NiO catalyst and also with a catalyst prepared from CaO/MgO/NiO, and they showed 100% conversion of the toluene already at 700°C. These results clearly demonstrate that Ni has high activity for tar reduction and is applicable to biomass gas upgrading. A Ni-based catalyst was therefore chosen as the reference catalyst for the present work. This catalyst, which was originally developed as an oxygen carrier for CLC, consists of 40wt.% NiO supported on an α-Al_2O_3 matrix. The particles (termed “S1 particles”) have been described previously[50]. This material shows high mechanical strength in a CFB and it has been applied as an oxygen carrier for 160 hours of operation in a 10-kW CLC unit[51].

As the use of Ni as raw material is expensive, the prepared catalyst needs to retain extensive time-on-stream to be economically viable. The preparation of the catalyst involves an environmentally hazardous process, as Ni is highly toxic and can be fatal if ingested by humans or animals. The toxicity of Ni incurs an extra cost, as the spent material needs to be sent for controlled disposal. Therefore, the identification of less-toxic and less-expensive catalytic materials is of importance for industrial actors interested in catalytic tar cleaning.

2.4 Integration of an indirect gasifier with a CLR system

The aim of this section is to provide a discussion as to how the energy flows are distributed between the gasifier and the CLR and the potential points of integration between an indirect gasifier and a CLR system.

Figure 10 shows a proposal for the integration process, whereby the indirect gasifier has been separated from the boiler and the actual fuel conversion in the gasifier has been divided into two steps: pyrolysis (*Py*); and char conversion (*X*). This arbitrary subdivision is to illustrate that the product gas yield (V_x) from the endothermic char conversion (*X*) in the gasifier has to be balanced with the overall heat requirements of the system supplied by char combustion (1-x) in the combustor. The raw gas ($V_x + V_p$) is then separated from the ash components and fed into the CLR system. Depending on the composition of the raw gas, the endothermic tar-reforming reactions in the CLR reactor require different amounts of additional heat, other than that produced through WGS reactions and coke regeneration, to sustain the heat balance. This heat demand (Q_{CLR}) can be satisfied by internal circulation of oxygen from the AR to the FR *via* the catalyst (*MeO*) or *via* combustion of a slipstream of the raw gas [1-$(V_x + V_p)$] in the AR.

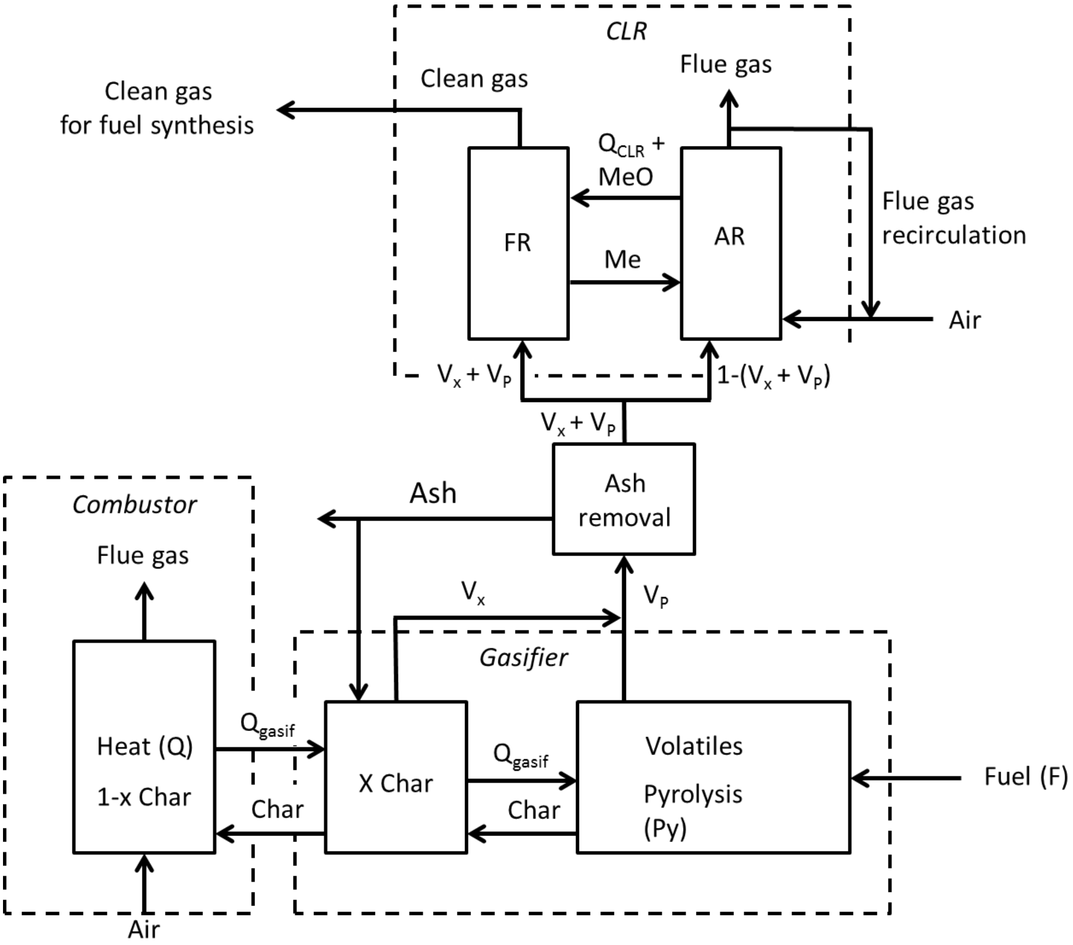

Figure 10. Schematic of an indirect gasification integrated with a CLR system.

During pyrolysis, the chemically stored energy in the fuel is distributed between the char, tar, and permanent gases, as exemplified by two extreme cases: (1) low-temperature pyrolysis (at 400°C); and (2) high-temperature pyrolysis (at 900°C). Figure **11, a** and **b,** which is based on the work of Neves et al.[52], presents an approximate distribution trend for the weight fraction and energy content in the char, tar, and permanent gas from pyrolysis of wood using nitrogen as the purge gas between 400°C and 900°C. **Figure 11a** presents the weight distribution of these species, in kg species/kg of dry ash-free fuel, as a function of the pyrolysis temperature. At 400°C, the major part of the fuel is converted to char and tar, whereas at 900°C, most of the fuel is converted to permanent gases. This shows that for increasing pyrolysis temperature, the trend is that the char and tar fraction is decreased, while the fraction of permanent gases is increased. The energy contents related to each of the fractions are shown in **Figure 11b**. At 400°C, almost all the chemically sequestered energy is bound to the char and tar fraction, whereas at 900°C, the char and tar account for approximately 40% of the chemically bound energy.

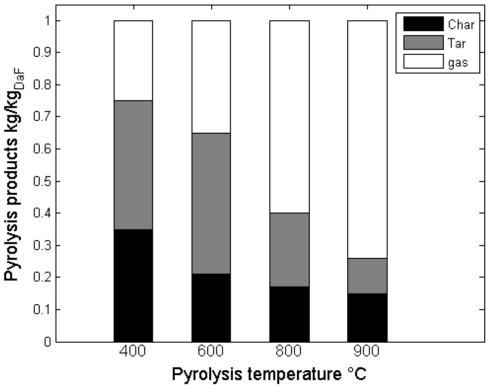

Figure 11a. Approximate wt.% distributions for char, tar, and permanent gases at different pyrolysis temperatures.

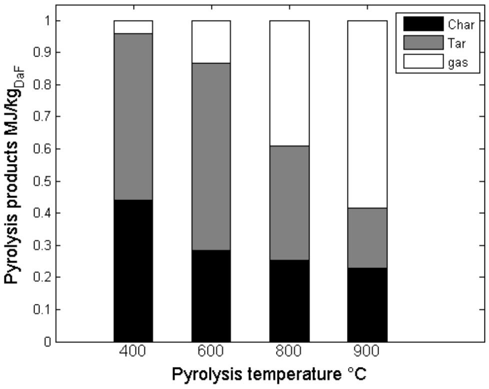

Figure 11b. Approximate energy distributions for char, tar, and permanent gases at different pyrolysis temperatures.

The toluene molecule was chosen as the tar component to exemplify theoretically the heat demand for the endothermic steam reforming of tars, as this has been designated as the tar component in several other investigations of tar reformation. In this example, the gasifier is operated at the temperatures of 400°, 600°, 800°, and 900°C, and up to 100 g_{tar}/kg_{daf} is considered in the estimation. Here, it is assumed that all the toluene is converted to CO and H_2 in the CLR at 900°C, according to Eq. (**8**).

$$C_7H_{8(g)} + 7H_2O_{(g)} \rightarrow 7CO_{(g)} + 11H_{2(g)} \quad \Delta H = 876\, KJ/mole \qquad (8)$$

A rough estimation of the heat needed for raising the temperature (ΔT) from the gasifier to the CLR and the heat needed for the tar reformation reactions are presented in **Figure 12.** The chemically stored energy levels in the tars are shown on top of the x-axis, and 50 g of tar correspond to around 2 MJ of chemically stored energy. The intersects between the solid lines and the y-axis for each of the temperature cases indicate the heat demands for increasing the temperature of the raw gas to 900°C. **Figure 12** shows that around 12% of the energy content in the fed fuel is needed to increase the temperature when the gasifier is operated at 400°C. The dotted line that intersects the different temperature cases indicates the break-even point at which the yield of chemically stored energy to the gas from tar reformation represents a gain in relation to the heat input. This means that CLR operation to the right side of the break-even line tends to increase the fuel to gas efficiency.

As mentioned above, when operating the CLR reactor, the heat demand can be provided through the combustion of a part of the raw gas either *via* oxygen-looping or *via* combusting the raw gas in the AR. The oxygen-looping offers the easiest path, as this can be accomplished by simply increasing the amount of air fed to the AR. However, increasing oxygen transport to the FR will results in less chemically stored energy in the reformed gas, due to the oxidation of hydrocarbons, hydrogen, and CO. When combusting a part of the raw gas in the AR, a slightly more complicated system is needed, as the raw gas has to be fed to both the FR and AR. However, the gain associated with this system is that the formed CO_2 is separated from the reformed gas; a similar feeding system is used at Chalmers University of Technology for the destruction of the raw gas fed from the gasifier to the boiler (see **Paper VII)**.

In summary, the heat needed for producing a tar-free gas in the CLR can be supplied in part by operating the gasifier at high temperature. However, this means that the energy stored in the char has to be sufficient to fulfill the energy balance across the boiler/gasifier system.

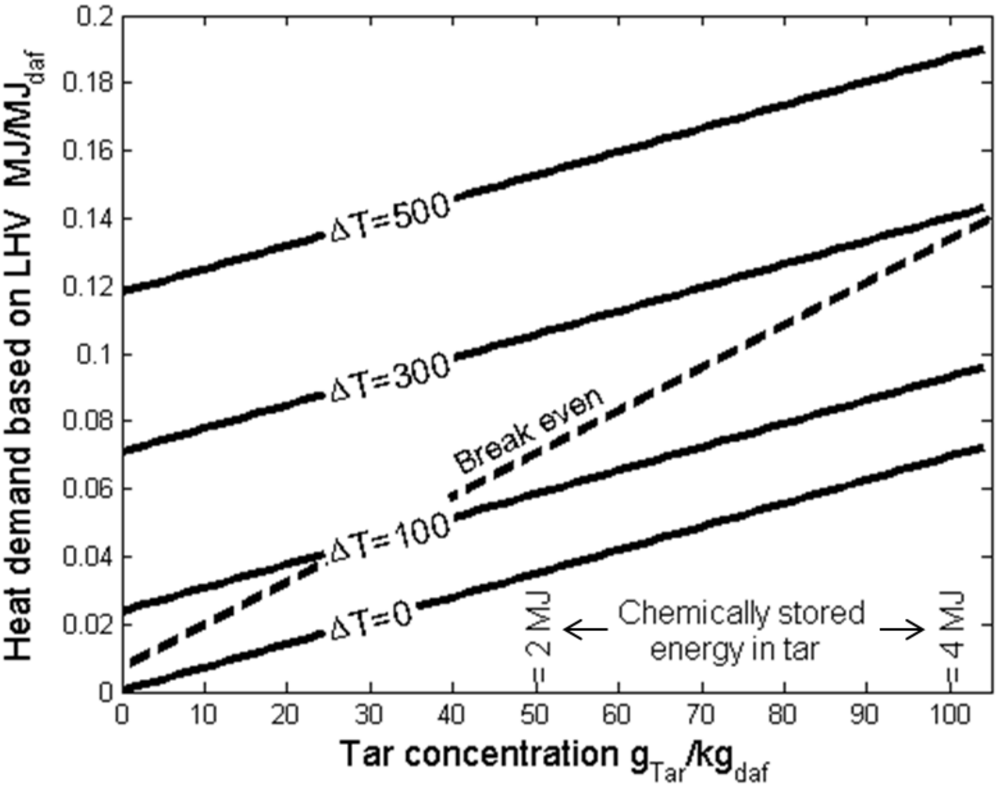

Figure 12. Heat demands for increasing the gas temperature from the gasifier and for reforming the tars in the CLR.

3 - Methodology and Experimental Setup

The present work is based on experiments conducted in three areas: 1) in the CLR system under cold conditions and under hot conditions; 2) moisture measurement experiments, which were conducted in the flue gases from the 8-MW_{th} grate-fired furnace at E.ON in Mölnlycke and in the flue gases from the 12-MW_{th} CFB boiler at Chalmers University of Technology; and 3) experiments with oxygen carriers in the above-mentioned CFB boiler.

The methodology used in this study can be categorized into three integrated blocks (**Fig. 13**). These three blocks cover the investigations made with the CLR system under cold conditions (blue block) and hot conditions (red block). The green block includes the investigations involving the moisture measuring unit and the investigations carried out with the oxygen carriers in the CFB boiler. The experimental setups, research questions, and the overlaps between the three blocks are discussed in the following section.

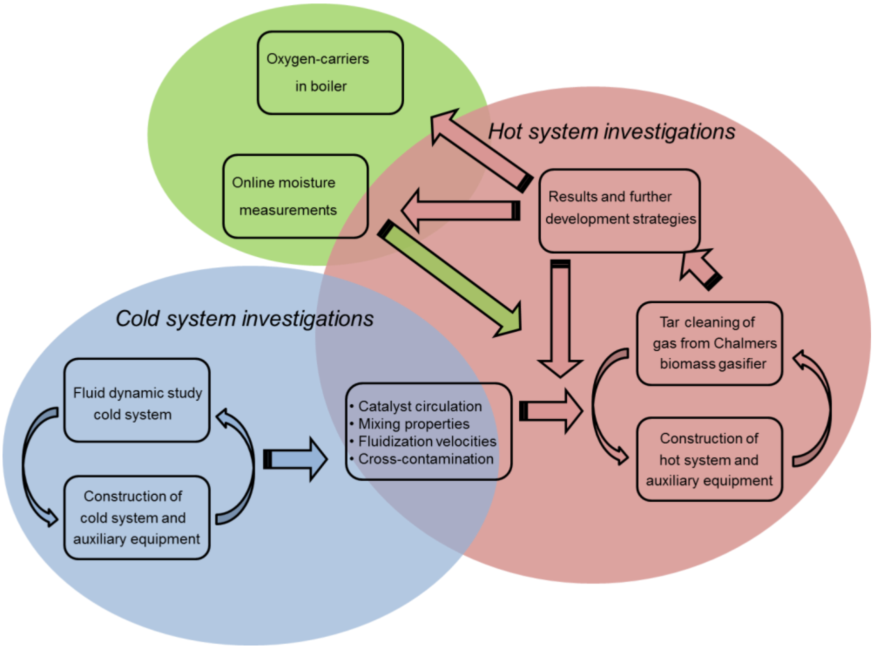

Figure 13 Schematic of the methodologies used in this work.

3.1 **Cold System investigations**

The cold CLR system is composed of a transparent Perspex material and is identical in size to the hot system, which is made of high-temperature-resistant steel. The rationale for conducting tests in a cold system is that it is possible to revise visually and understand the fluid dynamics, which cannot be achieved in the hot system, since visual access is impossible in the present setup. The reason for building cold and hot systems of identical size is that the fluid dynamics in a bench-scale reactor system is most likely influenced by wall effects; for comparative purposes, these effects should theoretically be less prominent. The integration of the cold and hot CLR systems involves the transfer of investigated fluid dynamic parameters from the cold system.

The simplified scaling relationships presented by Glicksman et al.[53] can be used to enable the transfer of fluidization data between hot and cold reactor systems. These authors showed by experiment that sufficient agreement between the data obtained from two systems can be achieved if the number of dimensionless numbers (**9**) is kept constant.

$$\frac{u_0^2}{gL}, \frac{\rho_s}{\rho_f}, \frac{u_0}{u_{mf}}, \frac{L_1}{L_2}, \frac{G_s}{\rho_s u_0}, \Phi, \mathit{Particle\ size\ distribution} \qquad \textbf{(9)}$$

The fluidization medium, particle density, and other parameters for the cold system were determined by comparing the dimensionless numbers for the hot and cold systems. **Table 2** summarizes the operating parameters and these dimensionless numbers for the AR and FR in the hot and cold systems. The gas density for air is 4-times lower in the hot system operated at 800°C than in the cold system operated at 25°C. If air is used as the fluidization medium in the cold system, then the particle density has to be increased by a factor of four to fulfill the density ratio between the solids and fluid. The scale analysis was conducted with pure nickel (5240 kg/m^3) as the reference catalyst in the hot system. In this case, a bed material with a density of 21,000 kg/m^3 would be needed. Therefore, it was decided to use helium (He) as the fluidization medium and to scale the particle density. The combination of silica sand (2600 kg/m^3) and He showed a sufficient match in terms of the dimensionless density ratio for the hot and cold systems, and was therefore chosen.

A schematic of the cold CLR system setup is shown in **Figure 14**. The cold system can be fluidized with air or He. To minimize effects of static electricity between the particles and the Perspex surfaces, the gas is humidified in an air-tight water bottle. Flow control valves are mounted on the outlets of the FR and AR to regulate the pressure in each reactor. In this manner, it is possible to recreate a potential difference in operating pressure between the FR and AR in the hot system. The flows of fluidization gas to the FR, AR, Inferior LS (ILS) and Superior LS (SLS) are controlled by rotameters. The system can be monitored *via* 24 pressure taps with accompanying pressure transducers. The pressure can be measured as the differential pressure between two taps in the system or as the differential pressure between one tap and the atmospheric pressure. A manually controlled valve is mounted in the downcomer for solid circulation rate measurements. The solid circulation is measured by closing the valve in the downcomer with simultaneous chronometer monitoring. Intermediate times are registered when the sand column reaches heights of 1, 2, and 3 cm in the downcomer. The registered heights (h_i') are recalculated in relation to the mass fluxes in the downcomer ($G_{s,Downcomer}$) from the density of the bed material (ρ_{solid}), according to Eq. (**10**):

$$G_{s,Downcomer} = \sum_{i=1}^{n} \frac{h_i'}{n} \cdot \rho_{solid} \quad \left[kg/m^2 s\right] \qquad (10)$$

Table 2 Operating parameters and dimensionless numbers for the hot and cold units.

Parameter	Units	Hot AR	Hot FR	Cold AR	Cold FR
Media	(gas)	Air	Raw gas	Helium/Air	Helium/Air
Temperature	T (K)	1173	1173	293	293
Pressure	P (Pa)	1×10^5	1×10^5	1×10^5	1×10^5
Gas viscosity	μ (Pa s)	4.59×10^{-5}	3.43×10^{-5}	1.96×10^{-5} /1.82×10^{-5}	1.96×10^{-5} /1.82×10^{-5}
Gas density	ρ_f (kg/m^3)	0.297	0.276	0.146/1.188	0.146/1.188
Bed geometry	(m)	L	L	L	L
Particle diameter	d_p (μm)	150	150	150	150
Solids density	ρ_s (kg/m^3)	5240	5240	2600	2600
Superficial velocity	u_o (m/s)	1.00	0.039	1.00	0.039
Sphericity	Φ	0.9	0.9	0.84	0.84
Particle size distribution	p	P	P	P	P
Solid flux	G_s (kg/m^{2}s)	G_s	G_s	$0.5 \times G_s$	$0.5 \times G_s$
Dimensionless number	ρ_s/ρ_f ($\times 10^4$)	1.76	1.89	1.58/0.218	1.58/0.218
Dimensionless number	u_0/u_{mf}	40.82	1.12	40.32/37.45	1.57/1.46

The cold system investigations are conducted to obtain an understanding of the fluid dynamics in the CLR system. The experimental work also contributes with skills and experience as to how to run the system in practice. Parameters that are considered to exert a strong influence on ensuring stable operation of the CLR are investigated in this work. These investigated parameters include:

- The potential to control catalyst circulation during fluidization with helium or air;
- Possibilities to transfer the governing data and robust operating conditions to the hot system;
- Cross-contamination of the effluents from the respective reactors, i.e., gas leakage.

Table 3 Geometric measures of the CLR system.

Reactor part	Cross-sectional (mm)	Height (mm)
Fuel reactor (FR)	50 × 50	380
Air reactor (AR)	20 × 20	460
Superior loop seal (SLS)	23 × 23	120
Inferior loop seal (ILS)	23 × 23	50

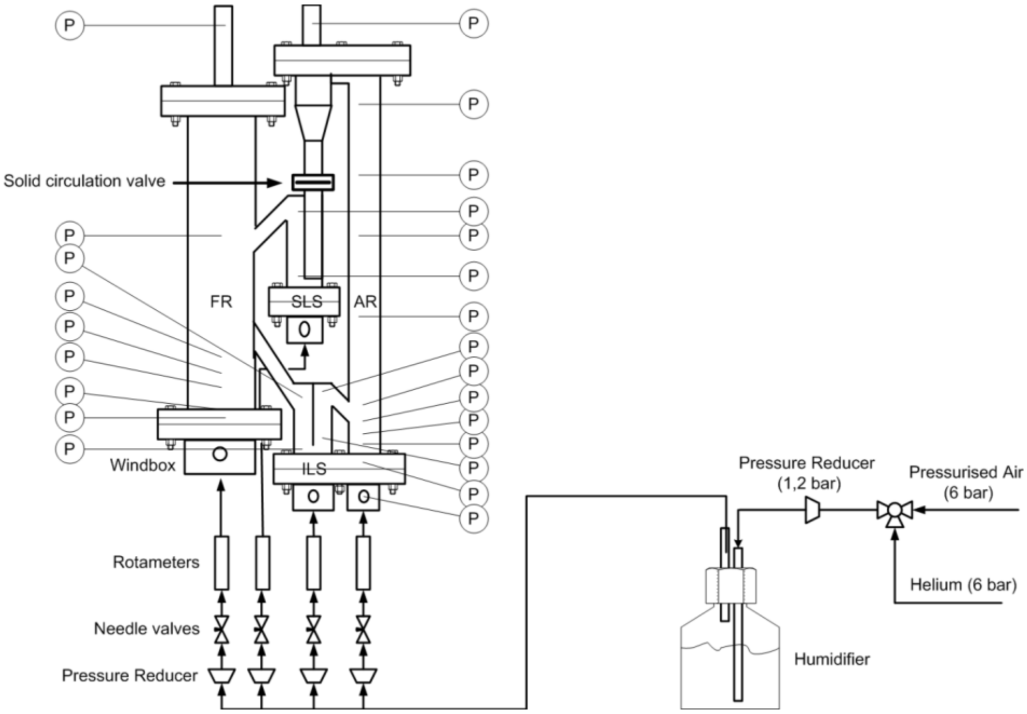

Figure 14 Cold system setup

3.2 Hot System investigations

The hot reactor with an auxiliary system was built in the vicinity of the Chalmers gasifier, and after almost two years of work the CLR system was operational. The CLR reactor within this project was developed for research purposes, and each part of the reactor can be monitored for temperature and pressure (**Fig. 15)**. The geometric dimensions of the reactor system are listed in **Table 3**. During operation of the CLR, samples of the catalyst can be collected *via* the secondary cyclone, which is implemented downstream of the AR (1). The particles from the secondary cyclone are transferred to the FR or to a sampling bottle by stepwise opening and closing of two control valves (2). With regard to temperature, the tar-reforming reactions and regeneration reactions can be optimized separately with a temperature difference of 200°C. This is achieved by separate heating of the two oven halves (3), together with an air-cooled jacket on the FR (4). Two separate mass flow regulators (5), one for air and one for nitrogen, are used for controlling the oxygen concentration in the inlet feed to the AR. The oxygen concentration can be varied from 0 mole% to 21 mole%. Helium is used to fluidize the SLS and ILS, and the flows are controlled by two separate mass flow regulators (6). Beyond the AR, the gas is cooled and dried in a gas-conditioning system (7). The contents of CO, CO_2, and O_2 in the gas that exits the AR are analyzed online by Non-Dispersive Infrared (NDIR) analyzers for CO and CO_2 and by a paramagnetic analyzer for O_2 (8). It is also possible to analyze the AR effluents in a micro-gas chromatograph (micro-GC; Varian 4900). The GC is used to determine the amount of He in the AR, which originates from the feed to the two LS (9).

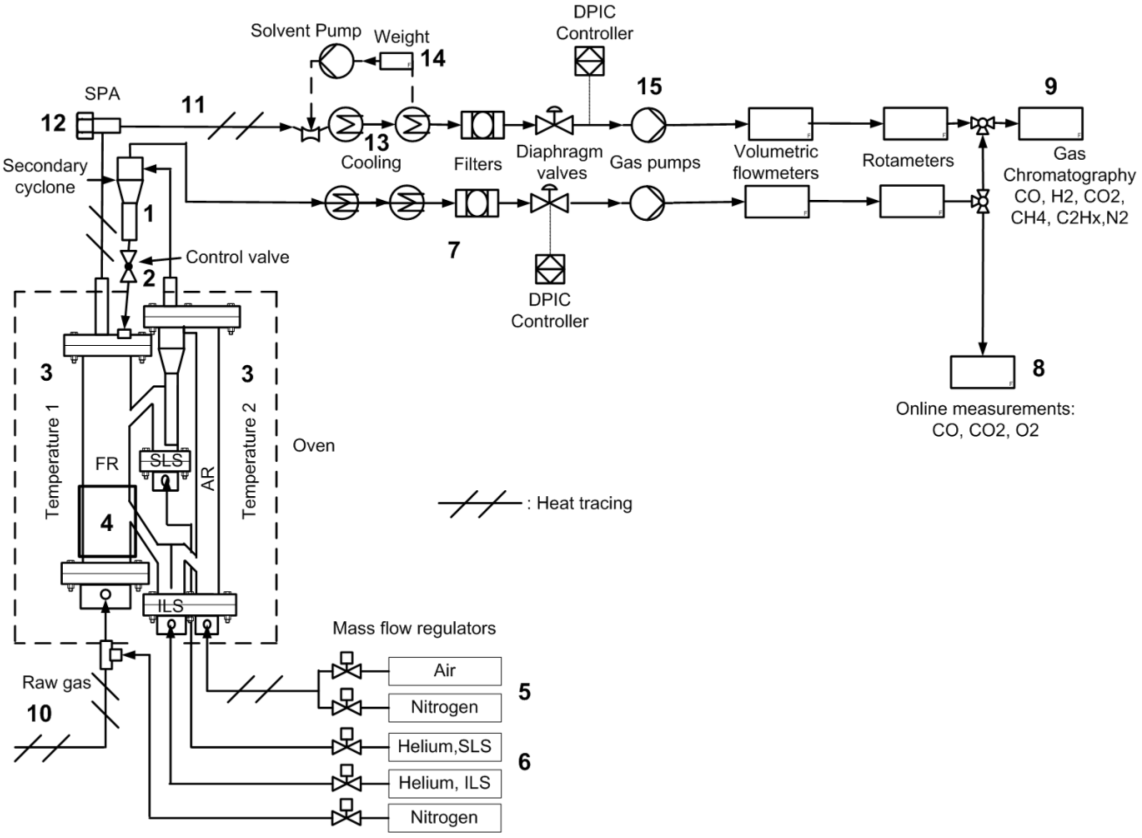

Figure 15. Schematic of the hot CLR setup.

The raw gas pipe between the FR and the gasifier (10), as well as the pipe connection between the FR and the gas-conditioning system (11), is heated to 400°C to preclude tar condensation. The concentration of tars in the reformed gas is measured by Solid Phase Adsorption (SPA) [54] located in the heated pipe between the FR and the gas conditioning system (12). The collected samples are then eluted and analyzed by Gas Chromatography followed by a Flame Ionization Detector (GC-FID). Detailed descriptions of the SPA sampling procedure and GC-FID analysis are provided in **Paper V**. The reformed gas leaving the FR is quenched by isopropanol in the heat exchanger (13), and the moisture content of the reformed gas is measured by weighing the condensate (14). The dry and cleaned reformed gas is further analyzed in a micro-GC (9). The tar concentration and the dry gas composition of the raw gas are measured by SPA followed by GC-FID and micro-GC, respectively, either in a separate system for monitoring the gasifier (**Papers II and III)** or just before the inlet to the FR (**Papers IV and V)**. A detailed description of the hot CLR system with accompanying analytic equipment can be found in **Paper II**.

Carbon transport from the FR to AR

Regeneration of coke deposits on the catalysts was evaluated by measuring the CO_2 and CO concentrations from the outlet of the AR. In all the experimental cases, for the start-up sequence and during nitrogen fluidization of the FR, the CO_2 and CO concentrations were below the detection limits of the instrument. The level of carbon deposits regenerated from the catalysts, $Y_{c,AR}$, was calculated as the ratio of the total integrated molar flows of carbon leaving the AR over the duration of the experiment to the total moles of carbon fed to the FR under stable operation in the CLR, according to Eq. (**11**):

$$Y_{C,AR} = \frac{\int_{t_{start}}^{t_{stop}} \left(\dot{n}_{AR,out} \left(CO_{2,ARout} + CO_{ARout} \right) \right) dt}{\int_{t_{start}}^{t_{stop}} \left(\dot{n}_{FR,in} \sum_i \xi_{C,i} C_{i,FRin} \right) dt} \qquad \textbf{(11)}$$

where $CO_{2,ARout}$ and $CO_{,ARout}$ are the concentrations of carbon contributed by CO_2 and CO, respectively, at the outlet of the AR, $C_{i,FRin}$ refers to all the measured carbonaceous species in the raw gas, and $\xi_{C,i}$ is the number of carbon atoms in carbonaceous species i in the raw gas.

Mole balance

When evaluating the performances of tar removal catalysts it is important to distinguish between gas upgrading and total tar decomposing efficiency. The difference lies in how the tar concentration in the reformed gas is valued. In the case of gas upgrading, the tar concentration in the reformed gas is simply measured, and the tar removal efficiency is calculated by comparing the tar concentrations entering and leaving the catalytic device. However, in the case of total tar decomposing efficiency, even the amount of produced gas, from, for example, hydrocarbon reformation and the Water-Gas shift (WGS), must be included in the calculation. This means that the surplus of permanent gases produced in the reactor is removed from the reformed gas, yielding the actual amount of removed tars. In this manner, a molar balance across the system that includes all the species needs to be defined.

A system-wide molar balance for the CLR system was derived (**Paper V**). This balance is used to clarify the manners in which the oxygen transfer and the gas yield from hydrocarbon reformation affect the efficiency of tar removal. Equations (**12a**) and (**12b**) provide the total mole flows of gases entering and leaving the FR. The concentrations of permanent gas species were measured in the raw gas ($Y_{i,in}$) and in the reformed gas

($Y_{i,out}$) using the micro-GC. The letter (r) in the summation symbol refers to the number of measured permanent gas components in the raw and reformed gases. The amounts of tar in the raw gas ($n_{Tar,in}$) and the reformed gas ($n_{Tar,Out}$), respectively, were estimated using SPA followed by GC-FID. A part of the He used as the fluidizing medium in the loop seals ends up in the reformed gas, and another part appears in the effluent from the AR. The total amount of He transported to the FR from ILS n_{ILS} and SLS n_{SLS} is obtained from the micro-GC measurements, together with the total flow of dry reformed gas. Here, γ_{FR} denotes the fraction of He transported to the FR. The oxygen transported from the AR to the FR is calculated *via* a molar balance across the AR. The mole flows of nitrogen ($n_{N2AR,in}$) and oxygen ($n_{O2AR,in}$) into the AR (**12c**) are set by the mass flow controllers. The amount of He entering the AR is calculated by subtracting the moles of He fed to the FR from the total moles of He fed to the system *via* the mass flow controllers. The amount of carbon transported from the FR to the AR ($Y_{CFR,Out}$) is calculated from Eq. (**11**) using the measured concentrations of CO_2 ($n_{CO2,ARout}$) and CO ($n_{CO,ARout}$) in the effluent gas of the AR. The transported oxygen ($n_{O2FR,in}$) is finally given by Eq. (**12e**), where the amount of oxygen used for converting the carbon deposits into CO_2 ($n_{CO2,ARout}$) and CO ($n_{CO,ARout}$), together with the potential oxygen leaving the AR ($n_{O2AR,out}$), are subtracted from the total amount of oxygen fed to the AR.

Mole flows in and out of the FR:

$$n_{FR,in} = n_{Rawgas} \cdot \sum_{1}^{r} Y_{i,in} + n_{Tar,in} + \gamma_{FR}\left(n_{ILS} + n_{SLS}\right) + n_{O_2\,FR,in} \qquad \textbf{(12a)}$$

$$n_{FR,out} = n_{FR,gas} \cdot \sum_{1}^{r} Y_{i,out} + n_{Tar,out} + \gamma_{FR}\left(n_{ILS} + n_{SLS}\right) + n_{CFR,out} \qquad \textbf{(12b)}$$

Mole flows in and out of the AR:

$$n_{AR,in} = n_{N_2,ARin} + \cdot n_{O_2,ARin} + n_{CFR,out} + \left(n_{ILS} + n_{SLS}\right) \cdot \left(1 - \gamma_{FR}\right) \qquad \textbf{(12c)}$$

$$n_{ARout} = n_{N_2,ARout} + n_{O_2,ARout} + n_{CO_2,ARout} + n_{CO,ARout} + \left(n_{ILS} + n_{SLS}\right) \cdot \left(1 - \gamma_{FR}\right) \qquad \textbf{(12d)}$$

$$n_{O_2\,FR,in} = n_{O_2,AR,in} - n_{CO_2,out} - 0.5 \cdot n_{CO,out} - n_{O_2,AR,out} \qquad \textbf{(12e)}$$

Equation (**13**) provides a measure of the chemically stored energy (Q) in the raw gas and the reformed gas, and is calculated by multiplying the moles of combustible gases (Y_i) with its respective lower heating value (LHV_i), according to Eq. (**13**). The letter (k) in the summation symbol is the number of combustible permanent gas components in the raw and reformed gases. This measure aims to bringing evidence on how the chemically stored energy changes within the gas as it is processed in the CLR system. Thus, no heat integrations are conducted and the sensible heat is not considered in this work.

$$Q = \sum_{1}^{k} Y_i \cdot LHV_i \qquad \textbf{(13)}$$

In the present work, the Residence Time (RT) or the gas/solid contact time in the bed is estimated in the same manner as for a fixed bed. Thus, the gained RT is the maximal gas/solid contact time that can be achieved in the CLR. This is because gas flows greater than the minimum fluidization velocity (u_{mf}) will flow through the low-resistance gas passages located in and between the bubbles, thereby allowing less time for contact between the gas and catalysts. As the FR is a bubbling fluidized bed with velocities several-fold higher than u_{mf}, the effective gas-to-solid contact will always be overestimated. This is so because the overall contact time for the gas flow will vary from almost nothing to that of packed bed. The RT is calculated according to Eq. (**14**), in which the volume of the bed V_{bed} is multiplied by the bed voidage ε_{bed}, thereby generating the total voidage in the emulsion phase, which is then divided by the average flow of the raw gas $V'_{Raw\ gas}$ plus the flow of the reformed gas ($V'_{Reformed\ gas}$), yielding the RT value (in seconds).

$$RT = \frac{V_{bed} \cdot \varepsilon_{bed} \cdot 2}{V'_{Raw\ gas} + V'_{\mathrm{Re}formed\ gas}} \qquad \textbf{(14)}$$

The proposed tar-cleaning method was investigated using ilmenite as the catalyst and raw gas (containing roughly 30 g_{tar}/m^3_{gas}) from the Chalmers biomass gasifier (**Papers II and V**). Further investigations were performed using a manganese catalyst (**Paper III**) and a nickel catalyst (**Papers IV and V**). Detailed experimental descriptions for each catalyst case are presented in the above-mentioned papers. The fundamental criteria used to assess the performance of the tar-cleaning method were as follows:

- The possibilities of obtaining continuous transport of catalysts and oxygen from the regenerator to the reformer;
- The possibilities of reforming tars in the reactor system using a natural ore, such as ilmenite, or manufactured catalysts such as M4MgZ1150 and NiO/Al_2O_3;
- Investigating how changes in oxygen concentration and temperature affect tar reformation and the gas composition in the FR;
- Investigating the possibility of maintaining high activity of the catalyst by continuous oxidation of the formed carbon in the regenerator reactor.

3.3 Development of online moisture measurement system

The online moisture measurement unit was originally developed for measuring the moisture contents of flue gases from a boiler. The underlying principle of the technique is that the relative humidity (RH) of the gas is determined from the sensitivity of the electrical conductivity of a polymer towards the moisture content of the surrounding gas. The volumetric moisture fraction ($X_{vol,m}$) in the gases is then determined from the relative humidity (φ) of the gas and the saturation pressure (P_{sat}) surrounding the sensor in relation to the atmospheric pressure (P), according to Eq. (**15**). The P_{sat} value is determined through integration of the Clausius-Clapeyron equation, with the assumption that the evaporation enthalpy is independent of temperature (**16**).

$$X_{vol,m} = \varphi \frac{P_{sat}}{P} \qquad \textbf{(15)}$$

$$P_{sat} = \exp(23.82 - 4193/(T - 32)) \qquad \textbf{(16)}$$

In addition to its application to measurements in boilers, this technique could potentially be used for the reformed gas after the CLR reactor, to improve the operation of the system and the evaluation of the experiments. In the CLR setup, the raw gas flow in the FR is controlled by a gas pump (15) (**Fig. 15)**, operating on the dry reformed gas. This means that the consumption of water from volume-increasing reactions in the FR, e.g., tar reforming and the WGS reaction, has to be considered. To obtain a constant gas flow between two experiments, an iterative procedure must be used. Furthermore, the activity of a catalyst can change during operation. For example, ilmenite increases in activity with cycles of oxidation and reduction. This means that monitoring moisture content in the reformed gas by weighing the condensate as a function of gas flow becomes too slow and inadequate for the application. In this respect, the technique presented here can, owing to its fast response time, also register dynamic fluctuations in the catalytic system.

A prototype that utilizes the method for RH was built and investigated in a transversal study for measuring moisture content in the flue gases from biomass-fired boilers. A schematic of the prototype is shown in **Figure 16**. The flue gas is extracted from the flue gas duct (1), separated from particles through a hot filter (2), and cooled to the target temperature in a tube that passes through a temperature-controlled oil bath (3). The RH, the temperature, and the pressure are measured in a cell (4). A manometer is used to measure the pressure, and a PT100 resistance detector is used for temperature detection, while the RH is determined by a sensor (supplied by the company Vaisala).

The dynamic behavior of the method was investigated in the 8-MW$_{th}$ grate-fired furnace in Mölnlycke during the burning of saw dust, and in the Chalmers 12-MW$_{th}$ research CFB boiler during the burning of wood chips; detailed descriptions of the experiments and experimental setup are presented in **Paper VII**. The main criteria investigated to assess the performance of the unit were:

- Measurements of RH and temperature in the extracted flue gas;
- Fourier Transform Infrared Spectroscopy FT-IR measurement of moisture content in (the same) extracted flue-gas for comparison;
- Water injection into the fuel feed (inducing step function).

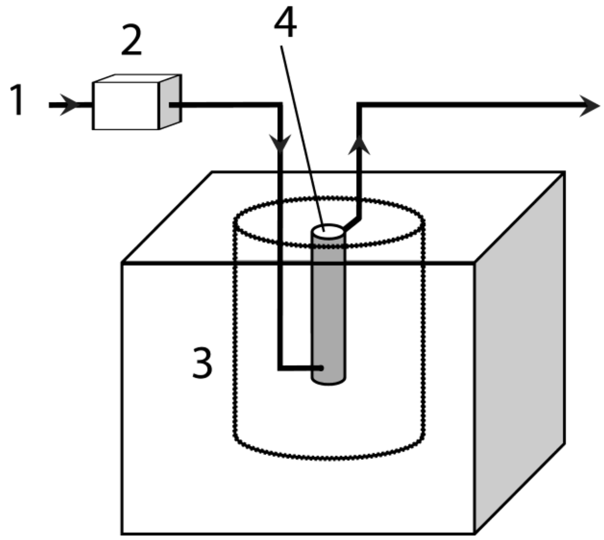

1. Extraction of flue gases from the duct
2. Filter
3. Temperature-controlled oil bath
4. Measurement cell

Figure 16. Device for measurement of moisture content of flue gases.

3.4 Investigation of oxygen carriers in the CFB boiler at Chalmers

During CLR operation with ilmenite, it was noted that the carbon deposits on the catalyst were oxidized to CO_2 in the AR, and no CO was detected. This occurred even though the concentration of oxygen in the inlet feed to the AR was very low. This promoted the idea that oxygen-carrying materials could be used to improve the combustion in a conventional CFB furnace. The addition of ilmenite to the solids inventory could potentially improve the distribution of oxygen throughout the furnace, owing to the ability of ilmenite to alternately take up and release oxygen. In this manner, less air is expected to be needed to maintain low emissions of CO and unreacted hydrocarbons during the combustion of highly volatile fuels, such as biomass. This idea was experimentally investigated in the present work, whereby up to 40 wt.% of the usually applied silica-sand was replaced by ilmenite.

Experiments were performed in the 12-MW_{th} CFB boiler/gasifier reactor system at Chalmers University of Technology, as presented in **Figure 2**. A detailed sketch of the boiler/gasifier is presented in **Figure 17**, in which the furnace (1) has a square cross-section of 2.25 m^2 and a height of 13.6 m, and the fuel is fed on top of the bed *via* the fuel chute (2). About 25% of the total fuel load to the system can be fed into the indirect gasifier (11) instead of the boiler. Around 70% of the fuel fed to the gasifier (14, 15) is converted to a raw gas, while the remaining char follows the bed material back to the boiler where it is combusted together with the fuel fed to the boiler. The produced raw gas is then directed to the center of the furnace freeboard, just below position H9 in **Figure 2**, where it is injected and combusted.

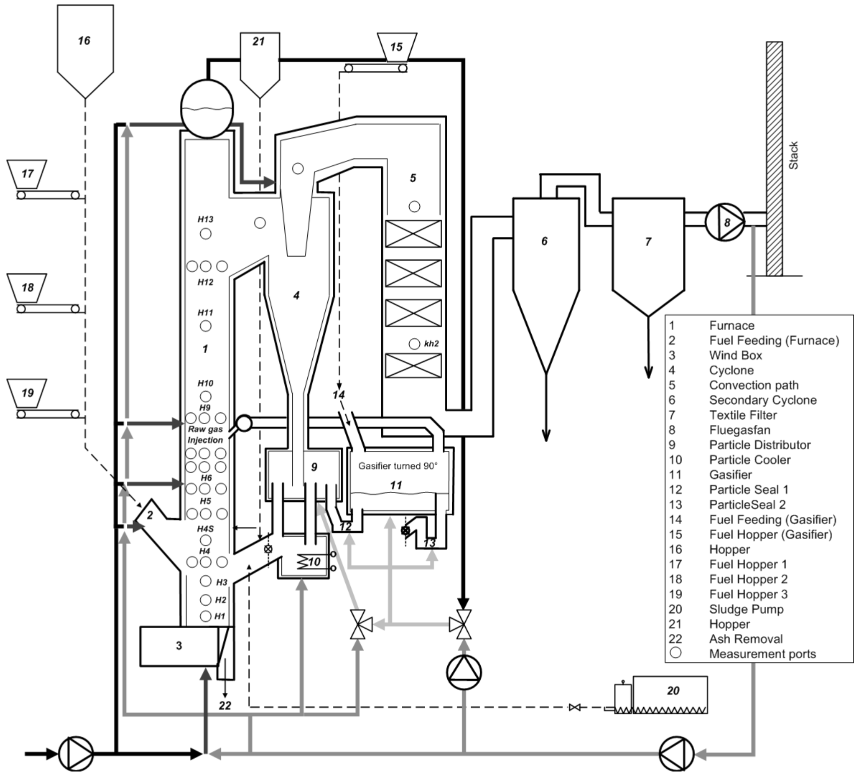

Figure 17. Chalmers boiler/gasifier reactor system.

The combustion process can be followed in detail by monitoring the temperature and pressure throughout the furnace body. Gases can be extracted by inserting a gas sampling probe through dedicated ports located throughout the furnace (referred to as H1–H13 in **Fig. 2**), upstream and downstream of the cyclone, in the convection path, and downstream of the flue gas fan. The concentrations of CO, O_2, NO, and total HC (THC) are measured by online gas analyzers; detailed descriptions of the probe and gas analyzers can be found in **Paper VII**.

The combustion experiments were conducted in two distinct phases. One phase included operation in the boiler only while the other involved both the boiler and the gasifier. In the gasifier experiments, the concentrated stream of combustible gases from the gasifier, containing around 1.4 MW of devolatilizing gases and steam, was forced to the furnace freeboard, and the corresponding performance was investigated. In this test, the concentrations of CO and THC were measured across the furnace horizontal cross-section at three different heights (**Fig. 2**): H7, which is located at a height of 7 m; H9, which is located right above the raw gas injection pipe; and H12 which is in the cyclone inlet. Nine gas measurements were conducted at each of H7, H9, and H12 according to the subdivision of the cross-section in the freeboard shown in **Figure 17**. These measurements were performed by stepwise horizontal insertion of the probe. In **Figure 18:** “Front” illustrates the wall of the furnace where the fuel is fed; “Back” corresponds to the wall opposite to the front; and “Center” indicates the in-between position. Furthermore, by operating the boiler/gasifier system initially with silica-sand and subsequently with increasing fractions of ilmenite in the sand, it was possible to assess whether the oxygen-carrier material improved mixing of the oxidizer and the fuel throughout the furnace geometry. Detailed descriptions of the results of these experiments are presented in **Paper VII**.

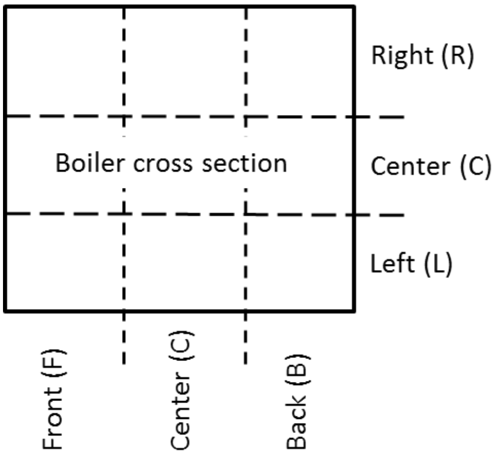

Figure 18. Measurement positions in the furnace cross-section (viewed from above) for gas extraction *via* the gas sampling probe.

The main criteria investigated to assess the performance of the ilmenite in the boiler were as follows:

- The possibility to maintain low emissions of unburned species in the exhaust from the boiler, even when operated close to stoichiometric combustion or with a low excess of oxygen;
- The possibility to even out the concentration profile of unburned species along the combustion furnace;
- The possibility to direct the combustion reactions to the furnace instead of to the cyclone.

4 - Results and Discussion

This section has for reasons of clarity been divided into four parts. The first and second parts, which comprise the main body of this work, deal with the CLR system operated under cold conditions (**Paper I)** and under hot conditions (**Papers II–V**). The third part deals with the development of the online moisture measuring unit (**Paper VI**), and the fourth part considers the operation of a biomass-fired CFB boiler with oxygen carriers as part of the bed material (**Paper VII**).

4.1 Cold system investigations

A fluid dynamics investigation of the cold CLR system was carried out to define the operating conditions that could be applied to the hot CLR system. One of the investigated parameters was the control of solid circulation rate, which is a fundamental requirement for the proposed tar-cleaning method to maintain carbon deposit-free surfaces of the catalysts. In **Figure 19**, solid circulation flux is plotted against the superficial velocity in the riser. The figure shows that regardless of the fluidization gas used, efficient control of solids circulation between the two reactors can be achieved by modulating the fluidization velocity in the riser. The two distinct plateaus seen in the experiments conducted with air as the fluidization medium indicate that it is possible to control the solid inventory in the FR using the ILS as a flow valve for solids. The throttling effect can be explained by wall friction, which is induced by the low volume in the ILS, and is in accordance with previous observations[55].

The cross-contamination of effluents from the respective reactors was investigated in the cold CLR. The oxygen concentrations in the effluents from the FR were measured, as the FR SLS and ILS were fluidized with nitrogen and the AR was fluidized with air. The oxygen concentration in the AR and the pressure difference between the AR and FR were plotted against the superficial velocity in the riser (**Fig. 20)**. The figure shows that the oxygen concentration in the FR is less than 0.4 mole% at the highest fluidization velocity in the riser, which indicates that the performance of the loop seals is adequate. Nevertheless, a trend is noted, with the oxygen concentration in the FR increasing with increased superficial velocity in the AR. The reason for the higher oxygen concentration is associated with the increase in pressure difference between the AR and FR, which is caused by the raised gas flow in the riser.

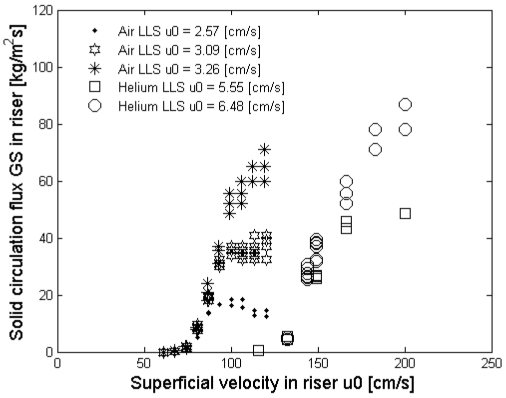

Figure 19. Solid circulation fluxes versus superficial gas velocity in the riser.

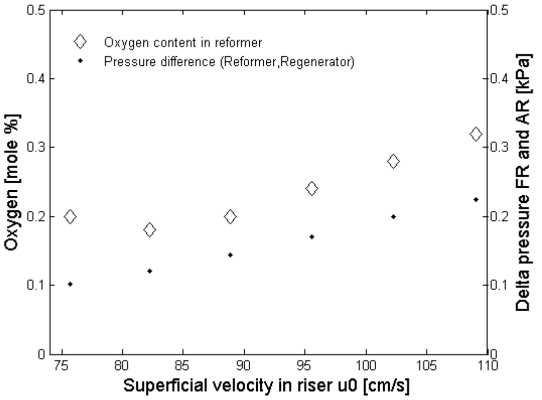

Figure 20. Oxygen leakage levels and pressure differences between the AR and FR versus the superficial velocity in the riser.

If the data from the cold system experiments are to be transferred to the hot system, it is important to have good agreement between the dimensionless numbers for the scaling relationship. The comparison of the dimensionless numbers between the hot and the cold system (**Table 2)** shows that the solid/gas density ratio is well adjusted for operation with He, with deviations of 11% in the AR and 20% in the FR. In contrast, the same dimensionless numbers for air operation differ by a factor of eight in the AR and a factor of nine in the FR. The ratio of the superficial velocity to the minimum fluidization velocity deviates by 1% for the AR and by 40% for the FR between the hot unit and the cold unit fluidized with He. In contrast, the ratio between the superficial velocity and minimum fluidization velocity deviates by 9% for the AR and by 30% for the FR between the hot unit and the cold unit fluidized with air. The deviation in the ratio between superficial velocity and minimum fluidization velocity for the FR is of less importance in the CLR than in the AR. The reason to this is that the solid flux, which is controlled by the fluidization properties in the riser, is more crucial for the operation.

4.2 Hot system investigations

The CLR system has been operated for more than 100 hours with different catalysts and at different temperatures in the range of 700°–880°C with raw gas from the Chalmers gasifier. However, the first two experiments were conducted as reference cases, in which only silica-sand was used as the bed material, so as to guarantee that no catalytic effects were induced by the reactor material itself (**Paper II**). The dry gas composition from one of the reference experiments, performed at an operational temperature of 800°C, is shown in **Figure 21**. The middle bar represents the gas composition downstream of the CLR, while the other bars represent the raw gas compositions from the gasifier before and after operation of the CLR. As shown in **Figure 21**, the CLR reactor operated with silica-sand has a negligible effect on gas composition.

Furthermore, the SPA analysis of this case confirmed that neither the tar content nor tar composition was affected by the CLR system. This suggests that no catalytic effects are produced by either the reactor material or the silica-sand.

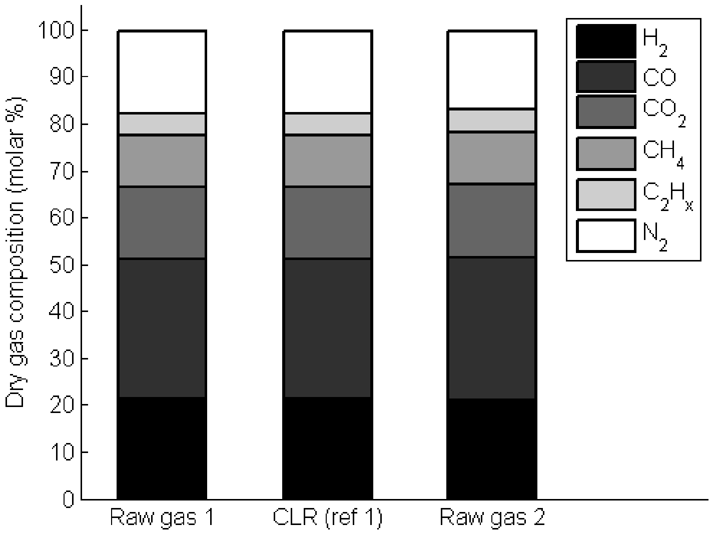

Figure 21. Dry gas compositions in the CLR reference experiments with silica-sand as bed material.

Table 4 Tar compositions of raw gas (Reference case) and reformed gas leaving the CLR for 60 wt.% ilmenite catalyst in the silica-sand and for 23 wt.% manganese catalyst in the silica-sand

Catalyst	Ilmenite		Manganese	
Measurement position	Reference	Reformed	Reference	Reformed
O_2 (mole%) in AR	-----	1.0	-----	2,2
Phenol	0.98	0.01	2.18	0.07
o-Cresol	0.03	0.00	0.26	0.00
m-Cresol	0.15	0.00	0.48	0.00
p-Cresol	0.04	0.00	0.15	0.00
Benzene	0.65	1.90	0.51	1.18
Toluene	0.71	0.17	0.66	0.60
m/p-Xylene	0.14	0.00	0.19	0.07
o-Xylene	1.06	0.16	1.10	0.85
Indan	0.05	0.17	0.06	0.16
Indene	2.94	0.05	3.76	0.61
Naphthalene	7.53	10.77	7.54	8.41
2-Methylnaphthalene	1.10	0.06	1.32	0.37
1-Methylnaphthalene	0.70	0.03	0.83	0.17
Biphenyl	0.47	0.84	0.54	0.65
Acenaphthylene	2.03	0.37	2.40	1.24
Acenaphthene	0.13	0.01	0.18	0.04
Fluorene	0.65	0.09	0.86	0.09
Phenanthrene	1.66	1.45	1.77	1.50
Anthracene	0.29	0.18	0.53	0.33
Fluoranthene	0.41	0.45	0.53	0.36
Pyrene	0.46	0.42	0.60	0.36
Unknowns	5.54	0.92	6.43	1.21
Total tar	27.70	18.04	32.89	18.27
Tar conversion	-----	35.0	-----	44.5

Tar reduction

During the first season of operation, the CLR gas-upgrading method was demonstrated using 60 wt.% ilmenite ($FeTiO_3$) in the silica-sand (**Paper II**). Subsequently, a mixture of silica-sand and 23 wt.% manganese catalyst (Mn_3O_4 supported on $MgZrO_3$) was used (**Paper III**). The tar-cleaning concept and the tar-reforming activities of the ilmenite and manganese catalysts were evaluated by comparing the tar contents of the gases entering and exiting the FR. Around 200 different tar components are typically detected in the raw gas by the GC-FID detector. Of these tar species, 21 have been chosen to reflect the distribution of tars, and the molecular masses of these range from that of benzene to that of pyrene. The remaining components were measured, but not specified as to species, and are referred to as 'unknowns'. **Table 4** summarizes the SPA results for the 21 analyzed tar components and the unknown species in the raw gas, as well as in the reformed gas leaving the CLR. In this case, the tar data were selected from the runs with the highest levels of tar reduction. The table is organized with respect to: the two investigated catalysts (ilmenite or manganese); the position of the tar measurement (reference gas or reformed gas); and the oxygen concentration in the air reactor (mole% O_2 in the AR). The greatest tar reduction (44.5%) was achieved with 23 wt.% manganese catalyst in silica-sand for CLR operation at 800°C. The case with 60 wt.% ilmenite in the silica-sand showed tar reduction of 35% at 800°C.

During the second season of CLR operation, three additional sets of experiments were conducted. The first set of experiments included operation with 100 wt.% manganese catalyst. The results of these experiments were too difficult to interpret and are therefore not considered here. However, two other sets of experiments were conducted: 1 using 100 wt.% ilmenite as the catalyst (**Paper V**); and 2) using 100 wt.% NiO/Al_2O_3 as the catalyst (**Papers IV and V**). The tar removal efficiencies for the gas-upgrading case, in which no compensation was made for the produced permanent gases, at different operating temperatures for the FR and at 1% and 2.2% O_2 are shown in **Figure 22a**. It is clear from **Figure 22a** that the Ni/Al_2O_3 catalyst has the strongest activities for tar removal at all the temperatures tested, and that increasing the temperature strongly influences the activity of the catalyst in terms of tar removal. At 700°C, the total tar conversion rate was 50%, and as much as 95% of the total tar content was removed at 880°C. In the cases that involved the ilmenite catalyst, around 25% of the tar was removed at 750°C and 60% of the tar was removed at 850°C. It is noteworthy that the reactivity of the ilmenite catalyst increased rapidly as the temperature was increased from 800°C to 850°C. Indeed, for an equivalent RT, tar removal was enhanced 4-fold, as compared with the level of tar removal when the temperature was increased from 750°C to 800°C. This may be explained by the nature of ilmenite activation. Ilmenite activity increases as the iron migrates to the surface of the particle, thereby creating active sites. Iron migration in the ilmenite is enhanced by repeated redox cycles and temperatures >800°C[46]. Overall, the level of oxygen transport from the AR to the FR appears to exert little influence on the rate of tar conversion by either catalyst, as shown in **Figure 22a**.

Figure 22b shows the actual amounts of decomposed tars on a mass basis, with compensation for the produced permanent gases acting as dilution media in the reformed gas. In this manner, total tar removal was decreased for both catalysts at all temperatures, as compared with the results shown in **Figure** 22a. In the case of the Ni/Al_2O_3 catalyst, tar decomposition drops from 95% to 86% at 880°C, as compared with the level of tar removal when the efficiency is calculated on the basis of normal cubic meter of dry gas (**Fig. 22a**). The same pattern is seen for the ilmenite catalyst, whereby tar decomposition decreases from 60% to around 42% at 850°C. The calculation of tar decomposition reveals that the amount of permanent gases produced in a reactor system can have a strong influence on the way in which the tar conversion efficiency is determined. Relying solely on gas concentration measurements, as in the gas-upgrading case, may be insufficient if the actual efficiency of tar decomposition is considered.

The results shown in **Figure 22b** suggest that tar conversion increases with increasing oxygen transport. However, this is most likely due to combustion reactions in the oxygen-rich zone above the bed. Some of the tar components remain more or less unreacted as they slip through the low-resistance gas passages in the bed. When these tars enter the oxygen-rich zone, more tars are combusted or partially combusted. This also explains the observed lack of change in the tar conversion rate for NiO/Al_2O_3 at 880°C for both oxygen concentrations; as most of the tars in the bed are already decomposed, the increased oxygen transfer has little impact on the rate of tar conversion.

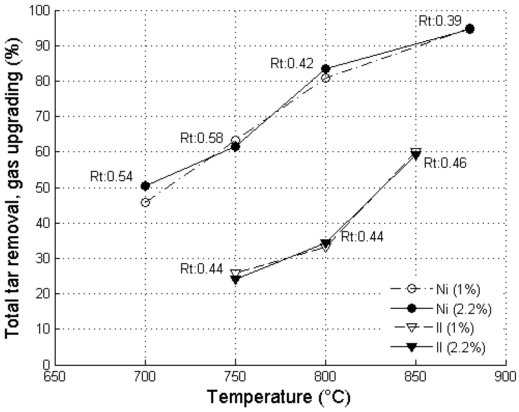

Figure 22a. Percentages of total tar removal in the gas-upgrading case using a NiO/Al_2O_3 catalyst (Ni) and ilmenite as catalyst (ilm) at 1.0% and 2.2% O_2 at different temperatures.

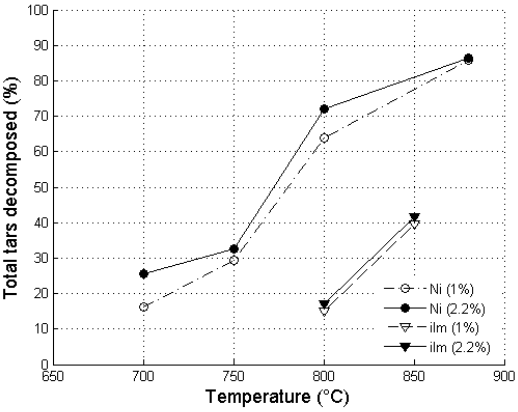

Figure 22b. Percentages of total tars decomposed by the NiO/Al_2O_3 catalyst and the ilmenite catalyst at 1.0% and 2.2% O_2 at different temperatures.

The analysis of the SPA samples gives in addition to the total amount of tars, information on the different tar molecules. This information reveals how the tar structures and tar distribution changes between the raw gas and the reformed gas after the CLR reactor. **Figure 23**, **a** and **b** shows the tar constitutions of the raw gas and the reformed gas at 1% O_2 in the AR and at 880°C for the case with 100 wt.% NiO/Al_2O_3 catalyst and at 850°C for the case with 100 wt.% ilmenite catalyst. Here, the tar components have been divided into six groups: phenols; benzene; 1-ring aromatic compounds with branches (1-ring branched); naphthalene; 2-ring aromatic compounds with branches (2-ring branched); and all aromatic compound with three or more rings (3-rings and larger). The right-most bars in **Figure 23, a** and **b** represent the total amounts of tars in the gases. The rationale for grouping the tar components in this way is to study the patterns of tar decomposition. Comparing the data in **Figure 23**, **a** and **b**, it is evident that both catalysts remove the phenolic compounds and a large proportion of the 1-ring branched tars. In the case of the NiO/Al_2O_3 catalyst, only benzene and a small amount of naphthalene remain in the reformed gas, whereas in the case of the ilmenite catalyst, although the actual levels are reduced, a spectrum of tars, ranging from benzene to aromatic compounds with ≥3 rings, remains. Moreover, the benzene fraction of the reformed gas is greater than that of the raw gas for both catalysts. This implies that more benzene is formed in the reactor than can be decomposed by the catalyst. One reason for this is that the benzene molecule itself is the most difficult form to dissociate owing to its resonance stabilization, thereby contributing to the observed phenomenon. In addition, since the benzene molecule is highly volatile, it is difficult to measure accurately, with the consequence that it is often not included in the definition of tars[27]. If benzene is not included as part of the tar spectrum, the total tar conversion rates for gas upgrading are: 99% for the NiO/Al_2O_3 catalyst; and 68% for the ilmenite catalyst. Similar figures showing the tar groupings for the 23 wt.% manganese case and the 60 wt.% ilmenite can be found in **Papers II and III**.

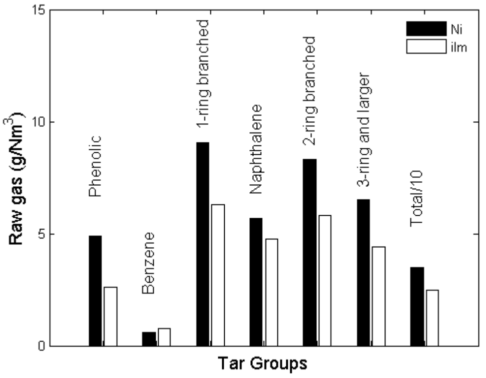

Figure 23a. Tar constituents of the raw gas before exposure to the NiO/Al_2O_3 catalyst (Ni) and the ilmenite catalyst (ilm).

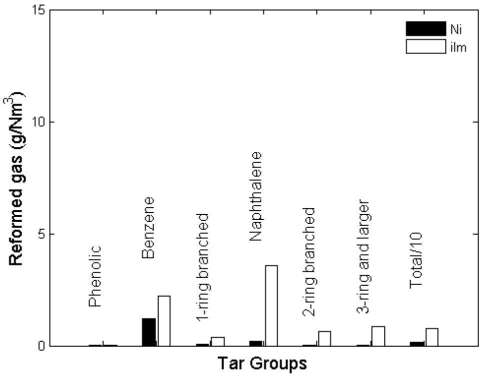

Figure 23b. Tar groupings in the reformed gas out of the CLR operated with the NiO/Al_2O_3 catalyst (Ni) at 880°C or with the ilmenite catalyst (ilm) at 850°C in the presence of 1% O_2.

The total tar conversion achieved with the NiO/Al_2O_3 catalyst at 880°C is in line with that reported in studies on syngas tar cleaning with Ni-based, steam-reforming catalysts performed by Corella et al.[36] and Aznar et al[48]. It should be emphasized that the raw gas in the present work was produced in a non-catalytic, industrial-sized gasifier. This yielded tar concentrations of up to 30-fold higher than those in the work performed by the aforementioned authors. However, a higher tar conversion rate with the NiO/Al_2O_3 catalyst would have been expected at 700°C, as Rownaghi and Huhnke[48] showed 95% conversion of toluene at a content of 30 g/nm^3 and at a similar temperature. However, the NiO/Al_2O_3 catalyst used in the present study was originally prepared to serve other purposes, i.e., as an oxygen carrier for CLC, where the aim is to transport as much oxygen as possible to achieve complete combustion of the fuel. The tar conversion rate for the ilmenite catalyst is lower than that obtained for the NiO/Al_2O_3 catalyst used in the present work, and even lower than that obtained for the Ni-based catalysts used in tar-cleaning experiments reported in the literature[9, 28, 29, 36, 48]. However, the ilmenite catalyst clearly shows tar removal activity and the efficiency of this reaction could possibly be increased by optimization of the CLR system for this catalyst. The tar-decomposing activity in the CLR reactor would be enhanced by a higher RT, as this is presently in the lower range of what has been reported in the literature. For instance, Dayton[9] collected data from over 70 tar-removal experiments and reported residence times of up to several seconds. Furthermore, the present work, together with studies performed on CLC, clearly suggests that to be properly activated, the ilmenite catalyst needs to be used in conjunction with repeated redox cycles at temperatures >800°C. However, with respect to tar reduction in biomass gases, these investigations suggest that regardless of the choice of metal oxide, temperatures >850°C are likely to be needed to achieve high rates of tar conversion.

Permanent gases: effects of temperature and oxygen loads

The dry composition of the raw gas was compared with the reformed gas after the CLR system, to investigate whether the catalysts have any catalytic effects on the permanent gases. In **Figure 24**, the gas compositions (mole%) from the 23 wt.% manganese experiments at 800°C are shown for the raw gas and the reformed gas at oxygen concentrations of 0.6, 1.0, and 2.2 mole% in the inlet feed to the AR. A general trend noted for all the investigated oxygen concentrations was that the H_2 and CO_2 concentrations increased while the CO concentration decreased. Furthermore, the concentrations of CH_4 and acetylene decreased slightly. The increase in H_2 can be explained by tar-reforming reactions and increased WGS activity, and the H_2/CO ratio being shifted from approximately 0.6 in the raw gas to 1.0 in the reformed gas.

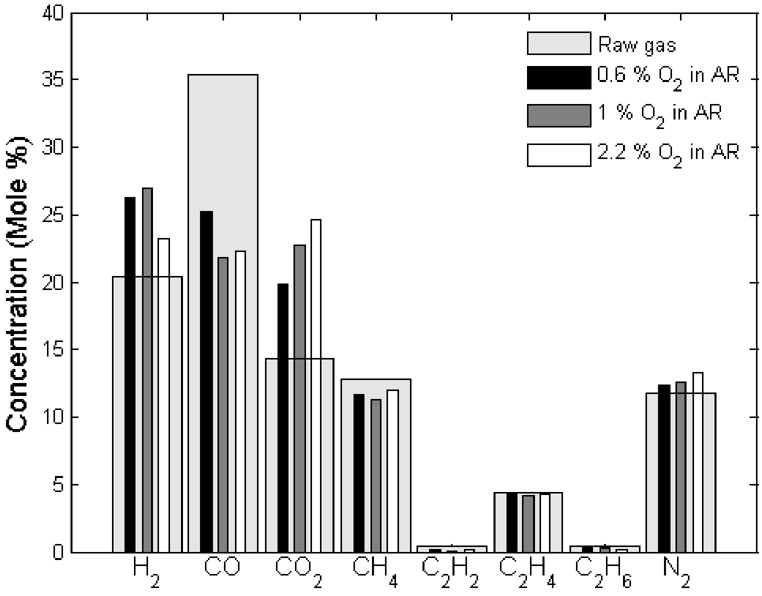

Figure 24. Dry gas compositions of the raw gas and reformed gas (23 wt.% manganese catalyst).

Figure 25, **a** and **b** shows the mole flows of the major gas components, H_2, CO, CO_2, CH_4, and light hydrocarbons expressed as $C_{2\text{-}3}H_X$ and including C_2H_2, C_2H_4, C_2H_6, and C_3H_6, at 1% O_2 for the 100 wt.% ilmenite catalyst case and for the 100 wt.% NiO/Al_2O_3 catalyst, respectively. The H_2 content of the reformed gas at 1% O_2 and with the NiO/Al_2O_3 catalyst clearly increased as the temperature was increased above 750°C (**Fig. 25a**). This can to a large extent be explained by the levels of reformed tar, CH_4, and light hydrocarbons, all of which are increased at higher temperature. At 880°C, the level of CH_4 was reduced by almost 50% and the levels of light hydrocarbons were decreased by 98%. Furthermore, at all temperatures, more CO_2 was formed than could be achieved through hydrocarbon oxidation, through the oxygen transported from the AR. This suggests that part of the hydrogen was formed *via* the WGS reaction. However, since the accuracy of the water measurements was insufficient, these could not be used to close the hydrogen balance.

The H_2 content was also increased in the reformed gas in the ilmenite catalyst experiments at 1% O_2 (**Fig. 25b**). The level of H_2 was approximately 8% higher at 850°C than at 800°C, which was as expected, since more tars were reformed. However, in contrast to the NiO/Al_2O_3 catalyst scenario, the CH_4 in the ilmenite catalyst cases was not consumed, and the levels of CH_4 in the reformed gas were slightly increased at both 800°C and 850°C. This suggests that CH_4 is produced in the system, and that the ilmenite catalyst has poor ability to reform this molecule. Nevertheless, the ilmenite catalyst showed a high propensity for reforming light hydrocarbons, with 87% of these compounds being reformed at 850°C.

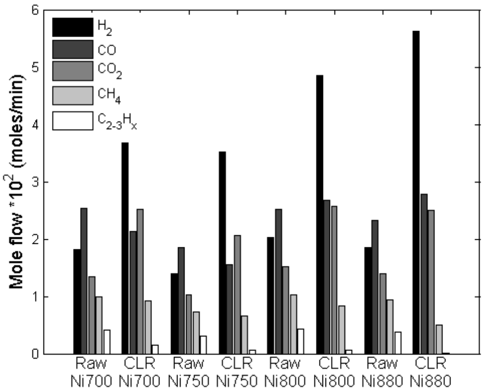

Figure 25a. Mole flow values of the gas species in the raw and reformed gases in the case of the NiO/Al_2O_3 catalyst at 1% O_2 and at the indicated temperatures (700°C, 750°C, 800°C, and 880°C).

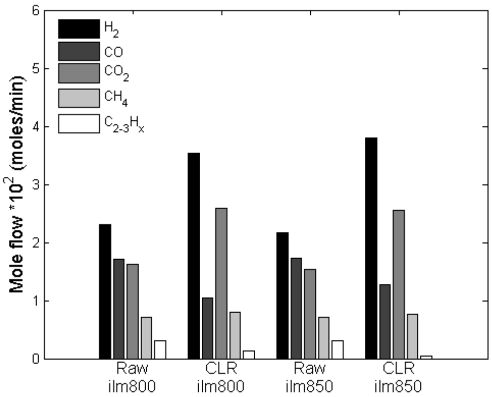

Figure 25b. Mole flow values of the gas species in the raw and reformed gases in the case of the ilmenite catalyst at 1% O_2 and at the indicated temperatures (800°C and 850°C).

The ratio of the increases in total permanent gas between the reformed gas and the raw gas for both catalysts at 1.0% and 2.2% O_2 are shown in **Figure 26a**. In almost all the cases, increased oxygen transport from the AR to the FR led to a decrease in the total level of permanent gases in the dry reformed gas (**Fig. 26a**). This implies that a fraction of the oxygen transported *via* the catalyst is involved in the oxidation of hydrogen and/or hydrocarbons, and that not all of the oxygen is consumed during tar oxidation, as suggested by Eq. (**2a**). In the cases involving the NiO/Al_2O_3 catalysts, the most likely reason for the decrease in total permanent gases is that higher oxygen transfer leads to increased oxidation of H_2 into water. This is supported by the data shown in **Figure 26b**, where the ratios of the change in the moles of H_2 and CO between the reformed gas and the raw gas for both catalysts at 1.0% and 2.2% O_2 are shown. The amount of H_2 produced in the Ni-catalyzed process was reduced at all temperatures as oxygen transport increased, whereas the CO content was essentially unaffected by increases in oxygen availability. The pattern of decreasing H_2 associated with increasing oxygen transport paralleled the decrease in total permanent gases (**Fig. 26a**). In the ilmenite catalyst cases, the influence of oxidation of the total permanent gases was first evident at 850°C (**Fig. 26a**), and the H_2 and CO contents were reduced as oxygen transport increased (**Fig. 26b**).

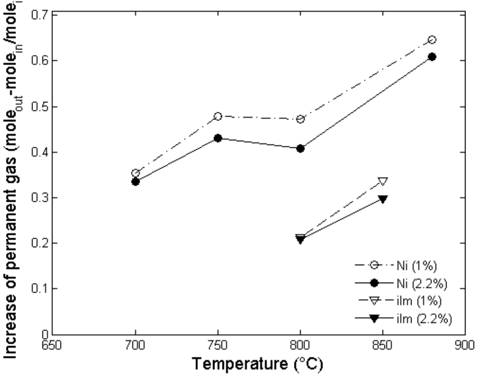

Figure 26a. Total molar increases in the permanent gas for the NiO/Al_2O_3 catalyst (Ni) and for the ilmenite catalyst in the CLR at 1.0% and 2.2% O_2.

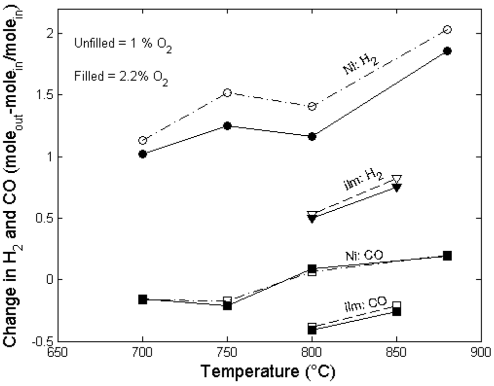

Figure 26b. Change in moles of H_2 and CO in the reformed gas compared to the raw gas used for the NiO/Al_2O_3 catalyst (Ni) and for the ilmenite catalyst as a function of temperature.

Figure 27 shows the level of chemically stored energy in the permanent gas and the raw gas used for the NiO/Al_2O_3 catalyst and the ilmenite catalyst as a function of temperature and oxygen transport. The chemically stored energy in the reformed gas increased with increasing operating temperature in the reactor system for both the NiO/Al_2O_3 catalyst and the ilmenite catalyst. The reason for this is that the formation of H_2 and CO increases as tars are decomposed *via* reforming reactions, which are enhanced at higher temperatures. In the case involving the NiO/Al_2O_3 catalyst, the levels of chemically stored energy in the reformed gas were higher than those in the raw gas with 1% O_2 at temperatures >750°C and with 2.2% O_2 at temperatures >800°C. At temperatures <750°C, catalysis is less active and the tar-reforming reactions do not outweigh the energy loss from oxidation of H_2, C_iH_j, and CO as a result of the oxygen transport. The oxidation of product gas into CO_2 and H_2O is also the reason why the chemically stored energy in the reformed gas for the NiO/Al_2O_3 catalyst is lower at 2.2% O_2 than at 1% O_2. In the case involving the ilmenite catalyst, the chemically stored energy was lower in the reformed gas than in the raw gas for all cases, which implies that the loss of stored energy through the oxidation of product gas is greater than the energy gained through tar reformation. However, the reasons as to why the energy content in the reformed gas is higher at 2.2% O_2 than at 1% O_2 at 850°C remain unclear.

Coke deposits on the catalysts

Coke deposition on catalytic surfaces is known to decrease the activity of the catalyst with respect to tar cracking, and the accumulation of coke can lead to complete deactivation of the catalyst. As described in the *Theory* section, tar-cracking and hydrocarbon-reforming reactions enhance the formation of coke on the surface of the catalyst, so it is important to conserve catalytic activity through continuous regeneration. As the experiments in the present work were conducted with raw gas that contained high levels of tars, carbon deposition was expected and the regeneration of catalyst was thoroughly monitored.

The CO and CO_2 concentrations in the effluent from the AR in all the experiments were measured online and within a timeframe of seconds. During all the experiments, before the raw gas was introduced into the FR, the levels of CO_2 and CO were below the detection limits of the instruments. The levels of CO_2 were measured in the outlet of the AR shortly after the introduction of the raw gas into the FR, and carbon deposits were found on the catalyst. The level of CO was always below the detection limit of the instrument, which implies that the amount of CO produced was negligible, and that all the coke deposits were oxidized to CO_2 in the AR. Furthermore, the oxygen level in the effluent from the AR was below the detection limit of the instrument during all the experiments, which implies that all the oxygen was consumed during either oxidation of the coke deposits or re-oxidation of the catalysts.

Figure 28 captures the regeneration of coke deposits on the catalyst and shows carbon transport from the FR to the AR as a function of the experimental temperature. Here, the results for $Y_{c,AR}$ are presented in wt.%. The highest level of carbon deposits was detected for the 100 wt.% ilmenite catalyst case at 850°C in 2.2% O_2; under these conditions, 0.25% of the total amount of carbon in the raw gas ended up as deposits on the catalyst. The highest level of carbon deposits for the 100 wt.% NiO/Al_2O_3 catalyst case, detected at 700°C in 1% O_2, was 0.11 % of the total amount of carbon in the raw gas. The amount of carbon transported from the FR to the AR by the catalysts underlines the advantages of combining tar cleaning with coke deposit regeneration. The results suggest that these types of catalysts can be applied in a CLR for processing raw gases that have high contents of tar, while at the same time maintaining catalyst activity without involving primary tar-reduction measures in the gasifier.

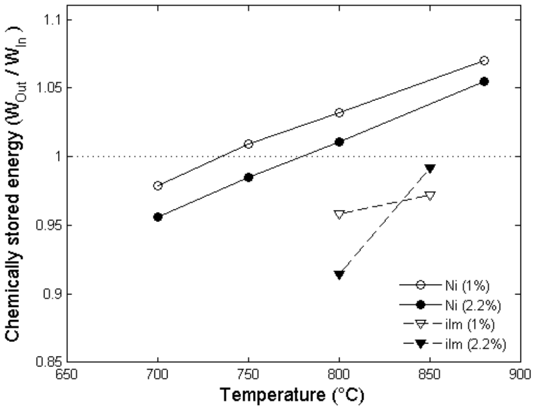

Figure 27. Chemically stored energy levels in the reformed gas compared to those in the raw gas used for the NiO/Al_2O_3 catalyst (Ni) and for the ilmenite catalyst at 1.0% and 2.2% O_2 as a function of temperature.

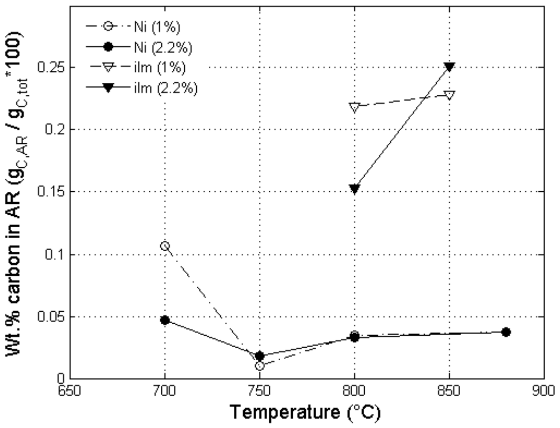

Figure 28. Weight percents (wt.%) of carbon transported from the FR to the AR as a function of temperature.

4.3 Development of the online water measurement system

The dynamic behavior of the calibrated method for water measurements was investigated in the Chalmers research CFB boiler, in which a step function of moisture in the flue gases was generated by adding water to the fuel feed. The results, presented in **Figure 29**, reveal that the RH sensor signal responds to frequencies within seconds, while the FT-IR analyzer detects the change in moisture approximately two minutes later. However, the used FT-IR analyzer filters the measurement signal retroactively on a per-minute basis; when treating the RH signal with the same filter, the outcomes from the RH sensor and FT-IR become comparable. The filtered signal from the RH measurement and the FT-IR measurement show no sign of hysteresis in the RH measurement, which means that the signals respond equally to both positive and negative changes in moisture content. Finally, using the method for detection of fluctuations yields moisture contents that are in the same order as the sampling time of the instrument (5 seconds).

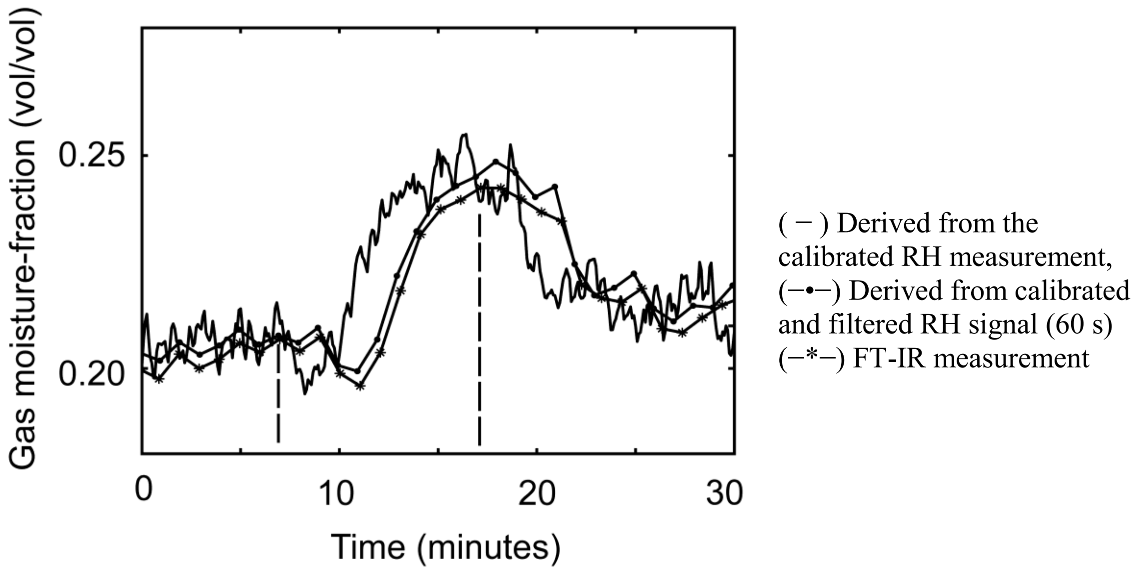

Figure 29. Moisture fractions of the flue gas during the dynamic test in the Chalmers CFB boiler.

4.4 Oxygen carriers in a biomass-fired CFB boiler

Boiler experiments

The concentrations of CO were measured at position “kh2” (**Fig. 17**) for all four cases: 0%, 20%, 17%, and 40% mass fractions of ilmenite in the total bed inventory. Three to four experimental points, corresponding to air-to-fuel ratios that ranged from 1.04 to 1.17, were considered for each of the cases. **Figure 30** shows the corresponding measured concentrations of CO, expressed in mg/nm^3 at 6% O_2, as a function of the air-to-fuel ratio. As seen in **Figure 30**, irrespective of the ilmenite content in the boiler, the CO level decreases as the air-to-fuel ratio are increases, which is in line with expectation. Moreover, as more ilmenite is introduced into the boiler, the concentrations of CO are decreased relative to the reference case. In particular, an abatement of almost 75% (from 54 to 13 mg/m$_n^3$) between the reference case and the 40 wt.% ilmenite case is evidenced at the air-to-fuel ratio of 1.12. This trend is even more pronounced at lower air-to-fuel ratios. For instance, at an air-to-fuel ratio of 1.08, an 80% drop in the CO concentration is achieved compared to the base case. The decrease in CO can be attributed to the oxygen-carrying properties of ilmenite. When an oxygen carrier is introduced into the furnace, the amount of fed oxygen is in theory evenly distributed along the whole furnace, which leads to increased conversion of the CO fraction. This can be compared with the higher amounts of CO seen in the reference case, where the bed inventory consisted solely of silica-sand and secondary air was injected as a distinct stream in the furnace freeboard, which resulted in poorer mixing of the fuel and oxygen.

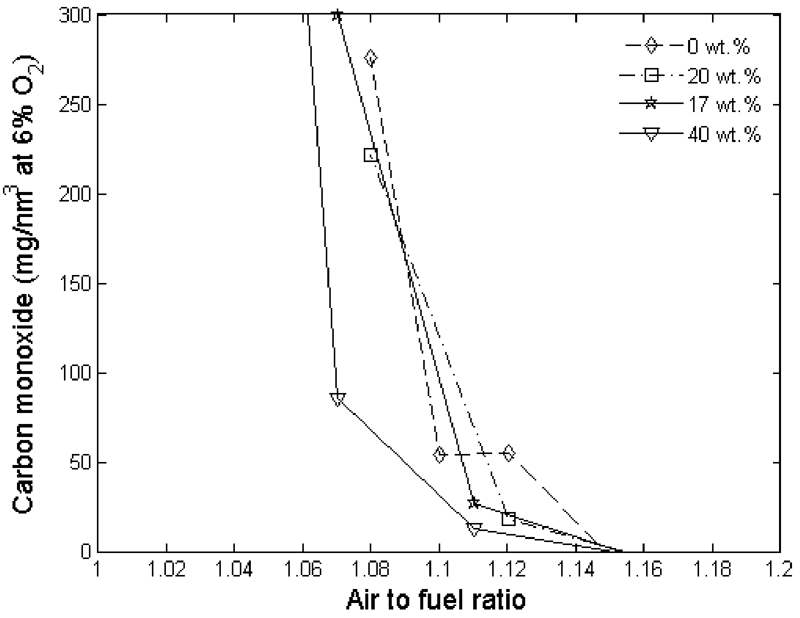

Figure 30. Concentrations of CO (mg/nm^3, at 6% O_2) measured at position "kh2" in the convection path as a function of the air-to-fuel ratios for silica-sand operation and for operation with ilmenite at 17–40 wt.% of the total bed inventory.

Boiler and gasifier experiments

Initially, only silica-sand was used as the bed material in the boiler/gasifier loop. This provided a reference case with which to compare operation with ilmenite inclusion in the bed. In these tests, measurements of O_2 and CO across the furnace horizontal cross-section were performed at three different heights, as described in *Methodology*. **Figure 31** shows the CO concentrations (mole%) at these heights in the furnace. On the left-hand side, the concentrations are from the reference case, while the values on the right-hand are those measured after the addition of 12 wt.% ilmenite to the total bed inventory. As previously stated, the raw gas produced in the gasifier is injected at an upper location alongside the "Back" side of the furnace (see **Fig. 17)**. More precisely, H7 and H9 are located respectively upstream and downstream of this injection point, which gives a basis for comparison. In **Figure 31**, the location of the injection point is clearly visible as a substantial increase in the CO concentration measured at H9. Moreover, the decrease in CO concentration observed between the two experimental configurations at H7 is consistent with the oxidation of CO in the presence of oxidized ilmenite in and above the furnace bed. In particular, on the "Front" side where fuel is fed to the furnace, the CO peaks are less pronounced in the ilmenite case. In general, using ilmenite seems to even out the CO peaks (left-hand sides in **Figure 31)**, confirming that this material enhances the mixing of the available oxygen in the furnace with combustible compounds. It seems that oxidation reactions are moved to the bed where fuel devolatilization occurs and in turn, volatile conversion is favored. This aspect is also evident higher up in the furnace, where entrained ilmenite at H12 continues to oxidize CO (see **Fig. 31)**. Taken together, this series of experiments involving both boiler and gasifier operation supports the notion that ilmenite promotes fuel and oxygen mixing in the furnace throughout its cross-section. This corresponds to the beneficial effect of ilmenite on CO detailed in the previous section.

Figure 32 shows the average temperature variations between the inlet and the outlet of the cyclone for the four cases (represented by bars 1 to 4): boiler with silica-sand; boiler/gasifier with silica-sand; boiler with the addition of 12 wt.% ilmenite; and boiler/gasifier with the addition of 12 wt.% ilmenite. During normal boiler operation with only silica-sand as the bed material, i.e., when the gasifier is not in operation and no raw gas is injected into the freeboard of the furnace, the temperature drop between the inlet and the outlet of the cyclone is usually around 35°C, owing to heat transfer to the surrounding walls (first bar in **Fig. 32)**. When the gasifier is in operation, the concentrated stream of combustibles into the furnace cannot achieve complete oxidation during the residence time along the freeboard. This is due to a lack of mixing of the available oxygen and unreacted species, as reflected in the measurements of CO concentrations (first column in **Fig. 31)** at H12. However, when the gas enters the well-mixed cyclone, these unreacted species come in contact with the oxygen and are combusted, which means that the cyclone works as an after-burner. The heat of reaction leads to an increase in the temperature of the gas inside the cyclone and therefore, the commonly observed temperature drop in the cyclone during normal boiler operation is clearly diminished during gasifier operation (second bar in **Fig. 32)**. Comparing the two cases of boiler and boiler/gasifier operation with the addition of 12 wt.% ilmenite (third and fourth bars, respectively, in **Fig. 32)**, the temperature drops in the cyclone are expanded by almost 50°C and 20°C, respectively. The reason for this is that less combustion occurs in the cyclone as more of the combustibles are converted already in the furnace. Thus, the oxygen-carrying properties of the ilmenite in combination with the well-distributed particles inside the furnace increase the mixing of the fuel and oxygen.

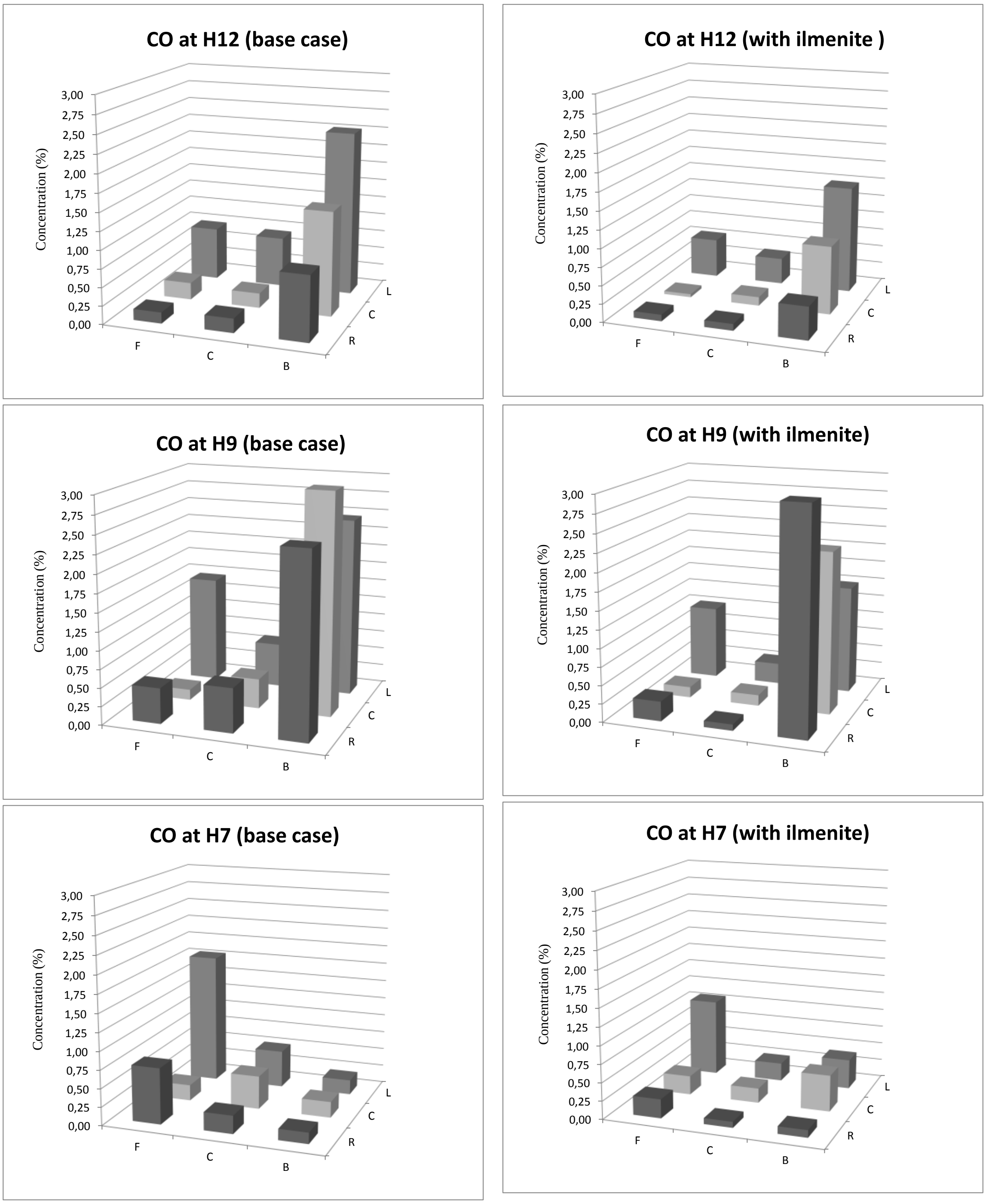

CO at H12 (base case)

CO at H12 (with ilmenite)

CO at H9 (base case)

CO at H9 (with ilmenite)

CO at H7 (base case)

CO at H7 (with ilmenite)

Figure 31. Carbon monoxide levels at three heights in the boiler cross-section for the reference case and the ilmenite case.

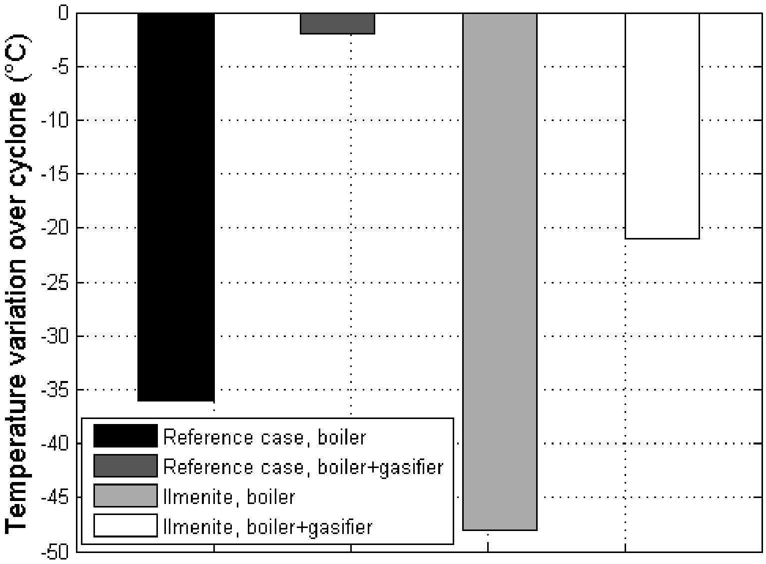

Figure 32. Average temperature differences between the inlet and outlet of the cyclone during the reference and ilmenite experiments in the boiler/gasifier system.

5 - Conclusions and Outlook

5.1 Cold system investigations

A novel method that combines tar cleaning and catalyst regeneration in Chemical Looping Reforming (CLR) was investigated. The method was evaluated by conducting experiments in identically sized dual fluidized bed reactor systems: a cold system for fluid dynamic experiments, and a system made of high-temperature-resistant steel for handling the raw gas from the Chalmers gasifier.

The possibilities to control the circulation rate of the catalyst in the reactor systems were investigated in a fluid dynamics study using the cold system (**Paper I**). The experiments, which were performed with air or He as the fluidization medium, indicate that, regardless of the fluidization gas used, the rate of circulation of solids can be efficiently controlled by the fluidization velocity in the riser. However, the throttling effect, which was seen during air fluidization in the ILS, was not seen in the hot system. The ILS could therefore not be used as a valve for controlling the rate of circulation of solids in the hot system. This was also evident already in the experiments with He as the fluidization medium. The dimensionless numbers (scaling laws by Glicksman et al. [53] for He and the gases in the hot system showed rather good agreement. This implies that the fluid dynamics patterns in the cold system potentially can be transferred to the hot system. The performed leakage experiment revealed that sufficient gas tightness of the loop seals can be achieved if the operating pressure difference between the FR and AR is kept low.

5.2 Hot system investigations

All the experiments in the hot system were conducted with raw gas from the Chalmers biomass gasifier, which contained 20–30 g_{tar}/Nm^3_{gas}. The CLR gas-upgrading method was initially demonstrated using 60 wt.% ilmenite ($FeTiO_3$) in silica-sand as the bed material (**Paper II**), and subsequently with a mixture of silica-sand and 23 wt.% manganese catalyst (Mn_3O_4 supported on $MgZrO_3$) (**Paper III**). The total tar content was reduced by 35% in the ilmenite catalyst case and by 44.5% in the manganese catalyst case, while no catalytic effects of the reactor material itself were observed. A general trend in both investigations was that the branched tars and phenols were largely converted to pure aromatic compounds, while more activation energy was required to open the stable ring structures of, for example, benzene and naphthalene. Both catalysts showed water-gas shift activity: the H_2/CO ratio increased from approximately 0.7 in the raw gas to 3.0 downstream of the reactor system for the ilmenite case and from 0.6 to 1.0 for the manganese case. The concentrations of light hydrocarbons and methane were not significantly affected by any of the catalysts.

Two additional sets of experiments were performed, one with 100 wt.% of the nickel catalyst (NiO/Al2O3; **Paper IV**) and one with 100 wt.% of ilmenite (**Paper V**). The derivation of a system-wide molar balance for the CLR system (**Paper V**) shows that it is important to specify the basis in which the tar efficiency calculations are conducted. When tar removal is calculated on the basis of dry reformed gas, as in the gas-upgrading case, the tar removal efficiencies are 95% for the NiO/Al_2O_3 catalyst at 880°C and 60% for the ilmenite catalyst at 850°C. The same calculation yields tar removal efficiencies of 86% and 42%, respectively, when the contribution of the produced permanent gases is removed from the reformed gas. Hydrogen production was enhanced by both catalysts, and 50% of the CH_4 and 98% of the light hydrocarbons were converted in the case of the NiO/Al_2O_3 catalyst at 880°C, as a result of reforming reactions. In the ilmenite catalyst case, 87% of the light hydrocarbons were reformed, although the production of CH_4 was higher than its consumption, resulting in a surplus of CH_4 in the reformed gas.

Overall, the ilmenite catalyst is less active than the NiO/Al_2O_3 catalyst as a tar-cleaning catalyst. The fate of the ilmenite catalyst in the present experimental set-up needs to be investigated under optimized conditions of operation, in which appropriate activation and improved gas/solid contact will be essential. Increased gas/solid contact and enhanced utilization of oxygen might be achieved by replacing the BFB reformer in the present setup with a CFB reformer.

In all the conducted experiments, all the catalysts were regenerated continuously from carbon deposits *via* oxidation to CO_2 (**Papers I–V**), and there was no indication of catalyst deactivation owing to carbon deposits.

5.3 Moisture measurements

A new cost-effective method for determining the moisture content of a gas stream within rapid response time was developed and experimentally validated in the present work. The goal was to enable online measurements of the water content of the reformed gas exiting the CLR reactor. Although the validation in the present study was carried out on the flue gas from a CFB boiler, the method can equally be applied downstream of the tar-cleaning reactor. In addition to its relative simplicity, the method showed good accuracy (<4% error). The results of the experiments show that this method detects variations in moisture content within a time-frame of seconds, without significant hysteresis.

5.4 Oxygen carriers in a biomass-fired CFB boiler

The possibilities to even out the concentrations of CO and unburned HC in a CFB furnace through the addition of the oxygen carrier ilmenite to the bed material inventory were experimentally investigated in the 12-MW$_{th}$ biomass-fired boiler/gasifier system at Chalmers University of Technology. The system was operated for a base case that involved silica-sand as the sole bed material, and subsequently for a set of cases in which up to 40 wt.% of the silica-sand was replaced by ilmenite. The air-to-fuel ratio was varied from 1.04 to 1.17, and the concentrations of CO, NO, and hydrocarbons were measured in the cross-section of the furnace at nine positions and at three different heights of the furnace, as well as at one position in the convection path. The investigation revealed that the content of CO was decreased by as much as 80% when 40% ilmenite was used, as compared with operation with only silica-sand. Already when 12 wt.% ilmenite was mixed with the ordinary bed material, the concentration profile of unburned species across the furnace tended to be less prominent in space, as compared with operation with only the silica-sand. The temperature profiles across the cyclone suggest that less combustion occurs in the actual cyclone when using ilmenite in the boiler, as compared with solely using silica-sand as the bed material. This implies that the distribution of oxygen in the furnace is improved by the incorporation of ilmenite.

5.5 Concluding Remarks and Outlook

Gas cleaning processes will be needed before the gas produced *via* biomass gasification can be utilized for synthesis into e.g. vehicle fuels. Several issues related to this gas cleaning operation have been emphasized in this thesis and the reactor system that has been presented could potentially address some of these. However, there are still challenges and questions that need to be answered before a fully developed CLR-system can be implemented in an industrial process. One of these challenges requiring further research is the reactor scale-up and how this will potentially affect the system and the operating parameters. How to optimally fulfill the heat demand for the endothermic tar reactions in the reactor system is one of such parameters. Information gained from operating the Chalmers boiler with oxygen carriers as part of the bed inventory can be used as a first input. The results suggest that a concentrated stream of gas can be injected into the freeboard and combusted to produce heat. This method can be transferred to the CLR-system where part of the produced raw gas could be combusted in the AR in a similar manner to heat the bed material. Furthermore, in comparison with using directly the raw gas from a gasifier, operating the lab-scaled reactor system with well-determined mass flows of synthetic gas and dedicated tar components would clearly be beneficial to evaluate the catalytic properties of different bed materials. These types of operations are also needed to enable proper heat and mass balances in the CLR-system, which in turn will give significant information to the up-scaling process.

It has also been shown that it is difficult to determine the water content in the effluent from a boiler, gasifier and gas cleaning unit. If the presented method for online monitoring of moisture is e.g. integrated with the CLR-system, a much more accurate determination of the moisture content in the effluent streams can be achieved. This will in turn result in that the water consumption from various reactions can be traced and a more correct hydrogen balance can be achieved. In this work, the measuring technique was tested in a lab-prototype with a primitive sensor for moisture detection. Today, there are multifunctional sensors available that could facilitate the use and decreases the size of the moisture measuring unit. In this manner, the method could be further developed for practical use in commercial operation of a boiler or in a potential gasification plant.

6 - Nomenclature

AR_{out}	From the effluent of the air reactor
CaO/MgO/NiO	Catalyst containing Calcium-oxide, Magnesium-oxide and Nickel-oxide
C_iH_j	Light hydrocarbons
CO_2	Carbon dioxide
CO	Carbon monoxide
C_nH_m	Representative tar molecule
C_7H_8	Toluene
CH_4	Methane
H_2	Hydrogen
H_2O	Water
He	Helium
Fe_2O_3	Hematite (iron-oxide)
FR_{out}	From the effluent of the fuel reactor
Gs	Solids flux (kg/m^{2}s)
g	Gravimetric constant (m/s^2)
g_{tar}/kg_{daf}	Gram tar per kilo gram dry and ash-free fuel
g_{tar}/Nm^3_{gas}	Mass of tars per normal cubic meter of product gas
ΔH	Heat of reaction
h_i	Height of bed material in cyclone downcomer (m)
L	Characteristic bed length (m)
M4MgZ1150	Manganese-oxide supported on Zirconia-oxide (manufactured catalyst)
MeO	Metal oxide
Me_xO_y	Oxidized metal oxide
Me_xO_{y-1}	Reduced metal oxide
Mn_3O_4	Manganese-oxide
NiO	Nickel-oxide
NO_x	Nitrogen oxides
MJ/kg_{daf}	Energy content, mega Joule per kilo gram dry and ash-free fuel
	MJ/MJ_{daf}: Ratio, mega Joule per mega Joule dry and ash-free fuel

n	Mole (mole) or molar flow (mole/m^3)
NiO/Al_2O_3	NiO supported on an α-Al_2O_3 matrix
P	atmospheric pressure (Pa)
P_{sat}	Saturation pressure (Pa)
Py	Pyrolysis
Q_{gasif}	Heat demand in gasifier X: Char conversion
Q_{CLR}	Heat demand in CLR
u_{mf}	Minimum fluidization velocity (m/s)
u_0	Superficial gas velocity (m/s)
V_x	Volume flow of gas produced from gasification of char
V_p	Volume flow of gas produced from pyrolysis
V	Volume (m^3)
V’	Volume flow (m^3/s)
Vol.%	Volume percent
WGS	Water-gas shift reaction
Wt.%	Weight percent
$X_{vol,m}$	Volumetric moisture fraction
$Y_{C,AR}$	Carbon deposits on the catalyst, ratio for the amount of carbon regenerated in the AR divided by the total amount of carbon fed to the FR ($g_{carbon,AR}/g_{carbon,tot}$)

Greek letters

ε_{bed}	Bed voidage
γ	Fraction of helium
ρ_f	Density of fluid (kg/m^3)
ρ_s	Density of solids (kg/m^3)
φ	Relative humidity

Abbreviations

AR	Air Reactor
BFB	Bubbling fluidized boiler
CFB	Circulating fluidized bed
CLC	Chemical Looping Combustion
CLR	Chemical Looping Reforming
DME	Dimethyl ether
FCC	Fluid Catalytic Cracking
FR	Fuel Reactor
F-T Diesel	Fisher-Tropsch Diesel
FTIR	Fourier Transform Infrared Spectroscopy
GC-FID	Gas chromatography followed by a flame ionization detector
HC	Hydrocarbons

ILS	Inferior Loop Seal
LHV	Lower heating value
LS	Loop Seal
Micro-GC	Micro-Gas Chromatography
PAH	Polycyclic aromatic hydrocarbons
PT100	Resistance detector for temperature detection
RH	Relative Humidity
RT	Residence time or gas/solid contact time
SLS	Superior Loop Seal
SNG	Substitute natural gas
SPA	Solid phase absorption
TGA	Thermogravimetric analysis
THC	Total hydrocarbons

7 - References

---

1. E. Ahlonsou, Y.D., D. Schimel, *Climate change 2001, The scientific basis, Chapter 1, Human-induced climate variations* 2001, IPCC.
2. Chum, H.L. and R.P. Overend, *Biomass and renewable fuels.* Fuel Processing Technology, 2001. **71**(1–3): p. 187-195.
3. Henrik Thunman, L.-E.Å., Bo Leckner, Filip Johansson, *A cost effective concept for generation of heat, electricity and transport fuel from biomass in fluidized bed boilers – using existing energy infrastructure*, in *Proceedings of the 15th European Biomass Conference & Exhibition - From research to market Deployment*2007: Berlin, Germany.
4. Thunman, H. and M.C. Seemann, *First experience with the new Chalmers gasifier*, in *20th International conference on fluidized bed combustion*, G.Z. Yue, H.; Zhao, C.; Luo, Z., Editor 2009: xi´an, China. p. 659 - 663.
5. Balat, M., et al., *Main routes for the thermo-conversion of biomass into fuels and chemicals. Part 2: Gasification systems.* Energy Conversion and Management, 2009. **50**(12): p. 3158-3168.
6. Pfeifer, C. and H. Hofbauer, *Development of catalytic tar decomposition downstream from a dual fluidized bed biomass steam gasifier.* Powder Technology, 2008. **180**(1-2): p. 9-16.
7. Devi, L., K.J. Ptasinski, and F.J.J.G. Janssen, *A review of the primary measures for tar elimination in biomass gasification processes.* Biomass and Bioenergy, 2003. **24**(2): p. 125-140.
8. Li, C.S. and K. Suzuki, *Tar property, analysis, reforming mechanism and model for biomass gasification-An overview.* Renewable & Sustainable Energy Reviews, 2009. **13**(3): p. 594-604.
9. Dayton, D., *A Review of the Literature on Catalytic Biomass Tar Destruction*, 2002, NREL.
10. Yung, M.M., W.S. Jablonski, and K.A. Magrini-Bair, *Review of Catalytic Conditioning of Biomass-Derived Syngas.* Energy & Fuels, 2009. **23**(4): p. 1874-1887.
11. Anis, S. and Z.A. Zainal, *Tar reduction in biomass producer gas via mechanical, catalytic and thermal methods: A review.* Renewable and Sustainable Energy Reviews, 2011. **15**(5): p. 2355-2377.
12. Larsson, A., M. Seemann, and H. Thunman, *Performance Evaluation of Industrial Scale Indirect Gasifiers - The Chalmers Gasifier.* To be submitted for publication, Spring 2013.
13. Patrick C.A Bergman, S.V.B.v.P., Harold Boerrigter, *The Novel "OLGA" technology for complete tar removal from biomass producer gas*, in *Pyrolysis and Gasification of Biomass and Waste, Expert meeting, 30* 2002: Strasbourg, France.

14. Semelsberger, T.A., R.L. Borup, and H.L. Greene, *Dimethyl ether (DME) as an alternative fuel.* Journal of Power Sources, 2006. **156**(2): p. 497-511.
15. Holmgren, K.M., et al., *System aspects of biomass gasification with methanol synthesis – Process concepts and energy analysis.* Energy, 2012. **45**(1): p. 817-828.
16. Mattisson T, a.L.A. *Applications of chemical-looping combustion with capture of CO2.* in *Second Nordic Minisymposium on Carbon Dioxide Capture and Storage, Göteborg, Sweden*. 2001.
17. Kunii, D. and O. Levenspiel, eds. *Fluidisation Engineering Second Edition*. ed. H. Brenner1991, Butterworth-Heinemann. 36-38.
18. Dutta, A., et al., *Techno-economics for conversion of lignocellulosic biomass to ethanol by indirect gasification and mixed alcohol synthesis.* Environmental Progress & Sustainable Energy, 2012. **31**(2): p. 182-190.
19. Neves, D., et al., *On-line measurement of raw gas elemental composition in fluidized bed biomass steam gasification*, in *World Bioenergy*2012: Jönköping-Sweden.
20. Strömberg, B., *Bränslehandboken*, 2004, Värmeforsk. p. 317.
21. Leckner, B., *Fluidized bed combustion: Mixing and pollutant limitation.* Progress in Energy and Combustion Science, 1998. **24**(1): p. 31-61.
22. Karlsson, S., et al., *Alkali Induced High Temperature Corrosion of Stainless Steel: The Influence of NaCl, KCl and CaCl2.* Oxidation of Metals, 2012. **78**(1): p. 83-102.
23. Baxter, L.L., et al., *The behavior of inorganic material in biomass-fired power boilers: field and laboratory experiences.* Fuel Processing Technology, 1998. **54**(1–3): p. 47-78.
24. Nielsen, H.P., et al., *The implications of chlorine-associated corrosion on the operation of biomass-fired boilers.* Progress in Energy and Combustion Science, 2000. **26**(3): p. 283-298.
25. Evans, R.J. and T.A. Milne, *Molecular characterization of the pyrolysis of biomass. 2. Applications.* Energy & Fuels, 1987. **1**(4): p. 311-319.
26. Evans, R.J. and T.A. Milne, *Molecular characterization of the pyrolysis of biomass.* Energy & Fuels, 1987. **1**(2): p. 123-137.
27. Milne, T.A. and R.J. Evans, *Biomass Gasifier "Tars": Their Nature, Formation, and Conversion*, 1998, National Renewable Energy Laboratory.
28. Bangala, D.N., et al., *Catalytic gas conditioning: Application to biomass and waste gasification*, in *Industrial & Engineering Chemistry Research*1997. p. 4184-4192.
29. Caballero, M.A., et al., *Biomass gasification with air in fluidized bed. Hot gas cleanup with selected commercial and full-size nickel-based catalysts.* Industrial & Engineering Chemistry Research, 2000. **39**(5): p. 1143-1154.
30. Delgado, J., M.P. Aznar, and J. Corella, *Biomass Gasification with Steam in Fluidized Bed: Effectiveness of CaO, MgO, and CaOâˆ'MgO for Hot Raw Gas Cleaning.* Industrial & Engineering Chemistry Research, 1997. **36**(5): p. 1535-1543.
31. Rapagnà, S., et al., *Steam-gasification of biomass in a fluidised-bed of olivine particles.* Biomass and Bioenergy, 2000. **19**(3): p. 187-197.
32. Seemann, M.C., et al., *The regenerative effect of catalyst fluidization under methanation conditions.* Applied Catalysis A: General, 2006. **313**(1): p. 14-21.

33. Baker, E.G., L.K. Mudge, and M.D. Brown, *Steam gasification of biomass with nickel secondary catalysts.* Industrial & Engineering Chemistry Research, 1987. **26**(7): p. 1335-1339.
34. Miyazawa, T., et al., *Catalytic performance of supported Ni catalysts in partial oxidation and steam reforming of tar derived from the pyrolysis of wood biomass.* Catalysis Today, 2006. **115**(1-4): p. 254-262.
35. Rydén, M., et al., *Waste products from the steel industry with NiO as additive as oxygen carrier for chemical-looping combustion.* International Journal of Greenhouse Gas Control, 2009. **3**(6): p. 693-703.
36. Corella, J., A. Orío, and J.-M. Toledo, *Biomass Gasification with Air in a Fluidized Bed: Exhaustive Tar Elimination with Commercial Steam Reforming Catalysts.* Energy & Fuels, 1999. **13**(3): p. 702-709.
37. Blanco, P.H., et al., *Characterization and evaluation of Ni/SiO2 catalysts for hydrogen production and tar reduction from catalytic steam pyrolysis-reforming of RDF.* Applied Catalysis B: Environmental, (0).
38. Uddin, M.A., et al., *Catalytic decomposition of biomass tars with iron oxide catalysts.* Fuel, 2008. **87**(4-5): p. 451-459.
39. Johansson, M., T. Mattisson, and A. Lyngfelt, *Investigation of Mn3O4 With Stabilized ZrO2 for Chemical-Looping Combustion.* Chemical Engineering Research and Design, 2006. **84**(9): p. 807-818.
40. Mendiara, T., et al., *Evaluation of different oxygen carriers for biomass tar reforming (II): Carbon deposition in experiments with methane and other gases.* Fuel, 2011. **90**(4): p. 1370-1382.
41. Mendiara, T., et al., *Evaluation of different oxygen carriers for biomass tar reforming (I): Carbon deposition in experiments with toluene.* Fuel, 2011. **90**(3): p. 1049-1060.
42. Min, Z., et al., *Catalytic reforming of tar during gasification. Part I. Steam reforming of biomass tar using ilmenite as a catalyst.* Fuel, 2011. **90**(5): p. 1847-1854.
43. Leion, H., et al., *The use of ilmenite as an oxygen carrier in chemical-looping combustion.* Chemical Engineering Research & Design, 2008. **86**(9A): p. 1017-1026.
44. Berguerand, N. and A. Lyngfelt, *Batch testing of solid fuels with ilmenite in a 10 kWth chemical-looping combustor.* Fuel, 2010. **89**(8): p. 1749-1762.
45. Leion, H., T. Mattisson, and A. Lyngfelt, *Solid fuels in chemical-looping combustion.* International Journal of Greenhouse Gas Control, 2008. **2**(2): p. 180-193.
46. Cuadrat, A., et al., *Behavior of ilmenite as oxygen carrier in chemical-looping combustion.* Fuel Processing Technology, 2012. **94**(1): p. 101-112.
47. Teresa Mendiara, A.J.a.P.G., *Chemical Looping Reforming of Generator Gas*, 2009, Department of Chemical and Biochemical Engineering: Lyngby, Denmark.
48. Aznar, M.P., et al., *Commercial Steam Reforming Catalysts To Improve Biomass Gasification with Steam−Oxygen Mixtures. 2. Catalytic Tar Removal.* Industrial & Engineering Chemistry Research, 1998. **37**(7): p. 2668-2680.
49. Rownaghi, A.A. and R.L. Huhnke, *Producing Hydrogen-Rich Gases by Steam Reforming of Syngas Tar over CaO/MgO/NiO Catalysts.* ACS Sustainable Chemistry & Engineering, 2012. **1**(1): p. 80-86.
50. Jerndal, E., et al., *NiO particles with Ca and Mg based additives produced by spray- drying as oxygen carriers for chemical-looping combustion.* Energy Procedia, 2009. **1**(1): p. 479-486.

51. Linderholm, C., et al., *160 h of chemical-looping combustion in a 10 kW reactor system with a NiO-based oxygen carrier.* International Journal of Greenhouse Gas Control, 2008. **2**(4): p. 520-530.
52. Neves, D., et al., *Characterization and prediction of biomass pyrolysis products.* Progress in Energy and Combustion Science, 2011. **37**(5): p. 611-630.
53. Glicksman, L.R., M. Hyre, and K. Woloshun, *Simplified scaling relationships for fluidized beds.* Powder Technology, 1993. **77**(2): p. 177-199.
54. Brage, C., et al., *Use of amino phase adsorbent for biomass tar sampling and separation.* Fuel, 1997. **76**(2): p. 137-142.
55. Pröll, T., et al., *Cold Flow Model Study on a Dual Circulating Fluidized Bed (DCFB) System for Chemical Looping Processes.* Chemical Engineering & Technology, 2009. **32**(3): p. 418-424.

Paper I

*The 13th International Conference on Fluidization - New Paradigm in Fluidization Engin*eering Vol. RP6, Article 115

Evaluation of Fluid Dynamics in a Hot and a Cold System of Interconnecting Fluidised Beds

Fredrik Lind*, Martin Seemann, Henrik Thunman
Department of Energy and Environment
Chalmers University of Technology
SE-412 96 Göteborg
T: +46 31 772 52 43; F: +46 31 772 35 92; E: fredrik.lind@chalmers.se

ABSTRACT

Operation controllability and fluid dynamics were evaluated in a system of interconnecting fluidised beds. Results indicate that the solid circulation is controllable and possible to determine from pressure measurements. Sufficient gas tightness of the loop-seals and flexibility in controlling of solid fluxes was indicated.

INTRODUCTION

Gasification is a promising method for converting crude biomass to renewable transport fuels, Devi et al (1). Nevertheless, the complications in handle the unwanted components in the raw gas, such as condensing hydrocarbons (often referred to as tars), are still a drawback and a major issue to solve, Li and Suzuki (2).

In this work, a novel technique for catalytic gas cleaning of biomass derived raw gas based on the concept for chemical lopping combustion (CLC), Lyngfelt et al (3) is investigated from an operational point of view. The concept of the gas cleaning system is to circulate catalytically active particles between two reactors, while the gases in the two reactors are kept separated. By means of the particles oxygen is transferred and reactions are catalysed. In contrast to CLC the required amount of oxygen transferred by the bed material is small, as only a share of the gas, the tars, should be combusted. Therefore, this work is focused on the control of the circulation rate as it is crucial for the development of this gas cleaning process. A survey of fluid dynamics is conducted in a cold system of interconnecting fluidised beds (IFBS), identical in size as an existing hot gas cleaning system.

The cold flow model used to determine the parameters relevant for circulation consists principally of a Circulating Fluidised Bed (CFB) and a Bubbling Fluidised Bed (BFB), Fig 1. The two beds are coupled by two fluidised loop-seals (LS); Superior Loop-Seal (SLS) and inferior Loop-Seal (ILS), which allows solid circulation, but prevents gas mixing between the two reactors. Inert gases are selected for the fluidization of the LS.

The identical design of the two systems is to avoid size related effects in fluid dynamics and to facilitate the transfer of fluidisation characteristics between the hot and the cold system. The advantage of the perspex cold system compared to the hot system is the possibility to visually revise the fluid dynamics and to measure the solid circulation rate. This knowledge received from the cold system is then transferable to the hot system by the simplified scaling laws presented by Glicksman et al (4).

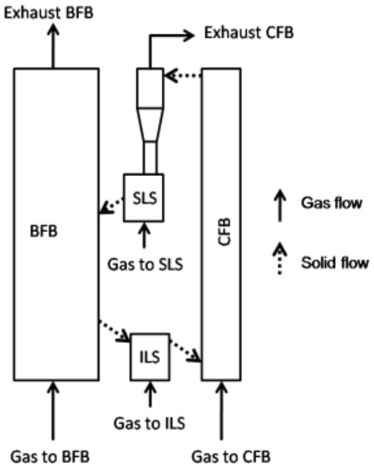

Figure 1 System of interconnecting fluidised beds

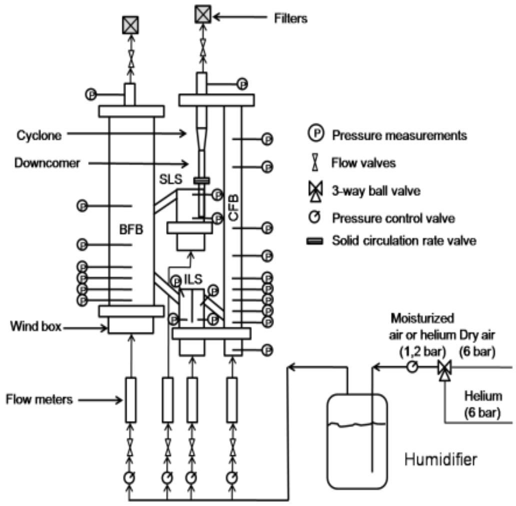

Figure 2 Cold system setup

Operations were conducted with both air and helium as fluidising media. Helium was selected because of the good agreement in fluidisation properties with the hot system.

The potential to control the operation of the gas cleaning IFBS is investigated from a set of experiments. The important criteria investigated in these measurements are:

i. **Solid circulation rate/solid flux:** Possibilities to control the solid flux between the CFB and BFB from varying the fluidisation velocity in the riser are investigated. The prospect of transferring the gained data between the cold and the hot model is evaluated from the simplified scaling laws by Glicksman (4). The solid flux determines the amount of oxygen that is transport via the solids to the BFB. In the gas cleaning unit this is important, as only enough oxygen supply for partial oxidations and breaking down of the unwanted components in the raw gas is desired.
ii. **Leakage via LS:** The influence in gas leakage from pressure difference between the CFB and BFB is evaluated. That this has a strong influence on the leakage has previously been shown by Eva Johansson et al (5).
iii. **System behaviour and supervision:** Relations between solid fluxes and pressure drop in the riser are investigated. The reason is to establish a relation to determine the solid fluxes in the hot unit from its pressure signals. Previously, Johnson et al (6) showed a correlation between the two parameters for a CFB boiler.
The behaviour of the fluidization in the system is characterised by the fluidisation regimes, which is determined from the sampled pressure signals. The different regimes in the riser reflect solid inventory and can be coupled to particle residence time, which is important for the oxidation of the catalyst.

iv. **Flexibility:** The possibility to control the solid fluxes by changing the velocity in the ILS is investigated. Pröll et al (7) indicated that regulating the fluidization in the LLS is influencing the solid flux in the system.

EXPERIMENTAL

The cold IFBS setup is shown in Fig 2. The system is supplied with air or helium at a pressure of 1.2 bars. To minimize effects from static electricity between the particles and the perspex surfaces the gas is humidified in an air tight water bottle. The moisturized gas is distributed to the four fluidising stems where the pressure is adjusted to a pressure slightly higher than atmospheric conditions, followed by manually tuning of the volumetric flow rates by the use of rotameters. The gas enters the reactor system via wind boxes, which are placed beneath the porous plates, in order to reduce potential pressure fluctuations in the gas feed. Flow control valves are mounted on the outlets of the CFB and BFB for regulation of pressure in each reactor. A filter is mounted after each flow control valve for collection of elutriated particles.

The system is equipped with 24 pressure taps and 24 pressure transducers. The pressure can be measured as differential pressure between two taps in the system or as differential pressure between one tap and atmospheric pressure. The pressure taps are inclined with an angel of 45° to prevent bed material from blocking the tubes. A manually controlled valve is mounted in the downcomer for solid circulation rate measurements.

Scaling Parameters

To transfer data between the cold and the hot reactor it is necessary to keep the following dimensionless numbers constant, Glicksman et al (4)

$$\frac{u_0^2}{gL}, \frac{\rho_s}{\rho_f}, \frac{u_0}{u_{mf}}, \frac{L_1}{L_2}, \frac{G_s}{\rho_s u_0}, \Phi, \mathit{Particle\ size\,distribution}$$

Table 1 summarizes the operating parameters and the dimensionless numbers for the CFB and BFB in the hot and cold system.

Table 1 Operation parameters and dimensionless numbers for the hot and cold unit

Parameter	Units	Hot CFB	Hot BFB	Cold CFB	Cold BFB
Media	gas	Air	Raw gas	Helium/Air	Helium/Air
Temperature	T (K)	1173	1173	293	293
Pressure	P (Pa)	1×10^5	1×10^5	1×10^5	1×10^5
Gas viscosity	µ (Pa s)	4.59×10^{-5}	3.43×10^{-5}	1.96×10^{-5} /1.82 $\times 10^{-5}$	1.96×10^{-5} /1.82 $\times 10^{-5}$
Gas density	ρ_f (kg/m^3)	0.297	0.276	0.146 / 1.188	0.146 / 1.188
Bed geometry	(m)	L	L	L	L
Particle diameter	d_p (µm)	150	150	150	150
Solids density	ρ_s (kg/m^3)	5240	5240	2600	2600
Superficial velocity	u_o (m/s)	1.00	0.039	1.00	0.039
Sphericity	Φ	0.9	0.9	0.84	0.84
Particle size distribution	p	P	p	p	p
Solid flux	G_s (kg/m^{2}s)	G_s	G_s	0.5 x G_s	0.5 x G_s
Dimensionless number	ρ_s / ρ_f (x10^4)	1.76	1.89	1.58 / 0.218	1.58 / 0.218
Dimensionless number	u_0/u_{mf}	40.82	1.12	40.32/37.45	1.57 / 1.46

Solid Circulation

Before each experiment, the system was refilled with new bed material and operated for 30 min in standard conditions with air, Table 2 to stabilize the conditions. Five sets of experiments for solid circulation were performed by varying the fluidisation velocity in the riser, from the highest velocity to the velocity were the bed started to have a slugging behaviour, Table 2 (Experimental run 1 – 5). The fluidisation velocity in the BFB, ILS and SLS was kept constant during each experiment.

The velocity in the riser was decreased with approximately 6 cm/s between each measurement for air and approximately 17cm/s for helium. The number of performed measurements at each fluidisation velocity of the riser is presented in Table 2. The solid circulation was measured by closing the valve in the downcomer with simultaneous start of timekeeping. Intermediate times were registered when the sand column reached 1, 2 and 3 cm of height in the downcomer. The registered heights (h_i') were recalculated to mass fluxes in downcomer ($G_{s,Downcomer}$) from the density of the bed material (ρ_{solid}) according to

$$G_{s,Downcomer} = \sum_{i=1}^{n} \frac{h_i'}{n} \cdot \rho_{solid} \quad \left[kg/m^2 s\right] \qquad (1)$$

Leakage

One leakage test was performed to investigate the potential slip of gases between the CFB and BFB. A gas chromatograph was coupled to the exhaust of the BFB and five measurements were performed at each fluidisation condition to determine the oxygen content. With the use of nitrogen in BFB, SLS, ILS and air in the CFB, the measured oxygen concentration in the BFB was coupled to the leakage of air from the CFB.

Before the experiment, the entire system was operated with nitrogen for 30 min with fluidisation velocities according to Table 2. The fluidisation velocity in the riser was varied from the highest velocity to the velocity were the bed started to have a slugging behaviour, Table 2.

Table 2 Experimental operation velocities for gases

Fluidisation media	Experimental run	CFB U_0 (cm/s)	BFB U_0 (cm/s)	SLS U_0 (cm/s)	ILS U_0 (cm/s)	Number of measurements[1]
Standard, Air	-----	100.22	3.92	3.60	3.09	-----
Air	1	120 → 61	3.92	3.60	2.57	2
Air	2	120 → 61	3.92	3.60	3.09	3
Air	3	120 → 61	3.92	3.60	3.26	3
Helium	4	201 → 116	5.65	5.73	5.55	3
Helium	5	201 → 132	5.65	5.73	6.48	5
Standard Nitrogen	-----	100.27	4.00	3.68	3.32	-----
Nitrogen (N) + Air (A)	6	107 → 74 (A)	4.00 (N)	3.68 (N)	3.32 (N)	5

[1] Number of measurements at each fluidisation velocity in the riser

RESULTS AND DISCUSSION

Scaling parameters

The dimensionless numbers for solid/gas density ratio between operation conditions for the hot and the cold unit operated with helium is well adjusted, with deviation of 11 % in the CFB and 20 % in the BFB. Whereas the dimensionless number for solid/gas density ratio in the comparison between the hot unit and the cold unit fluidised with air differs with a factor of 8 in the CFB and a factor 9 in the BFB. The ratio for superficial velocity and minimum fluidisation velocity deviates with 1 % for the CFB and 40 % for the BFB between the hot unit and the cold unit fluidised with helium. Whereas the ratio for superficial velocity and minimum fluidisation velocity deviates with 9 % for the CFB and 30 % for the BFB between the hot unit and the cold unit fluidised with air. The deviation in the ratio between superficial velocity and minimum fluidisation velocity for the BFB is of less importance in the gas cleaning IFBS compared to the same ratio for the CFB. The reason to this is that the solid flux, controlled by the fluidisation properties in the riser, is more vital for the operation.

Sufficient agreement in the dimensionless numbers for the scaling relationship between the hot unit and cold unit fluidised with helium indicates that fluid dynamic properties are transferable between the two systems. In the case air is used for the fluidization, the deviation in solid/gas density ratio between the hot unit and the cold unit implicates that results from transferring fluid dynamics between the systems are more approximate.

Solid Circulation

Figure 3 shows that, independent of gas, efficient control of solid circulation between the two reactors can be achieved by varying the fluidisation velocity in the riser. The scattering effect at high velocities in the riser is coupled to the visual reading of the sand column height in the downcomer during measurements of the solid flux; the height of the column is increasing too fast to get a precise measure with the applied method.

In the air experiments two distinct plateaus are formed in the experiments with low fluidisation velocity in the ILS. This indicates that the friction in the ILS exceeds the hydrostatic pressure of the sand column surplus in the BFB reactor and hinders a smooth particle transport. The lower solid circulation can be explained by wall friction induced by the small volume in the ILS and is in accordance with previous observation by Pröll et al (7). This effect gives one additional possibility to control the solid inventory in the BFB by using the ILS as solid flow valve.

From Fig 3, it is evident that the solid circulation controllability is valid for both air and helium operation, even if, the solid/gas density ratio is seven times higher for air than for helium.

Pressure Drop in Riser

In Fig 4, solid circulation is plotted as a function of pressure drop in the riser for the experimental runs 3 and 5. The results show that the pressure drop in the riser is an adequate parameter to determine the transport of solids between the CFB and BFB, which agrees well with work performed by Johnson et al (6). Close agreement is shown in the trends for air and helium. The agreement point to that the difference in gas properties between air and helium are of low importance for stipulating the solid flux, which indicates that the method for determine solid flux should be valid also in the hot system.

The amplitude of the sampled pressure drop signal in the riser reflects the fluidisation regime in the riser, Fig 5. During pneumatic transport a smooth and non oscillating signal is received whereas for the transition to a fast fluidised bed the signal starts to oscillate. During the transition from fast fluidised bed to slugging bed an even more oscillating signal with increased amplitude is received. The slugging bed regime in the riser is not a preferred operation condition, as the pressure fluctuations can have impact on the whole system. The possibility to observe different transitions in regimes indicates that pressure fluctuations, coupled to the bed movement in the riser, can be reduced.

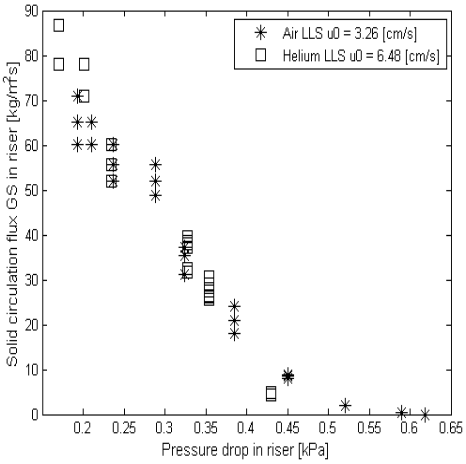

Figure 3 Solid circulation rates versus pressure drop in riser

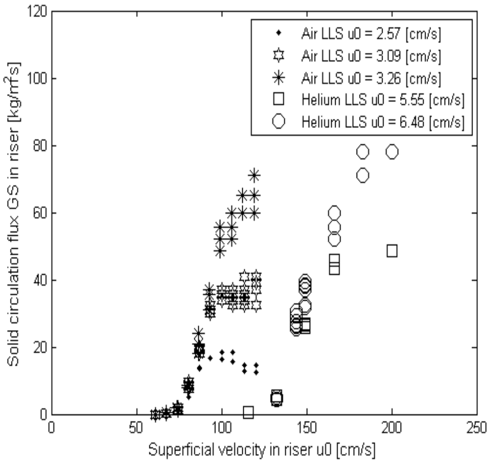

Figure 4 Solid circulation fluxes versus superficial gas velocity in riser

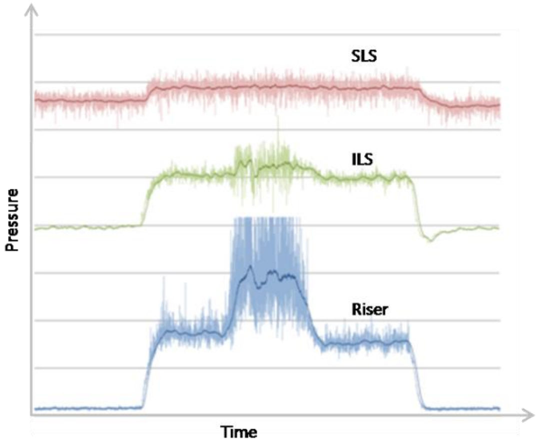

Figure 5 Pressure signals in riser

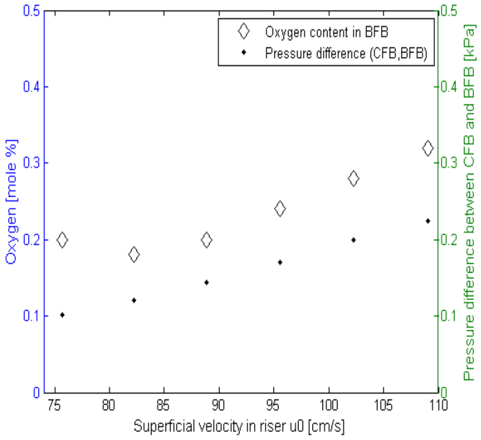

Figure 6 Oxygen leakage and pressure difference between CFB and BFB versus superficial velocity in riser

Leakage

In Fig 6, oxygen concentration in the CFB and pressure difference between the CFB and BFB are plotted against superficial velocity in the riser. The figure also shows that the oxygen concentration in the BFB is less than 0.4 mole % at the highest fluidisation velocity in the riser, which indicates that the performance of the loop-seals is sufficient. Nevertheless, a trend in oxygen concentration can be notable; the oxygen concentration in the BFB is increasing with increased superficial velocity in the CFB. The reason for the higher oxygen concentration is coupled to the increased pressure difference between the CFB and BFB, caused by the raised gas flow in the riser. The leakage related to this pressure difference agrees well with work performed by Johansson et al (5). The oxygen concentration profile during increased superficial velocity in the riser can most likely be levelled out by a slightly increase of the BFB operation pressure. In the hot and the cold unit the pressure in the BFB can be changed by throttling the exhaust gases.

CONCLUSION

The possibilities to control solid circulation rate in a system of interconnecting fluidised beds for cleaning of biomass derived raw gas have been investigated. Experiments were performed in a perspex cold system identical in size as an existing hot gas cleaning system. The difference in solid/gas density ratio between hot and cold system was compensated by the use of helium as fluidising media. The performed experiments points out that, independent of air or helium, solid circulation rate can be efficiently controlled by the fluidisation velocity in the riser. Good agreement of the dimensionless numbers from the scaling principles by Glicksman et al (4), between the helium experiments in the cold system and the gases in the hot system was achieved. The agreement implies that the measured solid fluxes in the cold system are transferrable to the hot system with the only correction for the difference in solids density between the systems. The results from the measurements are

- A coupling in solid circulation pattern between the air and helium experiments were presented, which prove that the less expensive air can be used as a complement to helium.
- Flexibility in controlling solid fluxes in the riser and solid inventory in the bubbling fluidised bed was demonstrated by using the inferior loop-seal as a solid throttling valve.
- The pressure profiles in the riser is shown to be an adequate parameter for determine solid circulation in the system.
- The height of the amplitude in the sampled pressure signal is a good indicator of the fluidisation regimes in the riser.
- Leakage experiment pointed out that sufficient gas tightness in the loop-seals is achieved for the reactor application.

NOTATION

IFBS: Interconnecting fluidised beds
CFB: Circulating fluidised bed
BFB: Bubbling fluidised bed
LS: Loop-seal
SLS: Superior loop-seal
CLC: Chemical looping combustion
ILS: Inferior loop-seal
h'_i : Height of sand column in downcomer per second [m/s]
$A_{c,downcomer}$: Cross-section area of downcomer [m]

REFERENCES

1. Lopamudra Devi, Krzysztof J. Ptasinski, Frans J. J G. Janssen. A review of the primary measures for tar elimination in biomass gasification processes. Biomass and Bioenergy, 24 (2003) 125 – 140
2. Chunshan Li, Kenzi Suzuki. Tar property, analysis, reforming mechanism and model for biomass gasification – an overview. Renewable and Sustainable Energy Reviews 13 (2009) 594 – 604
3. A. Lyngfelt, B. Leckner, T. Mattisson. A fluidized-bed combustion process with inherent CO2 separation; application of chemical-looping combustion. Chem Eng. Sci 56 (2001) pp. 3101 - 3113
4. L.R. Glicksman, M. Hyre, K. Woloshun. Simplified scaling relationships for fluidized beds. Powder Technology, 77 (1993) 177 – 199
5. E Johansson, A Lyngfelt, T Mattisson, F Johansson. Gas leakage measurements in a cold model of an interconnecting fluidized bed for chemical-looping combustion. Powder Technology 134 (2003) 210 – 217
6. F. Johnsson, A. Vrager, B. Leckner. Solids flow patter in the exit region of a CFB-furnace –influence of exit geometry. 15th Int. Conference on Fluidized Bed Combustion, Savannah, 1999
7. T. Pröll, K. Rupanovits, P. Kolbitsch, J. Bolhàr-Nordenkampf, H. Hofbauer. Cold flow model study on a dual circulating fluidized bed system for chemical looping processes. Chem. Eng. Technol. 32 (2009) No. 3 418 - 424

Paper II

I&EC research
Industrial & Engineering Chemistry Research

ARTICLE

pubs.acs.org/IECR

Continuous Catalytic Tar Reforming of Biomass Derived Raw Gas with Simultaneous Catalyst Regeneration

Fredrik Lind,[*,†] Martin Seemann,[†] and Henrik Thunman[†]

[†]Department of Energy and Environment, Division of Energy Technology, Chalmers University of Technology, SE-412 96 Gothenburg, Sweden

ABSTRACT: A novel concept for secondary catalytic tar cleaning with simultaneous regeneration of the catalysts is presented in this work. The process is demonstrated by an initial experiment with producer gas from the Chalmers biomass gasifier using ilmenite ($FeTiO_3$) as catalytic bed material. The tar cleaning system was operated at 800 °C and fed with raw gas from the Chalmers biomass gasifier, in which silica sand was used as bed material and the gasification was performed with steam. The tar content of the gas emerging from the gasifier was roughly 30 g_{tar}/Nm^3_{gas}. The experiment showed that the catalyst was continuously regenerated from carbon deposits, and the ilmenite reduced the total amount of tar by 35% at a gas residence time in the bed of 0.4−0.5 s. Branched hydrocarbons and phenols were more or less completely reformed, while there was an increase of stable aromatic rings (benzene, naphthalene). The catalyst showed high activity in water-gas shift reactions, and the H_2/CO ratio was shifted from around 0.7 prior to the reactor to almost 3 after the reactor.

INTRODUCTION

Gasification is recognized as an effective route for converting the chemical bound energy in lignocelluloses to a gaseous fuel. However, in addition to the major gas components (H_2, CO, CO_2, CH_4, H_2O, and light hydrocarbons), the raw gas generally contains unacceptable amounts of condensable hydrocarbons.[1−5] These hydrocarbons, often referred to as tars, start to condense already at 350 °C[6] and are associated with operational problems such as clogging and blockage of equipment downstream from the gasifier. Tars are included in a comprehensive classification of complex mixtures of hydrocarbons from 1 to 5-ring aromatic compounds, oxygen and sulfur-containing hydrocarbons.[2,3] The tar components preclude the immediate use of the raw gas as fuel for internal combustion engines and gas turbines. Consequently, upgrading the raw gas to a gaseous fuel or to a primary gas suitable for liquid fuel production requires gas cleaning either as a primary or as a secondary measure.

Extensive work has been performed in the area of tar cleaning along with gas conditioning, and several approaches suitable for gas cleaning are reported in the literature[1,7−10] and review papers.[2,5] In principal, hot gas cleaning is preferable to techniques for wet cleaning, since wet cleaning is associated with large quantities of wastewater/solvents and a thermodynamic penalty coupled with rapid gas cooling.[8] However, scrubbing is still state-of-the-art. Nevertheless, primary and secondary techniques associated with catalytic tar reforming are seen as the most promising hot gas cleaning methods. Primary catalytic tar cleaning involves catalytic bed material already in the gasification step itself,[2] to promote cracking of the tars. In this manner, the tar reactions take place under the same operating conditions as the gasification reactions. Secondary catalytic tar cleaning is performed in fixed or fluidized beds downstream from the gasifier and the technique can be summarized by means of three features: 1) catalyst reactor temperatures are thermally integrated with the gasifier exit temperature, 2) the composition of the product gas can be catalytically adjusted, and 3) steam can be added to the catalyst reactor to ensure complete reforming of tars.[5] In this manner, the technique for secondary tar cleaning becomes more flexible toward optimization in comparison to primary tar cleaning. But, regardless of primary or secondary measures, several studies[2,5,8,11,12] confirm that the tar content in the product gas can be reduced and the gas composition can be catalytically adjusted. However, the activity of the catalyst can decline over time, and the catalyst can finally become poisoned if it is continuously exposed to species like sulfur, chlorine, and alkali metals, components which all are present in the raw gas to some extent.[5] It is also concluded that high tar content involves carbon formation on the catalytic surfaces, which can cause severe deactivation of the catalyst after short operating time.[2,5]

Carbon formation on catalytic surfaces has been investigated by such scientists as Caballero et al.[8] They emphasized that the tar content in a feed to a downstream fixed bed catalytic tar reforming reactor with a nickel based catalyst should be kept below 2 g_{tar}/Nm^3_{gas} to avoid deactivation of the catalyst. Raw gas from gasification at low temperatures (below 1000 °C), that does not apply primary measures, yield a concentration of tar that is considerably higher than 2 g_{tar}/Nm^3_{gas}. For example, Rapagnà et al.[10] performed biomass gasification in a fluidized bed with silica sand at 770 °C and reported a tar content of 43 g_{tar}/Nm^3_{gas}.

Several approaches to minimize the tendency to form carbon on the surface of the catalyst are reported in the literature surveyed. For example, catalyst deactivation as a result of carbon deposits was compared in terms of fixed and fluidized beds for secondary tar cleaning by Baker et al.[13] They found that carbon deposits and catalyst deactivation was significantly lower on the catalysts in the fluidized bed. In parallel with secondary catalytic tar cleaning,

Received: March 30, 2011
Accepted: September 2, 2011
Revised: August 29, 2011
Published: September 07, 2011

dx.doi.org/10.1021/ie200645s | *Ind. Eng. Chem. Res.* 2011, 50, 11553–11562

Seemann et al.[14] reported that the internal catalyst circulation in a fluidized bed for methanation contributed to keeping the catalyst free of carbon deposits. The methanation experiments showed that carbon deposits were formed on the catalyst in the bottom zone of the bed, and as the catalyst was transported upward in the bed, the carbon deposits were removed by hydrogenation and gasification reactions with steam. Miyazawa et al.[15] reported a lower carbon yield on various nickel catalysts during partial oxidation than during steam reforming. This phenomenon can be explained by carbon combustion with O_2 during the catalyst fluidization. Another process dealing with both the conversion of hydrocarbons and formation of carbon on active surfaces is fluid catalytic cracking[16] (FCC). In FCC reactors, the problem of carbon formation is tackled by continuous regeneration of the catalyst surfaces, in this case a zeolite.

In this work a new method for secondary catalytic tar cleaning is demonstrated utilizing the experience of the FCC technology. The tar cleaning is performed in a dual fluidized bed reactor system that simultaneously removes carbon deposits on the catalyst surfaces, even at high tar contents. The proposed process is applicable to all types of biomass gasifiers, regardless of whether the gasifier technique includes primary measures for tar reduction or not. The tar cleaning system can be thermally integrated with the gasifier outlet temperature, which leads to minimal heat losses. The object is to reform the tar components to useful gas molecules by letting the tar containing producer gas react with both circulating oxidized and reduced metal oxides in a tar reformer reactor. Oxygen from the bed material is consumed as tars are partially oxidized, thereby producing a reduced metal oxide, which also acts as a tar reforming catalyst. The catalyst is then reoxidized and regenerated from carbon deposits in an air-fed oxidizing reactor followed by circulation back to the tar reforming reactor. Commercially available catalyst e.g. based on nickel, manganese, copper, or iron can be used in the system. However, the regeneration concept and the oxygen transport serve as an additional driving force for tar removal and opens possibilities for new catalytic bed materials. That is, using this method, probably less expensive and less toxic materials than the frequently used nickel can be applied as catalysts for secondary catalytic tar cleaning. In this manner, costs associated with long-term storage of hazardous waste can be neglected and it is possible to develop a green product, where the whole process chain is more environmentally friendly. The method can, depending on the choice of catalyst material and operating temperature, be further used to catalytically adjust the producer gas and transport molecules other than oxygen. An example of this is the possibility to reduce the sulfur content in the raw gas. Sulfur can be transported from the reformer reactor to the regenerator reactor, where it is oxidized simultaneously as the catalyst is regenerated in air.

The proposed catalytic process for reforming tars followed by catalyst regeneration resides to a large extent in the well-known technique of fluid catalytic cracking (FCC).[16] Integration of the proposed tar cleaning technique with a biomass gasifier is thereby comparable to an installation of a FCC unit in an oil refinery. This implies that increased process complexity induced to a gasifier system can be tackled with experience from FCC installations. The major difference between the two concepts is the properties of the catalysts. In the proposed method the tar cleaning catalysts support the tar reactions with catalytic surfaces, heat, and oxygen and can additionally be used for transporting other molecules within the system. The method is, therefore, called Chemical Looping Reforming (CLR). The technique is further investigated by means of a first experiment in a reactor system specially developed and erected within the project.

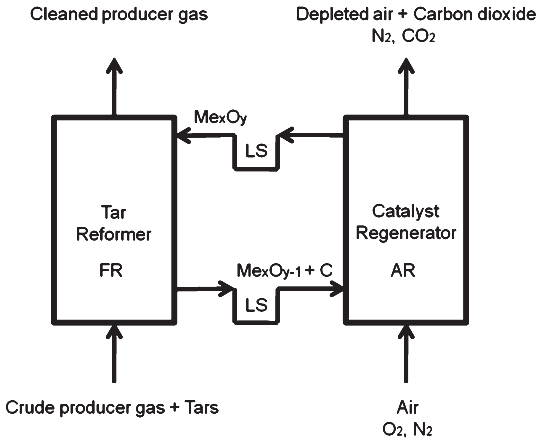

Figure 1. CLR system for tar removal.

In this experiment, a naturally occurring iron−titanium ore ($FeTiO_3$, known as ilmenite) was used as catalyst together with raw gas from the Chalmers biomass gasifier.[17,18] The fundamental criteria investigated to assess the performance of the tar cleaning method are as follows:

- The possibilities of obtaining continuous transport of catalysts and oxygen from the regenerator to the reformer are investigated.
- The possibilities of reforming tars in the reactor system by using a natural ore like ilmenite.
- Investigating the possibility of maintaining high activity of the catalyst by continuous oxidation of the formed carbon in the regenerator reactor.

THEORY

The tar cleaning process explored in this work is based on the CLR process, originally presented by Mattisson et al.[19] The reactor system is operated at atmospheric pressure and utilizes a circulating metal oxide (MeO) as catalyst, oxygen supplier, and heat carrier for reforming reactions and partial oxidation of the tar components into CO and H_2. The very small amount of transported oxygen by the MeO is what differs this principal of CLR the most from the originally presented process. This is also the reason for why the commonly used name oxygen carrier has been changed to catalyst in this proposed tar cleaning method.

The reactor system (CLR-system) consists of two reactors, one for air (AR) which is the regenerator reactor and one for the tar containing producer gas called fuel reactor (FR) or reformer reactor, Figure 1. Two loop seals (LS), fluidized with inert gas or steam, prevent gas cross-contamination of the effluents from the respective reactor but enable the catalyst to circulate between the two reactors. In the reformer reactor, the Me_xO_y is reduced to Me_xO_{y-1} during the partial oxidation of the tar components (C_nH_m) in the raw gas according to reaction 1, which usually is an endothermic reaction.[20] Besides the desired tar reforming reaction, additional carbon forming reactions cause carbon deposits on the Me

$$C_nH_m + (n - n_1)Me_xO_y \rightarrow (n - n_1)CO + (0.5m)H_2 + (n - n_1)Me_xO_{y-1} + n_1C \tag{1}$$

The reduced metal oxide Me_xO_{y-1} is also acting as catalyst for tar reforming in the presence of reforming mediums* like water

Table 1. Potential Tar Decomposing Reactions

reaction	equation	reaction number
steam reforming	$C_nH_m + nH_2O \rightarrow nCO + (n + 0.5m)H_2$	(3)
steam dealkylation	$C_nH_m + xH_2O \rightarrow C_iH_j + pH_2 + qCO$	(4)
hydro cracking	$C_nH_m + (n\cdot 2 - (m/2))H_2 \rightarrow nCH_4$	(5)
hydro dealkylation	$C_nH_m + xH_2 \rightarrow C_iH_j + qCH_4$	(6)
dry reforming	$C_nH_m + nCO_2 \rightarrow 2nCO + 0.5mH_2$	(7)
cracking	$C_nH_{2n+2} \rightarrow C_{n-1}H_{2(n-1)} + CH_4$	(8)
carbon formation	$C_nH_{2n+2} \rightarrow nC + (n + 1)H_2$	(9)

steam or carbon dioxide in the raw gas according to the simplified reaction 2

$$C_nH_m + Me_xO_{y-1} + H_2O^* + CO_2^* \rightarrow C_iH_j + H_2 + CO \tag{2}$$

Simultaneously, as the Me_xO_{y-1} is reoxidized to Me_xO_y in a strongly exothermic[20] reaction in the AR, carbon deposits on the catalytic surfaces are oxidized to CO_2 according to reaction 2a

$$n_1Me_xO_{y-1} + n_2C + (n_1/2 + n_2)(O_2 + 3.77N_2) \rightarrow n_1Me_xO_y + n_2CO_2 + (n_1/2 + n_2)(3.77N_2) \tag{2a}$$

To enable molecular (in this first step oxygen) transport, another type of catalyst than the zeolite-based has to be explored. Comprehensive work on finding suitable catalysts for primary and secondary tar cleaning along with oxygen-carriers for Chemical Looping Systems (CLS) has been undertaken over the past decade. Studies show that metal oxides, such as NiO,[5,8,21] Fe_2O_3,[5,11,21] Mn_3O_4,[21] and CuO[212] supported on various inert materials are promising.

So far, ilmenite has only been tested as a tar catalyst[22,23] once; however, ilmenite has been commonly used as oxygen-carrier for CLC operations.[24−26] CLC operations have demonstrated that ilmenite particles are not fully oxidized in their crude state. The degree of oxidation increases with repeated cycles in the CLS.[24] During the cyclical periods of oxidation and reduction, the porosity of the particles increases, while the reactivity also increases. The increasing reactivity can most likely be attributed to the enlarged surface area, as a result of the porous structure. A three-day CLC experiment carried out by Leion et al.[24] showed that the area increased from 0.11 to 0.28 m^2/g. The conclusion drawn in that work was that ilmenite is an attractive oxygen carrier for the CLC process, with no decrease in reactivity with pure methane or syngas (50% CO and 50% H_2). In addition to operating with gaseous fuel Berguerand and Lyngfelt[27] showed that the properties of ilmenite were sufficient in order to convert solid fuel in CLC.

The chemistry involved in catalytic tar decomposition of producer gas is a complex mix of hydrocarbon decomposition and equilibrium reactions. The tar reaction mechanisms have been investigated, for example, by Simell[28] et al., by using toluene as a tar component in hot catalytic gas cleanup. Based on these toluene experiments, they proposed a set of decomposition and equilibrium reactions (3−7 and 9) summarized in Table 1.

Table 2. Equilibrium Reactions

reaction	equation	reaction number
water-gas shift	$CO + H_2O \leftrightarrow H_2 + CO_2$	(10)
methanation	$CO + 3H_2 \leftrightarrow CH_4 + H_2O$	(11)
methanation	$2H_2 + C \leftrightarrow CH_4$	(12)
water gas	$CO + H_2 \leftrightarrow H_2O + C$	(13)
	$CO_2 + 2H_2 \leftrightarrow 2H_2O + C$	(14)
Boudouard	$C + CO_2 \leftrightarrow 2CO$	(15)

The proposed reaction scheme is complemented by reaction 8. In Table 1, toluene is replaced by C_nH_m, which is a general representation of the tar molecules in the producer gas from a biomass gasifier. In comparison to toluene, the tar composition in a gasifier includes at least 150 different tar molecules, which vary in molecular weights from that of benzene to weights higher than pyrene. As the molecular weight of the tars is increased so is usually also the dew point temperature, which normally increases the operating problems. The proposed reactions are here used to explain what might happen in the CLR system. In addition to the partial oxidation of the tar components, reaction 1, studies have shown that steam and dry reforming reactions (3 and 7) are catalyzed by metals from group VIII.[28−30] This implies that the Fe content of the ilmenite, together with the water and carbon dioxide content in the producer gas, will induce both steam and dry reforming. Calculations performed by Simell[28] et al. showed that dry reforming was more thermodynamically favored than steam reforming reactions at temperatures above 830 °C.

A drawback of the reforming catalyst is the risk of carbon forming reactions, which are also catalyzed by these metals. Three exothermic carbon forming reactions that are favored below 650 °C are listed in Table 2; the Boudouard reaction 15 and two water gas reactions 13 and 14. Reaction 9, listed in Table 1, is an additional carbon forming reaction which is enhanced at higher temperatures. Furthermore, the water-gas shift reaction 10 is reported to be catalyzed by Fe-based catalysts.[11]

■ EXPERIMENTAL SET UP AND PROCEDURE

A drawing of the CLR system is shown in Figure 2. The geometrical size of the reactor is given in Table 3, where the height is defined as the distance between the upper part of the porous plate and the top of each reactor or LS part. The system is manufactured from RA 253 MA, a high chromium austenitic stainless steel with a temperature resistance of up to 1100 °C. The CLR system is equipped with 10 pressure taps and 10 thermocouples for supervision. The pressure can be measured as the differential pressure between two taps in the system or as the differential pressure between one tap and the atmospheric pressure. The taps are inclined at an angle of 45° to prevent blocking of particles, and they are connected to a three-way ball valve to facilitate nitrogen purging. In this bench-scaled CLR system, the FR is designed as a bubbling fluidized bed to provide a good estimation of the gas/solid contact, but the FR can equally well be a circulating fluidized bed. The AR is a circulating fluidized bed, and the gas/solid separation is performed in a cyclone. The gases enter the reactor system by means of wind boxes, which are placed beneath the porous plates in FR, AR, SLS, and ILS to reduce potential fluctuations of pressure in the gas feed.

The experimental setup of the CLR system is shown in Figure 3. A jacket for air cooling is welded on the outside of

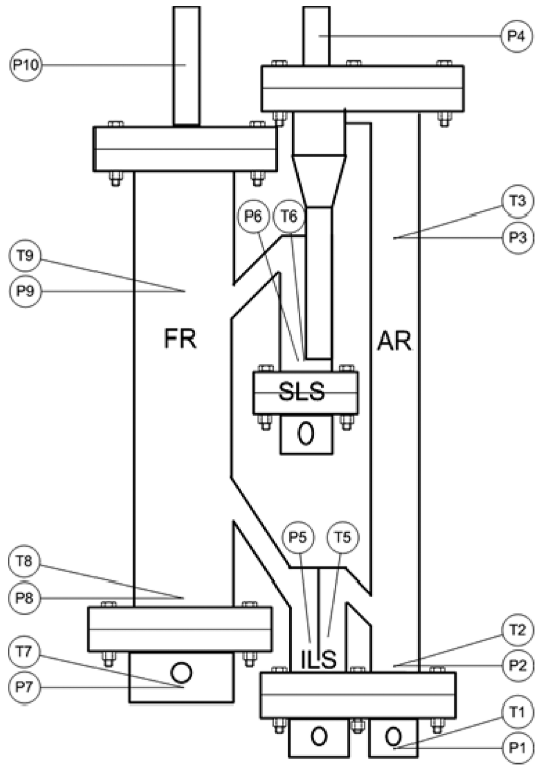

Figure 2. The CLR reactor.

Table 3. Geometrical Sizes of the CLR-System

	cross-sectional (mm)	height (mm)
fuel reactor (FR)	50 × 50	380
air reactor (AR)	20 × 20	460
superior loop seal (SLS)	23 × 23	120
inferior loop seal (ILS)	23 × 23	50

the FR (1), the cooling surface covering the reactor walls in a level corresponding to the height of the bed. The reactor system is placed in an oven consisting of two halves, where the two halves can be heated separately (2). Separate heating together with the air-cooled jacket on the FR enables the operation to take place with a temperature difference of around 200 °C between the two reactors. The reactor system is operated at a subatmospheric pressure of −4 to −6 kPa as a result of the pressure level in the gasifier, which due to safety considerations is operated slightly below atmospheric pressure. The gas for transportation and regeneration of the catalysts in AR is provided by two mass flow regulators connected in parallel, one regulator for air (3) and the other one for nitrogen (4).

The two regulators can be operated independently of each other in order to control inlet concentration of oxygen. The resulting gas mixture is preheated in an electrically heated Teflon tube (5) before being fed to the wind box. The SLS and the ILS are fluidized with helium, which is controlled by two independent mass flow regulators (6 and 7). The raw gas line (8) from the gasifier to the FR is heated to 400 °C in an electrically heated stainless steel tube to avoid tar condensation. A T-connection (9) for nitrogen supply from a mass flow regulator (10) is mounted on the raw gas pipe just before the inlet to the FR to enable inert conditions in the FR before introducing raw gas.

A tar measuring port (11) for SPA[31] sampling is integrated in the electrically heated outlet tube of the FR. The heated outlet tube downstream of the SPA-port is connected to a venturi nozzle (12), in which the raw gas is mixed with iso-propanol. The iso-propanol serves as a solvent for the remaining tar components to protect downstream equipment from tar fouling. A heated probe is immersed into the upper part of the nozzle in order to avoid tar condensation before the gas is mixed with the solvent. Downstream of the venturi nozzle, the solvent and gas mixture is cooled in a tube and shell heat exchanger (13). The condensate is separated from the gases by gravity and is transported from the bottom of the heat exchanger to a collecting vessel (14). A portion of the collected liquid is continuously recirculated back to the venturi nozzle by a pump. The gas is separated from the liquid slightly above the end of the heat exchanger and is transported through an additional cooling and drying step where the gas is cooled to 2 °C in a Peltier cooler (15). The remaining moisture is removed in a silica gel filter (16) to protect the downstream gas chromatograph. The aim with the second cooling step is to increase the operating time of the gas conditioning system. As the moisture content is minimized already in the Peltier cooler more operating time can be achieved without the need to regenerate the silica gel. As the physical size of the reactor system limits the height of the bed material column in the SLS, the differential pressure between AR and FR is kept below 500 Pa to prevent leakage between the two reactors. To retain this pressure difference despite external disturbances, for example from the gasifier, two pneumatic differential pressure control valves are installed, one downstream of the FR (17) and the other downstream of the AR (18). The two valves throttle the flow to the gas pumps in such a way that the differential pressure is kept within the allowed interval. After the gas pump (19), the dry reformed gas flow downstream the FR is measured by a volumetric membrane flow meter (20) followed by a rotameter (21). The composition of the cleaned producer gas (H_2, CO, CO_2, CH_4, C_2H_2, C_2H_4, C_2H_6, and N_2) is analyzed by means of a micro Gas Chromatograph (22) (Micro-GC Varian 4900). The micro-GC is equipped with a mole sieve 5A column that has argon as carrier gas and a PoraPLOT Q-column that has He as carrier gas. Entrained catalyst particles that follow the depleted air leaving the AR are separated from the gas in a secondary cyclone (23). The particles from the secondary cyclone are transferred through a tight gas lock back to the FR through the stepwise opening and closing of two control valves (24). Downstream of the secondary cyclone, the gas is conditioned in the same manner as downstream the FR with the exception that no iso-propanol is used as no tars are present here.

The content of CO, CO_2, and O_2 in the gas stream leaving the AR is analyzed online by Non Dispersive Infrared analyzers (25) for CO and CO_2, respectively, paramagnetic analyzer (25) for O_2, Table 4.

As the feeding temperature of the raw gas is around 400 °C, the control of the gas flow is performed on the cold side downstream the FR. This is done by throttling the diaphragm valve upstream the gas pump, operating with constant number of revolutions. Consequently, when controlling the gas flows and evaluating data from the CLR-system, one has to pay attention to water consuming and volume increasing reactions in the FR, e.g. the water-gas shift reaction. To obtain constant raw gas flow between two experiments, an iterative procedure is necessary.

A third gas sampling system, similar to the one described for the gas conditioning system used for the gas from the FR is

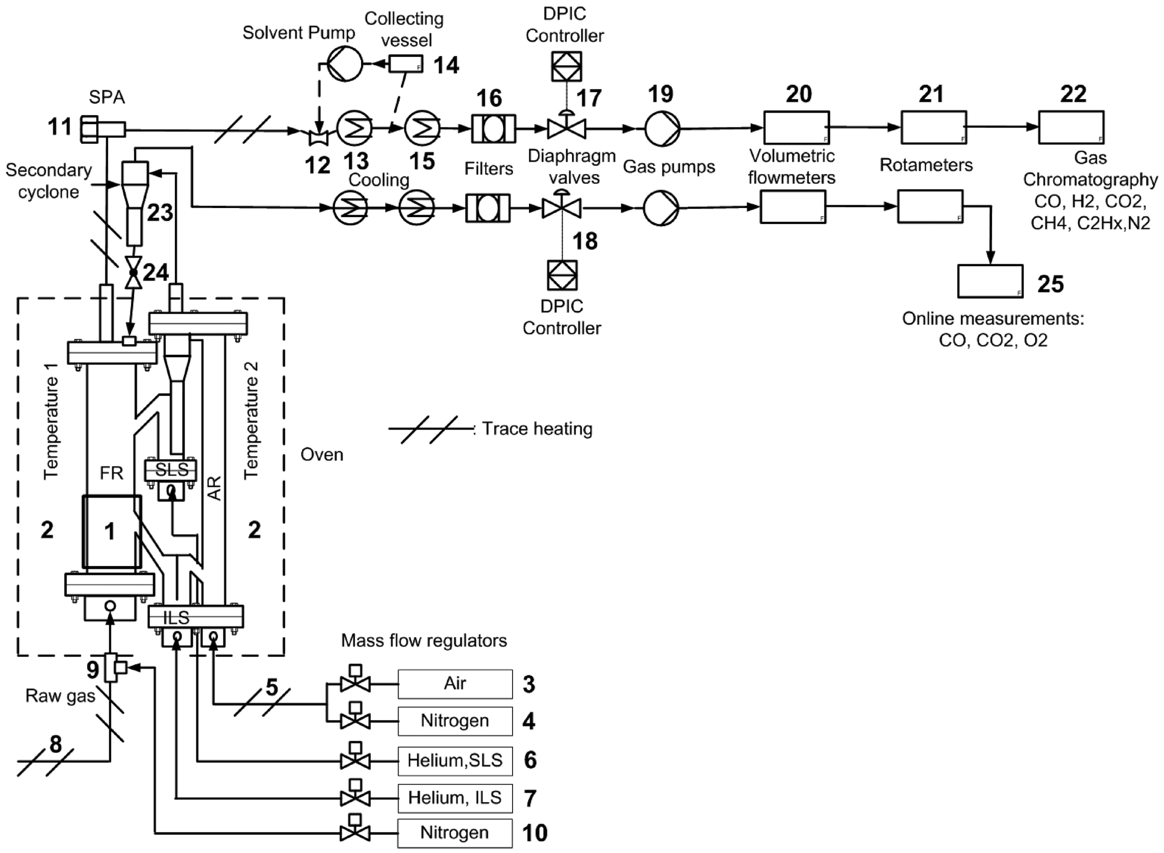

Figure 3. CLR system setup.

Table 4. Gas Analyzing Instruments Downstream of the AR

instrument	measuring interval (mole %)	detection limit (ppm)
O_2	0−25	1250
CO	0−1	50
CO_2	0−100	5000

employed to determine the gas composition and tar content of the raw gas from the gasifier. The raw gas feed to the gasifier sampling system is supplied by a separate heated stainless tube connected to the raw gas pipe downstream of the gasifier and the gas flow is controlled by a needle valve. The raw gas is analyzed using the same micro-GC as the CLR system.

Silica Sand. Two reference experiments was carried out to ensure that no catalytic effects were induced by the reactor material itself (containing 10% nickel), by comparing the dry gas composition and tar content in and out of the CLR system. The experiments were conducted with silica sand during two consecutive days at the temperatures 740 °C (Silica sand 740 °C) and 815 °C (Silica sand 815 °C) in the FR, Table 5.

Table 5 shows properties for the raw gas and operating conditions in the gasifier together with operating conditions and bed material properties for the CLR. The FR was fluidized with raw gas, i.e. the CLR system was run without solid circulation or oxygen supply. Both experiments, Silica sand 740 °C and Silica sand 815 °C, were started by defining the raw gas composition via the gasifier sampling system during the two-hour heating sequence of the CLR reactor. The dry raw gas composition was sampled every three minutes by the GC, and the tar composition was sampled with six SPA columns during a time period of 15 min at stable gasifier operation.

The gas flow in the FR, which was communicating with the atmosphere via the FR inlet, was adjusted by throttling the gas pumps with air. Completing the heating sequence, the raw gas pipe from the gasifier was connected to the CLR, and nitrogen was purged into the T-connection. The nitrogen flow was adjusted slightly higher than the measured gas pump flow to repel the raw gas back to the gasifier, operating at lower pressure. The CLR system was started with nitrogen to remove oxygen and to enable a smooth transition from inert fluidization to full raw gas operation. Silica sand was poured into the FR, after which the procedure to reach full raw gas operation was initiated. The nitrogen feed to the FR was stepwise decreased by 5% (0.25 L/min), to replace the nitrogen by raw gas. Thus, the raw gas was introduced to the FR by a stepwise increasing concentration gradient until the nitrogen was fully replaced by raw gas. The FR was fluidized with raw gas for 2 h, at operating conditions according to Table 5.

Sampling of the dry gas composition from the FR was done every third minute in the micro-GC, and the sampling of tar was performed by a set of six SPA samples during a time period of 15 min at stable CLR operation. After the completed raw gas run, the CLR system was shut down in the reverse order of the start-up procedure, i.e. nitrogen was stepwise introduced with 0.25 L/min until no hydrocarbons were detected by the GC. The raw gas pipe was removed from the FR inlet, and the reactor system was cooled during fluidization with air from the surrounding. An additional two hour period of raw gas sampling was performed via the gasifier sampling system for both Silica sand 740 °C and Silica sand 815 °C. This repeated experiment was performed in

Table 5. Operating Properties for Gasifier and CLR, Together with Raw Gas Composition from Gasifier

properties	units	Silica sand 740 °C	Silica sand 815 °C	Ilmenite 800 °C
gasifier:				
fuel	------	wood pellets	wood pellets	wood pellets
bed temperature	(°C)	800	780	800
bed material	-----	silica sand	silica sand	silica sand
raw gas composition (dry):				
hydrogen	(mole%)	20.5	21.3	22.6
carbon monoxide	(mole%)	29.5	29	33.2
carbon dioxide	(mole%)	16.3	15.8	15.2
methane	(mole%)	11	10.9	12.5
light hydrocarbons (C_2H_x)	(mole%)	4.9	4.7	5.0
nitrogen	(mole%)	18.2	17.1	11.2
condensable:				
tars	(gtar/Nm^{3}gas)	≈31	≈27	≈27
steam content, raw gas	(mole%)	55	57	53
CLR:				
temperature	(°C)	740	815	800
air feed in AR	(L/min)	-----	-----	0.26
nitrogen feed in AR	(L/min)	-----	-----	5.04
helium feed in ILS	(L/min)	-----	-----	0.21
helium feed in SLS	(L/min)	-----	-----	0.35
raw gas feed FR (wet)	(L/min)	≈3.7	≈3.8	≈4
silica sand:				
particle diameter (mean)	(μm)	150	150	150
solids density (bulk)	Ps,S (kg/m^3)	1600	1600	1600
amount silica sand	g	370	370	264
ilmenite:				
particle diameter (mean)	(μm)	-----	-----	150
solids density (bulk)	Ps,I (kg/m^3)	-----	-----	2600
amount ilmenite	g	-----	-----	396
wt% of total bed inventory	%	-----	-----	60
gas residence time (reactor)	s	-----	-----	≈2.6−2.7
gas residence time (bed)	s	-----	-----	≈0.4−0.5

the same way, i.e. the gas composition was sampled every third minute via the GC and the tar composition was sampled by a set of six SPA-samples after an hour.

Ilmenite. The reference measurements were followed by an experiment where the prospect was to demonstrate the possibilities of reforming tars in the CLR process. In this experiment, ilmenite was used as catalyst for reforming the tar components. The ilmenite used in this experiment was supplied by Titania A/S in Norway. It was 94.3% pure and concentrated from a naturally occurring ore containing 40% ilmenite, 37% plagioclase, 8.6% ortopyroxene, 6.5% klinopyroxene, 4.2% biotitt, and some minor other phases. To initiate the experiment, the CLR system was heated to 800 °C without bed material. The CLR reactor was also disconnected from the gasifier and air flowed through the FR. The air flow was determined in the FR in the same manner as in the reference experiments. After completing the heating sequence, the gas flows of air and nitrogen in the AR (containing 1 mole% of oxygen) and the helium flow in the ILS and SLS were adjusted to the mass flow regulators according to Table 5. The bed material containing only ilmenite was then poured into the air fluidized FR. After a few minutes a solid circulation problem was detected by the resulting pressure signals. By disassembling the system, it was shown that ilmenite particles had agglomerated in the limited cyclone leg. To address this issue it was, therefore, decided to conduct the experiment by mixing silica sand 40 wt % and ilmenite 60% wt. In a fluid dynamic study[32] performed in a cold model identical in size to the hot system, it was found that ilmenite could mix with silica sand and that two bed materials contained sufficient mixing properties. The start-up procedure of the CLR system was once more performed. As the CLR system reached 800 °C, the bed material mix was poured into the air fluidized FR. The resulting pressure signals in the AR and the FR indicated that solid circulation was re-established.

No defluidization problems were observed, and stable operating conditions were obtained. The raw gas pipe was connected to the FR together with a nitrogen flow, slightly exceeding the gas pump capacity, to ensure inert operation in the FR. The nitrogen flow was, thereafter, stepwise decreased by 5% (0.25 L/min) until full raw gas operation was achieved.

The oxygen content in the feed to the AR was kept at 1 mol %, and the experiment was performed during one hour. The sampling of O_2, CO, and CO_2 in the outlet of the AR was performed every second during the entire experiment. Sampling of the reformed gas composition out of the FR was performed every three minutes, and six tar samples were collected by SPA at the end of the run. After the experiment was completed, the CLR system was shut

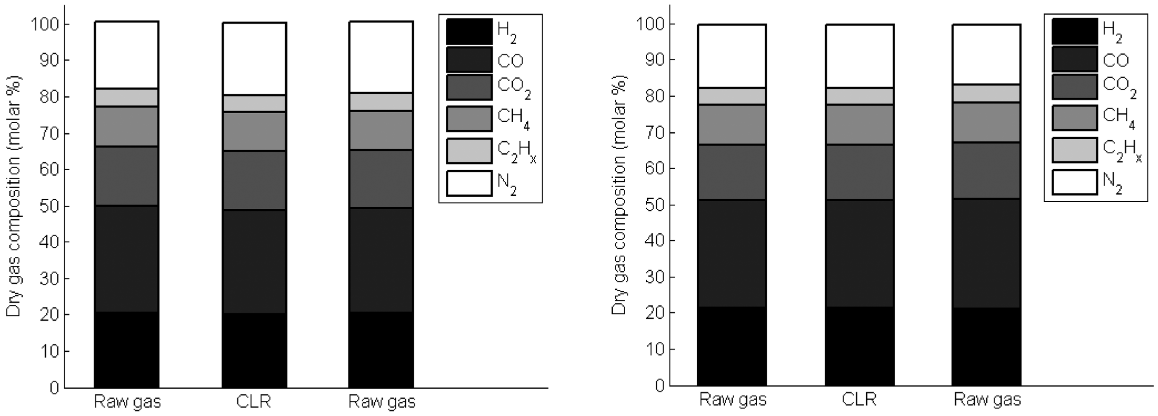

a, Silica sand 740°C (740 °C)

b, Silica sand 815°C (815 °C)

Figure 4. CLR reference experiments with silica sand.

down in accordance with the procedure used in the reference experiments.

The raw gas composition feed to the FR was determined via the gasifier sampling system for two hours after the experiment. Dry gas composition was sampled every three minutes via the GC, and the tar composition was sampled by a set of six SPA-samples after an hour.

RESULTS AND DISCUSSION

Experiments Silica sand 740 °C and Silica sand 815 °C were carried out to confirm that no catalytic effects were observed from the reactor material or the silica sand. The dry gas composition of the two reference experiments with silica sand are shown in Figure 4 a and b, where a is the 740 °C scenario and b is the 815 °C scenario. The middle bars in both figures represent the gas composition after the CLR, and the bars to the left and to the right represent the raw gas composition of the gasifier before and after the operation of the CLR. As shown in Figure 4, the CLR reactor operated with silica sand has a negligible effect on the gas composition of both Silica sand 740 °C and Silica sand 815 °C. Furthermore, the SPA-analysis from these two experiments also confirmed that the tar content or composition was unaffected by the CLR system. This suggests that no catalytic effects are produced by either the reactor material or by the silica sand.

Catalyst circulation in the CLR-system is a fundamental requirement to transport oxygen and recover catalytic surfaces. A circulating catalyst is consuming oxygen during the reoxidation in the AR. The oxygen concentration of the gas leaving the AR reveals whether or not the catalyst is consuming oxygen, thus indicating recirculation of the reduced catalysts from FR to AR. The catalyst circulation was studied during the experiment with ilmenite. Figure 5 displays the evolution of the oxygen content leaving the AR during the consecutive phases of fluidization: air, nitrogen, or raw gas fluidization in the FR during the entire experiment. The oxygen content is stable during the first period of air and nitrogen fluidization, indicating that the catalysts are oxygen-saturated. The fact that the oxygen content is unaffected during the transition from air to inert conditions confirms that no gas is transported via the LS from the FR to the AR. When the nitrogen is switched to raw gas, there is an initial sequence, during which the oxygen concentration slowly levels out. The oxygen concentration remains close to zero during the entire period of raw gas operation. This result verifies that the catalysts are continuously circulated in the system and that all the accessible oxygen in the AR is consumed by the reoxidation of the catalyst and by the oxidation of the carbon deposits on the catalyst surfaces.

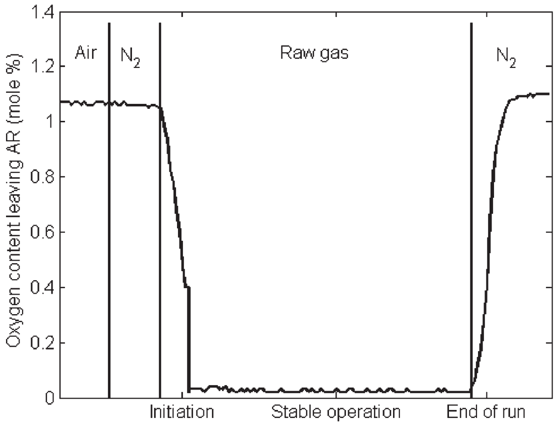

Figure 5. Oxygen concentrations in AR for air, N_2, and raw gas fluidization in the FR.

The regeneration of carbon deposits on the catalysts was investigated by measuring CO_2 and CO concentration in the outlet of the AR. During air and nitrogen fluidization in the FR, both CO_2 and CO concentrations were below the detection limit of the instruments (CO_2: 5000 ppm and CO: 50 ppm). In the transition to full raw gas operation, the CO_2 concentration starts to increase until it levels out and is stabilized at 0.13 mol %, corresponding to 0.5 mass % of the total amount of carbon input into the FR. Even though the measured CO_2 showed an increase in concentration between nitrogen and raw gas fluidization, the value of 0.13 mol % is below the detection limit of the instrument and has to be regarded as an approximate value. On the other hand, the CO concentration was below the detection limit of the instrument during the entire experiment, which confirms that the deposits of carbon on the catalysts in the FR are oxidized to CO_2 in the AR. It was not possible to detect any deactivation of the catalyst from other sources, e.g. sulfur or chlorine poisoning as the operating time was too short.

The continuous circulation and regeneration of catalysts are once more verified at the end of the experiment, Figure 5. When the raw gas is switched to nitrogen, the oxygen concentration

Table 6. Tar Compositions in Raw Gas and Reformed Gas Downstream of the CLR-System

compound	Reference (gasifier) (g_{tar}/Nm^3gas)	Ilmenite 800 °C (g_{tar}/Nm^3gas)
phenol	0.98	0.01
o-cresol	0.03	n.d
m-cresol	0.15	n.d
p-cresol	0.04	n.d
benzene	0.65	1.90
toluene	0.71	0.17
m/p-xylene	0.14	n.d
o-xylene	1.06	0,16
indan	0.05	0.17
indene	2.94	0.05
naphthalene	7.53	10.77
2-methylnaphthalene	1.10	0.06
1-methylnaphthalene	0.70	0.03
biphenyl	0.47	0.84
acenaphthylene	2.03	0.37
acenaphthene	0.13	0.01
fluorene	0.65	0.09
phenanthrene	1.66	1.45
anthracene	0.29	0.18
fluorantene	0.41	0.45
pyrene	0.46	0.42
unknowns	5.54	0.92
total tar	27.70	18.04

leaving the AR starts to increase. The increasing oxygen concentration shows that in the absence of raw gas in the FR, catalysts are gradually reoxidized in the circulation loop. After a few minutes, the initial oxygen concentration in the AR is reached, showing that all the catalyst particles are oxygen-saturated and that all the carbon deposits have been oxidized into CO_2.

The tar cleaning concept and the tar reforming activity of ilmenite are evaluated by comparing the tar content of the gas in and out of the FR. Table 6 summarizes the tar components analyzed in SPA samples from the raw gas (Reference) as well as in the reformed gas leaving the CLR (Ilmenite 800 °C); tar components that were detectable in the raw gas but were not detectable downstream of the CLR are marked not detectable (n.d) in Table 6.

The total amount of tars was reduced from 27.70 to 18.04 $g/Nm^3{}_{gas}$, which corresponds to a tar reduction of 35%. This value can appear as low, but there are some reasons that can explain this. This is the first experiment performed in the CLR, which shows that it is possible to use a natural ore as tar reforming catalyst in the system. However, to reach higher tar reduction and thereby be competitive with commercially available nickel catalysts (where tar reduction close to 100% is possible) the activity of the ilmenite and operating conditions needs to be optimized. This optimization can be conducted by increasing the gas/catalyst contact, i.e. using 100% ilmenite as bed material, increasing the bed height and augment the active surface on the catalyst by proper activation of the ilmenite. The fact that surface area plays a major role for tar decomposition with iron oxide catalysts has been demonstrated by Uddin et al.[11] Further investigations of using ilmenite as tar reforming catalyst are interesting as there is potential for reaching acceptable tar conversion by using a nontoxic catalyst with a bulk price comparable to hard coal.

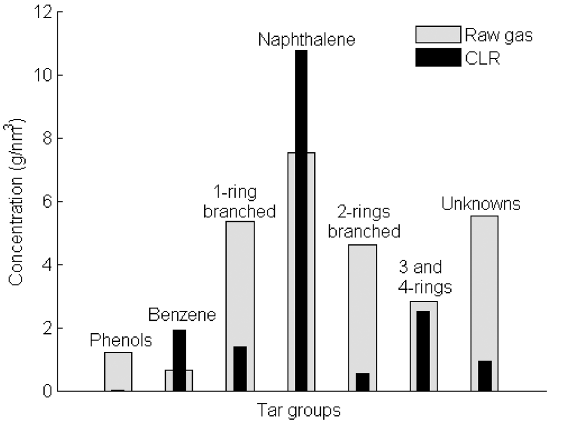

Figure 6. Tar groups for raw gas and reformed gas.

The analysis of the SPA samples gives, in addition to the total tar, also information on different tar molecules. This information reveals how tar structures change during CLR operation. Figure 6 shows overall changes in tar composition. Here, the tar compounds are divided into the following groups: phenols, benzene, 1-ring aromatic compounds with branches, naphthalene, 2-ring aromatic compounds with branches, 3- to 4-ring aromatic compounds without branches and unknowns. The yields of these groups before and downstream of the FR are presented. Tar components are grouped to visualize the changes in tar molecules and give information about the tar decomposition path. As seen from the numbers, the amount of phenols and 1-ring aromatic compounds with branches decreases and the amount of benzene increases. In other words, phenols and branched tar molecules are stripped of their alkyl and hydroxyl groups, respectively, forming pure aromatic rings. Almost all phenols and about 75% of branched tars are converted, whereas the fraction of the more stable benzene more than doubles. The same pattern of stripping branches from the molecules can be seen in the case of 2-ring aromatic compounds. The naphthalene fraction increases by 43%, while the branched 2-ring aromatic compound decreases by almost 90%. Besides the decomposition of 1- and 2-ring branched compounds and phenols, the decomposition of tars from the group of unknowns also contributes to the increase in benzene and naphthalene. The group of unknowns involves approximately 150 unidentified tar molecules with molecular weights spread from that of benzene to molecular weights greater than pyrene. The 3- and 4-ring nonbranched aromatic compounds decrease by 12%, while the group of unknowns decreases by 84%. The decomposing of unknowns with molecular weight greater than pyrene together with heavier molecules, so-called non-GC detectable, are most likely to contribute to the group of 3- and 4-ring nonbranched aromatic compounds. In this manner, the tar composition distribution can be explained as a result of consumed versus formed molecules. Hence, a greater amount of stable aromatic molecules are formed than are broken down.

The dry composition of the raw gas is compared to the reformed gas from the CLR system to investigate whether or not ilmenite shows any catalytic effect on the permanent gases. The left bar in Figure 7 shows the dry gas composition of the raw gas, and the right bar shows the dry reformed gas downstream of the CLR. The nitrogen content in the outlet stream of the FR is 21%

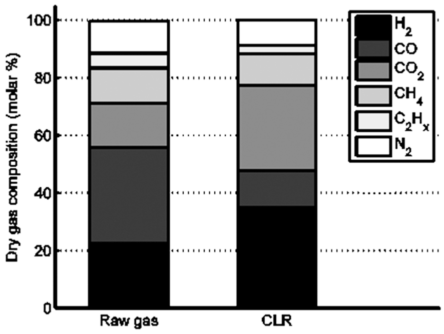

Figure 7. Dry gas compositions from gasifier and CLR.

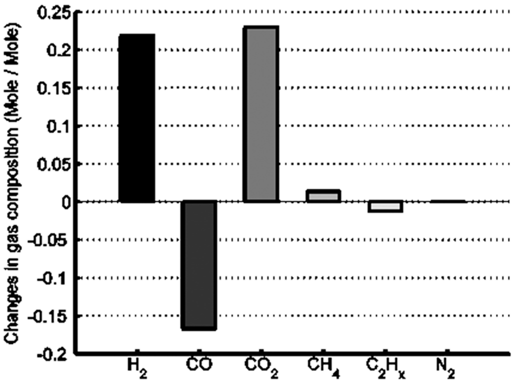

Figure 8. Changes in gas composition between reformed gas and raw gas.

lower than the fed raw gas. Since the same amount of nitrogen is fed to the FR, the reduced nitrogen concentration is linked to an overall volume increase of permanent gases. The difference in concentration between the reformed gas and the raw gas is presented in Figure 8, in which the raw gas and the reformed gas are normalized with regards to their respective nitrogen content.

The increase in H_2 and CO_2 together with the decrease in CO, Figure 8, can to a large extent be explained by increased water-gas shift activity induced by the ilmenite. The H_2/CO-ratio, when comparing the raw gas to the reformed gas leaving the CLR system in Figure 7, shifts from approximately 0.7 to 3. Increased water-gas shift activity attributed to an iron-based catalyst in the presence of steam has been demonstrated before by, for example, Uddin et al.[11] However, as the increase of H_2 and CO_2 is not covered fully by the decrease in CO the water-gas shift reaction alone is not responsible for this result. The extra amount of CO_2 can be attributed to the catalyst oxygen transfer between the AR and the FR, resulting in oxidation of some CO and other hydrocarbons. Sources of excess hydrogen might be partial oxidation of tars (reaction 1), steam reforming reactions (reaction 3), steam dealkylation of tars (reaction 4), and carbon forming reactions (reaction 9). The reformed gas shows a slight increase in methane content, Figure 8. The increase in methane corresponds to the decrease of light hydrocarbons, and cracking reactions are presumably the source of this development.

■ CONCLUSION

A novel method for combining tar cleaning and catalyst regeneration using oxygen carrying catalysts in a dual fluidized bed system has been investigated. Thanks to the continuous regeneration of carbon deposit, the concept shows the potential for managing producer gas with high tar content without decreasing catalyst activity. The catalyst circulation also expands the range of application as molecules other than oxygen could be transported within the system. Suitable catalysts are based on metal oxides with oxygen transporting properties.

In this work, the method is demonstrated by using ilmenite ($FeTiO_3$) as a catalyst together with producer gas from the Chalmers biomass gasifier with a tar content of roughly 30 g_{tar}/Nm^3_{gas}. Based on the results of the investigation, the following conclusions may be drawn:

(1) The tar cleaning concept was proven as the ilmenite was continuously transporting oxygen in the system, and the total tar content was reduced by 35%. The branched tars and phenols were to a large extent converted to pure aromatic compounds, while more activation energy was required to open the stable ring structure, i.e. benzene and naphthalene. No catalytic effects were observed from the reactor material itself or from the silica sand fillers

(2) Carbon deposits on the ilmenite were continuously removed by oxidation into CO_2. Neither deactivation of the ilmenite nor disturbance in oxygen transfer was observed during the operating time.

(3) The reactor system proved sufficient in order to catalytically adjust the producer gas. Ilmenite demonstrated high water gas shift reaction activity, and the H_2/CO-ratio rose from approximately 0.7 in the raw gas to 3 downstream of the reactor system. A decrease in light hydrocarbons was observed, while the methane content was slightly increased downstream of the reactor system.

■ AUTHOR INFORMATION

Corresponding Author

*Phone: +46 (0)31 772 52 43. E-mail: Fredrik.Lind@chalmers.se.

■ ACKNOWLEDGMENT

This work has been financially supported through the Era-Net program and by E.On. The operation of the gasifier was made possible by grants from Göteborg Energi, Metso, Akademiska Hus, and the Swedish Energy Agency. The authors also wish to acknowledge K.T.H. for the tar analysis and research engineer Rustan Marberg for his work with the experimental equipment.

■ NOMENCLATURE

g_{tar}/Nm^3_{gas}: mass of tars per normal cubic meter of product gas
CLC: chemical looping combustion
CLR: chemical looping reforming
CLS: chemical looping systems
AR: air reactor
FR: fuel reactor
LS: loop-seal
SLS: superior loop seal
ILS: inferior loop seal
FCC: fluid catalytic cracking
SPA: solid phase adsorption
MeO: metal oxide
Me_xO_y: oxidized metal oxide
Me_xO_{y-1}: reduced metal oxide
micro-GC: micro gas chromatography

■ REFERENCES

(1) Pfeifer, C.; Hofbauer, H. Development of catalytic tar decomposition downstream from a dual fluidized bed biomass steam gasifier. *Powder Technol.* **2008**, *180* (1−2), 9–16.

(2) Devi, L.; Ptasinski, K. J.; Janssen, F. J. J. G. A review of the primary measures for tar elimination in biomass gasification processes. *Biomass Bioenergy* **2003**, *24* (2), 125–140.

(3) Li, C. S.; Suzuki, K. Tar property, analysis, reforming mechanism and model for biomass gasification-An overview. *Renewable Sustainable Energy Rev.* **2009**, *13* (3), 594–604.

(4) Taralas, G.; Kontominas, M. G.; Kakatsios, X. Modeling the thermal destruction of toluene (C7H8) as tar-related species for fuel gas cleanup. *Energy Fuels* **2003**, *17* (2), 329–337.

(5) Dayton, D. *A Review of the Literature on Catalytic Biomass Tar Destruction*; TP-510-32815; NREL: 2002.

(6) Bergman, P. C. A.; van Paasen, S. V. B.; Boerrigter, H. The Novel "OLGA" technology for complete tar removal from biomass producer gas. In *Pyrolysis and Gasification of Biomass and Waste, Expert meeting, 30* Strasbourg, France, 2002.

(7) Bangala, D. N.; Abatzoglou, N.; Martin, J. P.; Chornet, E. Catalytic gas conditioning: Application to biomass and waste gasification. *Ind. Eng. Chem. Res.* **1997**, *36*, 4184–4192.

(8) Caballero, M. A.; Corella, J.; Aznar, M. P.; Gil, J. Biomass gasification with air in fluidized bed. Hot gas cleanup with selected commercial and full-size nickel-based catalysts. *Ind. Eng. Chem. Res.* **2000**, *39* (5), 1143–1154.

(9) Delgado, J.; Aznar, M. P.; Corella, J. Biomass Gasification with Steam in Fluidized Bed: Effectiveness of CaO, MgO, and CaO−MgO for Hot Raw Gas Cleaning. *Ind. Eng. Chem. Res.* **1997**, *36* (5), 1535–1543.

(10) Rapagnà, S.; Jand, N.; Kiennemann, A.; Foscolo, P. U. Steam-gasification of biomass in a fluidised-bed of olivine particles. *Biomass Bioenergy* **2000**, *19* (3), 187–197.

(11) Uddin, M. A.; Tsuda, H.; Wu, S. J.; Sasaoka, E. Catalytic decomposition of biomass tars with iron oxide catalysts. *Fuel* **2008**, *87* (4−5), 451–459.

(12) Olivares, A.; Aznar, M. P.; Caballero, M. A.; Gil, J.; Frances, E.; Corella, J. Biomass gasification: Produced gas upgrading by in-bed use of dolomite. *Ind. Eng. Chem. Res.* **1997**, *36* (12), 5220–5226.

(13) Baker, E. G.; Mudge, L. K.; Brown, M. D. Steam gasification of biomass with nickel secondary catalysts. *Ind. Eng. Chem. Res.* **1987**, *26* (7), 1335–1339.

(14) Seemann, M. C.; Schildhauer, T. J.; Biollaz, S. M. A.; Stucki, S.; Wokaun, A. The regenerative effect of catalyst fluidization under methanation conditions. *Appl. Catal., A* **2006**, *313* (1), 14–21.

(15) Miyazawa, T.; Kimura, T.; Nishikawa, J.; Kado, S.; Kunimori, K.; Tomishige, K. Catalytic performance of supported Ni catalysts in partial oxidation and steam reforming of tar derived from the pyrolysis of wood biomass. *Catal. Today* **2006**, *115* (1−4), 254–262.

(16) Kunii, D.; Levenspiel, O. *Fluidisation Engineering*, 2nd ed.; Butterworth-Heinemann: 1991; pp 36−38.

(17) Thunman, H.; Åmand, L.-E.; Leckner, B.; Johansson, F. A cost effective concept for generation of heat, electricity and transport fuel from biomass in fluidized bed boilers − using existing energy infrastructure. In *Proceedings of the 15th European Biomass Conference & Exhibition - From research to market Deployment*, Berlin, Germany, 2007.

(18) Larsson, A.; Pallarés, D.; Neves, D.; Seemann, M.; Thunman, H. Zero-dimensional modeling of indirect fluidized bed gasification. In *International conference on fluidization, Fluidization XIII*, Gyeong-ju Korea, 2010; Vol. 16th to 21st of May, pp 845−852.

(19) Mattisson, T.; Lyngfelt, A. In *Applications of chemical-looping combustion with capture of CO2*, Second Nordic Minisymposium on Carbon Dioxide Capture and Storage, Göteborg, Sweden, April 18−20, 2001; 2001; pp 163−168.

(20) Ryden, M.; Lyngfelt, A.; Mattisson, T. Synthesis gas generation by chemical-looping reforming in a continuously operating laboratory reactor. *Fuel* **2006**, *85* (12−13), 1631–1641.

(21) Rydén, M.; Cleverstam, E.; Lyngfelt, A.; Mattisson, T. Waste products from the steel industry with NiO as additive as oxygen carrier for chemical-looping combustion. *Int. J. Greenhouse Gas Control* **2009**, *3* (6), 693–703.

(22) Mendiara, T.; Johansen, J. M.; Utrilla, R.; Geraldo, P.; Jensen, A. D.; Glarborg, P. Evaluation of different oxygen carriers for biomass tar reforming (I): Carbon deposition in experiments with toluene. *Fuel* **2011**, *90* (3), 1049–1060.

(23) Mendiara, T.; Johansen, J. M.; Utrilla, R.; Jensen, A. D.; Glarborg, P. Evaluation of different oxygen carriers for biomass tar reforming (II): Carbon deposition in experiments with methane and other gases. *Fuel* **2011**, *90* (4), 1370–1382.

(24) Leion, H.; Lyngfelt, A.; Johansson, M.; Jerndal, E.; Mattisson, T. The use of ilmenite as an oxygen carrier in chemical-looping combustion. *Chem. Eng. Res. Des.* **2008**, *86* (9A), 1017–1026.

(25) Berguerand, N.; Lyngfelt, A. Batch testing of solid fuels with ilmenite in a 10 kWth chemical-looping combustor. *Fuel* **2010**, *89* (8), 1749–1762.

(26) Leion, H.; Mattisson, T.; Lyngfelt, A. Solid fuels in chemical-looping combustion. *Int. J. Greenhouse Gas Control* **2008**, *2* (2), 180–193.

(27) Berguerand, N.; Lyngfelt, A., Batch testing of solid fuels with ilmenite in a 10 kWth chemical-looping combustor. *Fuel 89*, (8), 1749-1762.

(28) Simell, P. A.; Hepola, J. O.; Krause, A. O. I. Effects of gasification gas components on tar and ammonia decomposition over hot gas cleanup catalysts. *Fuel* **1997**, *76* (12), 1117–1127.

(29) Rostrup-Nielsen, J. R. Production of synthesis gas. *Catal. Today* **1993**, *18* (4), 305–324.

(30) Rönkkönen, H.; Simell, P.; Reinikainen, M.; Krause, O.; Niemelä, M. V. Catalytic clean-up of gasification gas with precious metal catalysts - A novel catalytic reformer development. *Fuel* **2010**, *89* (11), 3272–3277.

(31) Brage, C.; Yu, Q.; Chen, G.; Sjöström, K. Use of amino phase adsorbent for biomass tar sampling and separation. *Fuel* **1997**, *76* (2), 137–142.

(32) Lind, F.; Semann, M.; Thunman, H. Evaluation of fluid dynamics in a hot and a cold system of interconnecting fluidised beds. In *International conference on fluidization, Fluidization XIII*, Gyeong-ju Korea, 2010; pp 869−876.

Paper III

Biomass Conv. Bioref.
DOI 10.1007/s13399-012-0042-6

ORIGINAL ARTICLE

Manganese oxide as catalyst for tar cleaning of biomass-derived gas

Fredrik Lind · Mikael Israelsson · Martin Seemann · Henrik Thunman

Received: 22 September 2011 / Revised: 7 March 2012 / Accepted: 5 April 2012

Abstract The possibilities to upgrade raw gas with the use of a manganese oxide have been investigated in an application for secondary tar cleaning of biomass-derived gas. Experiments were conducted in a reactor system where a novel technique that combines tar cleaning with catalyst regeneration is applied. Raw gas from the Chalmers non-catalytic steam biomass gasifier—containing roughly 32 g_{tar}/Nm_{gas}^3—was fed to the tar cleaning reactor. The tar reforming qualities of the manganese oxide were evaluated in the reactor system using a mixture of 23 wt.% catalysts in silica sand at the temperatures 700 and 800°C. Experiments showed that the catalyst was continuously regenerated from carbon deposits and that the total amount of tars was decreased by as much as 44.5 % at a gas residence time of 0.4 s in the bed. The catalyst showed activity in water–gas shift reaction and the H_2/CO ratio increased from 0.6 in the raw gas to a peak value of 1 in the reformed gas at 800°C. Only a slight decrease in methane and acetylene content was observed for both operating temperatures.

Keywords Biomass · Tar · Gas cleaning · Catalysts · Gasification · Dual fluidized bed

1 Introduction

Biomass is a resource that can be used as fuel in various applications in order to replace fossil fuels. For example, biomass can be synthesized to transport fuels such as: synthetic natural gas, dimethyl ether, or methanol [1]. In order to process biomass to bio-fuels, there is a need to first convert the solid biomass to, for example, gas. This step can be done in a thermo-chemical conversion process called gasification. As biomass is gasified, condensable hydrocarbons, often referred to as tars, are formed as a by-product [2–6]. Tars start to condense already at 350°C [7] and are associated with operation problems such as clogging and blockage of equipment downstream the gasifier. The tars propensity to condense precludes direct use of the raw gas as feedstock for fuel synthesis or as a fuel in gas turbines/engines without implementation of a sufficient tar cleaning. The development of efficient tar cleaning systems is, therefore, a crucial parameter for commercializing the biomass gasification technology.

In principle, there are two available routes for cleaning the raw gas from tars: wet or dry gas cleaning. Wet cleaning is performed in scrubber units where the raw gas is rapidly cooled by a liquid. In this process, the tars are physically removed from the gas by condensation onto water or oil droplets. The wet cleaning—based on scrubber technology—is a well-established technology but is associated with significant amounts of waste water/solvents and thermodynamic penalties coupled to the rapid cooling of the raw gas [8]. Dry cleaning most often refers to catalytic or a high temperature cleaning (thermal cracking of tars). Catalytic cleaning can be integrated with the gasifier outlet temperature, whereas high-temperature cleaning needs to be performed at elevated temperatures (>1,100°C) to reach high conversion efficiencies [6]. Some of the product gas needs to be consumed together with additional oxygen to increase the exit temperature of the gasifier (from around 800 to 1,100°C). Therefore, catalytic tar cleaning is the preferred method as the heat losses can be minimized [6] and the chemically stored energy within the tars can be recovered in the product gas. However, so far catalytic

---

F. Lind (✉) · M. Israelsson · M. Seemann · H. Thunman
Division of Energy Technology, Department of Energy and Environment, Chalmers University of Technology,
412 96 Gothenburg, Sweden
e-mail: Fredrik.Lind@chalmers.se

systems have not been feasible for use in industrial applications. This is mainly because of problems associated with deactivation of the catalysts. It is known that catalysts with long-term exposure from components such as sulfur, chlorine, alkali, etc., can be deactivated, but the catalyst can also lose its activity after only a short operating time if carbon is depositing on the active surfaces [3, 6, 8]. In this work, a method that combines tar cleaning with regeneration of carbon deposits on the catalyst is applied to investigate the possibilities of using manganese oxide as a reforming catalyst. In this first experiment, a well-defined manufactured catalyst was used to study the tar decomposing activity of the manganese oxide itself, whereas the long-term goal is to use naturally occurring ores containing manganese.

The tar reforming properties of the catalyst are evaluated in a system of dual fluidized beds [9], which is based on the chemical looping reforming (CLR) technique originally presented by Mattisson et al. [10]. The CLR system is fed with raw gas—containing about 32 $g_{tar}/Nm_{raw\ gas}^3$—from the Chalmers 2–4 MW biomass research gasifier [11, 12]. The idea with the tar cleaning method is to reform tar components (C_nH_m) into useful gas molecules. The reactor system consists of two reactors: a regenerator reactor also called air reactor (AR) and reformer reactor (FR) fluidized with raw gas (Fig. 1). Two loop seals, fluidized with inert gas or steam, prevent gas cross-contamination of the effluents from respective reactor, while enabling the catalyst to circulate between the two reactors. In the reformer reactor, the Me_xO_y is reduced to Me_xO_{y-1} during the partial oxidation of the tar components (C_nH_m) in the raw gas according to reaction (1), which usually is an endothermic reaction [13]. Besides the desired tar reforming reaction, additional carbon-forming reactions cause carbon to deposit on the Me.

$$\begin{aligned} C_nH_m + (n-n_1)Me_xO_y &\rightarrow (n-n_1)CO \\ &+ (0.5\,m)H_2 + (n-n_1)Me_xO_{y-1} + n_1C \end{aligned} \tag{1}$$

The reduced metal oxide Me_xO_{y-1} is also acting as catalyst for tar reforming in the presence of reforming media* such as water steam or carbon dioxide in the raw gas according to the simplified reaction (2).

$$\begin{aligned} &C_nH_m + Me_xO_{y-1} + H_2O^* + CO_2^* \\ &\rightarrow Me_xO_{y-1} + C_iH_j + H_2 + CO \end{aligned} \tag{2}$$

Simultaneously, as Me_xO_{y-1} is re-oxidized to Me_xO_y in a strongly exothermic [13] reaction in the AR, carbon deposits on the catalytic surfaces are oxidized to CO_2 according to reaction (3)

$$\begin{aligned} &n_1Me_xO_{y-1} + n_2C + (n_1/2 + n_2)(O_2 + 3.77N_2) \\ &\rightarrow n_1Me_xO_y + n_2CO_2 + (n_1/2 + n_2)(3.77N_2) \end{aligned} \tag{3}$$

The concept of reforming tars in the CLR system was proven by Lind et al. [9] using ilmenite ($FeTiO_3$) as tar reforming catalyst.

The catalyst (M4MgZ1150) used in this work consists of 40 % manganese oxide (Mn_3O_4) supported on 60 % stabilized magnesium–zirconium oxide ($MgZrO_3$) and was originally developed as an oxygen carrier for the chemical-looping combustion process (CLC) [14]. Johansson et al. [15] investigated the potential of the M4MgZ1150 as oxygen carrier in CLC operations and confirmed that the material was suitable as it could withstand continuous redox reactions and in the same time showed high reactivity. This implies that the material is even suitable for the CLR system where the catalyst is continuously exposed to reduction and oxidation reactions. Mendiara et al. [16, 17] investigated the tar reforming activity of the M4MgZ1150 in batch experiments with toluene as representative tar component at 600 and 800°C. They concluded that the material showed high reactivity towards toluene, which was decomposed to a large extent at both temperatures. In this work, the tar reforming properties of M4MgZ1150 is investigated in a system that has been developed one step closer to an industrial application. The experiment gives additional information about the catalyst activity, as more than 170 tar components are present in the raw gas from the gasifier and 21 of them are analyzed. The fundamental investigated criteria to assess the tar reforming quality of the catalyst and the suitability to use the catalyst in the CLR system are:

- How reactor temperature variations influence the tar reforming activity
- How various oxygen loads on the catalyst influence the tar reforming activity
- The possibilities to regenerate active surfaces from carbon deposits while remaining of catalytic activity
- How reactor temperature and oxygen load influences the permanent gas composition

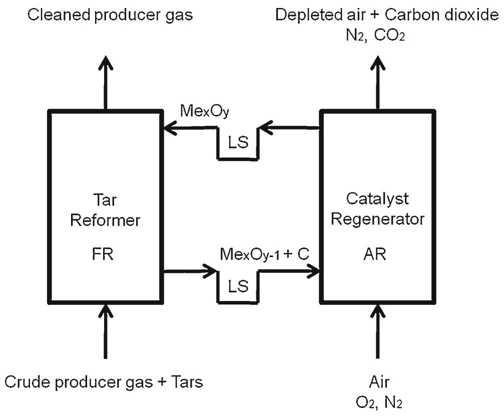

Fig. 1 Dual fluidized bed system for tar removal

2 Experimental

A drawing of the 0.5 meter high CLR system is shown in Fig. 2. In this bench-scaled CLR system, the FR (1) is designed as a bubbling fluidized bed to provide a good estimation of the gas/solid contact, but the concept could also be applied to two circulating fluidized beds. The regenerator reactor (AR) (2) is a circulating fluidized bed and gas/solid separation is achieved in a cyclone. The gases (Table 1) enter the reactor system via wind boxes, which are placed beneath the porous plates in FR, AR, superior loop seal (SLS), and inferior loop seal (ILS) in order to reduce pressure fluctuations in the gas feed. The tar reforming reactions and regeneration reactions can, with respect to temperature, be optimized separately with a temperature difference up to above 200°C. The temperature control is achieved by separate heating of the two oven halves (3), together with an air-cooled jacket on the FR (4). The gas feed to the AR is controlled by two separate mass flow regulators (5), which enable operation with air and/or nitrogen. Downstream the AR, the gas is cooled and dried in a gas conditioning system (6). The content of CO, CO_2, and O_2 in the gas exhausting from the AR are analyzed online by non-dispersive infrared analyzers for CO and CO_2, respectively paramagnetic analyzer for O_2 (7). The gas flows of Helium to the SLS and ILS are controlled by two separate mass flow regulators (8). The FR in the CLR system is connected to the Chalmers gasifier, which is operated at a pressure slightly lower than the atmospheric pressure, due to safety reasons. As a consequence, the CLR operating pressure is −4 to −6 kPa and

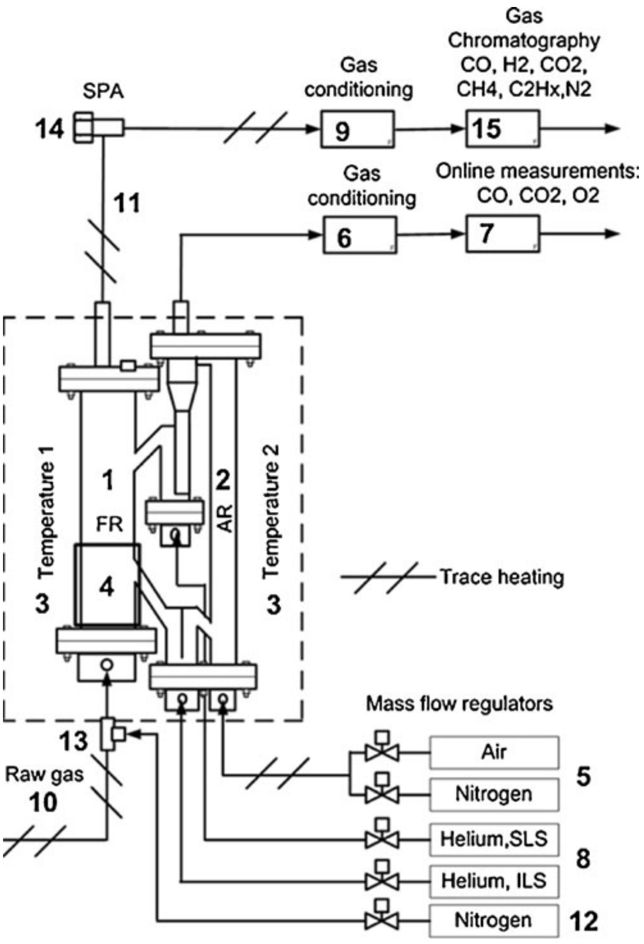

Fig. 2 Drawing of the CLR setup

Table 1 Operation conditions in gasifier and chemical looping reforming (CLR)

Properties	Units	700°C in CLR		800°C in CLR	
Gasifier					
Fuel	–	Wood pellets		Wood pellets	
Bed temperature	°C	830		825	
Bed material	–	Silica sand		Silica sand	
Dry raw gas composition					
Hydrogen	mol%	21.02		20.42	
Carbon monoxide	mol%	35.35		35.40	
Carbon dioxide	mol%	14.47		14.37	
Methane	mol%	12.85		12.85	
Acetylene	mol%	0.41		0.38	
Ethylene	mol%	4.45		4.40	
Ethane	mol%	0.40		0.43	
Nitrogen	mol%	11.06		11.75	
Tars	g/nm^3	32.89		32.90	
Steam content. raw gas	mol%	50.71		51.25	
CLR					
Temperature	°C	700		800	
Air feed in AR	l/min	0.26	0.56	0.26	0.56
Nitrogen feed in AR	l/min	5.04	4.74	5.04	4.74
Helium feed in ILS	l/min	0.29		0.29	
Helium feed in SLS	l/min	0.37		0.37	
Raw gas feed FR (dry)	l/min	≈2.5		≈2.5	
Silica sand					
Particle diameter (mean)	Mm	230		230	
Solids density (bulk)	kg/m^3	1,470		1,470	
Amount silica sand	G	388		388	
Gas residence time (reactor)	s	≈3.0		≈3.0	
Gas residence time (bed)	s	≈0.4		≈0.4	
M4MgZ1150					
Particle diameter (mean)	µm	230		230	
Solids density (bulk)	kg/m3	1,560		1,560	
Amount catalysts	g	116		116	
wt.% of total bed inventory	%	23		23	

CLR chemical looping reforming, *AR* air reactor, *FR* reformer reactor, *SLS* superior loop seal, *ILS* inferior loop seal the gas flow through the reactor is controlled by a gas pump in the gas conditioning system (9). The raw gas pipe between the FR and the gasifier (10), as well as, the connecting pipe between the FR and the gas conditioning system (11) are electrically heated to 400°C to avoid tar condensation. A T-connector for nitrogen supply (from a mass flow regulator (12)) is mounted on the raw gas pipe upstream the inlet to the FR (13). This enables inert conditions in the FR before and after the introduction of raw gas. The concentrations of tars in the raw gas and the reformed gas are measured by solid phase adsorption [18] (SPA). The tar samples for the reformed gas are collected in the heated pipe between the FR and the gas conditioning system (14) while an additional system is used for tar sampling of the raw gas [9]. The adsorbed tars are dissolved in a solvent and sent for analysis in a gas chromatography followed by flame ionization detector (GC-FID). The reformed gas leaving the FR is cooled and dried in the gas conditioning system (9) and thereafter, analyzed by a micro gas chromatograph (15), micro-GC (Varian 4900). A detailed description of the analysis equipment, CLR and the gasifier measuring system can be found in Lind et al. [9].

3 Experimental procedure

A reference experiment with silica sand was carried out at 740 and 815°C to ensure that no catalytic effects was induced by the sand or the reactor material itself (containing 10 % nickel). The experiment which was performed by comparing the dry gas composition and tar content in and out of the CLR system showed that the silica sand and the reactor material had negligible effect on both gas and tar composition. Detailed description and results from the reference experiment can be found in Lind et al. [9].

The manganese experiments were conducted with a mixture of 23 % M4MgZ1150 in 77 % silica sand as bed inventory to investigate how the tar decomposing/reforming properties are influenced by a change in temperature and oxygen load. A detailed description of the catalyst preparation can be found in Johansson et al. [15]. The catalyst activity and the regeneration of the catalyst was evaluated at 700 and 800°C with two different oxygen concentrations—1.0 and 2.2 mol% O_2—in the inlet feed to the AR (Table 1). The same bed material was used in both experiments.

The bed material mixture was poured into the FR, which was heated to 800°C, and the raw gas pipe connected under nitrogen purging. Thus, the raw gas was gradually replacing the nitrogen until the nitrogen was fully exchanged to raw gas.

The regeneration of carbon deposits on the catalysts was investigated by measuring CO_2 and CO concentration from the outlet of the AR. For the start-up sequence in both 700 and 800°C cases, and during nitrogen fluidization in the FR, the CO_2 and CO concentrations were below the detection limit of the instrument. Table 2 shows the measuring interval and detection limit for the analysis instruments downstream the AR. The amount of carbon deposits that was regenerated from the catalysts $Y_{\mathrm{c,AR}}$ has been calculated as the ratio between total integrated mass of carbon at the outlet of the AR and total mass of carbon fed to the FR during steady-state operation in the CLR, according to Eq. 4. Where $m\mathrm{CO}_{2,\mathrm{ARout}}$ and $m\mathrm{CO}_{,\mathrm{ARout}}$ is the carbon contribution from the carbon dioxide and carbon monoxide at the outlet of the AR and $\mathrm{mC}_{i,\mathrm{FRin}}$ denotes all the carbonaceous species in the raw gas.

$$Y_{C,\mathrm{AR}} = \frac{\int_{t_{\mathrm{start}}}^{t_{\mathrm{stop}}} \left(\dot{m}\,\mathrm{CO}_{2,AR\,\mathrm{out}} + \dot{m}\,\mathrm{CO}_{AR\,\mathrm{out}} \right) \mathrm{d}t}{\int_{t_{\mathrm{start}}}^{t_{\mathrm{stop}}} \left(\sum_{i=j}^{n} \dot{m}\,\mathrm{C}_{i,\mathrm{FR\,in}} \right) \mathrm{d}t} \tag{4}$$

The oxygen content in the feed to the AR was kept at 1.0 mol% for 1 h. Sampling of O_2, CO, and CO_2 in the outlet of the AR was performed every second during the entire experiment. Sampling of the reformed gas composition out from the FR was performed every third minute and 6 tar samples were collected by SPA when stable operation was achieved. Thereafter, the oxygen concentration was switched from 1.0 to 2.2 mol% during 1 h. Sampling of tars and dry gas components was conducted in the same manner as in the 1.0 mol% oxygen case.

The composition of the raw gas fed to the FR was determined via the gasifier sampling system for 2 h following the CLR experiment. Dry gas composition was sampled every third minute via the GC and tar composition was sampled by one set of six SPA samples after 1 h. The same procedure was repeated for the 700°C experiment, except that the bed material was already in the CLR during the start-up.

4 Results and discussion

The aim of this work was to evaluate if the M4MgZ1150 could be suitable as a reforming catalyst in a system for secondary continuous catalytic tar cleaning. The tar reforming activity of the catalyst was evaluated at the temperatures

Table 2 Gas-analyzing instruments downstream of the AR

Instrument	Measuring interval (mol%)	Detection limit (ppm)
O_2	0–25	1,250
CO	0–1	50
CO_2	0–100	5,000

of 700 and 800°C by comparing the tar components in the raw gas with the reformed gas after the CLR system. Table 3 summarizes the concentrations (g_{tar}/Nm^3) of the 21 analyzed tar components from the SPA-samples, in the raw gas, as well as in the reformed gas leaving the CLR. The table is organized in accordance to: the two investigated temperatures (cases), the position for tar measuring (measure position) and the oxygen concentration in the inlet feed to the air reactor (mole% O_2 in AR). The highest degree of tar reduction (44.5 %) was achieved at a CLR operating temperature of 800°C. At a temperature of 700°C in the CLR the highest reduction of tar was nearly 22 %. These values can seem low if compared with, e.g., values for tar reforming with a nickel based catalyst, where tar conversions can be close to 100 %. However, in this experiment the amount of catalyst was only 23 wt.% of the total bed inventory and consequently the gas solid contact was very restricted.

In addition to the total amount of tars, the SPA samples also provide information about the different tar molecules and how the tar structures change. Figure 3a, b shows the overall changes in tar composition—divided into seven groups—between the raw gas and the reformed gas at 700 and 800°C. The groupings display the general patterns for the catalytic decomposition of the tars. The tar groups are as follows: phenols, benzene, one-ring aromatic compounds with branches (1-ring), naphthalene, two-ring aromatic compounds with branches (2-ring), three- to four-ring aromatic compounds without branches (3- and 4-rings), and finally "unknowns." The results from experiment performed at 800°C (Fig. 3a) show how the amount of phenols and 1-ring tars decreases, while the amount of benzene increases for both oxygen concentrations. This implies that the decomposition of phenols and1-ring tar molecules takes place via a reaction stripping off the hydroxyl or alkyl group from the branched molecule to form pure benzene. Almost all phenols (98 %) and more than half (55 %) of the 1-ring branched aromatic compounds are converted at 800°C with oxygen concentration of 2.2 mol% in the AR.

Table 3 Tar composition for raw gas (gasifier) and reformed gas at 700 and 800°C leaving the CLR using 23 wt.% M4MgZ1150 in silica sand

Cases	700°C in CLR (g_{tar}/Nm^3)			800°C in CLR (g_{tar}/Nm^3)		
	Measure position (mol% O_2 in AR)					
	Gasifier (–)	CLR (1.0)	CLR (2.2)	Gasifier (–)	CLR (1.0)	CLR (2.2)
Phenol	1.39	0.88	0.39	2.18	0.09	0.07
o-cresol	0.06	0.08	0.03	0.26	0.00	0.00
m-cresol	0.20	0.02	0.00	0.48	0.00	0.00
p-cresol	0.06	0.00	0.00	0.15	0.00	0.00
Benzene	0.75	0.80	0.77	0.51	1.18	1.18
Toluene	0.81	0.82	0.72	0.66	0.68	0.60
m/*p*-xylene	0.21	0.20	0.15	0.19	0.08	0.07
o-xylene	1.33	1.23	1.05	1.10	0.83	0.85
Indan	0.04	0.08	0.06	0.06	0.17	0.16
Indene	3.85	2.08	1.32	3.76	0.65	0.61
Naphthalene	8.01	7.97	8.69	7.54	9.68	8.41
2-methylnaphthalene	1.29	1.03	0.90	1.32	0.52	0.37
1-methylnaphthalene	0.83	0.64	0.55	0.83	0.24	0.17
Biphenyl	0.56	0.58	0.71	0.54	0.81	0.65
Acenaphthylene	2.46	2.13	2.16	2.40	1.51	1.24
Acenaphthene	0.17	0.09	0.08	0.18	0.06	0.04
Fluorene	0.86	0.55	0.42	0.86	0.14	0.09
Phenanthrene	1.71	1.75	2.17	1.77	2.02	1.50
Anthracene	0.51	0.51	0.61	0.53	0.47	0.33
Fluorantene	0.52	0.49	0.61	0.53	0.51	0.36
Pyrene	0.58	0.56	0.71	0.60	0.53	0.36
"Unknowns"	6.72	4.25	3.60	6.43	2.00	1.21
Total tar	32.90	26.73	25.70	32.89	22.18	18.27
Conversion (%)	–	18.8	21.8	–	32.6	44.5

CLR chemical looping reforming, *AR* air reactor

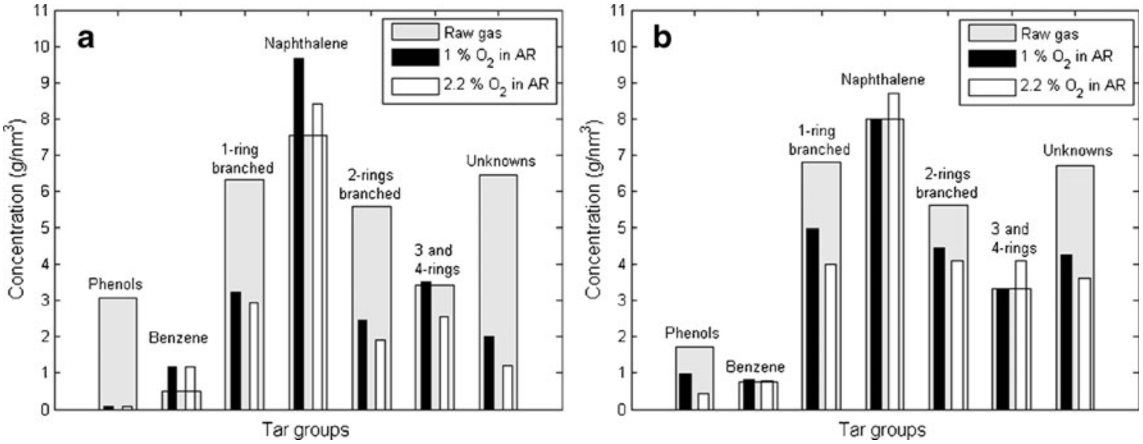

Fig. 3 **a** Composition of tar divided into seven groups for raw gas and reformed gas at 800°C. **b** Tar group composition for raw gas and reformed gas at 700°C

A similar tar decomposing pattern can be seen for the 2-ring tar molecules, where the alkyl group is stripped off forming pure naphthalene. The 2-ring compounds are decreased by as much as 66 % at an oxygen concentration of 2.2 mol% in the AR. Besides the decomposition of phenols and 1- and 2-rings, the decomposition of tars from the group "unknowns" also contributes to the increase in benzene and naphthalene. The "unknowns" comprise at least 150 unidentified tar molecules with molecular weights spread from that of benzene to molecular weights greater than pyrene. The reforming of unknown molecules greater than pyrene may explain why the amount of 3- to 4-rings is higher in the reformed gas than in the raw gas for the 1.0 mol% oxygen case. The elevated concentrations of 3- and 4-rings may well also origin from the decomposition of the heaviest tar molecules, so called non-GC detectable, i.e., not possible to measure via GC-FID.

A general trend for the 800°C case (Fig. 3a) is that increased oxygen concentration increases the conversion of phenols, 1- to 2-rings and "unknowns." In other words, the tar reforming reactions benefit from increased oxygen transfer from the AR to the FR. The tar decomposition pattern of forming pure aromatic compounds (benzene and naphthalene) from branched aromatic compounds and phenols agrees well with results from an experiment involving ilmenite as a tar reforming catalyst in the same system [9].

A similar pattern in reforming phenols and 1-ring compounds can be seen at 700°C (Fig. 3b) but in this case the catalyst activity is lower. At 2.2 mol% O_2 in the AR, the phenols and the 1-ring is reduced by 75 and 41 % in comparison to 98 and 55 % at 800°C. The fraction of benzene is more or less unchanged in comparison to the raw gas for both oxygen concentrations at 700°C. This implies that the rate of benzene decomposition is equal to its rate of formation. A change in oxygen concentration from 1.0 to 2.2 mol% in the AR increases the rate of formation for naphthalene at 700°C (Fig. 3b). The same pattern is seen for the group 3- and 4-rings at the higher oxygen concentration, which can be explained by increased decomposition of "unknowns" and non-GC detectable tars. This implies that the oxygen transfer via the catalyst has greater effect on the decomposition rate of branched molecules than on pure aromatics.

In general, the tar reforming activity of a catalyst decreases and can completely disappear if carbon is depositing on the active sites. As tar cracking and reforming reactions enhance the formation of carbon on the surface of the catalyst, it is therefore important to regenerate and recover the active surface of the catalyst. During CLR operation, the concentration of carbonaceous gases leaving the AR as well as the total gaseous carbon fed to the FR are monitored. The pressure in the AR is kept 200–300 Pa higher than in the FR to preclude raw gas leakage to the AR. The measured CO concentration was below the detection limit of the instrument in both the 700 and 800°C case, which confirms that the deposits of carbon on the catalyst in the FR are nearly fully oxidized to CO_2 in the AR. The measured CO_2 content was in the same order as the detection limit of the instrument, so even though there was a definite increase in CO_2 when comparing the raw gas experiment with the nitrogen fluidization in the FR, the result should be interpreted as trends and not absolute values. However, integrating values under steady-state condition gives an indication of the proportion of carbon deposit actually regenerated in the AR. The calculated mass fraction of carbon in the AR (according to Eq. 4) is shown for the two different oxygen loads at 700 and 800°C in Fig. 4. It can be observed that the increase in oxygen concentration from 1.0 to 2.2 mol% oxygen in the inlet feed to the AR increases the amount of carbon deposits at both 700 and 800°C. This can be explained by the enhanced tar reforming activity in the FR from elevated oxygen transport via the catalyst,

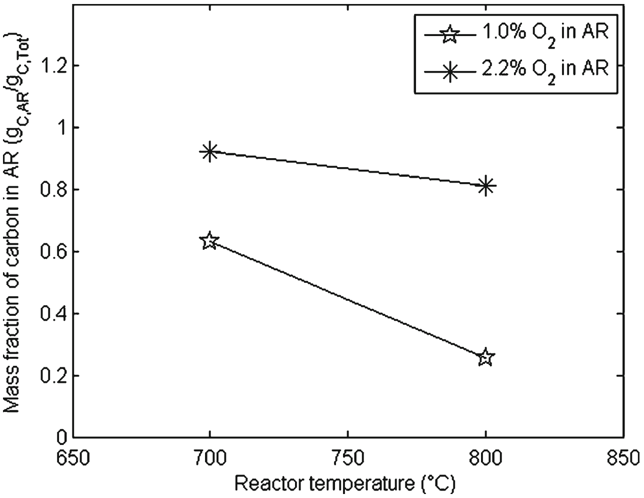

Fig. 4 Mass fraction of carbon in AR

which in turn increases the carbon deposits on the catalyst. The highest amount of carbon deposits were detected at 700°C, where the amount of carbon leaving the AR corresponds to almost 1 % of the total amount of the carbon fed to the FR. The fact that greater amounts of carbon are formed on the catalysts at 700 than at 800°C is a consequence of the endothermic gasification reactions occurring in the FR. The result is that a greater amount of carbon deposits follows the catalysts to the AR where it is converted to CO_2.

The dry composition of the raw gas is compared with the reformed gas after the CLR system, to investigate if the M4MgZ1150 shows any catalytic effect on the permanent gases. The changes in gas compositions are shown for the raw gas and for the reformed gas at 800°C (Fig. 5a). A general trend at 800°C is that the H_2 and CO_2 concentrations increase, while the CO concentration decreases. Furthermore, the concentrations of CH_4 and acetylene decrease slightly. The increase in H_2 can to a large extent be explained by an increased water–gas shift activity (WGS), resulting in that the H_2/CO ratio being shifted from approximately 0.6 in the raw gas to 1 in the reformed gas. However, when comparing the concentrations of the measured gas components in the raw gas and the reformed gas, the decrease in CO, CH_4, and light hydrocarbons is not fully compensated by the increase in CO_2. A possible explanation to this could be that there has been a change in raw gas composition between the measurements on the raw gas and those performed on the reformed gas after the CLR system. Moreover, gas cross-contamination between the AR and the FR—operated at a slightly lower pressure—may have occurred. This would also explain the increased nitrogen content in the reformed gas. Therefore, the changes in gas components between the raw gas and the reformed gas should be regarded as trends and not as absolute numbers.

In Fig. 5b, the gas compositions are shown for the raw gas and the reformed gas at 700°C. In the 1.0 mol% oxygen case, there is a slight increase in H_2 concentration, and for the 2.2 mol% there is a slight decrease in H_2. This shows that the M4MgZ1150 catalyst also induces some activity in WGS reactions at 700°C, but when the oxygen concentration is increased from 1.0 to 2.2 mol%, the produced H_2 is oxidized to water by the catalyst. Just as in the 800°C case, there is a slight decrease in CH_4 and acetylene.

5 Conclusions

A metal oxide named M4MgZ1150, consisting of 40 % Manganese oxide (Mn_3O_4) supported on 60 % $MgZrO_3$, has been investigated as tar reforming catalyst in an application for secondary catalytic tar reforming. The available amount of catalysts was only sufficient to constitute one fourth of the bed material and silica sand was, therefore, used as filler material. The mixed bed material was circulated in a reactor system of dual fluidized beds, where one of the beds was operated as a tar reformer and the second as a

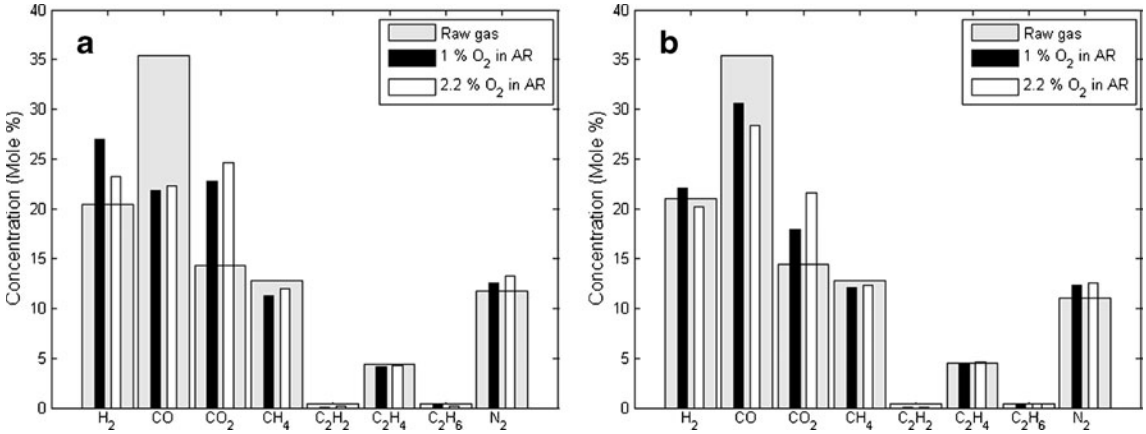

Fig. 5 **a** Gas composition for raw gas and reformed gas at 800°C. **b** Gas composition for raw gas and reformed gas at 700°C

catalyst regenerator. The tar reforming reactor was fed with raw gas from the Chalmers biomass gasifier—containing approximately 32 $g_{tar}/Nm_{raw\ gas}^3$—and the regenerator was fed with two different fractions of oxygen in nitrogen. From the results of the investigation, the following conclusions were drawn:

1. The catalyst showed tar reforming activity, where the small bed—consisting of 23 wt.% M4MgZ1150 in silica sand—generating a gas/catalyst residence time of approximately 0.4 s resulted in a total tar reduction of up to 44.5 % at 800°C. The tar decomposing rate was enhanced with increased oxygen load on the catalyst and tar groups containing branched aromatics and phenols were more easily decomposed by the catalyst than the pure ring structures, i.e., benzene and naphthalene.
2. The catalyst was continuously regenerated from carbon deposits via oxidation into CO_2 in the regenerator reactor. No catalyst deactivation due to carbon deposits was detected, even though a maximum of 1 % of the total amount of fed carbon to the FR was regenerated from the catalyst in the AR.
3. A general trend of increased CO_2 and decreased CO was seen with increased oxygen transport via the catalyst. The catalyst showed activity in water-gas shift reaction at both 700 and 800°C and only a slight decrease in methane and acetylene contents were observed at both temperatures.

Acknowledgments This work has been financially supported through the Era-Net program, E.ON Sverige AB and by Svenskt Förgasningscentrum SFC. The operation of the gasifier has been possible by support from Göteborg Energi, Metso, Akademiska Hus and Swedish Energy Agency. The authors also acknowledge KTH for the tar analysis and research engineer Rustan Marberg for his work with the experimental equipment.

References

1. Engvall K, Kusar H, Sjöström K, Pettersson LJ (2011) Upgrading of raw gas from biomass and waste gasification: challenges and opportunities. Top Catal 54:949–959
2. Pfeifer C, Hofbauer H (2008) Development of catalytic tar decomposition downstream from a dual fluidized bed biomass steam gasifier. Powder Technol 180(1–2):9–16
3. Devi L, Ptasinski KJ, Janssen FJJG (2003) A review of the primary measures for tar elimination in biomass gasification processes. Biomass Bioenergy 24(2):125–140
4. Li CS, Suzuki K (2009) Tar property, analysis, reforming mechanism and model for biomass gasification—an overview. Renew Sustain Energy Rev 13(3):594–604
5. Taralas G, Kontominas MG, Kakatsios X (2003) Modeling the thermal destruction of toluene (C_7H_8) as tar-related species for fuel gas cleanup. Energy Fuel 17(2):329–337
6. Dayton D (2002) A review of the literature on catalytic biomass tar destruction. NREL/TP-510-32815.
7. Bergman PCA, van Paasen SVB, Boerrigter H (2002) The Novel "OLGA" technology for complete tar removal from biomass producer gas. In: Pyrolysis and gasification of biomass and waste, expert meeting 30, Strasbourg, France
8. Caballero AM, Corella J, Aznar MP, Gil J (2000) Biomass gasification with air in fluidized bed. Hot gas cleanup with selected commercial and full-size nickel-based catalysts. Ind Eng Chem Res 39(5):1143–1154
9. Lind F, Seemann M, Thunman H (2011) Continuous catalytic tar reforming of biomass derived raw gas with simultanious catalyst regeneration. Ind Eng Chem Res 50:11553–11562
10. Mattisson T, Lyngfelt A (2001) Applications of chemical-looping combustion with capture of CO_2. In: Second nordic minisymposium on carbon dioxide capture and storage, Gothenborg, Sweden
11. Thunman H, Åmand L-E, Leckner B, Johnsson F (2007) A cost effective concept for generation of heat, electricity and transport fuel from biomass in fluidized bed boilers—using existing energy infrastructure. In: Proceedings of the 15th European biomass conference and exhibition—from research to market deployment, Berlin, Germany
12. Larsson A, Seemann M, Thunman H (2010) Zero-dimensional modeling of indirect fluidized bed gasification. In: International conference on fluidization, fluidization XIII, Gyeong-ju, Korea, pp 845–852
13. Ryden M, Lyngfelt A, Mattisson T (2006) Synthesis gas generation by chemical-looping reforming in a continuously operating laboratory reactor. Fuel 85(12–13):1631–1641
14. Lyngfelt A, Leckner B, Mattisson T (2001) A fluidized-bed combustion process with inherent CO_2 separation; application of chemical-looping combustion. Chem Eng Sci 56(10):3101–3113
15. Johansson M, Mattisson T, Lyngfelt A (2006) Investigation of Mn_3O_4 with stabilized ZrO_2 for chemical-looping combustion. Chem Eng Res Des 84(9):807–818
16. Mendiara T, Johansen MJ, Utrilla L, Geraldo P, Jensen AD, Glarborg P (2011) Evaluation of different oxygen carriers for biomass tar reforming (I): carbon deposition in experiments with toluene. Fuel 90(3):1049–1060
17. Mendiara T, Johansen MJ, Utrilla L, Geraldo P, Jensen AD, Glarborg P (2011) Evaluation of different oxygen carriers for biomass tar reforming (II): carbon deposition in experiments with methane and other gases. Fuel 90(4):1370–1382
18. Brage C, Qizhuang Y, Chen G, Sjöström K (1997) Use of amino phase adsorbent for biomass tar sampling and separation. Fuel 76 (2):137–142

Paper IV

I&EC research
Industrial & Engineering Chemistry Research

Article

pubs.acs.org/IECR

Use of Nickel Oxide as a Catalyst for Tar Elimination in a Chemical-Looping Reforming Reactor Operated with Biomass Producer Gas

Nicolas Berguerand,*[,†] Fredrik Lind,[†] Mikael Israelsson,[†] Martin Seemann,[†] Serge Biollaz,[‡]
and Henrik Thunman[†]

[†]Department of Energy and Environment, Chalmers University of Technology, SE-412 96 Göteborg, Sweden
[‡]Paul Scherrer Institut (PSI), Laboratory of Energy and Material Cycles, CH-5232 Villigen PSI, Switzerland

ABSTRACT: A secondary tar-cleaning process based on chemical-looping reforming (CLR) was investigated for upgrading biomass producer gas, derived from the Chalmers University of Technology 2-4 MW indirect gasifier. The experiments were conducted in a bench-scale CLR reactor using a manufactured nickel oxide (NiO) catalyst. Although Ni is a well-documented and efficient steam-reforming catalyst, it is susceptible to rapid deactivation under tar-rich conditions. The aim of this study was to explore the advantages of CLR as a gas-cleaning application, a process which offers continuous regeneration of the carbon deposits on catalysts. The tar-reforming performance of this Ni material and its influence on the gas composition and in particular its potential to increase the H_2/CO ratio, were studied. The system was tested at reforming temperatures that ranged from 700 to 880 °C and at oxygen concentrations of 1.0% and 2.2% in the inlet feed to regenerator section. The results confirm the strong ability of the catalyst to reform tars. Higher process temperatures clearly promoted tar conversion, with 96% overall conversion at 880 °C (99% if benzene is excluded), as compared with 45% conversion at 700 °C. The hydrogen production was favored when temperature was raised, though, a maximum ratio of H_2/CO of 2.2 was observed at 750 °C. Finally, no time-on-stream deactivation of the catalyst in the CLR was observed during the test, which lasted almost 7 h.

■ INTRODUCTION

Biomass gasification, which is an attractive technology to produce gaseous fuels from the chemically stored energy in lignocelluloses, could play a prominent role in the current efforts to diversify the energy supply. In general, an increase in biomass use to replace fossil fuels as feedstocks in industrial processes is an important part of the strategy to meet environmental concerns and demands. However, a major drawback of gasification is the formation of differing contents of tars in the producer gas stream.[1−4] These tars consist of complex mixtures of hydrocarbons, commonly one- to five-ring aromatic compounds, some of which contain oxygen and sulfur. The correspondingly high dew-points, with some tars already condensing at ≥350 °C, raise downstream issues with regard to equipment that is prone to fouling.[5] Consequently, efficient removal of tar from the raw gas exiting the biomass gasifier is a prerequisite for widespread application of the gasification concept. Thus, there is a need for substantial gas conditioning using different techniques. In this respect, the most pertinent options are hot gas cleaning and wet cleaning. Although wet cleaning relies on well-established scrubbing methods, it creates an additional waste stream and a heat penalty as a result of rapid cooling; these problems are not associated with hot gas cleaning. Moreover, the requirement for a constant supply of new scrubbing solvent affects the overall efficiency of the wet cleaning method.

The present study investigates a secondary catalytic tar-cleaning process that is based on dual circulating fluidized beds (CFB). This process exploits the advantages of catalytic tar cleaning and inherent catalyst regeneration. To advance this process, detailed experimentation needs to be conducted. A crucial aspect of this research is the development of suitable and economically viable catalysts that can achieve high conversion rates for tars while remaining active despite exposure to repeated redox cycles and contaminants. In this respect, the present study evaluates the catalytic qualities of a manufactured Ni-based catalyst with regard to tars and the permanent gas composition. For this purpose, we use the CFB reactor concept, which differs from the traditional approaches to gas upgrading. Although such catalysts are expensive to produce, they could become an interesting option for tar cleaning if their duration of activity in operation is maintained by continuous regeneration. The use of Ni-based catalysts (some of which are commercially available) for tar elimination have been thoroughly investigated, principally in fixed-bed applications, and the results have been reported[6−12] and summarized.[6,11,12] These studies describe how not only sulfur, chlorine, and alkali metals, but also rapid coke formation on the catalyst can all act as catalyst poisons.[6,8] Some of the advantages of the reactor system used in the present work over the fixed bed configuration are examined below.

■ THEORY

Chemical-Looping Reforming. The technique presented here is called chemical-looping reforming (CLR) and is derived from the chemical-looping combustion (CLC) principle, which over the past decade has been developed to process gaseous, solid, and liquid fuels.[13−17] The idea of CLR was first presented in a patent by Arnold Conrad of the Standard Oil Development

Received: October 16, 2012
Revised: December 7, 2012
Accepted: December 10, 2012
Published: December 10, 2012

Company in the 1950s[18] and was reintroduced by Mattisson et al. in 2001.[19] Subsequently, the concept was experimentally established for the production of hydrogen in a 300 W prototype by Rydén et al.,[20] while its application for tar cracking was demonstrated by Lind et al.[21−23]

In the CLR concept, partial oxidation of the raw gas in the fuel reactor (FR) is achieved by means of partial oxidation of the oxygen carrier in the air reactor (AR) using nitrogen-diluted air (Figure 1). Reactions 1 and 2 illustrate the principal pathway for reforming the tar component (C_nH_m) in the FR. It should be noted that the level of oxygen transport will affect the composition of the permanent gases, as a minor proportion of the hydrocarbons and/or hydrogen will be partly or fully oxidized. However, in the present case, it is mainly the tar components that are considered.

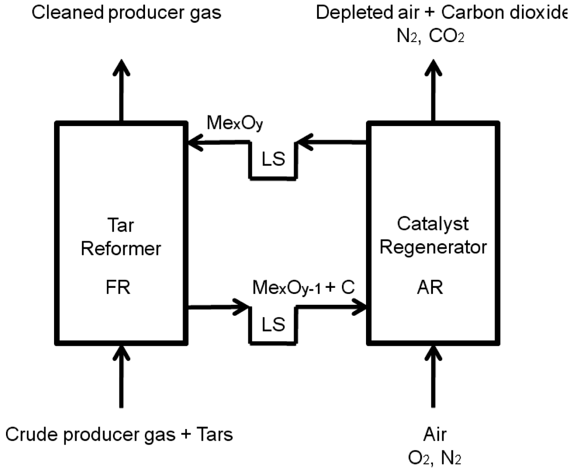

Figure 1. Dual fluidized bed system for tar reforming.

$$C_nH_m + (n - n_1)Me_xO_y \rightarrow (n - n_1)CO + (0.5m)H_2 + (n - n_1)Me_xO_{y-1} + n_1C \qquad (1)$$

$$C_nH_m + Me_xO_{y-1} + H_2O * + CO_2* \rightarrow C_iH_j + H_2 + CO \qquad (2)$$

In reaction 1, the oxygen carried by the catalyst is consumed to convert some of the tars into mainly CO and H_2. Thus, the reduced catalyst particles act as both tar-reforming catalysts and reactants with the reforming media, such as steam and CO_2, according to the general reaction 2. As tar is being removed from the crude producer gas *via* reactions 1 and 2, an undesired carbon deposit is formed on the catalyst. This phenomenon has been observed in several studies.[8,24,25] In industrial applications, the resulting catalyst decay represents a major problem for continuous operation and makes the implementation of an effective regeneration step compulsory. In the present study, in contrast to the fixed-bed configuration, the circulation loop (see Figure 1) enables catalyst rejuvenation in the AR. More precisely, the carbon deposit is oxidized to form CO_2 and the catalysts are reoxidized following reaction 3:

$$n_1Me_xO_{y-1} + n_2C + (n_1/2 + n_2)(O_2 + 3.77N_2) \rightarrow n_1Me_xO_y + n_2CO_2 + (n_1/2 + n_2)(3.77N_2) \qquad (3)$$

In reactions 1−3, Me_xO_y and Me_xO_{y-1} represent the oxidized and reduced forms, respectively, of the catalyst.

Thus, in CLR, the circulation of solids between the reactors offers the possibility to regenerate the catalyst, which makes the system applicable even to producer gases with high concentrations of tars. This reactor configuration with continuous regeneration evokes the fluid catalytic cracking (FCC) technology, in which the process includes reformation of hydrocarbons, and the carbon deposits supply the heat for the endothermic cracking reactions.[26] Reaction 1 is often endothermic, whereas reaction 2 is strongly exothermic. Two loop-seals (LS) fluidized with inert gas prevent cross-contamination of the gas effluents from the AR and FR, thereby allowing sampling and analyses of the respective outlets (Figure 1).

In addition to reactions 1 and 2, the tar removal mechanisms can proceed through other pathways. Simell et al.,[9] using toluene as a representative tar component together with various catalysts including NiO, proposed a set of possible decomposition reactions. These reactions include steam reforming or steam dealkylation. Lind et al.[21] have summarized the main mechanisms. Since reforming reactions are endothermic, they are favored at higher temperatures. In addition, several equilibrium reactions can take place in the FR, some of which occur only in the gas phase, while others involve the carbon deposit.[21] Steam-reforming reactions and the water gas shift equilibrium (WGS) are particularly interesting considering that the steam content of the raw gas is usually high (typically 50−60 mol %).

For the experimental operations described in the present study, the crude producer gas was delivered by the Chalmers indirect biomass gasifier, which was operated at 2 MW. A description of the facility is provided elsewhere.[27,28] The gas composition of the inlet stream and its tar content vary somewhat depending on gasifier operation.

■ EXPERIMENTAL SECTION

CLR reactor. The CLR reactor system is constructed in stainless austenitic chromium−nickel steel (253 MA) and has a maximal operational temperature of 1100 °C. The setup of the reactor is shown in Figure 2. The CLR comprises an FR in the form of a bubbling fluidized bed attached to an AR, designed as a riser with a smaller cross-section. Ascending particles in the suspended gas flow leaving the AR are efficiently collected by cyclonic separation before they proceed to the FR *via* a loop-seal (LS). The loop-seals have rectangular cross sections and include the upper loop-seal (ULS), located beneath the cyclone leg, and lower loop-seal (LLS), located in the transfer line back to the regenerator. The reactor is a bench-scale system that is not self-supporting in terms of energy; the heat supply is delivered by an oven inside which the unit is inserted. The separate heating system also means that there is the possibility to induce different temperatures in the AR and FR.

During operation, the FR is fluidized with raw gas from the gasifier while the LLS and ULS are fluidized with helium. The partial oxidation of the catalyst in the AR is achieved by fluidizing the corresponding bed with a mixture of air and nitrogen, thereby diluting the inlet stream to the desired oxygen concentration that is, air-to-fuel ratio. Pressure taps, of which there are 10 in total, are located alongside the reactors, wind-boxes, loop-seals, and exit ducts and allow monitoring of the differential pressures in the system, as well as indirect tracking of the bed material. Moreover, 10 thermocouples ensure

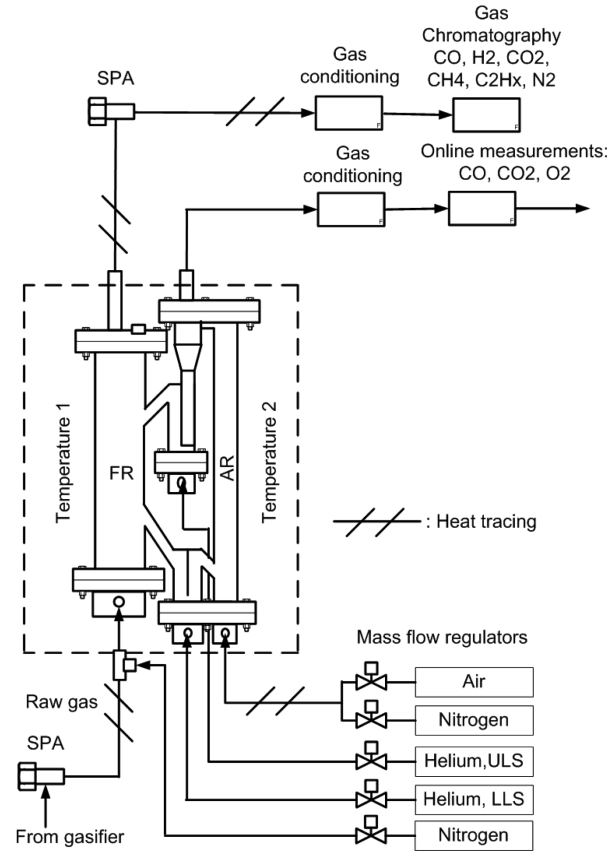

Figure 2. CLR setup.

temperature supervision. Detailed descriptions of the reactor system and its dimensions are provided elsewhere.[21]

Bed Material. The bed material used in the present experiments comprises nickel oxide supported on an α-Al_2O_3 matrix. These near-spherical particles were prepared by spray-drying, and the active NiO content was 40% wt. The apparent density of the particles was 2850 kg/m^3 and the particle size distribution (PSD) was in the range of 125−180 μm. More information on the preparation and properties of the catalyst is provided in a previous publication,[29] where the material is referred to as "S1 particles". In previous investigations using the CLR, experiments with various proportions of catalyst, ranging from 20% to 60%, were conducted in combination with silica−sand as the inert fraction.[21−23] The catalysts used were ilmenite, an iron titanium oxide, and manufactured particles that consisted of 40% manganese oxide (Mn_3O_4) on a 60% magnesium−zirconium (Mg-ZrO_2) matrix. The results indicated promising tar-removing abilities for both catalysts used in the process.[21−23] In a fully deployed system, the solids inventory would most likely consist of 100% of the chosen catalyst material, as was the case in the present investigation.

Operating Conditions. To minimize the risk of leakage of toxic gases, the Chalmers gasifier is operated at a pressure slightly below the atmospheric pressure. This implies that the CLR system itself must be run at subatmospheric pressures, that is, −6 to −4 kPa in this case. As no functional flow control equipment can handle a raw gas inlet temperature of nearly 350 °C, a pump was mounted in the FR exhaust line, which meant that the driving force for bed fluidization was exerted downstream of the CLR. To maintain the variations in pressure between the reactors at reasonable levels and thereby prevent gas leakage, a similar pump was placed at the outlet of the AR. During the start-up of the CLR system, the AR and FR were air-fluidized while the temperature was gradually ramped to the set-point. The LS were fluidized with helium. Once catalyst circulation was established and the temperature was stabilized, the FR fluidization was replaced with N_2 fluidization. The raw gas line was then attached to a T-connector upstream of the FR (Figure 2). At this stage, the FR was still fluidized with N_2, while part of the incoming stream could leak backward into the gasifier. Raw gas operation was initiated by decreasing in a stepwise manner the flow of N_2 until all the supply of N_2 was discontinued. A steady-state was normally reached within 30−45 min.

In the present work, the FR was tested at 700, 750, 800, and 880 °C. The gasifier was operated with wood pellets at slightly differing temperatures, ranging from 800 to 830 °C. The total bed inventory of the gasifier was typically 900−1000 kg, and the heat requirement was met by the circulation of hot silica-sand between the boiler and the gasifier.[27,28] Variations in fuel quality and gasifier operation over time can affect the properties of the raw gas to be fed into the CLR. Table 1 recapitulates the main operating parameters used in the CLR during the course of an experiment. Oxygen constituted either 1.0% or 2.2% of the gas entering the AR. The lambda (λ) term is defined as the ratio between the amount of oxygen provided to the system in the air flow to the AR ($F_{O,AR}$) and the oxygen that would be needed to combust completely the raw gas ($F_{O,needed}$), according to eq 4:

Table 1. Operating Parameters for the CLR

fuel	raw gas
temperature range (°C)	700−880
bed material	NiO on α-Al_2O_3
total bed inventory (g)	500
FR fluidization, dry gas (L_n/min)	~3.1
λ values	~0.024 (1% O_2), ~0.050 (2.2% O_2)
steam content in raw gas (%)	~50−55
helium fluidization LLS/ULS (L_n/min)	0.25/0.40
gas−solids contact time (s)	0.29−0.35
gas residence time in reactor (s)	2.25−2.66

$$\lambda = \frac{F_{O,AR}}{F_{O,needed}} \tag{4}$$

Note the high steam content of the raw gas fed to the CLR (Table 1).

Tar and Gas Analyses. Sets of solid phase adsorption (SPA) samples were extracted to yield the tar composition in both the inlet and outlet streams of the reformer reactor (see Figure 2 for the locations of the SPA sampling ports). The SPA methodology was developed at Kungliga Tekniska Högskolan (Stockholm, Sweden) by Brage and colleagues.[30] Details of the SPA sampling in this unit are provided elsewhere.[21] Typically, the producer gas contains numerous tar compounds, with signals from at least 200 different components being detected. In the present study, the focus was on total tar concentrations, as well as on the levels of specific tar components that are present in representative quantities and that are indicative of decomposition pathways.

Moreover, during the course of the experiment, analyses of the dry raw gases and reformed gases were carried out in a Varian 4900 microgas chromatograph (micro-GC) using a setup placed in parallel to the CLR by Jörg Schneebeli (Paul Scherrer Institute, Switzerland). The permanent gases measured in this way included: N_2, CO, CO_2, CH_4, H_2, C_2H_2, C_2H_4, C_2H_6, and C_3H_8. Finally, from the AR, the levels of O_2, CO, and CO_2 were detected by online gas analysis.

RESULTS AND DISCUSSION

Effect of Temperature on the Amount and Composition of Tar. To investigate the effect of temperature on the levels and compositions of the tars in the reformed gas, a series of tests was conducted at four temperatures: 700, 750, 800, and 880 °C. Using SPA, the concentrations in the raw gas line and at the outlet of the FR were evaluated. Figure 3 compares the total concentrations in these streams at the four temperatures investigated, for the delivery of 1.0% O_2 to the AR ($\lambda \approx 0.024$). When similar experiments were conducted in a previous study using inert silica–sand as the reference bed material, no appreciable level of tar conversion was detected.[21]

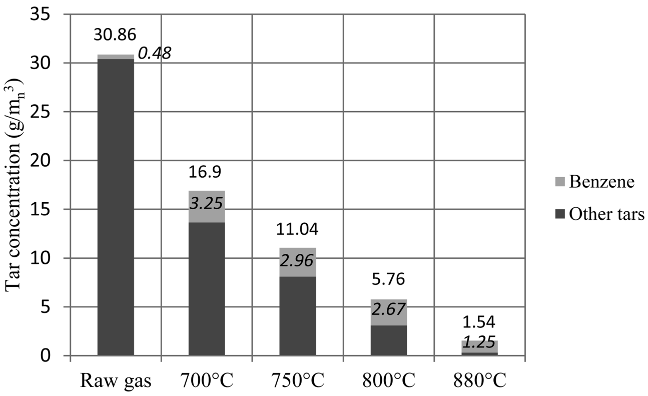

Figure 3. Total levels of tars in the raw gas and reformed gas using at four different temperatures and in 1.0% O_2 (i.e., $\lambda \approx 0.024$).

From the data in Figure 3, it is clear that catalytic tar reforming occurs in the FR, as the total amounts of tar are lower in the reformed gas than in the raw gas, for example, reduced by 46% at 700 °C. Moreover, a clear effect of temperature is observed. At higher temperatures, more tars are converted. The highest temperature of 880 °C yields a conversion rate of 95%. The amounts of benzene in the different cases are shown in Figure 3. While benzene represents only a small percentage of the total tars in the raw gas, its share in the reformed gas increases significantly, until at 880 °C almost all the tars consist of benzene. It must be emphasized that benzene, being more volatile than the heavier tars, is more difficult to measure accurately using SPA.[30] This is one of the reasons why some research groups do not include benzene in their definition of tars.[3] If benzene is excluded, the data in Figure 3 indicate a 99% reduction in tar levels at the highest temperature. This is comparable to the highest tar cracking efficiencies achieved using fixed beds and nickel catalysts, as reported previously.[6] In particular, Zhang et al.[7] claimed to have eliminated >99% of heavy tars using a combined guard bed and a reactor filled with Ni catalysts. Moreover, in the present work, the inlet concentrations of tar measured directly in the gasifier raw gas stream were generally higher and the gas–solids residence times in the CLR were similar or lower than those cited in the aforementioned studies, in which guard beds or scrubbing methods were usually placed upstream of the actual catalyst beds.[7,11] For instance, Han et al.[11] reported on tar cracking with residence times in the catalytic bed of several seconds, as compared with gas–solids contact times of <0.5 s in the present study. Finally, a comparatively shorter residence time may also explain the lower rate of tar conversion observed in the CLR at a low operating temperature.

A comparison performed for the case involving an O_2 load of 2.2% showed similar trends and rather similar outlet concentrations of tars in the reformed gas for the respective temperatures. The findings that the O_2 load to the regenerator has little influence on the efficiency of tar reforming in the reformer means that for a real system, O_2 transport should be optimized so as to minimize oxidation of the permanent gases in the reformer, while ensuring complete regeneration of the catalyst and maintenance of the heat balance.

Table 2 compares the amounts (in g/m_n^3) of the principal tar components in the raw and reformed gases for the four temperatures studied. The results show that for all the temperatures studied, the levels of phenols, one-ring branched and two-ring branched hydrocarbons decreased after passage through the reformer. In contrast, the level of benzene increased. This is consistent with a decomposition pathway that involves the removal of the alkyl or hydroxyl groups from the one-ring branched hydrocarbons and phenols, to form benzene. These trends appeared to be substantially enhanced at higher temperatures (Table 2). In particular, virtually all the phenols were converted at 800 °C. This is expected, as the main reactions involving tar decomposition are endothermic, which means that they are enhanced at higher temperatures.[20] Moreover, these results are in accordance with a tar decomposition process that is exacerbated by the presence of group VIII transition metals, that is, Ni in this case.[9]

Table 2. Principal Tar Components in the Raw and Reformed Gas (g/m_n^3)

		reformed gas			
tar species	raw gas	700 °C	750 °C	800 °C	880 °C
benzene	0.479	2.604	2.366	2.240	1.047
toluene	0.893	1.788	0.952	0.394	0.020
xylene	0.329	0.138	0.048	0	0
phenol	2.962	0.365	0.112	0.029	0
indene	3.032	0.085	0.030	0.020	0
cresol	0.848	0	0	0.007	0.005
naphthalene	5.070	4.888	3.511	1.597	0.158
methylnaphthalene	1.569	0.219	0.064	0.024	0.004
biphenyl	0.378	0.364	0.222	0.066	0
acenaphthylene	1.222	0.035	0.012	0.009	0
acenaphthene	0.125	0	0	0	0
fluorene	0.595	0.244	0.128	0.030	0
phenanthrene	1.213	1.003	0.573	0.198	0.012
anthracene	0.338	0.107	0.047	0.011	0
fluoranthene	0.282	0.112	0.046	0.013	0
pyrene	0.343	0.428	0.265	0.082	0

Naphthalene degradation was more temperature sensitive than, for example, benzene degradation (Table 2). Basically, at 880 °C, only the most hardly decomposed benzene and naphthalene remained in the reformed gas. Overall, reasonably efficient removal of tar can be achieved using this nickel catalyst in the CLR system, even at relatively low temperatures and O_2 levels. More importantly, temperature clearly has an effect on the performance of the system.

Effect of Temperature on the Composition of the Reformed Gas. The influence of temperature on the composition of the permanent gases was examined. The system was tested at 700, 750, 800, and 880 °C. For comparison, O_2 levels of 1.0% and 2.2% in the inlet feed to the AR were tested. The aim was to investigate the ability of the bed material to adjust catalytically the gas composition. In this section, C_2H_x regroups C_2H_2, C_2H_4, and C_2H_6.

Figure 4 displays the gas concentrations as a function of time for samples taken at the outlet of the FR, for a single day of the experiment during which two temperature cases and two O_2 levels were investigated. In Figure 4, there is no clear evidence that the O_2 content in the AR *per se* had any effect on the gas composition in the reformed gas. However, a higher temperature promoted the formation of H_2, while almost half of the CH_4 was consumed. It is evident from Figure 4 that the conditions at a given temperature are fairly stable. Moreover, there is no indication that any loss of catalytic activity occurred over the 7-h duration of the experiment.

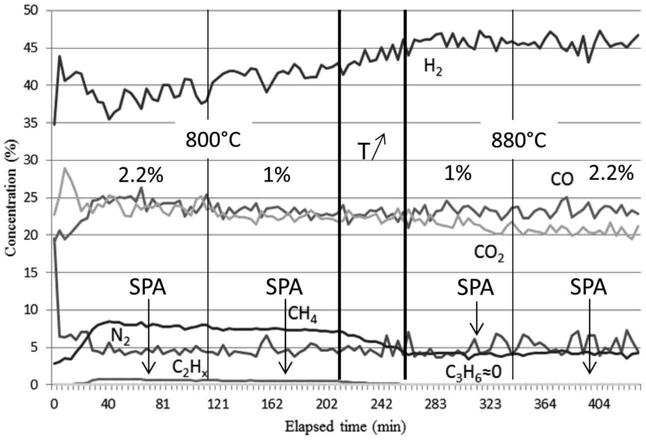

Figure 4. Gas concentration profiles versus time elapsed at the outlet of the FR at 800 and 880 °C and with oxygen loads of 1.0% and 2.2% (i.e., $\lambda \approx 0.024$ and 0.050, respectively).

Figures 5 and 6 present the gas distributions in the raw and reformed gases for the four respective temperatures. Note that for the FR inlet, average values are presented as the composition varied only slightly between experiments.

Figure 5 indicates a trend toward an increase in H_2 in the reformed gas, as compared with the raw gas, as the temperature is increased. Provided that no leakage occurs from the AR to the FR, the only source of N_2 is the raw gas itself. Thus, a constant N_2 content would indicate that the total flow of dry gas entering and leaving the FR is unchanged. In contrast, a decrease in the N_2 content would imply an increase in the dry raw gas flow. The latter is observed in Figure 5: as the temperature rises, the N_2 content decreases. The increase in dry flow is a result of various reactions, such as steam or dry reforming of the tars, methane reforming, and possibly the WGS, all of which processes produce more permanent gases than they consume. The WGS might also explain the apparent increases in H_2 and CO_2 relative to the raw gas composition (Figure 5). Endothermic reforming reactions, which are favored at higher temperatures, produce mainly H_2 and CO. However, CO is partly consumed through the WGS, which explains why the CO content is less affected than the H_2 content. These reactions result in increases in the dry gas flow leaving the FR (Figure 5) at 800 and 880 °C. In particular, half of the methane is consumed at higher temperatures, since methane steam reforming is enhanced. In addition, at higher temperatures, gasification of the carbon deposited on the catalyst is promoted, yielding CO and H_2. Note that the levels of C_3H_6 in the reformed gas are too low (<0.05%) to be perceptible in Figure 5. Finally, at 750 °C, virtually all the C_2H_x were already converted. This is advantageous with respect to the potential implementation of downstream methanation, as C_2H_x is associated with downstream catalyst deactivation.[31]

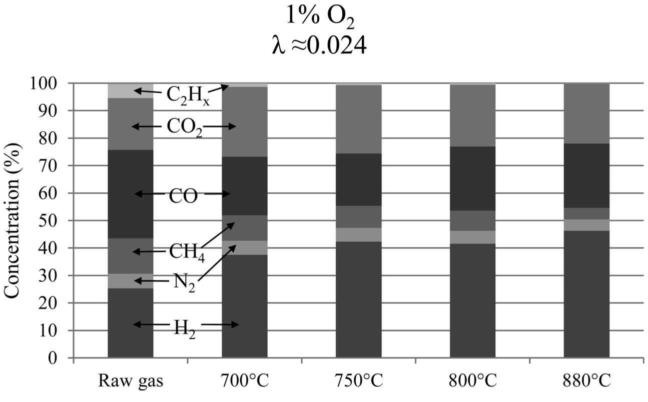

Figure 5. Average gas compositions of raw and reformed gases at four different temperatures with oxygen load of 1.0% (i.e., $\lambda \approx 0.024$).

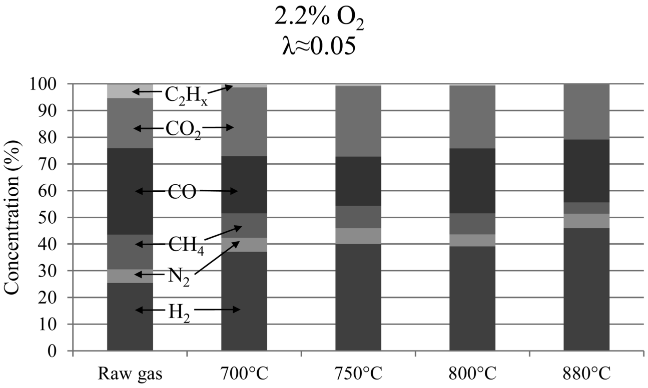

Figure 6. Average gas composition of raw and reformed gases at four different temperatures and oxygen load of 2.2% (i.e., $\lambda \approx 0.050$).

Figure 6 shows the results for 2.2% O_2 load in the regenerator. Results similar to those shown in Figure 5 were obtained, with increases in H_2 levels as the temperature increased. These results indicate that the degree of catalyst oxidation has little influence on the permanent gas composition in the FR, confirming the deductions made from the data in Figure 4.

The H_2/CO ratios (in Figures 5 and 6) were examined for the different operating conditions and regrouped in Figure 7. Even if a tenuous trend toward increases in ratios with increasing temperatures is suggested by the data in these figures, a maximum ratio of 2.2 is already reached at 750 °C. A ratio approaching 3 appears to be favorable for a downstream methanation step.

Finally, Figure 8 summarizes the effect of O_2 load at a given temperature. The case involving the process temperature of 800 °C was considered.

Figure 8 confirms the observation that the O_2 load to the AR reactor has little influence on the outcome in the FR reactor

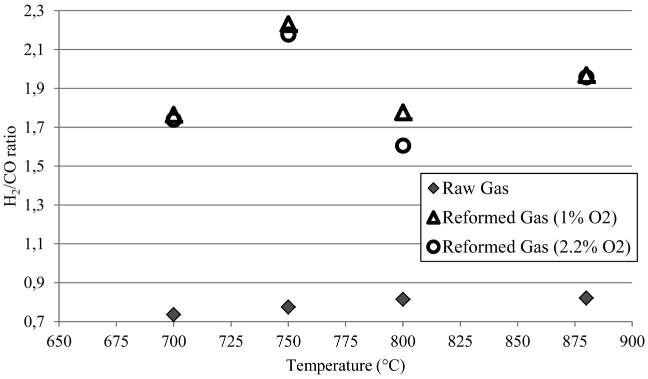

Figure 7. H_2/CO ratios in the raw and reformed gases at four different temperatures with oxygen loads of 1.0% and 2.2% (i.e., $\lambda \approx 0.024$ and 0.050, respectively).

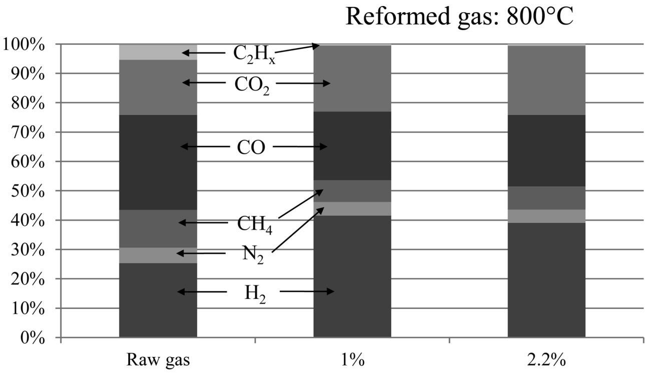

Figure 8. Average gas composition of raw and reformed gases at oxygen levels of 1.0% and 2.2% and 800 °C.

when it comes to modifying the permanent gas composition. With the exception of some minor consumption of H_2, no major differences were noted between the two O_2 load cases.

Carbon Transport and Catalyst Deactivation. The concentrations of CO and CO_2 leaving the AR were monitored. With the given sensitivity and lower detection limit of the analyzers, no appreciable levels of CO_2 were detected at the outlet of the regenerator. Moreover, there was no evidence of time-on-stream deactivation caused by catalyst poisoning due, for example, to carbon deposition. This suggests that either the conditions in the reformer were sufficiently favorable to inhibit formation of carbon deposits or that precursors for deposits were efficiently removed from the catalyst before this latter proceeded to the regenerator. That the operating conditions in a fluidized bed can have carbon-regenerative effects on Ni catalysts has been shown by Seemann et al.[32] Both of the above scenarios are plausible and represent advantages of the CLR configuration over fixed beds, despite the fact that the experiment was limited to a few hours. However, it should be stressed that with such high levels of tar in the raw gas (typically 30 g/m_n^3), a fixed bed of Ni catalyst would probably have lost activity very rapidly during this time period.[33] Taken together, these findings strengthen the promise of the CLR process for tar-reforming applications, even if longer-term experiments are needed to confirm these preliminary observations.

■ CONCLUSIONS

We investigated the performance of a bench-scale CLR reactor in combination with a manufactured nickel-based catalyst with respect to decreasing the tar levels from a biomass-generated crude gas. The experiments involved testing at four different temperatures, 700, 750, 800, and 880 °C, as well as two distinct oxygen concentrations (1.0% and 2.2%) in the inlet feed to the regenerator reactor or air reactor (AR). These values correspond to air-to-fuel ratios of 0.024 and 0.050, respectively.

The results of these experiments indicate that the following: (i) The NiO catalyst showed strong tar-reforming abilities and is suitable for the complex process of upgrading biomass producer gas. (ii) The NiO catalyst exhibits a capacity to convert tars in the raw gas, even at low temperatures. Indeed, at 700 °C, 45% of the total tars in the raw gas were eliminated after passing through the CLR. At 750 °C, the corresponding tar-removal rate was 66%. (iii) At 880 °C, 96% of the tars are eliminated. If benzene is not taken into account, 99% of the tars are eliminated; this is comparable to the gas-conditioning efficiencies of fixed beds that use nickel catalysts. (iv) The catalyst showed a tendency to shift the H_2/CO ratio from approximately 0.7 in the raw gas to 2.2 at the higher temperature (800 °C). H_2/CO ratios closer to 3 could be favorable in downstream methanation processes. (v) The oxygen load has little influence on either tar conversion or permanent gas composition. (vi) Thanks to the CLR reactor configuration offering inherent catalyst regeneration within the loops of solids, no loss in catalyst activity was observed during almost 7 h of experimentation.

■ AUTHOR INFORMATION

Corresponding Author

*E-mail: nicoberg@chalmers.se. Tel: +46 (0)31 772 52 41.

Notes

The authors declare no competing financial interest.

■ ACKNOWLEDGMENTS

This work was made possible by financial support from E.On. Operation of the gasifier was supported by Göteborg Energi, Metso, Akademiska Hus, and the Swedish Energy Agency (Energimyndigheten). The authors thank research engineers Rustan Marberg, Jessica Bohwalli, and Johannes Öhlin for their valuable help with the experimental equipment and Jörg Schneebeli (PSI, Switzerland) for the gas analysis.

■ NOMENCLATURE

AR = air reactor
CFB = circulating fluidized bed
CLC = chemical-looping combustion
CLR = chemical-looping reforming
FCC = fluid catalytic cracking
FR = fuel reactor
LLS = lower loop seal
LS = loop-seal
Me_xO_y = oxidized metal-oxide
Me_xO_{y-1} = reduced metal-oxide
ULS = upper loop seal
SPA = solid phase adsorption

■ REFERENCES

(1) Pfeifer, C.; Hofbauer, H. Development of catalytic tar decomposition downstream from a dual fluidized bed biomass steam gasifier. *Powder Technol.* **2008**, *180* (1–2), 9–16.

(2) Devi, L.; Ptasinski, K. J.; Janssen, F. J. J. G. A review of the primary measures for tar elimination in biomass gasification processes. *Biomass Bioenergy* **2003**, *24* (2), 125–140.

(3) Milne, T. A., Evans, R. J. Abatzoglou, N. *Biomass gasifier "tars": Their nature, formation, and conversion*; National Renewable Energy Laboratory: Golden, CO, November 1998; No. NREL/TP-570–25357.

(4) Li, C. S.; Suzuki, K. Tar property, analysis, reforming mechanism and model for biomass gasification—An overview. *Renew. Sustain. Energy Rev.* **2009**, *13* (3), 594–604.

(5) van Paasen, S. V. B., Kiel, J. H. A. Tar formation in a fluidized-bed gasifier—Impact of fuel properties and operating conditions, Energy Research Center of the Netherlands: Petten, The Netherlands, March 2004; No. PECN-C-04-013.

(6) Dayton. D. *Review of the Literature on Catalytic Biomass Tar Destruction—Milestone Completion Report*; National Renewable Energy Laboratory: Golden, CO, December 2002; No. NREL/TP-510–32815.

(7) Zhang, R.; Brown, R. C.; Suby, A.; Cummer, K. Catalytic destruction of tar in biomass derived producer gas. *Energy Converse. Manage.* **2004**, *45*, 995–1014.

(8) Coll, R.; Salvado, J.; Farriol, X.; Montane, D. Steam reforming model compounds of biomass gasification tars: conversion at different operating conditions and tendency towards coke formation. *Fuel Process. Technol.* **2001**, *74*, 19–31.

(9) Simell, P.; Kurkela, E.; Ståhlberg, P.; Hepola, J. Catalytic hot gas cleaning of gasification gas. *Catal. Today* **1996**, *27*, 55–62.

(10) Courson, C.; Makaga, E.; Petit, C.; Kiennemann, A. Development of Ni catalysts for gas production from biomass gasification. Reactivity in steam- and dry-reforming. *Catal. Today* **2000**, *63*, 427–437.

(11) Han, J.; Kim, H. The reduction and control technology of tar during biomass gasification/pyrolysis: An overview. *Renew. Sustain. Energy Rev.* **2008**, *12* (2), 397–416.

(12) Sutton, D.; Kelleher, B.; Ross, J. R.H. Review of literature on catalysts for biomass gasification. *Fuel Process. Technol.* **2001**, 73, 155–173.

(13) Lyngfelt, A.; Leckner, B.; Mattisson, T. A fluidized-bed combustion process with inherent CO_2 separation; application of chemical-looping combustion. *Chem. Eng. Sci.* **2001**, *56* (10), 3101–3113.

(14) Linderholm, C.; Mattisson, T.; Lynfelt, A. Long-term integrity testing of spray-dried particles in a 10 kW chemical-looping combustor using natural gas as fuel. *Fuel* **2009**, *88* (11), 2083–2096.

(15) Leion, H.; Mattisson, T.; Lyngfelt, A. Solid fuels in chemical-looping combustion. *Int. J. Greenhouse Gas Control* **2008**, *2*, 180–93.

(16) Berguerand, N.; Lyngfelt, A. Design and operation of a 10 kWth chemical-looping combustor for solid fuels—Testing with South African coal. *Fuel* **2008**, *87* (12), 2713–2726.

(17) Moldenhauer, P.; Rydén, M.; Mattisson, T.; Lyngfelt, A. Chemical-looping combustion and chemical-looping reforming of kerosene in a circulating fluidized-bed 300 W laboratory reactor. *Int. J. Greenhouse Gas Control* **2012**, *9*, 1–9.

(18) Arnold, C. Process for production of carbon monoxide and hydrogen. Standard Oil Development Company Patent GB636206, 1950.

(19) Mattisson, T., Lyngfelt, A. Applications of Chemical-Looping Combustion with Capture of CO_2. Second Nordic Minisymposium on Carbon Dioxide Capture and Storage, Göteborg, Sweden, 2001.

(20) Ryden, M., Hydrogen Production from Fossil Fuels with Carbon Dioxide Captures, Using Chemical-Looping Technologies. Ph.D. Thesis, Dept. of Energy and Environment, Division of Energy Conversion, Chalmers University of Technology, 2008, Göteborg, Sweden.

(21) Lind, F.; Seemann, M.; Thunman, H. Continuous catalytic tar reforming of biomass derived raw gas with simultanious catalyst regeneration. *Ind. Eng. Chem. Res.* **2011**, *50*, 11553–11562.

(22) Lind, F.; Israelsson, M.; Seemann, M.; Thunman, H. Manganese oxide as catalyst for tar cleaning of biomass-derived gas. *Biomass Convers. Biorefin.* **2012**, *2*, 133–140.

(23) Berguerand, N.; Lind, F.; Seemann, M.; Thunman, H. Producer gas cleaning in a dual fluidized bed reformer using two catalysts. *Compend. Int. Conf. Polygener. Strat.* **2011**, 147–155.

(24) Aznar, M. P.; Corella, J. Improved steam gasification of lignocellulosic residues in a fluidized bed with commercial steam reforming catalyst. *Ind. Eng. Chem. Res.* **1993**, *32*, 1–10.

(25) Baker, E. G. Steam gasification of biomass with nickel secondary catalysts. *Ind. Eng. Chem. Res.* **1978**, *26*, 1335–1339.

(26) Kunii, D., Levenspiel, O. *Fluidization Engineering*, 2nd ed.; Butterworth-Heinemann Series in Chemical Engineering, Butterworth-Heinemann; Boston, MA, 1991; Chapter 14, p 338

(27) Thunman H., Seemann, M. First experience with the new Chalmers gasifier. 20th International Conference on Fluidized Bed Combustion, Xı́an, China. Yue, G.Z.H., Zhao, C., Luo, Z., Eds.; 2009; p 659–663.

(28) Seemann, M., Thunman, H. The new Chalmers research-gasifier. International Conference on Polygeneration Strategies, Vienna University of Technology, 2009.

(29) Jerndal, E.; Mattisson, T.; Thijs, I.; Snijkers, F.; Lyngfelt, A. NiO particles with Ca and Mg based additives produced by spray-drying as oxygen carriers for chemical-looping combustion. *Energy Procedia.* **2009**, *1*, 479–486.

(30) Brage, C.; Yu, Q.; Chen, G.; Sjostrom, K. Use of amino phase adsorbent for biomass tar sampling and separation. *Fuel* **1997**, *76* (2), 137–142.

(31) Bartholomew, C. H. Mechanisms of catalyst deactivation. *Appl. Catal. A* **2001**, *212*, 17–60.

(32) Seemann, M. C.; Schildhauer, T. J.; Biollaz, S. M. A.; Stucki, S.; Wokaun, A. The regenerative effect of catalyst fluidization under methanation conditions. *Appl. Catal. A* **2006**, *313* (1), 14–21.

(33) Caballero, M. A.; Corella, J.; Aznar, M. P.; Gil, J. Biomass gasification with air in fluidized bed. Hot gas cleanup with selected commercial and full-size nickel-based catalysts. *Ind. Eng. Chem. Res.* **2000**, *39* (5), 1143–1154.

Paper V

energy&fuels

Article

pubs.acs.org/EF

Ilmenite and Nickel as Catalysts for Upgrading of Raw Gas Derived from Biomass Gasification

Fredrik Lind,* Nicolas Berguerand, Martin Seemann, and Henrik Thunman

Department of Energy and Environment, Division of Energy Technology, Chalmers University of Technology, SE-412 96 Gothenburg, Sweden

Supporting Information

ABSTRACT: Two metal oxides, naturally occurring ilmenite (iron titanium oxide) and manufactured nickel oxide supported on an α-Al_2O_3 matrix (NiO/AL_2O_3), were compared as catalysts for secondary biomass gas upgrading. The experiments were conducted in a chemical-looping reforming (CLR) reactor, which combines biomass gas upgrading with continuous regeneration of coke deposits. The CLR system was fed with a tar-rich producer gas from the Chalmers 2−4-MW biomass gasifier, and the possibilities to reduce the tar fraction and to increase the yield of hydrogen were evaluated for temperatures between 700 and 880 °C. A system-wide molar balance was established to enable calculations of tar removal efficiency on a mass basis; these results were further compared with those for the more widely used tar-to-reformed gas ratio, yielding tar concentrations in units of grams of tars per normal cubic meter of product gas (g_{tar}/Nm^3_{gas}). Both materials exhibited activity with respect to tar decomposition and increased the yield of hydrogen. In addition, both tar removal and hydrogen production were increased with increasing temperature. All the phenolic compounds and a large proportion of the one-ring branched tars were decomposed at 800 °C by the two catalysts, despite the fact that the tar load in the raw gas was as high as 30 g_{tar}/Nm^3_{gas}. Results from the mole balance showed that it is important to specify on what basis the tar removal efficiency is calculated. The tar removal efficiency was calculated as 95% for the Ni/Al_2O_3 catalyst at 880 °C and as 60% for the ilmenite catalyst at 850 °C on tar-to-reformed gas basis. When the produced permanent gases were removed from the reformed gas, the same calculations yielded tar removal efficiency of 86% and 42%, respectively. The testing of serial samples of the effluent stream from the regeneration reactor for carbon oxides showed that coke was removed from the catalyst, and no deactivation by coke deposits was detected during the 8 h of operation of the CLR reactor.

1. INTRODUCTION

Biomass is a renewable energy source (RES) that can be used in several energy applications to substitute fossil fuels. One of these applications is vehicle fuels, which can be produced synthetically from lignocelluloses, for example, substitute natural gas (SNG), ethanol, dimethyl ether (DME), and Fischer−Tropsch diesel (F-T diesel).[1] However, before fuel synthesis can be realized, the chemically stored energy in the native fuel has to be accessible. One way to achieve this is by gasification, which is a thermochemical process that is approaching commercialization and is seen as a promising technology for converting large quantities of green solid fuel into raw gas. Typically, the raw gas obtained from the process consists of H_2, CO, CO_2, CH_4, H_2O, and light hydrocarbons, as well as higher molecular hydrocarbons and small amounts of contaminants, such as H_2S, NH_3, and Cl. However, one of the obstacles to direct utilization of the raw gas is that condensable hydrocarbons or "tars"[2−6] are formed during the gasification process. The tar fraction usually consists of a variety of aromatic compounds (usually with 1−5 rings) and oxygenated and sulfur-containing species.[1,7] Condensation of tars onto downstream equipment leads to the failure of compressors, turbines, and pumps, as well as major clogging of pipes. Furthermore, tar deposition and nonreversible accumulation of sulfur on the active sites of a fuel synthesis catalyst can lead to its complete deactivation downstream of the gasification unit.[6] Therefore, a satisfactory gas-cleaning and gas-upgrading system needs to be implemented upstream of the actual fuel synthesis. Although gasification technology is approaching feasibility on the industrial scale, issues remain regarding the development of an energy-efficient gas-cleaning method that would produce a synthesis feedstock gas of high purity and appropriate gas composition for downstream fuel synthesis. Therefore, extensive research efforts in the areas of gas cleaning and gas conditioning are mandatory before the chain from native biomass to high-quality fuels can be realized in an energy-efficient manner, which is a prerequisite for full commercialization.[5]

Catalytic gas cleaning is a promising method for dealing with the tar issue, and it opens up possibilities for adjusting the gas composition so as to make it suitable for downstream fuel synthesis. With this technique, the chemically bound energy within the tars can be utilized and the latent heat in the producer gas can, to a large extent, be recovered through heat-exchanging feeds, either internally or via steam production. However, to date, this method has not been considered feasible for implementation in industrial processes, as the catalyst-related costs have been too high. This is due mainly to the fact that the time-on-stream for the catalyst has been insufficient,

Received: December 17, 2012
Revised: January 22, 2013

owing to catalyst poisoning through rapid coke formation and sulfur deterioration.

In the present work, catalytic gas upgrading is evaluated and two metal oxides are investigated and compared as potential catalysts for downstream upgrading of raw gas derived from biomass gasification. The first catalyst, which contains nickel oxide supported on alumina oxide (NiO/Al_2O_3), was manufactured and used as the reference catalyst. The second catalyst is the naturally occurring ore ilmenite, which is an iron titanium oxide ($FeTiO_3$ in its most reduced form). The catalysts were applied to the chemical-looping reforming (CLR) system proposed by Lind et al.,[8] which overcomes the problem of coke formation on the catalysts by continuous regeneration of catalyst in one of the beds. A similar concept for tar cleaning in a twin-bed system and cost estimations for the process have been proposed by Dutta et al.[9]

The overall goal of the present work was to experimentally investigate the possibility of applying an inexpensive, nontoxic ore to secondary gas upgrading. For this material, once it has been mined, the grinding operation is essentially the only refining process, which means that the cost of producing this catalyst is low compared to manufactured catalysts. The present study compares the tar-reducing activity and gas-conditioning properties of the ilmenite catalyst with those of the reference catalyst. The determination of catalyst tar activity is here based on the actual tar conversion, and this is determined from measurements of the tar concentration in and out of the experimental unit. The choice of reference catalyst was motivated by the facts that Ni-based catalyst shows very high activity in tar reformation and many tar-cleaning studies have been performed in which Ni-based catalysts have been used. Therefore, in the present study, it is possible to quantify the tar-reducing efficiencies of the two catalysts through comparisons with similar investigations reported in the literature.

The tar-cleaning activities of the catalysts and their influences on hydrogen production were evaluated by varying the reactor temperature within the range 700−880 °C, with two different oxygen loads in the regeneration reactor. In comparison to earlier work performed with the CLR reactor system,[8,10] a molar balance is proposed. This balance is employed to clarify the manner in which oxygen transfer and gas yield from hydrocarbon reformation affect the efficiency of tar removal.

2. THEORY

2.1. Chemical-Looping Reformation Tar-Cleaning Concept.

The tar-reforming properties of the metal oxides were evaluated in the CLR system originally presented by Mattisson and Lyngfelt.[11] The CLR system is fed with raw gas, which contains 20−30 $g_{tar}/Nm^3{}_{rawgas}$, from the Chalmers 2−4-MW biomass research gasifier. The idea behind the tar-cleaning method is to reform tar components (C_nH_m) into useful gas molecules. The reactor system consists of two reactors: (1) a regenerator reactor, also called the air reactor (AR); and (2) a reformer reactor, also referred to as the fuel reactor (FR), which is fed with the raw gas (Figure 1). Two seals, the superior (SLS) and inferior (ILS) loop seals, which are fluidized with inert gas or steam, prevent gas cross-contamination of the effluents from the respective reactors while enabling overall catalyst circulation. In this bench-scale system, the oxidized metal oxide Me_xO_y exits the SLS and descends through the gas phase for about 15 cm before reaching the bubbling bed, which creates an oxygen-rich zone. During the descent, part or all of the Me_xO_y is reduced to Me_xO_{y-1} as hydrocarbons (C_iH_j), H_2, and CO are available for combustion according to the reaction:

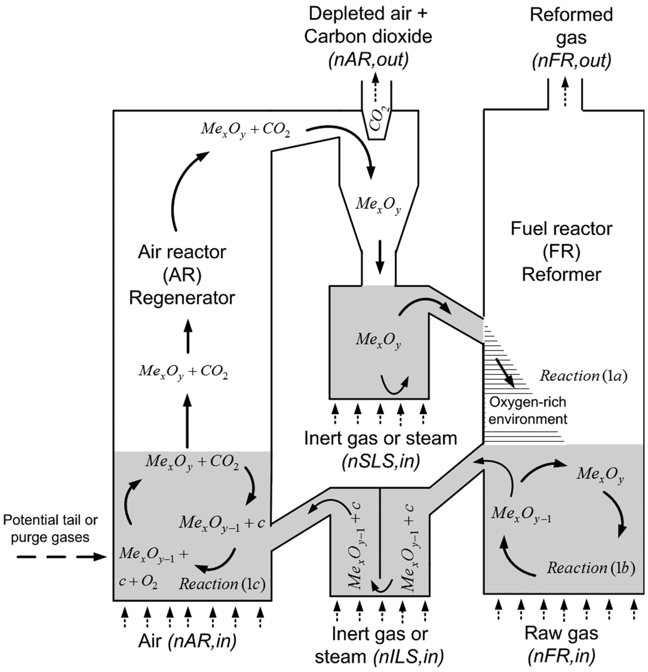

Figure 1. Concept of CLR for secondary upgrading of biomass producer gas.

$$C_iH_j + nH_2 + zCO + [2i + 0.5(j + z) + n]Me_xO_y \rightarrow (i + z)CO_2 + (j/2 + n)H_2O + [2i + 0.5(j + z) + n]Me_xO_{y-1} \quad (1a)$$

The reduced metal oxide Me_xO_{y-1} in the bed acts as a catalyst for reforming the tars (C_nH_m) in the presence of reforming media (indicated by an asterisk), such as steam (H_2O^*) or $CO_2{}^*$ in the raw gas, according to the simplified reaction 1b. Apart from the desired tar-reforming reaction, additional carbon-forming reactions cause carbon to be deposited on the particles.

$$C_nH_m + Me_xO_{y-1} + H_2O^* + CO_2{}^* \rightarrow C_iH_j + H_2 + CO + Me_xO_{y-1} + C \quad (1b)$$

While the Me_xO_{y-1} is reoxidized to Me_xO_y in a strongly exothermic reaction in the AR, carbon deposits on the catalytic surfaces are oxidized to CO_2 according to reaction 1c. The oxidation of coke deposits contributes to maintaining the heat balance, as the formed heat is transported via the catalyst back to the FR, and thereafter used in the endothermic tar reactions. Heat production from the regeneration of coke in a catalytic twin-bed system is a well-known concept and is the driving force behind the commercially applied process of fluid catalytic cracking, which is used to boost the yield of gasoline from heavy crude distillates in oil refineries.[12] It should be noted that oxygen transport will affect the composition of the permanent gases, given that a minor part of the hydrocarbons and/or hydrogen and carbon monoxide will be either partly or fully oxidized. These reactions might also be essential if the heat contribution from the oxidation of coke deposits is insufficient to sustain the heat balance. Depending on process integration, the heat balance in the CLR can be achieved by combusting in the regenerator the tail and purge gases from potential downstream fuel synthesis, as indicated in Figure 1. This concept integrated with a downstream ethanol synthesis was proposed by Dutta et al.[9] However, in the present study, heat integration is not the major target and tar removal is the main consideration.

$$n_1\mathrm{Me}_x\mathrm{O}_{y-1} + n_2\mathrm{C} + [(n_1/2) + n_2](\mathrm{O}_2 + 3.77\mathrm{N}_2) \rightarrow n_1\mathrm{Me}_x\mathrm{O}_y + n_2\mathrm{CO}_2 + [(n_1/2) + n_2]3.77\mathrm{N}_2 \quad (1c)$$

2.2. Catalysts for Tar Cleaning. Research on catalytic tar cleaning has been conducted for several decades.[3,5,7,13,14] In particular, since Ni catalysts have shown rather high activities for tar reformation, these are frequently used as catalysts for gas upgrading. Several studies involving Ni-based catalysts have been conducted. For instance, Corella et al.[15] reported biomass tar conversions of 99.5% with commercial Ni-based steam reforming catalysts, while Aznar et al.[16] showed that tar conversion with >98% efficiency could be achieved in the temperature range 650−820 °C. Bangala et al.[17] used a Ni-based catalyst to study the possibility for steam reformation of naphthalene, which is one of the major biomass tar components, and they showed that complete conversion of naphthalene could be achieved at 750 °C. Rownaghi and Huhnke[18] conducted experiments in a fixed bed with toluene and steam over a NiO catalyst and further with a catalyst prepared from CaO/MgO/NiO and showed 100% conversion of the toluene already at 700 °C. These results clearly demonstrate that Ni has high ability for tar reduction and is applicable to biomass gas upgrading. However, the use of Ni as raw material is expensive and the prepared catalyst needs extensive time-on-stream to become economically viable. Preparation of the catalyst involves an environmentally hazardous process, as Ni is highly toxic and can be fatal if ingested by humans or animals. The toxicity of Ni incurs an extra cost, as the spent material needs to be sent for controlled disposal. Therefore, the identification of less toxic and less expensive catalytic materials is of importance for industrial actors interested in catalytic tar cleaning.

Ilmenite is a nontoxic, naturally occurring ore that is, in industrial applications, mainly used for titanium refinement. The bulk price for ilmenite[19] is comparable to that of hard coal and corresponds to about 1% of the bulk price for crude Ni.[20] The cost of preparation for ilmenite catalysts can be low compared to those for manufactured catalysts, as grinding of the ore is essentially the only process required. In fact, the price of ilmenite as a catalyst is only 2−3 times that of ordinary silica sand. Owing to the low cost of ilmenite, the time-on-stream for the material is not as essential as for manufactured catalyst.

The use of ilmenite as an oxygen carrier in chemical-looping combustion (CLC) has been investigated in detail.[21−23] Ilmenite demonstrates high mechanical strength during repeated redox cycles of CLC, which is a prerequisite for chemical-looping technologies and in particular for CLR. However, raw ilmenite is not fully oxidized and needs to be activated during continuous redox cycles at temperatures >800 °C.[24] Cuadrat et al.[25] conducted experiments in which they activated ilmenite during repeated redox cycles and concluded that the porosity of the ilmenite particles increased and that an external Fe-rich shell was formed on the particle.

Ilmenite has also been applied as a tar-reforming catalyst. Min et al.[26] conducted experiments in a fixed bed using ilmenite as a steam-reforming catalyst for the conversion of tars formed during pyrolysis of Australian Mallee wood. They observed that although ilmenite catalyst exhibited good activity for tar decomposition, it also generated high levels of coke deposits, which in the case of fixed beds would clearly be detrimental. Lind et al.[8] used ilmenite as a tar catalyst in the CLR system. In these experiments, a tar-rich raw gas stream from the Chalmers biomass gasifier was used with 60 wt % ilmenite catalyst in silica sand. The results indicated that the ilmenite catalyst had promising tar-removal ability and that the levels of coke deposits could be kept low due to the regeneration cycle.[10] In the present work, the investigation is performed with 100 wt % ilmenite catalyst as the bed inventory in the CLR system. A mole balance is proposed to facilitate calculations of tar removal efficiency on a mass basis, thereby enhancing applicability to hydrocarbon reformation.

3. EXPERIMENTAL SECTION

3.1. Experimental Setup. The potentials of the two metal oxides for gas upgrading were investigated in the CLR system, using raw gas from the 2−4-MW indirect gasifier at Chalmers University of Technology. Ashes and other solid impurities are removed from the raw gas in an electrically heated ceramic filter and then fed via an electrically heated tube (400 °C) to the CLR reactor. The CLR-reactor system, tar sampling positions, and gas analysis equipment for monitoring the permanent gas into and out of the CLR have been detailed in previous publications[8,10] and will not be treated in this work. However, the micro gas chromatograph (micro-GC) used here contains four channels instead of the two used in previous investigations. The GC (Varian 4900) is equipped with two molecular sieve 5a columns with argon as the carrier gas and two PoraPlot U-columns with helium as the carrier gas. All tar sampling was performed via solid-phase adsorption (SPA).[27]

3.2. Experimental Performance. All the experiments that involved the two catalysts were initiated in the same manner. The reactor system was heated to the desired temperature. The catalyst was poured into the FR, and the raw gas pipe from the gasifier was connected under nitrogen purging. The nitrogen flow was slowly decreased and the raw gas was added to gradually replace the nitrogen until eventually the nitrogen was fully replaced with raw gas. The catalyst activity and the regeneration of the catalyst were evaluated with two different O_2 concentrations in the inlet feed to the AR, 1.0 and 2.2 mol % O_2 (see Table 1 in Supporting Information). These two concentrations of O_2 will be referred to hereinafter as 1% O_2 and 2.2% O_2, respectively. Processes with the Ni/Al_2O_3 catalyst were operated at 700, 750, 800, and 880 °C; processes with the ilmenite catalyst were conducted at 750, 800, and 850 °C. The catalyst time-on-stream was around 8 h for both ilmenite and NiO/Al_2O_3 catalysts. Detailed information on the experiments is given in Table 1 in Supporting Information.

3.3. Tar Sampling and Analysis by Solid-Phase Adsorption. The tar composition of the reformed gas was tested by collecting a series of SPA samples for each oxygen concentration used, and this process was repeated for each of the investigated temperatures. Each series comprised six individual samples, whereby a needle was attached to the inlet of a solid-phase extraction (SPE) column that contained 500 mg of silica-based amino phase (NH_2), Supelclean LC-NH_2 SPE (Sigma−Aldrich). A gastight connection between the outlet of the SPE column and a plastic tube connected to a 100-mL plastic syringe was prepared. The needle was injected through a heat-resistant septum (Thermogreen LB-2 septum; Sigma−Aldrich) into the center of the pipe that carried the reformed gas. Reformed gas was then sucked through the amino phase with a specially designed robot, and a total of 100 mL of dry gas was collected in the syringe during sampling for 1 min. The needle was pulled out of the septum and the SPE column was removed from the plastic tube. A cap was placed over the needle and another cap was placed on the end of the column. The column was then put into an ice-containing cooler bag until all six samples were collected. The same procedure was carried out for tar sampling of the raw gas.

The tars adsorbed in the amino phase were dissolved by using dichloromethane and 2-propanol and thereafter analyzed in a gas chromatograph with flame ionization detector (GC-FID). Detailed information on the tar sampling for SPA technique and the procedure for dissolving the tars in the amino phase is available elsewhere.[27] The GC-FID apparatus used was a GC-430 from Bruker, which was equipped with a column of type BR-17 ms (30 m × 0.25 mm), and the FID was of type DEFC 11 (Bruker). The procedure for temperature ramping was as follows: 50 °C for 5 min, followed by ramping at 8 °C/min to 350 °C, and then maintenance at this temperature for an additional 12.5 min.

3.4. Catalysts. The Ni catalyst, which was originally developed as an oxygen carrier for CLC, consists of 40 wt % NiO supported on an α-Al_2O_3 matrix. The particles (termed S1 particles) have been described previously.[28] This material shows high mechanical strength in a circulating fluidized bed (CFB), and it has been applied as an oxygen carrier for 160 h of operation in a 10-kW CLC unit.[29] The bulk density of the NiO/Al_2O_3 catalyst was determined as 2850 kg/m^3, with a particle size distribution (PSD) of 125−180 μm.

The natural ore ilmenite, $FeTiO_3$ in its most reduced form, was supplied by the Norwegian company Titania A/S. A detailed description of the ilmenite ore is provided elsewhere.[8,21,30] The bulk density was determined to be 2600 kg/m^3 at a PSD of 125−180 μm.

3.5. Coke Deposits. Regeneration of coke deposits on the catalysts was evaluated by measuring the CO_2 and CO concentrations from the outlet of the AR. In all the experimental cases, for the start-up sequence and during nitrogen fluidization of the FR, the CO_2 and CO concentrations were below the detection limit of the instrument. The level of carbon deposits regenerated from the catalysts, $Y_{C,AR}$, was calculated as the ratio of the total integrated molar flows of carbon leaving the AR over the duration of the experiment to the total moles of carbon fed to the FR under stable operation in the CLR, according to eq 2:

$$Y_{C,AR} = \frac{\int_{t_{start}}^{t_{stop}} [\dot{n}_{ARout}(CO_{2,ARout} + CO_{ARout})]\,dt}{\int_{t_{start}}^{t_{stop}} (\dot{n}_{FRin} \sum_i \xi_{C,i} C_{i,FRin})\,dt} \tag{2}$$

where $CO_{2,ARout}$ and CO_{ARout} are the concentrations of carbon contributed by CO_2 and CO, respectively, at the outlet of the AR; $C_{i,FRin}$ refers to all the measured carbonaceous species in the raw gas; and $\xi_{C,i}$ is the number of carbon atoms in carbonaceous species i in the raw gas.

3.6. Evaluating Tar Removal and Molar Flows in the Chemical-Looping Reformation System. When the performances of tar removal catalysts are evaluated, it is important to distinguish between gas upgrading and total tar decomposing efficiency. The difference lies in how the tar concentration in the reformed gas is valued. In the case of gas upgrading, the tar concentration in the reformed gas is simply measured, and the tar removal efficiency is calculated by comparing the tar concentrations entering and leaving the catalytic device. However, in the case of total tar decomposing efficiency, even the amount of produced gas from, for example, hydrocarbon reformation and the water−gas shift (WGS), must be included in the calculation. This means that the surplus of permanent gases produced in the reactor is removed from the reformed gas, yielding the actual amount of removed tars. In this manner, a molar balance across the system that includes all species needs to be defined.

The mole flows in and out of the CLR system were estimated via a system-wide molar balance calculation. As the temperature of the raw gas entering the FR was 400 °C, it was not possible to measure the inlet gas flow in the present setup. However, this gas flow can be derived from measurements, as it is possible to determine the cooled dry gas flow out of the FR via the volumetric flow meter. The quality of the water measurements before and after the CLR was not sufficiently high to allow their inclusion as an input to the molar balance. Therefore, the mole balance calculation was performed on the dry gases. It should be emphasized that the measuring technique used in the present work constitutes a degree of uncertainty, since hydrocarbons in the range of C4−C5 are not quantified and C3 and C6 hydrocarbons are only partially captured. These compounds have molecular masses that are too high to give sufficient resolution in time in a micro-GC, while they are too small and volatile to be effectively captured by the amine in the SPA column. As a portion of these hydrocarbons may also be dissolved and captured in a potential scrubber liquid, it is not possible to measure them in the gases downstream of the scrubber unit. Furthermore, these hydrocarbons in the raw gas may be converted into measurable permanent gases in the CLR, as a result of reforming reactions. If they are converted in the CLR, these hydrocarbons will increase the yield of carbon and hydrogen in the reformed gas, and the moles of permanent gases entering the system will be overestimated. The problems associated with measuring accurately the levels of volatile hydrocarbons prompt some researchers to exclude benzene from the definition of "tar".[31]

Equations 3a and 3b provide the total mole flows of gases entering and leaving the FR. The concentrations of permanent gas species were measured in the raw gas ($Y_{i,in}$) and in the reformed gas ($Y_{i,out}$) by use of the micro-GC. The letter r in the summation refers to the number of measured permanent gas components in the raw and reformed gases. The amounts of tar in the raw gas ($n_{tar,in}$) and the reformed gas ($n_{tar,out}$) were estimated via SPA followed by GC-FID. A part of the helium used as the fluidizing medium in the loop seals ends up in the reformed gas and a part appears in the effluent from the AR. The total amount of helium transported to the FR from ILS (n_{ILS}) and SLS (n_{SLS}) is given by the micro-GC measurements, together with the total flow of dry reformed gas. Here, γ_{FR} denotes the fraction of helium transported to the FR. The oxygen transported from the AR to the FR is calculated via a molar balance over the AR. The mole flows of nitrogen ($n_{N_2,ARin}$) and oxygen ($n_{O_2,ARin}$) into the AR (eq 3c) are set by the mass flow controllers. The amount of helium entering the AR is given by subtracting the moles of He fed to the FR from the total moles of He fed to the system via the mass flow controllers. The amount of carbon transported from the FR to the AR ($Y_{C,FRout}$) is calculated from eq 2 by use of the measured amounts of CO_2 ($n_{CO_2,ARout}$) and CO ($n_{CO,ARout}$) in the effluent gas of the AR. The transported oxygen ($n_{O_2,FRin}$) is finally given by eq 3e, where the amount of oxygen used for converting the carbon deposits into CO_2 ($n_{CO_2,ARout}$) and CO ($n_{CO,ARout}$), together with the potential oxygen leaving the AR ($n_{O_2,ARout}$) are subtracted from the total amount of oxygen fed to the AR.

Mole flows in and out of the fuel reactor:

$$n_{FRin} = n_{rawgas} \sum_{i=1}^{r} Y_{i,in} + n_{tar,in} + \gamma_{FR}(n_{ILS} + n_{SLS}) + n_{O_2,FRin} \tag{3a}$$

$$n_{FRout} = n_{FRgas} \sum_{i=1}^{r} Y_{i,out} + n_{tar,out} + \gamma_{FR}(n_{ILS} + n_{SLS}) + n_{C,FRout} \tag{3b}$$

Mole flows in and out of the air reactor:

$$n_{ARin} = n_{N_2,ARin} + n_{O_2,ARin} + n_{C,FRout} + (n_{ILS} + n_{SLS})(1 - \gamma_{FR}) \tag{3c}$$

$$n_{ARout} = n_{N_2,ARout} + n_{O_2,ARout} + n_{CO_2,ARout} + n_{CO,ARout} + (n_{ILS} + n_{SLS})(1 - \gamma_{FR}) \tag{3d}$$

$$n_{O_2,FRin} = n_{O_2,ARin} - n_{CO_2,out} - 0.5n_{CO,out} - n_{O_2,ARout} \tag{3e}$$

Equation 4 provides a measure of the chemically stored energy (Q) in the raw gas and the reformed gas, and is calculated by multiplying the moles of combustible gases (Y_i) by its respective lower heating value (LHV_i) according to eq 4. The letter k in the summation is the number of combustible permanent gas components in the raw and reformed gases. This measure aims to bringing evidence on how the chemically stored energy changes within the gas as it is processed in the CLR system. Thus, no heat integrations are conducted and the sensible heat is therefore not considered in this work.

$$Q = \sum_{i=1}^{k} Y_i \mathrm{LHV}_i \tag{4}$$

In the present work, the residence time (RT) or the gas/solid contact time in the bed is estimated in the same manner as for a fixed bed. Thus, the gained RT is the maximal gas/solid contact time that can be achieved in the CLR. This is because gas flows higher than the minimum fluidization velocity (u_{mf}) will flow through the low-resistance gas passages located in and between the bubbles, thereby giving less time for contact between the gas and catalysts. As the FR is a bubbling fluidized bed with velocities severalfold higher than u_{mf} (Table 1 in Supporting Information), the effective gas to solid contact will always be overestimated, since the overall contact time for the gas flow will vary from almost none to that of packed bed. The RT is calculated according to eq 5, in which the volume of the bed V_{bed} is multiplied by the bed voidage $\varepsilon_{\mathrm{bed}}$, thereby generating the total voidage in the emulsion phase, which is then divided by the average flow of the raw gas V'_{rawgas} plus the flow of the reformed gas ($V'_{\mathrm{reformedgas}}$), yielding the RT value (in seconds):

$$\mathrm{RT} = \frac{V_{\mathrm{bed}}\varepsilon_{\mathrm{bed}}2}{V'_{\mathrm{rawgas}} + V'_{\mathrm{reformedgas}}} \tag{5}$$

4. RESULTS AND DISCUSSION

4.1. Tar Removal Efficiency with Respect to Gas Upgrading and Tar Decomposition. Tar removal for the gas upgrading case at different operating temperatures in the FR, and at 1% and 2.2% O_2, is shown in Figure 2a. It is clear from Figure 2a that the Ni/Al_2O_3 catalyst has the strongest activities for tar removal at all temperatures and that increasing the temperature strongly influences the activity of the catalyst in terms of tar removal. At 700 °C the total tar conversion was 50%, and as much as 95% of the total tar content was removed at 880 °C. In the cases involving the ilmenite catalyst, around 25% of the tar was removed at 750 °C and as much as 60% of the tar was removed at 850 °C. It is noteworthy that the reactivity of the ilmenite catalyst increases rapidly as the temperature is increased from 800 to 850 °C. Indeed, for an equivalent RT, tar removal is enhanced 4-fold compared to the level of tar removal when the temperature is increased from 750 to 800 °C. This may be explained by the nature of ilmenite activation. Ilmenite activity increases as the iron migrates to the surface of the particle, thereby creating active sites. Iron migration in the ilmenite is enhanced by repeated redox cycles and temperatures >800 °C.[25] Overall, the level of oxygen transport from the AR to the FR appears to exert little influence on the rate of tar conversion by either catalyst, as shown in Figure 2a.

Figure 2b shows the actual amount of decomposed tars on a mass basis, with compensation for the produced permanent gases acting as dilution media in the reformed gas. In this manner, total tar removal is decreased for both catalysts at all temperatures, as compared with the results shown in Figure 2a. In the case of the Ni/Al_2O_3 catalyst, tar decomposition drops from 95% to 86% at 880 °C, as compared with the level of tar removal when the efficiency is calculated on the basis of dry normal cubic meter of gas (Figure 2a). The same pattern is seen for the ilmenite catalyst, whereby tar decomposition decreases from 60% to around 42% at 850 °C. The calculation of tar decomposition reveals that the amount of permanent gases produced in a reactor system can have a strong influence on the way in which the tar conversion efficiency is determined. Relying solely on gas concentration measurements, as in the gas upgrading case, may be insufficient if the actual efficiency of tar decomposition is considered.

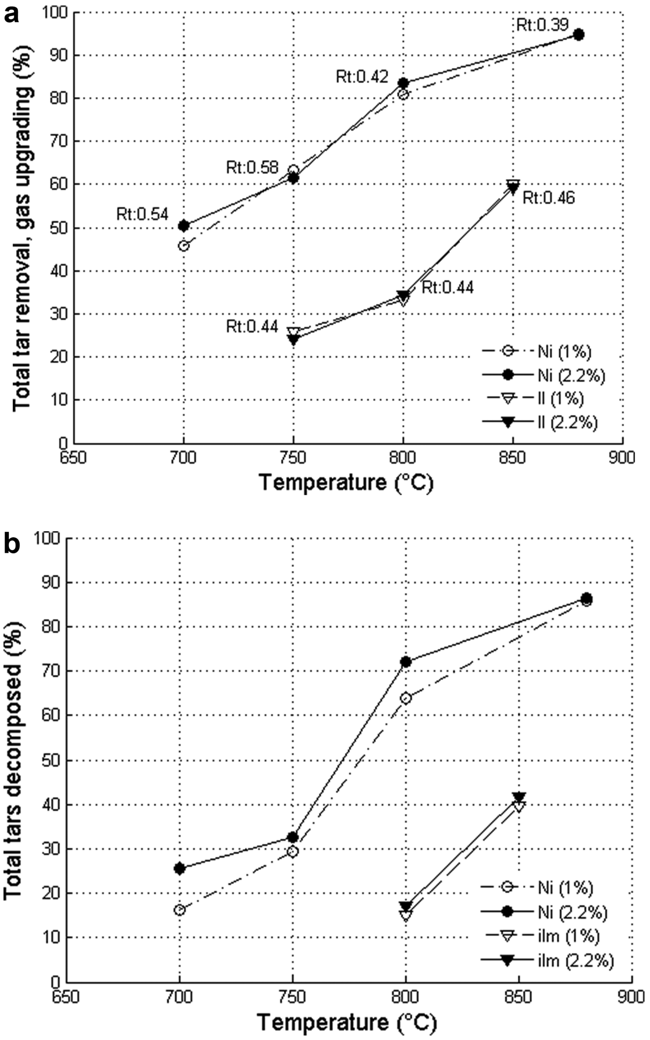

Figure 2. (a) Percentages of total tar removal in gas upgrading for NiO/Al_2O_3 (Ni) and ilmenite (Il) catalysts at 1.0% and 2.2% O_2 at different temperatures. (b) Percentages of total tars decomposed by NiO/Al_2O_3 and ilmenite catalysts at 1.0% and 2.2% O_2 at different temperatures.

The results shown in Figure 2b suggest that tar conversion is enhanced with increasing oxygen transport. However, this is most likely due to combustion reactions in the oxygen-rich zone above the bed. Some of the tar components will remain more or less unreacted as they slip through the low-resistance gas passages in the bed. When these tars enter the oxygen-rich zone, more tars are combusted or partially combusted. This also explains the observed lack of difference in the tar conversion rate for NiO/Al_2O_3 at 880 °C: most of the tars in the bed are already decomposed, so the increased oxygen transfer has little impact on tar conversion.

Figure 3 shows the tar constitutions of raw gas and reformed gas in 1% O_2, at 880 °C for NiO/Al_2O_3 catalyst and at 850 °C for ilmenite catalyst. The tar components were categorized into six distinct groups. In this classification, all the measured tars were assigned a group on the basis of size and structure, and they represent the overall tar composition. This grouping

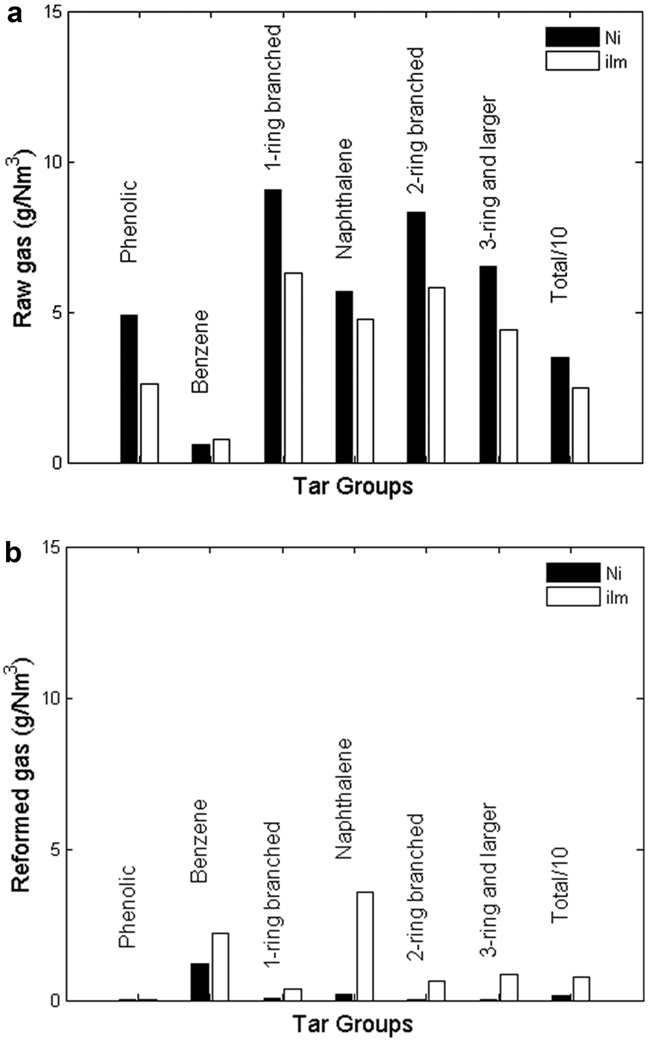

Figure 3. (a) Tar constituents of the raw gas when subjected to NiO/Al_2O_3 (Ni) and ilmenite (ilm) catalysts. (b) Tar groups in the reformed gas out of the CLR when operated with NiO/Al_2O_3 catalyst (Ni) at 880 °C or with ilmenite catalyst (ilm) at 850 °C in the presence of 1% O_2.

system can be used to reveal the general patterns for tar decomposition. The groups are as follows: phenols; benzene; 1-ring aromatic compounds with branches (1-ring branched); naphthalene; 2-ring aromatic compounds with branches (2-ring branched); and 3-ring aromatic compounds and larger. It should be stressed that the total tar concentration in the raw gas delivered to the CLR can differ depending on the operating conditions and the choice of fuel used in the gasifier. For instance, in the case of 880 °C with NiO/Al_2O_3 catalyst, the total tar concentration in the raw gas was 29.8 g/Nm^3, while in the case of ilmenite catalyst at 850 °C, the total tar concentration in the raw gas was 19.2 g/Nm^3 (Figure 3a).

When the data in Figure 3 panels a and b are compared, it is evident that both catalysts have removed the phenolic compounds and a large proportion of the 1-ring branched tars. In the case of NiO/Al_2O_3 catalyst, only benzene and a small amount of naphthalene remain in the reformed gas, whereas in the case of ilmenite catalyst, although the levels are reduced, a spectrum of tars, ranging from benzene to aromatic compounds with $\geq$3 rings, remains.

Moreover, the benzene fraction of the reformed gas is higher than that in the raw gas for both catalysts. This implies that more benzene is formed in the reactor than can be decomposed by the catalyst. One reason for this is that the benzene molecule itself is the most difficult to dissociate due to its resonance stabilization, thus contributing to the observed phenomenon. In addition, since the benzene molecule is highly volatile, it is difficult to measure accurately, with the consequence that it is often not included in the definition of tars.[31] If benzene is not included as part of the tar spectrum, the total tar conversion rates for gas upgrading are 99% for NiO/Al_2O_3 catalyst and 68% for ilmenite catalyst.

In the ilmenite catalyst case, the naphthalene fraction was not reduced to the same extent as the fractions of 2- and 3-ringed tars. This implies that the 2-ring branched tars and the polycyclic aromatic hydrocarbons form naphthalene, which in turn can decompose into benzene if the RT and energy supply is sufficient to disrupt the molecular bonds.

Overall, in terms of gas upgrading, the total tar conversion rate for NiO/Al_2O_3 catalyst at 880 °C is in line with that reported for experimental work on syngas tar cleaning with Ni-based, steam-reforming catalysts performed by Corella et al.[15] and Aznar et al.[16] It should also be emphasized that the raw gas in the present work was produced in a noncatalytic industrial-sized gasifier. This yielded tar concentrations up to 30 times higher than those in the work performed by the aforementioned authors. However, higher tar conversion with NiO/Al_2O_3 catalyst could have been expected at 700 °C, as Rownaghi and Huhnke[18] showed 95% conversion of toluene at a content of 30 g/Nm^3 and at similar temperature. On the other hand, the NiO/Al_2O_3 catalyst used here was originally prepared to serve other purposes, that is, as an oxygen carrier for CLC, where the aim is to transport as much oxygen as possible to reach complete combustion of the fuel. The tar conversion rate for the ilmenite catalyst is lower than that obtained for the NiO/Al_2O_3 catalyst used in the present work and even lower than that for the Ni-based catalysts used in tar-cleaning experiments reported in the literature.[5,13,15−17] However, the ilmenite catalyst clearly shows activity for tar removal, and the efficiency of this reaction might be increased if the CLR system were optimized for this catalyst. The tar-decomposing activity in the CLR reactor would be enhanced by a higher RT, as this is in the lower range of what has been reported in the literature. For instance, Dayton[5] collected data from over 70 tar-removal experiments and reported residence times of up to several seconds. Furthermore, the present work, together with studies performed within CLC investigations, clearly suggests that for properly activation the ilmenite catalyst needs to be used in conjunction with repeated redox cycles at temperatures >800 °C.

Tar groupings for the two catalysts at 800 °C and 1% O_2 are shown in Figure 4. The overall tar-decomposition pattern follows the one described for ilmenite catalyst at 850 °C. For both catalysts, almost all the phenolic compounds are removed at 800 °C and the benzene fraction is higher in the reformed gas than in the raw gas. At this temperature, the naphthalene fraction for the ilmenite catalyst is higher in the reformed gas than in the raw gas, which implies that the RT and/or energy supply to the system are not sufficient to break the naphthalene bonds.

4.2. Permanent Gases: Effects of Temperature and Oxygen Load. The gas compositions of raw gas and reformed gas during the experiments were analyzed online in a micro-

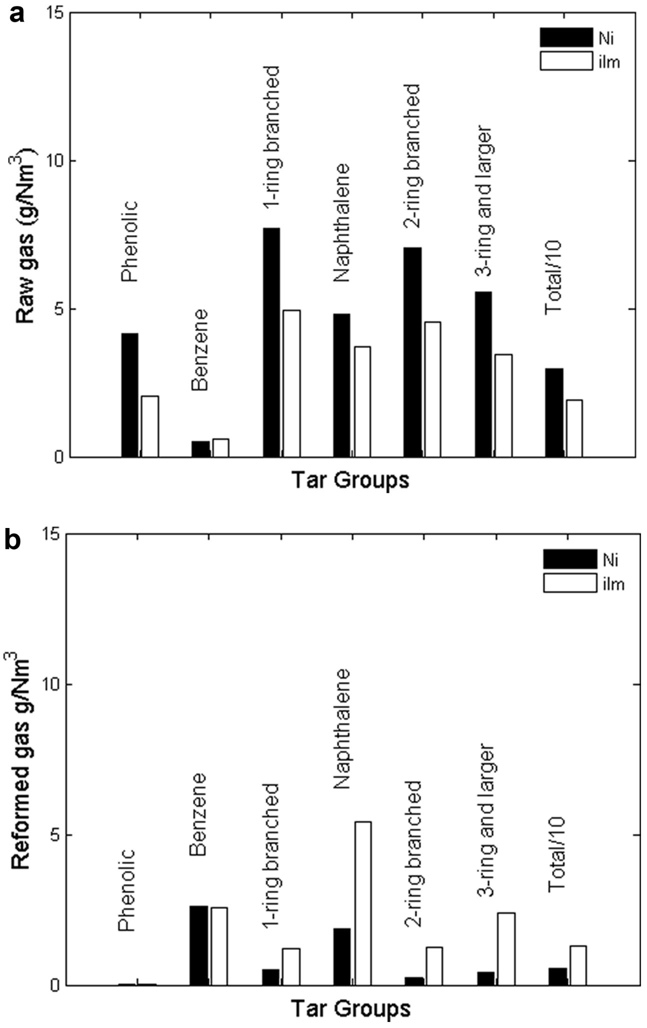

Figure 4. Tar groups in (a) raw gas and (b) reformed gas for NiO/Al_2O_3 (Ni) and ilmenite (ilm) catalysts.

GC. Figure 5 shows the mole flows of the major gas components H_2, CO, CO_2, CH_4, and light hydrocarbons, expressed as $C_{2-3}H_x$ and including C_2H_2, C_2H_4, C_2H_6 and C_3H_6, at 1% O_2 for NiO/Al_2O_3 and ilmenite catalysts.

The H_2 content of the reformed gas at 1% O_2 with NiO/Al_2O_3 catalyst clearly increased with increasing temperature above 750 °C (Figure 5a). To a large extent, this can be explained by the levels of reformed tar, CH_4, and light hydrocarbons, all of which are increased at higher temperature. At 880 °C, the level of CH_4 was reduced by almost 50% and the levels of light hydrocarbons were decreased by 98%. Furthermore, at all temperatures, more CO_2 was formed than could be achieved through hydrocarbon oxidation, through the oxygen transported from the AR. This suggests that part of the hydrogen was formed via the WGS reaction. However, since the accuracy of the water measurements was not sufficient, these could not be used to close the hydrogen balance.

The H_2 content was also increased in the reformed gas for ilmenite catalyst experiments at 1% O_2 (Figure 5b). In this instance, the reaction at 750 °C has been excluded due to the lack of raw gas data. The increase in H_2 is approximately 8% higher at 850 °C compared to 800 °C, which again is expected, since more tars are reformed. However, in contrast to the NiO/Al_2O_3 catalyst scenario, CH_4 in the ilmenite catalyst cases was not consumed and the amount of CH_4 actually increased by a few percentage points in the reformed gas at both 800 and 850 °C. This suggests that CH_4 is produced in the system and that the ilmenite catalyst shows poor ability to reform this molecule. However, the ilmenite catalyst shows a high propensity for reforming light hydrocarbons, with 87% of these compounds reformed at 850 °C.

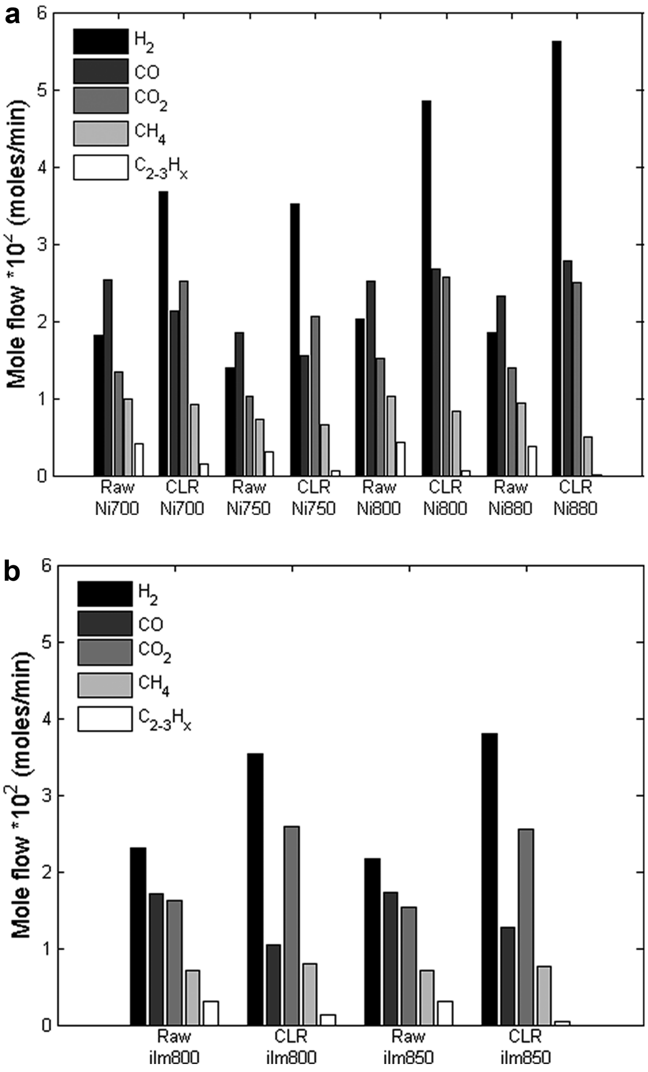

Figure 5. Mole flow values of gas species in raw and reformed gases for (a) NiO/Al_2O_3 catalyst at 1% O_2 at 700, 750, 800, and 880 °C and for (b) ilmenite catalyst at 1% O_2 at 800 and 880 °C.

The ratio of the total permanent gas increase between the reformed gas and the raw gas for both catalysts at 1.0% and 2.2% O_2 is shown in Figure 6a. In almost all cases, increased oxygen transport from the AR to the FR leads to a decrease in the total level of permanent gases in the dry reformed gas (Figure 6a). This implies that a share of the oxygen transported via the catalyst is involved in the oxidation of hydrogen and/or hydrocarbons and that not all of the oxygen is consumed in the process of tar oxidation as suggested in eq 1a. For NiO/Al_2O_3 catalyst, the most likely reason for the decrease in total permanent gases is that higher oxygen transfer leads to increased oxidation of H_2 into water. This is supported by the data in Figure 6b, where the ratio change in the moles of H_2 and CO between the reformed gas and the raw gas for both catalysts at 1.0% and 2.2% O_2 is shown. The amount of H_2

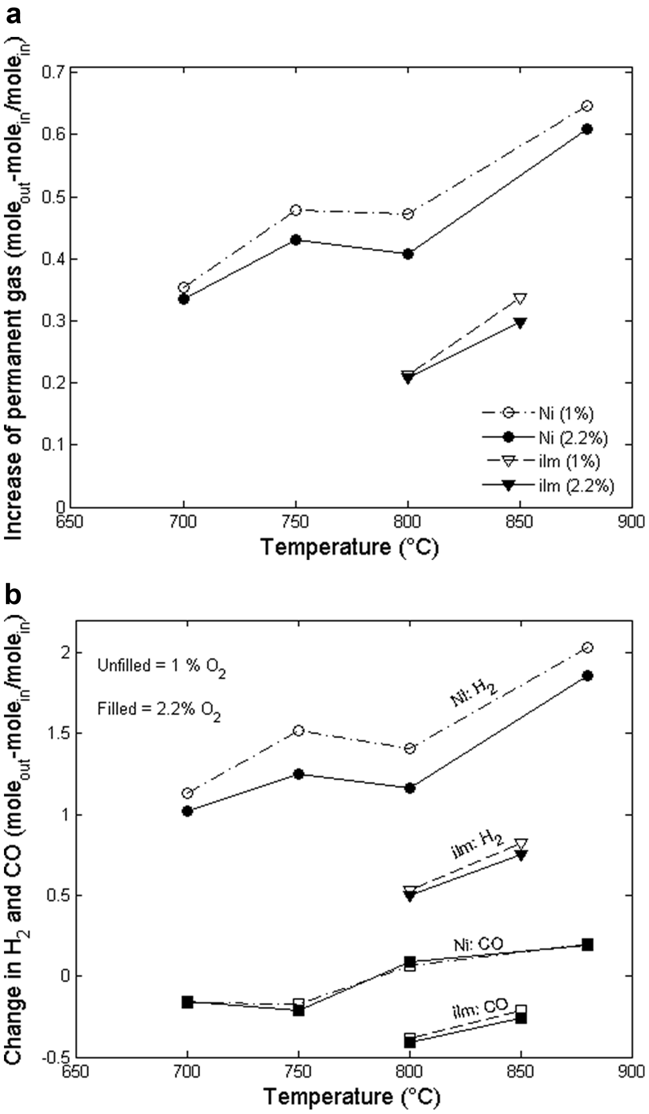

Figure 6. (a) Total molar increases in the permanent gas for NiO/Al_2O_3 (Ni) and ilmenite (ilm) catalysts in the CLR at 1.0% and 2.2% O_2. (b) Change in moles of H_2 and CO in the reformed gas compared to the raw gas used for NiO/Al_2O_3 (Ni) and ilmenite (ilm) catalysts as a function of temperature.

produced in the Ni-catalyzed process was reduced at all temperatures as oxygen transport increased, whereas the CO content was essentially unaffected by increases in oxygen availability. The pattern of decreasing H_2 associated with increasing oxygen transport matched well the decrease in total permanent gases (Figure 6a). For ilmenite catalyst, the influence of oxidation of the total permanent gases was first evident at 850 °C (Figure 6a), and the H_2 and CO contents were reduced as oxygen transport increased (Figure 6b).

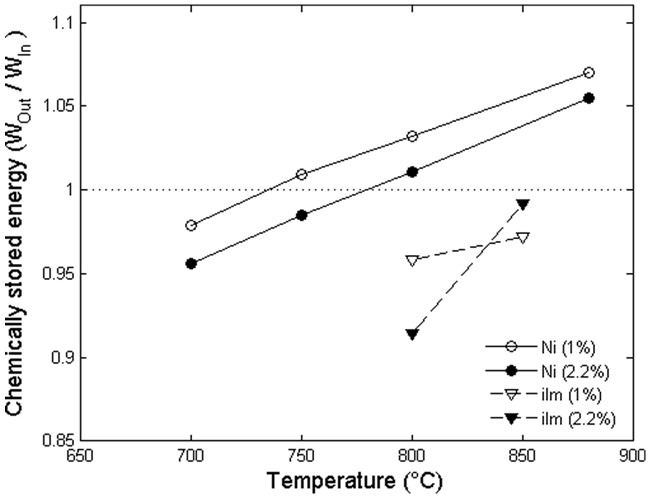

Figure 7. Chemically stored energy in the reformed gas compared to the raw gas used for NiO/Al_2O_3 (Ni) and ilmenite (ilm) catalysts at 1.0% and 2.2% O_2 as a function of temperature.

Figure 7 shows the chemically stored energy in the permanent gas compared to the raw gas used for NiO/Al_2O_3 and ilmenite catalysts as a function of temperature and oxygen transport. The chemically stored energy in the reformed gas increases with increasing operating temperature in the reactor system for both catalysts. The cause for this is that more H_2 and CO are formed as tars are decomposed via reforming reactions, and these reactions are enhanced at higher temperatures. For NiO/Al_2O_3 catalyst, this leads to the chemically stored energy in the reformed gas being higher than in the raw gas with 1% O_2 above 750 °C and with 2.2% O_2 above 800 °C. At temperatures below 750 °C, the catalysis is less active and the tar reforming reactions do not outweigh the energy loss from oxidation of H_2, C_iH_j, and CO as a result of the oxygen transport. The oxidation of product gas into CO_2 and H_2O is also the reason why the chemically stored energy in the reformed gas for NiO/Al_2O_3 catalyst is lower at 2.2% O_2 than at 1% O_2. For ilmenite catalyst, the chemically stored energy is lower in the reformed gas than in the raw gas for all cases, which implies that the loss of stored energy from oxidation of product gas is greater than the gained energy from tar reforming. However, there are no obvious reasons that the energy content in the reformed gas is higher at 2.2% O_2 than at 1% O_2 at 850 °C.

Overall, oxidation of permanent gases led to a loss of product gas. This means that, for fully developed systems, the operating conditions need to be optimized so that most of the permanent gases are preserved while the heat balance is fulfilled and the oxygen supply to the AR is enough to ensure sufficient regeneration of coke deposits on the catalyst. Furthermore, the results from the present work indicate that using a CFB reactor as the reformer would have been more beneficial than the bubbling fluidized bed (BFB) used in the present setup. The main reasons for this are that (1) gas/solid contacts would be enhanced in a CFB and (2) the oxygen supplied via the catalyst could be concentrated to the tar-rich zone in the bottom bed instead of the tar-poor gas phase above the bed, as in the present setup (Figure 1).

4.3. Coke Regeneration and Catalyst Deactivation.

Coke deposition on catalytic surfaces is known to decrease the activity of the catalyst with respect to tar cracking, and the accumulation of coke can lead eventually to complete deactivation of the catalyst. As described in the Introduction, tar cracking and hydrocarbon-reforming reactions enhance the formation of coke on the surface of the catalyst, so it is important to recover catalytic activity through continuous regeneration. As the experiments in this work were conducted with raw gas that contained high levels of tars, carbon deposition was expected and the regeneration of catalyst was thoroughly monitored.

The CO and CO_2 concentrations in the outlet of the AR during all experiments were measured online and on a second basis. During all experiments, before the raw gas was introduced into the FR, the levels of CO_2 and CO were below the detection limits of the instruments. The levels of CO_2 were measured in the outlet of the AR shortly after introduction of raw gas into the FR, and it was clearly shown that carbon deposits had formed on the catalyst. The level of CO was always below the detection limit of the instrument, which implies that the amount of CO produced could be neglected and that all coke deposits were oxidized to CO_2 in the AR. Furthermore, the oxygen level in the effluent from the AR was below the detection limit of the instrument during all experiments, which implies that all the oxygen was consumed by either oxidation of coke deposits or reoxidation of catalysts.

Figure 8 captures the regeneration of coke deposits on the catalyst and shows carbon transport from the FR to the AR as a function of the experimental temperature. Here, the results for $Y_{C,AR}$ are presented as weight percent. The highest level of carbon deposits was detected for the ilmenite catalyst at 850 °C in 2.2% O_2; under these conditions, 0.25% of the total carbon in the raw gas ended up as deposits on the catalyst. The highest level of carbon deposits for the NiO/Al_2O_3 catalyst, detected at 700 °C in 1% O_2, was 0.11% of the total carbon in the raw gas. The amount of carbon transported from the FR to the AR by the catalysts underlines the advantages of combining tar cleaning and coke deposit regeneration. The results suggest that these types of catalysts can be applied in a CLR for processing raw gas with high contents of tar, while at the same time maintaining catalyst activity without involving primary tar measures in the gasifier.

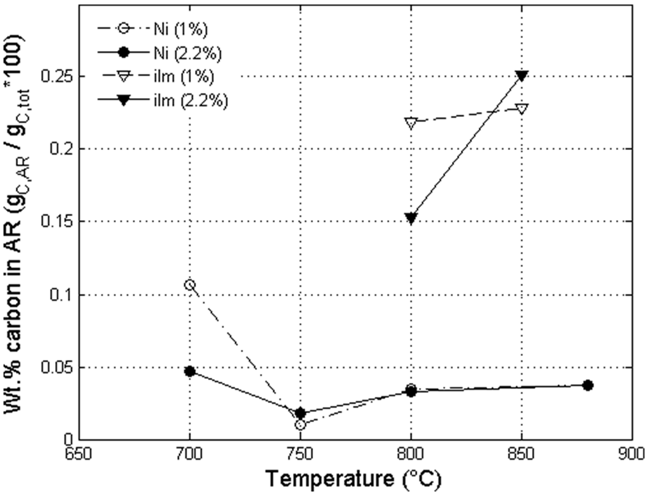

Figure 8. Weight percents (wt %) of carbon transported from the FR to the AR as a function of temperature.

5. CONCLUSIONS

The potentials of using NiO/Al_2O_3 and ilmenite catalysts for gas upgrading were investigated with respect to application to secondary catalytic tar cleaning of biomass-derived gas. The NiO/Al_2O_3 catalyst was manufactured and the ilmenite catalyst is a naturally occurring ore that consists of iron titanium oxide. Raw producer gas with high tar content from the Chalmers 2–4-MW biomass gasifier was fed into the reactor system, which was operated within the temperature range 700–880 °C. The efficiency of tar removal was evaluated by two different approaches: (1) gas-upgrading efficiency, whereby the tar efficiency was calculated from the tar concentrations before and after the reactor; and (2) a tar-decomposing efficiency, in which compensation was made for the dilution effects of the permanent gases from WGS, tar, CH_4, and light hydrocarbon reformation. Owing to continuous regeneration of carbon deposits, the system also displayed promising abilities to handle producer gases with very high tar contents without apparent deactivation of the catalyst. Based on these results, the following conclusions are drawn:

- The two catalysts show tar-reforming activities, which are clearly enhanced with increasing temperature. Increased oxygen transport via the catalyst slightly improves the efficiency of tar removal but decreases the yield of product gas. The NiO/Al_2O_3 catalyst shows rather high activity for tar removal already at 700 °C. For ilmenite catalyst, total tar removal was increased 4-fold as the temperature was increased from 800 to 850 °C, as compared to the increase in conversion when the temperature was increased from 750 to 800 °C.
- It is important to specify on what basis the tar efficiency calculations are conducted. When tar removal is calculated on the basis of dry reformed gas, that is, the gas-upgrading case, tar removal efficiency is 95% for the NiO/Al_2O_3 catalyst at 880 °C and 60% for the ilmenite catalyst at 850 °C. The same calculation yields tar removal efficiencies of 86% and 42%, respectively, if the contribution from produced permanent gases is removed from the reformed gas.
- Hydrogen production is enhanced by both catalysts, and 50% of the CH_4 and 98% of the light hydrocarbons are converted for NiO/Al_2O_3 catalyst at 880 °C, due to reforming reactions. For ilmenite catalyst, 87% of light hydrocarbons are reformed, although the production of CH_4 is higher than its consumption, leading to a surplus of CH_4 in the reformed gas.
- The accumulation of coke on the catalyst was minimized, as the transported carbon was continuously oxidized to CO_2 in the regenerator, even though 30 g_{tar}/Nm^3_{gas} was feed into the reformer reactor. No deactivation of the two catalysts was detected during the 8-h time scale of the experiments.
- Overall, the ilmenite catalyst is less active as a tar-cleaning catalyst than the NiO/Al_2O_3 catalyst. The fate of the ilmenite catalyst in this experimental setup needs to be investigated under optimized operating conditions, in which appropriate activation and improved gas/solid contact would be essential. Increased gas/solid contact and better utilization of oxygen might be achieved by replacing the BFB reformer in the present setup with a CFB reformer.

■ ASSOCIATED CONTENT

Ⓢ Supporting Information

One table, listing operating parameters for the gasifier and CLR. This information is available free of charge via the Internet at http://pubs.acs.org/.

■ AUTHOR INFORMATION

Corresponding Author

*E-mail Fredrik.Lind@chalmers.se; tel +46 (0)31 772 52 43.

Notes

The authors declare no competing financial interest.

■ ACKNOWLEDGMENTS

This project is supported financially by E.On and the Swedish Gasification Centre (Svenskt Förgasningscentrum; SFC). The operation of the gasifier was facilitated by Göteborg Energi, Metso, Akademiska Hus, and the Swedish Energy Agency. We thank Jörg Schneebeli and Serge Biollaz (Paul Scherrer Institute, Switzerland) for their help with the gas chromatography measurements and research engineers Rustan Marberg, Jessica Bowhalli, and Johannes Öhlin for their work with the experimental and analysis equipment.

■ NOMENCLATURE

CLR = chemical-looping reforming
g_{tar}/Nm^3_{gas} = mass of tars per normal cubic meter of product gas
RES = renewable energy sources
SNG = substitute natural gas
DME = dimethyl ether
F-T diesel = Fischer−Tropsch diesel
AR = air reactor
FR = fuel reactor
SLS = superior loop seal
ILS = inferior loop seal
Me_xO_y = oxidized metal oxide
Me_xO_{y-1} = reduced metal oxide
C_nH_m = representative tar molecule
C_iH_j = representative molecule for hydrocarbons
CLC = chemical-looping combustion
BFB = bubbling fluidized bed
CFB = circulating fluidized bed
SPA = solid-phase Adsorption
SPE = solid-phase extraction
micro-GC = micro gas chromatography
GC-FID = gas chromatography followed by a flame ionization detector
WGS = water−gas shift
RT = residence time

■ REFERENCES

(1) Balat, M.; Balat, M.; Kırtay, E.; Balat, H. Main routes for the thermo-conversion of biomass into fuels and chemicals. Part 2: Gasification systems. *Energy Convers. Manage.* **2009**, *50* (12), 3158−3168.

(2) Pfeifer, C.; Hofbauer, H. Development of catalytic tar decomposition downstream from a dual fluidized bed biomass steam gasifier. *Powder Technol.* **2008**, *180* (1−2), 9−16.

(3) Devi, L.; Ptasinski, K. J.; Janssen, F. J. J. G. A review of the primary measures for tar elimination in biomass gasification processes. *Biomass Bioenergy* **2003**, *24* (2), 125−140.

(4) Li, C. S.; Suzuki, K. Tar property, analysis, reforming mechanism and model for biomass gasification: An overview. *Renewable Sustainable Energy Rev.* **2009**, *13* (3), 594−604.

(5) Dayton, D. *A Review of the Literature on Catalytic Biomass Tar Destruction*; TP-510-32815; National Renewable Energy Laboratory, Golden, CO, 2002.

(6) Yung, M. M.; Jablonski, W. S.; Magrini-Bair, K. A. Review of catalytic conditioning of biomass-derived syngas. *Energy Fuels* **2009**, *23* (4), 1874−1887.

(7) Anis, S.; Zainal, Z. A. Tar reduction in biomass producer gas via mechanical, catalytic and thermal methods: A review. *Renewable Sustainable Energy Rev.* **2011**, *15* (5), 2355−2377.

(8) Lind, F.; Seemann, M.; Thunman, H. Continuous Catalytic Tar Reforming of Biomass Derived Raw Gas with Simultaneous Catalyst Regeneration. *Ind. Eng. Chem. Res.* **2011**, *50* (20), 11553−11562.

(9) Dutta, A.; Talmadge, M.; Hensley, J.; Worley, M.; Dudgeon, D.; Barton, D.; Groenendijk, P.; Ferrari, D.; Stears, B.; Searcy, E.; Wright, C.; Hess, J. R. Techno-economics for conversion of lignocellulosic biomass to ethanol by indirect gasification and mixed alcohol synthesis. *Environ. Prog. Sustainable Energy* **2012**, *31* (2), 182−190.

(10) Lind, F.; Israelsson, M.; Seemann, M.; Thunman, H. Manganese oxide as catalyst for tar cleaning of biomass-derived gas. *Biomass Convers. Biorefin.* **2012**, *2* (2), 133−140.

(11) Mattisson, T., Lyngfelt, A. Applications of chemical-looping combustion with capture of CO_2. In *Proceedings of Second Nordic Minisymposium on Carbon Dioxide Capture and Storage*, Göteborg, Sweden, April 18−20, 2001; pp 46−51.

(12) Kunii, D.; Levenspiel, O. *Fluidisation Engineering*, 2nd ed.; Butterworth-Heinemann: Oxford, U.K. 1991; pp 36−38.

(13) Caballero, M. A.; Corella, J.; Aznar, M. P.; Gil, J. Biomass gasification with air in fluidized bed. Hot gas cleanup with selected commercial and full-size nickel-based catalysts. *Ind. Eng. Chem. Res.* **2000**, *39* (5), 1143−1154.

(14) Delgado, J.; Aznar, M. P.; Corella, J. Biomass gasification with steam in fluidized bed: Effectiveness of CaO, MgO, and CaO−MgO for hot raw gas cleaning. *Ind. Eng. Chem. Res.* **1997**, *36* (5), 1535−1543.

(15) Corella, J.; Orío, A.; Toledo, J.-M. Biomass gasification with air in a fluidized bed: Exhaustive tar elimination with commercial steam reforming catalysts. *Energy Fuels* **1999**, *13* (3), 702−709.

(16) Aznar, M. P.; Caballero, M. A.; Gil, J.; Martín, J. A.; Corella, J. Commercial steam reforming catalysts to improve biomass gasification with steam−oxygen mixtures. 2. Catalytic tar removal. *Ind. Eng. Chem. Res.* **1998**, *37* (7), 2668−2680.

(17) Bangala, D. N.; Abatzoglou, N.; Martin, J. P.; Chornet, E. Catalytic gas conditioning: Application to biomass and waste gasification. *Ind. Eng. Chem. Res.* **1997**, *36*, 4184−4192.

(18) Rownaghi, A. A.; Huhnke, R. L. Producing hydrogen-rich gases by steam reforming of syngas tar over CaO/MgO/NiO catalysts. *ACS Sustainable Chem. Eng.* **2012**, *1* (1), 80−86.

(19) Consensus Economics, http://www.consensuseconomics.com/Ilmenite_Price_Forecasts.htm; accessed online 01-17-2013.

(20) Consensus Economics, http://www.consensuseconomics.com/Nickel_Price_Forecasts.htm; accessed online 11-21-2012.

(21) Leion, H.; Lyngfelt, A.; Johansson, M.; Jerndal, E.; Mattisson, T. The use of ilmenite as an oxygen carrier in chemical-looping combustion. *Chem. Eng. Res. Des.* **2008**, *86* (9A), 1017−1026.

(22) Berguerand, N.; Lyngfelt, A. Batch testing of solid fuels with ilmenite in a 10 kWth chemical-looping combustor. *Fuel* **2010**, *89* (8), 1749−1762.

(23) Leion, H.; Mattisson, T.; Lyngfelt, A. Solid fuels in chemical-looping combustion. *Int. J. Greenhouse Gas Control* **2008**, *2* (2), 180−193.

(24) Schwebel, G. L.; Leion, H.; Krumm, W. Comparison of natural ilmenites as oxygen carriers in chemical-looping combustion and influence of water gas shift reaction on gas composition. *Chem. Eng. Res. Des.* **2012**, *90* (9), 1351−1360.

(25) Cuadrat, A.; Abad, A.; Adánez, J.; deDiego, L. F.; García-Labiano, F.; Gayán, P. Behavior of ilmenite as oxygen carrier in chemical-looping combustion. *Fuel Process. Technol.* **2012**, *94* (1), 101−112.

(26) Min, Z.; Asadullah, M.; Yimsiri, P.; Zhang, S.; Wu, H.; Li, C.-Z. Catalytic reforming of tar during gasification. Part I. Steam reforming of biomass tar using ilmenite as a catalyst. *Fuel* **2011**, *90* (5), 1847−1854.

(27) Brage, C.; Yu, Q.; Chen, G.; Sjöström, K. Use of amino phase adsorbent for biomass tar sampling and separation. *Fuel* **1997**, *76* (2), 137−142.

(28) Jerndal, E.; Mattisson, T.; Thijs, I.; Snijkers, F.; Lyngfelt, A. NiO particles with Ca and Mg based additives produced by spray- drying as oxygen carriers for chemical-looping combustion. *Energy Procedia* **2009**, *1* (1), 479−486.

(29) Linderholm, C.; Abad, A.; Mattisson, T.; Lyngfelt, A. 160 h of chemical-looping combustion in a 10 kW reactor system with a NiO-

based oxygen carrier. *Int. J. Greenhouse Gas Control* **2008**, *2* (4), 520–530.

(30) Leion, H.; Jerndal, E.; Steenari, B.-M.; Hermansson, S.; Israelsson, M.; Jansson, E.; Johnsson, M.; Thunberg, R.; Vadenbo, A.; Mattisson, T.; Lyngfelt, A. Solid fuels in chemical-looping combustion using oxide scale and unprocessed iron ore as oxygen carriers. *Fuel* **2009**, *88* (10), 1945–1954.

(31) Milne, T. A.; Evans, R. J. *Biomass Gasifier "Tars": Their Nature, Formation, and Conversion*; NREL/TP-570-25357; National Renewable Energy Laboratory, Golden, CO, 1998.

Paper VI

CHEMICAL ENGINEERING RESEARCH AND DESIGN 89 (2011) 2470–2476

Contents lists available at ScienceDirect

Chemical Engineering Research and Design

journal homepage: www.elsevier.com/locate/cherd

On-line monitoring of fuel moisture-content in biomass-fired furnaces by measuring relative humidity of the flue gases

*Sven Hermansson**, *Fredrik Lind, Henrik Thunman*

Department of Energy and Environment, Chalmers University of Technology, SE-412 96 Göteborg, Sweden

ABSTRACT

Combustion of biomass for heat and power production is continuously growing in importance, because of incentives for replacing fossil energy resources with renewable ones. In biomass combustion, the moisture content of the fuel is an essential operation parameter, which often fluctuates for biomass fuels. Variation in moisture content complicates the operation of the furnaces and results in an uncertainty in the energy content of the fuel delivered to a plant. The fuel moisture-content in a furnace may be determined either by direct measurement on the entering fuel or by measuring the moisture and oxygen contents of the flue gases deriving the moisture content of the fuel. However, reliable methods of a motivated cost for the small to medium-scale furnaces are today not available. An exception is if the furnace is equipped with flue-gas condenser, which can be used to estimate the moisture content of the flue gases. A limitation of this method is, though, that not all furnaces have flue-gas condensers and that the measured signal has an inherent time delay.

In this work, measurement of the relative humidity (RH) of the flue gases from a furnace is investigated as the central component in the on-line monitoring of the moisture content of the fuel in a furnace. The method was analysed with humid air in a laboratory environment and tested for accuracy and dynamical behaviour in two biomass-fired heat-production units, one circulating fluidised-bed boiler (CFB) and one grate furnace. The results show that the method, which is easy to calibrate on site, can be used to predict the moisture content of the biomass fuel in the grate furnace with very good precision (<4% error). Furthermore, the method detects variations in moisture content of the furnace flue gases due to changes in the moisture content of the combusted fuel within the order of seconds. Since the transport time of the flue gases from the furnace to the measurement position is of the same order of magnitude, the total time for detection of a change in the moisture content of the fuel is small enough for the signal to be used to control both the fuel feed and the combustion air in a grate furnace.

Keywords: Combustion; Biomass; Moisture content; Relative humidity; Grate furnaces; Sensors

1. Introduction

Combustion of biomass for heat and power production is expanding due to the search for renewable alternatives to fossil fuels. An important parameter when using biomass is the moisture content of the fuel, which normally is a blend of different batches typically varying between 30 and 55%, related to the total mass of biomass as delivered. Variation in moisture content complicates the operation of the combustors and results in an uncertainty in the energy content of the fuel delivered to a plant. This is especially problematic for smaller units where the economical and technical resources are more limited than in larger ones. Within this segment of boilers, the most common conversion method is grate firing. Grate furnaces are typically installed in heat production plants with capacities below 40 MW_{th}. For example, in Sweden there are about 350 furnaces operated with reciprocating grate for production above 1 MW_{th} (Svensk Fjärrvärme AB, 2007) and in the rest of Europe and North America the technique is increasingly applied in the segment below 20 MW_{th}.

---

* *Corresponding author*. Tel.: +46 31 772 1455; fax: +46 31 772 3592.
E-mail addresses: sven.hermansson@chalmers.se, sven.j.hermansson@gmail.com (S. Hermansson).

Received 10 November 2010; Received in revised form 28 March 2011; Accepted 29 March 2011

doi:10.1016/j.cherd.2011.03.018

Nomenclature

c_p	specific heat (J/kg K)
LHV	lower heating value (J/kg)
m	mass flow (kg/s)
P	pressure (Pa)
Q	heat (W)
R	calibration factor
t	time (s)
T	temperature (K)
X	volume fraction (m^3/m^3)
Y	mass fraction (kg/kg)
ΔH_{evap}	heat of evaporation of water (J/kg)
η	efficiency
φ	relative humidity, RH

Indices

b	furnace boiler
err	error
d	delay
dry	dry matter
fg	flue gases
cond	flue-gas condenser
fuel	fuel
m	moisture
sat	saturation
uncomb	products of incomplete combustion

A major advantage with the grate furnace is its ability to manage a variety of wet fuels (Yin et al., 2008). However, even if a grate furnace is reasonably stable to changes in fuel quality, fluctuations still are challenges to the operation. One important parameter to maintain a stable operation is the moisture content, which commonly varies both between and within delivered fuel batches. Today, the standard procedure to determine the moisture content of the fuel in small to medium-scale grate furnaces is to analyse a number of manually collected samples from each fuel batch delivered to the plant. Such a crude method only serves as a rough estimation to calculate the price of an entire truck load. Furthermore, it is not accurate enough to predict the moisture content of the fuel-mix that continuously enters the furnace; a change in moisture content of the fuel-mix needs to be detected at high-frequent resolution (seconds) to enable a correct response from the combustion-air system or within minutes to produce a response from the fuel-feed system. More accurate methods for monitoring of the moisture content of the fuel are, therefore, requested. However, to make the methods available to small to medium scale plants the investment cost of such installations must be within reasonable limits.

On-line measurements of the moisture content of a fuel mix are carried out with direct or indirect methods. Direct methods focus on the fuel itself, while the indirect methods derive the fuel moisture-content from quantities measured in the flue gases and in the combustion air. Methods for direct measurements of the fuel moisture-content are near-infrared spectroscopy (NIR), dual X-ray, radio frequent, microwave and nuclear magnetic resonance (NMR) measurements (Nyström and Dahlquist, 2004). Especially NIR has been investigated and implemented as a promising method to analyse the fuel for moisture content either by automatic sampling at delivery or, for control purposes, in the fuel mix before it is injected into the furnace (Berg et al., 2005). However, these methods are hard to motivate for small-scale combustors on economical basis and, furthermore, they demand measurement set-up, calibration and handling skills (Aulin and Karlsson, 2008). Therefore, the direct measurement-methods often become unfeasible in the capacity area of grate furnaces.

The alternatives to the direct methods are the indirect methods for determining the moisture content, which are both easier to handle and less costly. The key to the indirect method for finding the moisture content of a solid fuel is to determine the moisture content of the flue-gases. From the measurement of gas moisture-content, the moisture content of the fuel can then be derived by a mass balance, including the moisture content of the combustion air, the elementary composition of the fuel and the composition of the combustion-air (Nyström and Dahlquist, 2004; Marklund and Schuster, 1991). In this process, the only inherent delay of measurement signal is the transport time of the gas from the combustion chamber to the measurement position. This time delay is approximately less than 2 s, opening up possibilities of controlling both the combustion air and fuel feed. However, the large dimensions of the flue-gas ducts and the temperature levels in the flue gas system, which normally is above 150 °C, are complicating factors; Fourier-transform infrared technology (FT-IR) qualifies as the sole method among the available methods summarised in Table 1 to determine the moisture content with enough accuracy while approaching a reasonable cost level in relation to the combustion unit. Still, the accuracy of the FT-IR is sensitive to the absolute temperature level, pressure, temperature gradients and particles carried with the gas, complicating measurements directly in the flue-gas duct. As an alternative to FT-IR – also listed in Table 1 – in combustion units equipped with a flue-gas condensation-unit, the moisture content may be estimated from a heat balance over the condenser (Eriksson et al., 2008). On the other hand, this measurement signal is delayed because of the heat transfer resistance in the heat exchangers. This method is, therefore, limited to detection of low-frequent fluctuations, in the order of minutes, which in most cases is sufficient for control of the fuel feed (Bood et al., 2010), while too crude to be used for control of the combustion air.

Recently, sensors have been developed for measuring relative humidity (RH) in gases up to 200 °C, qualifying the method for determining the moisture content in the temperature range of flue gases. These RH-sensors use chemically modified polymers as detector materials, responding by capacitance to the RH of the surrounding gas (Sakai, 1993), which have been shown to be resistant to environments contaminated with different organic compounds (Ikonen et al., 2006). In addition, and as listed in Table 1, the cost of the sensors is reasonable and the handling skills required are less than for FT-IR. However, the accuracy of the RH-sensors in high temperature flue gases is too low to be used for indirect determination of the moisture content of the fuel in furnaces (Eriksson et al., 2008) because of the low RH-level (<0.01) typical for biomass flue-gases. In this work, the method using a RH-sensor is developed with the aim of improving the accuracy to levels acceptable for indirect determination of the moisture content of the fuel in a biomass furnace. This is achieved by cooling of an extracted flue-gas stream, elevating the RH of the flue gases, before performing the measurement. The method is tested for accuracy and dynamic behaviour in laboratory environment and in two heat production units, one multi-fuel circulating fluidised-bed

Table 1 – Ways to measure moisture content in flue gases.

Measurement device	Result	Complexity	Detection delay	Accuracy	Approx. cost	Reference
FT-IR	Directly	High	Seconds to minutes	High	$20,000	Yokelson et al. (1996); Jaakkula et al. (1998); Bak and Clausen (2002); De Palma, 2010
Flue gas condenser	Via heat balance	Low	Minutes	Acceptable	N.A.	Marklund and Schuster (1991)
Relative humidity/temperature sensor	From modelled saturation pressure	Low	Seconds	Poor	$1000	Eriksson et al. (2008); Ikonen et al. (2006).

boiler (CFB) burning wood chips of approximately 42% moisture and one grate furnace burning saw dust of approximately 54% moisture.

2. Indirect determination of fuel moisture-content

The moisture content of a solid fuel, Y_m, is normally defined as the mass of moisture in the fuel, $m_{m,fuel}$, related to the total mass of the wet fuel, m_{fuel}, according to,

$$Y_m = \frac{m_{m,fuel}}{m_{fuel}}. \tag{1}$$

The indirect method for determining the moisture content of a solid fuel is based on measured moisture and oxygen contents of the flue gas. With additional information of the elementary composition of the fuel and of the combustion air, together with the humidity of the latter, the moisture content of the fuel, Y_m, can be calculated from a mass balance across the furnace.

As an alternative to measurement in the flue gases, the moisture content in the flue gases can be determined from the heat of condensation of the moisture in the flue gases. A combined heat balance for the flue-gas condenser and the boiler is then arranged,

$$Q_{cond} = \sum_i m_{i,fg} \int_{T_{fg}}^{T_{cond}} c_{p,i}\ dT + m_{m,cond}(-\Delta H_{evap})_{T_{cond}} \tag{2}$$

$$Q_b = \sum_i m_{i,fg} \int_{T_{ref}}^{T_{fg}} c_{p,i}\ dT + m_{fuel,dry}\eta_b(LHV) - m_{m,fuel}\eta_b(-\Delta H_{evap}) \tag{3}$$

where Q is heat from the flue-gas condenser and boiler, c_p is heat capacity, ΔH_{evap} is heat of evaporation of water, T is temperature, η is efficiency and *LHV* is lower heating value of the fuel. Indices are *cond* for condenser, *fg* for flue gas, *m* for moisture, *evap* for evaporation, *ref* reference point, *dry* for dry part of fuel and *b* for furnace boiler. A limitation with this method is, as already mentioned, the inherent delay in response, which is caused by the heat-transfer resistance of the heat exchangers in the condenser. To quantify the delay, the signal can be compared with a second reference signal by statistical cross-correlation,

$$r = \frac{\sum_i^d[(Y_{m1,i} - \bar{Y}_{m1})(Y_{m2,i} - \bar{Y}_{m2})]}{\sqrt{\sum_i^d (Y_{m1,i} - \bar{Y}_{m1})^2}\sqrt{\sum_i^d (Y_{m2,i} - \bar{Y}_{m2})^2}} \tag{4}$$

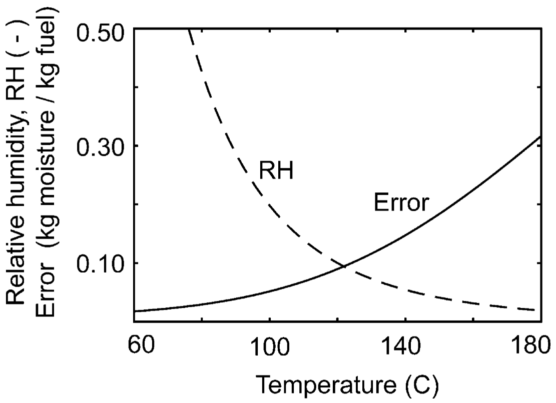

Fig. 1 – Error of calculated fuel moisture-content and attributable RH-measurement for a typical biomass (Ragland and Aerts, 1991) flue gas of 20% moisture content.

$$\bar{Y}_m = \frac{1}{\Delta t}\sum_i^n Y_{m,i}\Delta t_i \tag{5}$$

where *r* is the normalised cross-correlation factor, *d* the range of the investigated delay, Δt the extension in time of each value of Y and indices 1 and 2 represent the compared signals. The range of the normalised cross correlation is between zero and one, where a high value indicates that the two signals correlate at that particular delay.

Using a RH-sensor, the moisture fraction of the gases is determined from the saturation pressure, P_{sat}, according to,

$$X_{vol,m} = \varphi\frac{P_{sat}}{P} \tag{6}$$

$$P_{sat} = \exp\left(\frac{23.82 - 4193}{T - 32}\right), \tag{7}$$

where X_{vol} is the volumetric fraction, φ is the RH, P is the total pressure in the gas (Eq. (7) is an integration of the *Clausius–Clapeyron* equation under the assumption that the evaporation enthalpy is independent of temperature). Additionally, the temperature needs to be measured to find the saturation pressure. The major challenge with this method, as indicated above, is the low RH-level of hot flue gases, typically below 1% for biomass combustion, which results in substantial uncertainties in the RH-measurement (Eriksson et al., 2008). This is exemplified in Fig. 1, where the measured RH of a flue gas and the resulting expected error of the calculated moisture content of the fuel, Eq. (1), are plotted against the temperature of the gas. A flue-gas of 3.5% oxygen (dry) from a typical biomass (Ragland and Aerts, 1991) of moisture content of 20%

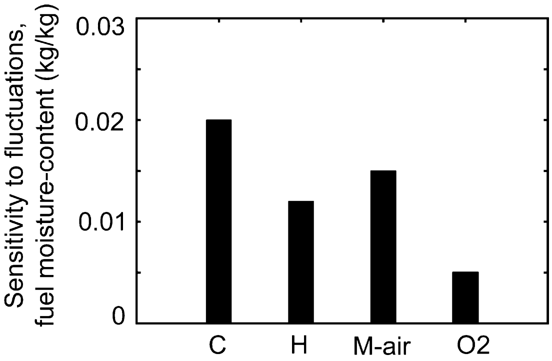

Fig. 2 – Sensitivity of the calculated fuel moisture-content to elementary composition (C, carbon; H, hydrogen) of ±2%-units, and to 10% error in moisture content of the combustion air (M-air) and in oxygen concentration of the flue gases (O_2).

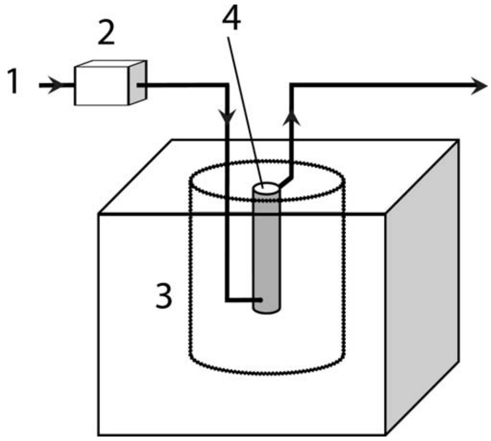

Fig. 3 – Outline of measurement set-up: (1) extraction of flue-gases from the duct; (2) filter; (3) temperature controlled oil bath; (4) measurement cell.

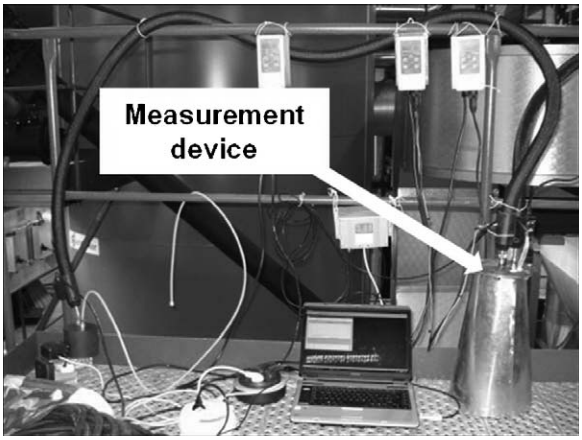

Fig. 4 – Measurement set-up.

has been used in the calculation. The definition of the measurement error for a RH-sensor (Ikonen et al., 2006) available on the market is

$$\varphi_{err} = \pm(0.015\varphi + 0.015), \tag{8}$$

where φ_{err} is the expected error in measured RH and φ is the RH measurement-value. It can be seen in the figure that for temperatures above 150 °C, the error of the fuel moisture content, Y_m, is at least 0.15 kg moisture per kg fuel, which corresponds to approximately 50% of the total fuel moisture-content. This should be compared with the expected errors attributable to the other variables in the mass balance, i.e. the oxygen content in the flue gas, the moisture content of the combustion air and the elementary composition of the fuel, which are presented in Fig. 2 and that all are below 0.02. In the sensitivity analysis presented in Fig. 2, deviations of 2%-units of the elementary composition (50% C, 42% O and 6% H; Ragland and Aerts, 1991) was used, together with 10% deviations of the moisture content of the combustion air and of the oxygen fraction of flue-gases. Thus, to reduce the error caused by the RH-measurement to the same level as for the other uncertainties, the RH of the flue gases should be increased to at least 0.4. For this typical flue gas, such a level is reached by cooling the flue gases to approximately 80 °C.

3. Measurement set-up

The measurement arrangement is illustrated in Figs. 3 and 4. The flue-gas is extracted from the flue-gas duct (1), separated from particles by a filter (2) and cooled to the targeted temperature in a tube that passes through a temperature-controlled oil bath (3). The RH, the temperature and the pressure are measured in a cell (4); a manometer is used for the pressure and a PT100 resistance detector for temperature detection, while the RH is determined from the sensitivity in electrical conductivity of a polymer to the surrounding gas moisture-content (Sakai, 1993; Ikonen et al., 2006).

Earlier, the RH-sensor used in this work was validated in clean air and in air contaminated with organic compounds (Ikonen et al., 2006). Here, the suitability of the sensor as a central component to determine the moisture content in flue gases from biomass combustion was investigated in the following tests:

1. Determination of operational RH-range of the experimental set-up:
   - sensitivity to condensation, using air of approximately 10% moisture-content.
2. Accuracy of the method in controlled biomass flue-gas environment (Chalmers research 12 MW_{th} circulating fluidised bed (CFB)-boiler, 8 h continuous operation):
   - measurement of relative humidity and temperature in extracted flue-gas;
   - sampling of fuel feed every half hour;
   - registration of operational conditions.
3. Dynamic behaviour of the method in the Chalmers research 12 MW_{th} CFB-boiler:
   - measurement of relative humidity and temperature in extracted flue-gas;
   - measurement of moisture content FT-IR analyser in (the same) extracted flue-gas;
   - water injection to the fuel feed (inducing step function).
4. Field experiment in an E.ON 8 MW_{th} grate-fired furnace burning saw dust (3 h):
   - measurement of relative humidity and temperature in extracted flue-gas;
   - registration of the heat output from the flue-gas condenser;
   - sampling of fuel every half hour.

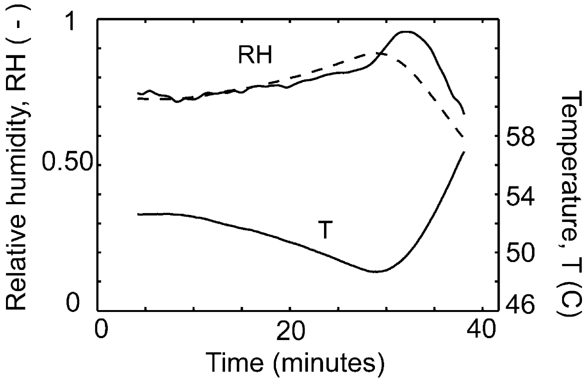

Fig. 5 – Relative humidity in the measurement cell for variation in temperature (in air of 10% moisture). (—) Measured temperature and RH; (- - -) theoretic RH.

4. Results and discussion

The operational limits of the method were determined by investigating the sensitivity to condensation in the measurement set-up when using 150 °C air of approximately 10% moisture content. The target temperature of the cooled sensor cell was gradually decreased towards the expected dew point of 43 °C and eventually increased again. The measured RH for the trial and the predicted RH of the air, calculated according to Eqs. (6) and (7), are given in Fig. 5. The measured RH is seen to follow the prediction well up to approximately a RH of 75% (50 °C). When further decreasing the temperature, the measured RH overshoots the predicted value. This behaviour was interpreted as start of condensation in the cell. Even though the trial was interrupted by increasing the target temperature, the measured RH continued to rise for approximately 3 min. This confirms that condensate had been formed in the cell, which contributed to the prolonged increase of RH by evaporation. According to these results, the sensor cell should not be operated at RH below 0.5–0.6. According to Fig. 1, the maximal accuracy of the fuel moisture-content will then, theoretically, be 0.025 kg moisture per kg fuel. This is in the same order of magnitude as the errors produced in the sensitivity analysis, illustrated in Fig. 2.

The accuracy of the RH-sensor in flue gases from biomass combustion was investigated in the Chalmers CFB-boiler during 8 h of stable operation. According to the repeated fuel-sampling, the fuel contained 0.421 kg moisture per kg fuel on average. The calculated fuel moisture content from measured RH (41% on average) and temperature, presented in Fig. 6, resulted in an average fuel moisture-content of 0.374 kg moisture per kg fuel. The registered operational conditions and fuel properties used in the calculation are listed in Table 2. The discrepancy between the sampled moisture content and the calculation (0.047 kg moisture per kg fuel) coincides well with the expected accuracy of the RH-sensor, given in Fig. 1. The discrepancy is either due to inaccuracies in the RH measurement or due to the uncertainties in the fuel and air properties. Here, the elementary composition of the fuel and operation parameters was rigorously documented, which indicates that the discrepancy of the measurement principally is caused by the RH-measurement. When measuring within the same range of RH in other furnaces, burning similar biomass under similar conditions, it can be assumed that the error is constant. Therefore, the accuracy test is used to calibrate the RH signal until the calculated result coincides with the sampled value. The calibration factor, R, for the RH sensor is determined to 1.087.

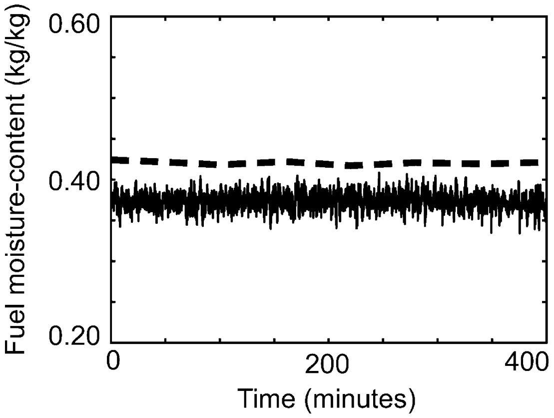

Fig. 6 – Moisture content of the fuel in the accuracy test in the Chalmers research CFB-boiler. (—) Calculated from the measured RH; (- - -) determined from fuel-sample analysis.

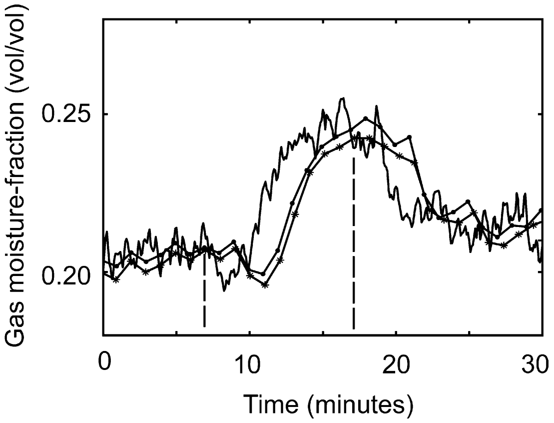

Fig. 7 – Moisture fraction of the flue gas during the dynamic test in Chalmers CFB-boiler. The period bounded with dashed lines defines the time period during which water was added to the fuel. (—) Derived from the calibrated RH-measurement; (●) derived from calibrated and filtered RH-signal (60 s); (—∗—) FT-IR measurement.

The dynamic behaviour of the calibrated method was investigated in the Chalmers research CFB-boiler, producing a step function of moisture in the flue gases by adding water to the fuel feed. The results, presented in Fig. 7, reveal that the RH-sensor signal responds to frequencies within 1 min, while the FT-IR analyser detects the change in moisture approximately 2 min later. However, the used FT-IR analyser filters the measurement signal retroactively on minute-basis; when treating the RH signal with the same filter they become comparable. The filtered signal from the RH-measurement and the FT-IR measurement show no sign of hysteresis in the RH-measurement, meaning that the signals respond equally to both positive and the negative change in moisture content. This validates the method for detection of fluctuations in moisture content in the same order as the sampling time of the instrument (5 s).

The result from the field experiment in the 8 MW_{th} grate fired furnace is given in Fig. 8 as fuel moisture content derived from the calibrated RH-measurement and from the registered heat of flue-gas condensation together with the fuel samples. The mean value of the period was determined to 0.525 from the calibrated measurement of RH, to 0.544 from the fuel sam-

Table 2 – Operational conditions and fuel properties during the trials in the Chalmers research 12 MW_{th} CFB-boiler and in the E.ON 8 MW_{th} grate-fired furnace.

	Chalmers CFB, 12 MW_{th}	E.ON grate furnace, 8 MW_{th}
Operating conditions (on average)		
Fuel	Wood chips	Saw dust
Power output (MW_{th})	6.8	3.8 + 0.8 (fg condenser)
Fuel flow (kg/s)	0.636	n/a
Air flow (kg/s)	2.67	n/a
Oxygen in fg (m^3/m^3)	0.039	0.025
Fuel composition (kg/kg dry matter)		
Carbon	0.496	0.499
Hydrogen	0.060	0.060
Oxygen	0.433	0.438
Nitrogen	0.0015	0.0006
Sulphur	0.0001	<0.0001
Chlorine	0.0001	<0.0001
Ash	0.009	0.003

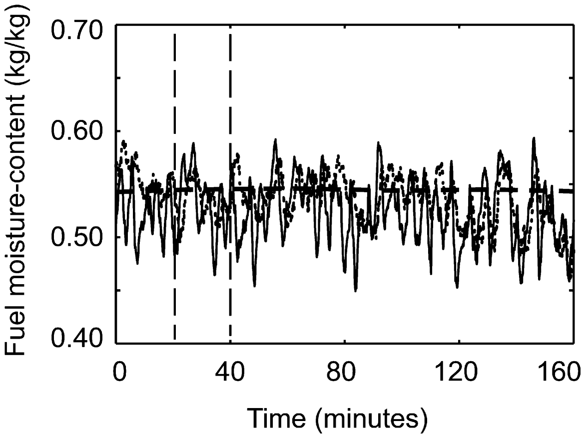

Fig. 8 – Moisture content of the fuel in the 8 MW_{th} grate furnace with sample (bold dashed line). The time-period shown in Fig. 9 is, here, bounded with vertical dashed lines. (—) Calculated from calibrated RH-measurement; (●) calculated from the heat of flue-gas condenser; (- - -) determined from fuel-sample analysis.

ples and to 0.531 from the method based on the heat of the flue-gas condenser. The values have been adjusted for a hidden water leakage in the convectional part of the furnace, leading to increased moisture concentration, that was discovered during a succeeding maintenance stop. By analysing the frequency of refilling of the boiler system the leakage could be determined to 1 m^3 per 24 h, resulting in an error of calculation of 0.008 kg moisture per kg wet fuel. Operational conditions and analysed fuel properties used in the calculations are listed in Table 2. The results show that that the determination of the moisture content of the fuel with the calibrated RH-measurement coincides well both with the sampled fuel moisture-content and with the condenser-based calculation. The discrepancy between the RH-based method and the two other methods is less than 4% of the sampled value. According to the theoretical accuracy of the un-calibrated sensor RH-measurement, Eq. (8), the median error in the moisture content of the fuel should be at least 7.5% of the calculated mean value during the period. Here, it is seen that such a magnitude of error is not reached, but that the accuracy of the method has been improved significantly by the in situ calibration. The calibration procedure may in future applications be carried out by sampling of the fuel, as was performed in the CFB-boiler. An alternative or complement to this method would be to condense the extracted flue-gas stream while during a sufficient time period measuring the mass of condensate together with the dry gas flow.

Analysis of an extracted part of the test in the 8 MW_{th} grate fired furnace shows that the method based on the calibrated RH-measurement responds faster than the method based on the condenser-heat. The part of the trial used for investigation is marked with dashed lines in Fig. 8 and magnified in Fig. 9a. A cross-correlation analysis of the two series, according to Eqs. (4) and (5), gives a correlation ($r = 0.56$) at a shift of 1.5 min between the two signals. When applying this shift, as

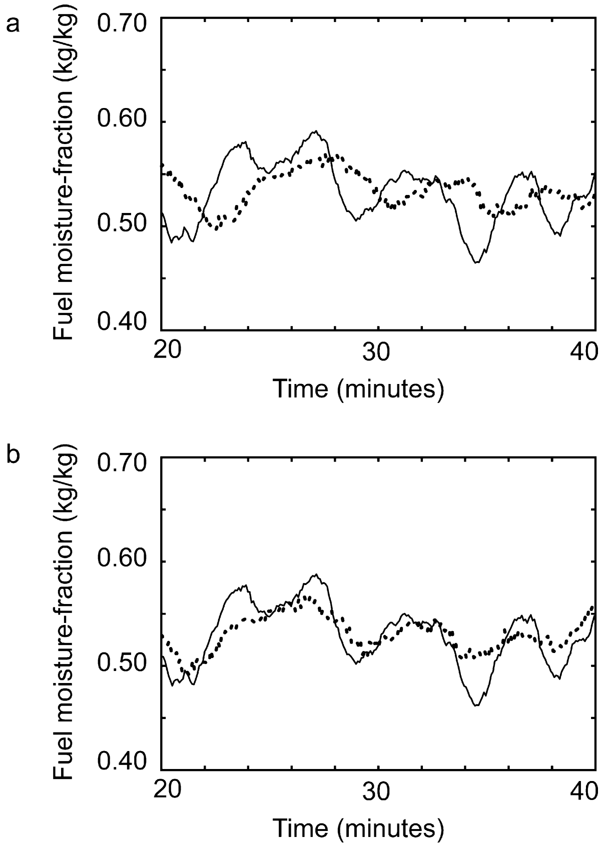

Fig. 9 – Fuel moisture-content during the trial in the 8 MW_{th} grate furnace (extracted part, defined in Fig. 8). (—) Calculated from calibrated RH-measurement; (●) calculated from the heat of flue-gas condenser. (a) Original signals; (b) after reducing the response time of the condenser-heat based according to the cross-correlation (1.5 min).

presented in Fig. 9b, the two signals match each other. The identified delay between the signals is in accordance with the result from the test of dynamics, where the sensor was seen to respond within the order of seconds to changes in moisture content. The method based on heat of condensation of the flue gases is, as already discussed, expected to respond slower due to the resistance in the transfer of the heat of condensation from the flue-gas side to the cooling-water side in the condenser.

5. Conclusions

Relative humidity (RH) was investigated as alternative to existing methods for measuring the moisture content in flue-gases from biomass combustion to indirectly determine the moisture content of the fuel. From an economical point of view, an RH-sensor in combination with measurement of temperature is more favourable for small-scale biomass furnaces than a flue-gas condenser or an FT-IR detector. Furthermore, the demand of an RH-sensor on the measurement set-up and calibration is less than for an FT-IR. The drawback with the RH-sensor is that the accuracy normally is lower than for the alternative methods when the measurement is performed directly in the flue gas duct. In this work, a method to increase the accuracy was developed. The method consists in cooling of a partial stream of the flue gases, raising the RH-level of the measurement gas and transferring the accuracy of the measurement into an acceptable range. The proposed measurement set-up was tested both in humid air and in flue gas from two heat production units – one grate furnace burning saw dust of approximately 54% moisture and one CFB-boiler burning wood chips of approximately 42% moisture.

The results show that the method developed predicts the moisture content of the biomass fuel in the grate furnace with very good precision (<4% error) after calibration of the RH measurement sensor under similar conditions in the CFB-boiler. The calibration of the sensor can be performed by determining the moisture content of fuel samples – a method applied in this work and in accordance with present standard for economical classing of the fuel. A suggested alternative method is to evaluate the moisture content of the flue gas by condensing a given gas stream during a sufficient time period. Furthermore, the result of the tests shows that the method is able to detect variations in moisture content within the order of seconds, without any significant hysteresis. Thus, the method developed can be used to control both the fuel feed and the combustion air in a grate furnace, while the method based on the condenser heat was shown to be limited to control the fuel feed.

Acknowledgements

The authors would like to thank E.ON Värme AB, especially Bengt-Åke Andersson and Conny Eriksson, for the co-operation and support along the project and the measurement campaign in the grate furnace in Mölnlycke, Sweden. Maria Bergh, Mikaela Flodin, Pia Flydén and Ulrika Gustafsson are acknowledged for their assistance with the design and constructing of the measurement device.

References

Aulin, R., Karlsson, M., 2008. Standardisation of Moisture Measurement using NIR Spectroscopy for Delivery Control, Värmeforsk rapport. Värmeforsk, Stockholm, ISSN 1653-1248.

Bak, J., Clausen, S., 2002. FTIR emission spectroscopy methods and procedures for real time quantitative gas analysis in industrial environments. Meas. Sci. Technol. 13, 150–156.

Berg, M., Wiklund, S.E., Karlsson, M., Tryzell, R., 2005. Automatic Determination of Moisture Content in Biofuels based on NIR-measurements, Värmeforsk rapport 935. Värmeforsk, Stockholm, ISSN 1653-1248.

Bood, J., Liljeström, E., Lindberg, G., Persson, C., Rådegård, E., Turesson, M., 2010. Indikering av bränslefukthalt med hjälp av indirekt mätning av fukthalten i rökgasen på fliseldade pannor (Indication of fuel moisture content by measuring moisture content of flue gases in wood-chips fired boilers), Thesis for bachelors degree. Chalmers University of Technology, Göteborg, Sweden.

De Palma, A., 2010. FTIR spectroscopy: picking up steam in nontraditional markets. Lab Manager Mag. 5 (4), 43.

Eriksson, L., Filipsson, P., Johansson, E., Lorentsson, R., Palm, R., Smitt Meyer, C., 2008. Förbättringsmöjligheter för småskalig biobränsleförbränning (Potentials for improving small scale biomass combustion), Thesis for bachelors degree. Chalmers University of Technology, Göteborg, Sweden.

Ikonen, S., Stormbom, L., Ranta-aho, T., 2006. Chemical interference test results of a novel humidity sensor. In: 5th International Symposium on Humidity and Moisture , ISHM 2006 Brazil, Rio de Janeiro, April 2006.

Jaakkula, T.J., Vahlman, T.A., Roos, A.A., Saarinen, P.E., Kauppinen, J.K., 1998. On-line analysis of stack gas composition by a low resolution FT-IR gas analyzer. Water Air Soil Pollut. 101, 79–92.

Marklund, J., Schuster, R., 1991. Indirekt fuktbestämning av bränsle (In-direct determination of fuel-moisture content), Värmeforskrapport 406. Värmeforsk, Stockholm, ISSN 0282-3772.

Nyström, J., Dahlquist, E., 2004. Methods for determination of moisture content in woodchips for power plants—a review. Fuel 83, 773–779.

Ragland, K.W., Aerts, D.J., 1991. Properties of wood for combustion analysis. Bioresour. Technol. 37, 161–168.

Sakai, Y., 1993. Humidity sensors using chemically modified polymeric materials. Sens. Actuator B: Chem. 13–14, 83–85.

Svensk Fjärrvärme AB, 2007. Fjärrvärmeföreningens Pannregister (Directory of Heat Production Furnaces in Sweden). Svensk Fjärrvärme AB, Stockholm.

Yin, C., Rosendahl, L.A., Kær, S., 2008. Grate-firing of biomass for heat and power production. Prog. Energy Combust. Sci. 34, 725–754.

Yokelson, R.J., Griffith, D.W.T., Ward, D.E., 1996. Open-path Fourier transform studies of large-scale laboratory biomass fires. J. Geophys. Res. 101 (D15), 21067–21080.

Paper VII

Using an oxygen-carrier as bed material for combustion of biomass in a 12-MW_{th} circulating fluidized-bed boiler

Henrik Thunman[1], *Fredrik Lind*[1]*, *Claes Breitholtz*[2], *Nicolas Berguerand*[1],
Martin Seemann[1]

[1]Department of Energy and Environment, Division of Energy Technology, Chalmers University of Technology, SE-412 96 Gothenburg, Sweden

[2] Metso Power AB, PO Box 8734. SE-402 75 Gothenburg, Sweden

*E-mail: fredrik.lind@chalmers.se, Tel: +46 (0)31 772 52 43

Keywords: Biomass Combustion, Oxygen Carriers, Combustion Emissions, Mass Transfer Issues, Ilmenite

Abstract

The initial experiences of using an oxygen-carrying metal oxide, ilmenite, in the 12-MW_{th} circulating fluidized bed (CFB) boiler/gasifier system at Chalmers University of Technology are presented. The rationale for the addition of ilmenite to the solids inventory is that ilmenite has the ability to alternately take up and release oxygen, and thereby improve the distribution of oxygen throughout the furnace. As a consequence, less air is needed to maintain low emissions from carbon monoxide (CO) and unreacted hydrocarbons (HC) during the combustion of volatile-rich fuels, such as biomass. One of the conducted experiments involved only the boiler, and the reference case corresponded to operation solely with silica-sand as the bed material, while in an additional three cases, ilmenite in various amounts was added to make up to 40wt.% of the total bed inventory. During the experiments, the concentrations of CO and nitric oxide (NO) in the convection path of the boiler were measured. The addition of ilmenite to the silica-sand decreased the concentrations of CO and NO by 80% and 30%, respectively. Additional experiments were performed in which a concentrated stream of raw gas produced in the indirect gasifier was injected into the freeboard of the boiler. In one experiment, only silica-sand was used, while 12wt.% ilmenite was added to the bed material in a separate experiment. The concentrations of CO and HC were measured at three different heights in the boiler and at nine positions over a cross-section of the furnace. The concentrations of CO and total HC in the furnace cross-section during concomitant gasification operation were reduced by the addition of ilmenite.

Introduction

In most commercial combustion applications, the most important part is the consumption of gaseous oxygen. Combustion efficiency depends to a large extent on the facilitation of adequate mixing of the fuel and oxygen both spatially and temporally[1]. A commonly applied measure in combustion plants to control the level of oxygen in relation to fuel-specific properties is to adjust the level of excess air. However, increasing the oxygen supply to the furnace usually requires that an excess of air has to be fed into the combustion unit, which results in loss of boiler efficiency. This can also generate a situation in which there is irregular release of heat inside the combustion chamber, owing to the uneven distribution of oxygen and fuel in space and time. The resulting maldistribution can in turn lead to emission-related issues, such as the release of NO_x and SO_x species and the escape of unreacted hydrocarbons (HC) and CO in the flue gases; extensive efforts have been made to resolve this problem. Furthermore, as a consequence of the uneven heat release, high-temperatures zones can be formed within small volumes inside the furnace. These temperature gradients are likely to induce the melting of ash components, which promotes the formation of sticky ash, which may be deposited onto cooling surfaces. The condensation of ash onto super-heater and heat exchanger surfaces in the convection path may lead to severe fouling and create degraded heat transfer and corrosion problems[2-4].

Currently, measures that can be applied to ameliorate these problems are in two main categories: 1) measures that focus on the preparation and feeding of the fuel; and 2) measures related to the introduction of air together with - in many cases - recirculated flue gases[5]. The first category of measures is essential when solid fuels are to be combusted, as the preparative step aims to yield a fuel that is as homogeneous as possible. Nevertheless, this operation has to have a reasonable energy penalty for the process in terms of affordable equipment and operating cost. For all the different fuel types, and particularly for the solid fuels, optimization of the feeding is a significant challenge[6]. In many cases, this can be seen as the most concealed part of the boiler design from different manufactures of combustion technologies. The feeding system must distribute the fuel to the furnace in an optimal manner while ensuring robust operation of the overall boiler.

The second category of measures is concerned with the implementation of a satisfactory air register. For this, choosing the appropriate number and location of feeding ports for air injection is the key to ensuring complete combustion of the fuel - and possibly limiting combustion to the boiler body itself - and to restricting the levels of harmful emissions. In general, the two categories of measures are combined, and the feeding streams ensure that the fuel and the gaseous oxygen are adequately mixed, i.e., to guarantee that the temperature and stoichiometry are favorable for the specific boiler operation[5]. This also explains why most of the boiler development over the past century has been devoted to furnace design, with a focus on the injection positions for the air and recirculated flue gases. All of these actions reflect the fact that heat release is typically connected to the location of fuel oxidation, which is the general principle for most of the current commercial combustion processes. However, if complete fuel oxidation could be achieved during controlled heat release throughout the furnace volume and at close to stoichiometric combustion, the efficiency and ash-related issues for particularly heterogeneous fuel combustion could be greatly improved. Nevertheless, to overcome mass transfer issues and to make the operation feasible at close to the stoichiometric condition, two crucial conditions need to be fulfilled: 1) the amount of fed oxygen needs to be accessible throughout the whole furnace geometry, to ensure complete combustion of the fuel; and 2) the fed oxygen needs to be retained to benefit the specific reactions coupled to the heterogeneity of the fuel. Taking biomass conversion as an example, the appropriate amounts of oxygen have to be distributed so as to convert the char fraction in the same time as the volatiles fractions are being fully oxidized before entering the convection path.

In the present work, these conditions were considered with the aim of improving the combustion of biomass in a circulating fluidized bed (CFB). The underlying rationale is to replace the totality or a fraction of the usual bed material with an oxygen-carrying metal oxide, as depicted in Figure 1. This metal oxide, which has the ability to absorb and release oxygen during redox reactions at the temperatures used, will theoretically, owing to its reactions with gaseous HC and the fluid dynamics in the riser furnace, facilitate simultaneous oxygen supply across the entire boiler geometry, thus fulfilling condition (1). When the oxidized metal oxide (MeO) is conveyed upwards through the furnace geometry, the bound oxygen is converted through reactions with the volatiles (C_iH_j) into carbon dioxide and water, and the metal oxide is reduced (to *Me*). The reduced form (*Me*) is then separated from the flue gases in the cyclone and recirculated to the bottom bed. The air feed to the furnace can then be balanced from based on the oxygen consumption needed to convert the char fraction (*nChar*) to CO_2, together with the need for oxygen for re-oxidizing the reduced metal oxide (*Me*) and thereby completing the redox cycle. This process fulfills condition (2).

In a general sense, the system presented here shares similarities with the oxygen storage device in the universally used three-way catalyst (TWC) for gasoline engines[7], which was developed to reduce simultaneously the emissions of NOx, CO, and unburned HC under close to stoichiometric conditions. The TWC concept involves a type of downstream gas cleaning and relies on continuous adjustment of the air to fuel ratio to create alternately slightly rich and slightly lean oxygen conditions in the engine, leading to either an excess of oxygen or a lack of oxygen in the exhaust gases. Under conditions of excess oxygen the catalyst absorbs oxygen and under low-oxygen conditions it releases oxygen. This oxygen looping in the TWC is used to finalize the combustion of unburned species, and in this respect it corresponds to the addition of a metal oxide to the boiler. Therefore, the catalyst in the TWC system and the metal oxide in the boiler act as oxygen buffers, to ensure low-level emissions of harmful species, even under the dynamic conditions present in an engine or a boiler.

The concept of applying a metal oxide to a combustion process, exploiting the continuous oxidation and reduction of the metal, is familiar from the principle of Chemical-Looping Combustion (CLC)[8]. However, the CLC system is more complex, as the aim is to combust fuels for heat and power production while at the same time the CO_2 is separated and sent for storage. In the present study, the emissions of CO_2 are of less importance, since biomass is regarded as a CO_2-neutral fuel. Nevertheless, research on CLC has generated much knowledge regarding materials that are suitable for use as oxygen carriers[9, 10] and this knowledge is pertinent for a standard CFB boiler.

More specifically, in the present work, the idea of using an oxygen carrier in a CFB boiler was explored through experiments conducted in a commercially operated boiler. The experiments were conducted with biomass as the fuel in the 12-MW boiler/gasifier system at Chalmers University of Technology, where up to 40 wt.% of the ordinarily used silica-sand bed material was replaced with the metal oxide ilmenite. Ilmenite is a naturally occurring ore, $FeTiO_3$ in its most reduced form. To assess the performance of ilmenite in the boiler, the following criteria were investigated:

- The possibility to maintain low-level emissions of unburned species in the exhaust from the boiler, even when the boiler was operated close to stoichiometric combustion or with a small excess of oxygen.
- The possibility to distribute evenly the concentration profile of the unburned species along the combustion furnace.

The potential benefits of applying the concept are discussed from a theoretical point of view, and important observations made by the operating staff are presented.

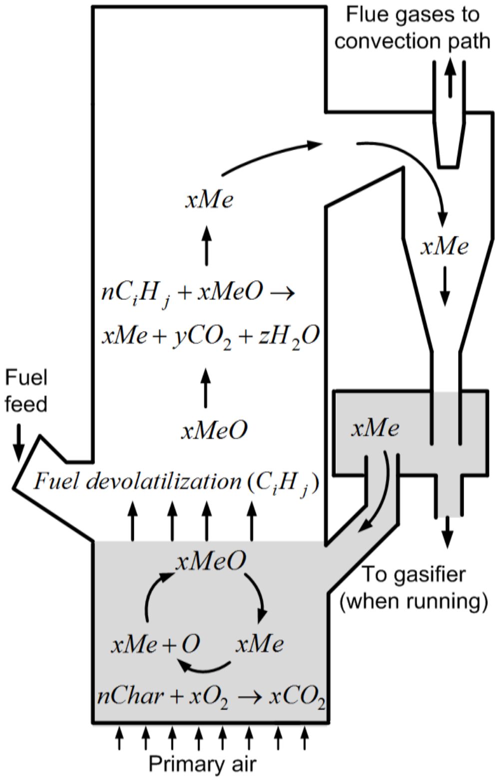

Figure 1. Reactions involving fuel and oxygen carriers in the boiler.

1. Theory

Traditionally, most of the oxygen carriers used in CLC are manufactured from metal oxides, such as NiO, Fe_2O_3, Mn_3O_4, and CuO. Thus, the desired properties of suitable oxygen carriers are very similar to those of catalysts: 1) the carriers should exhibit high resistance to mechanical stress; and 2) they should also have a long operational lifetime and show high activity in the reaction. These features are essential if the oxygen carrier is to transport a sufficient amount of oxygen to complete the fuel conversion process. However, the increased interest in combustion of solid fuels in CLC has raised the issue of problems with the ash. For example, agglomeration or sintering of the bed material, which leads to disruption of operation, is not an uncommon feature of fluidized bed combustion processes that use biomass. The usual way of handling this type of problem is to replace continuously part of the bed with new bed material. In this way, as much as 30% of the bed can be replaced daily when using particularly problematic fuels. However, this makes the use of manufactured oxygen carriers less viable economically. Therefore, research on the development of new and less-expensive oxygen carriers has been increasingly directed towards finding naturally occurring minerals that are able to transport oxygen and that essentially require only grinding before use. Consequently, when introducing an oxygen carrier in a biomass-fired furnace, these particles do not need to have a long functional lifetime but they do need to be cheap. In the present work, the focus is therefore on the mineral ilmenite, which has a bulk price similar to that of the silica-sand delivered to the Chalmers boiler (i.e. \$180/ton).

Ilmenite is an iron titanium oxide that has promising characteristics in that it withstands continuous oxidation and reducing conditions. According to Eq. (1), the heat of reaction for the oxidation of ilmenite to its most-oxidized state of “pseudobrookite plus rutile” is 235 kJ/mole O[11]. The respective heats of reaction when ilmenite is reduced by CO, CH_4, and H_2 are given by Eqs. (2-4). These species are common components of the volatiles biomass.

$$\mathrm{2FeTiO_3} + 1/2O_2 \Leftrightarrow Fe_2TiO_5 + TiO_2 \quad (\Delta H = -235\,KJ/mol\,O) \tag{1}$$

$$CO + Fe_2TiO_5 + TiO_2 \Leftrightarrow \mathrm{2FeTiO_3} + \mathrm{C}O_2 \quad (\Delta H = -48\,KJ/mol\,O) \tag{2}$$

$$1/4CH_4 + Fe_2TiO_5 + TiO_2 \Leftrightarrow \mathrm{2FeTiO_3} + 1/4\mathrm{C}O_2 + 1/2H_2O \quad (\Delta H = 35\,KJ/mol\,O) \tag{3}$$

$$H_2 + Fe_2TiO_5 + TiO_2 \Leftrightarrow \mathrm{2FeTiO_3} + H_2O \quad (\Delta H = -8\,KJ/mol\,O) \tag{4}$$

Reactions (2-4) indicate that the conversion of the volatiles in the boiler should be roughly thermally neutral, which indicates that high-temperature gradients could be avoided in the gas phase. In theory, the gaseous combustion reactions can be provided with an excess of evenly distributed oxygen at any time if the boiler is operated with only ilmenite as the bed material. Indeed, as the fuel only constitutes a small proportion of the total bed volume in a CFB boiler, the oxygen-carrying capacity of the bed material may be rather low but may still be sufficient for oxidizing the volatiles. Estimations based on the oxygen transport capacity of the material together with the fuel feed indicate that the amount of oxygen absorbed by the ilmenite particles is sufficient to oxidize the fuel combustibles released over a 30-second period.

In general, the CFB combustor is regarded as an isothermal system. However, the conversion of the char fraction gives rise to particles at high temperatures, leading to zones with high temperatures within the furnace. Measurements performed by Palchonok et al.[12] have shown that char particles with temperatures of approximately 350°C are detectable in a CFB boiler and that the magnitude of this excess temperature in the boiler is strongly linked to the surrounding oxygen concentration and particle size. Those authors concluded that the highest measured temperatures could likely be attributed to the conversion of small char particles that follow oxygen-rich gas streams. The influence of these oxygen-rich gas streams, which are the result of poor distribution of the oxidizer within the furnace, is likely to increase when the boiler is operated with an excess of oxygen, which (as described in the *Introduction*) is the usual way to operate commercial boilers. If the boiler is operated with ilmenite and close to stoichiometric combustion, these oxygen-rich streams may theoretically be kept low, as the metal oxide is spread across the entire furnace geometry, and oxygen is consumed when the *Me* is re-oxidized into *MeO*. Furthermore, this exothermic oxidation is located within the ilmenite particle. A direct benefit is that the excess temperature of the ilmenite particles, which is due to the oxidation, becomes limited to approximately 100°C. Activated ilmenite has an oxygen-carrying capacity of 3.3%, and it is assumed that 15% of this O_2 is consumed in the combustion reactions. Thus, for each kilo of ilmenite, 4.95 g of oxygen (i.e., 0.31 moles of oxygen) are consumed in the oxidation process. The heat of reaction of the oxidation, as derived from Eq. (1), then releases 69 kJ. As the heat capacity of the particles is approximately 0.85 kJ/kg K, the maximum increase in temperature under these conditions is 81°C. This is the maximum temperature because heat transfer from the ilmenite particles is not considered. This is a consequence of the high heat capacity of the oxygen carrier, as well as its restricted oxygen-carrying capacity, which can be compared with excess temperatures of 300°–350°C for char particles [12].

2. Experimental

The experiments were performed in the CFB-boiler/gasifier reactor system at Chalmers University of Technology (Fig. 2). The-12 MW biomass-fired boiler produces hot water for district heating, with the major part of the produced heat being consumed within the Chalmers University of Technology campus. The boiler is operated around the clock during the colder half of the year, from early November to late April, when there is heavy demand for domestic heating. Regarding the components of the boiler, as depicted in Figure 2: the furnace (1) has a square cross-section of 2.25 m^2 and a height of 13.6 m; the fuel is fed at the top of the furnace bed *via* the fuel chute (2; the entrained bed material is separated from the flue gases in the water-cooled cyclone (4); and then transported to the particle distributer (9); through the particle distributer, it is possible to re-circulate the bed material back to the combustion furnace either *via* the gasifier (11) or I the external particle cooler (10); the flue gases leave the furnace *via* the cyclone into the convection path (5), where the gases are cooled in heat exchangers using water, which is subsequently used for district heating; the flue gases that exit the convection path are cleaned of ashes in a secondary cyclone (6) and thereafter using bag filters (7).

About 25% of the total fuel load to the system can be fed into the indirect gasifier instead of the boiler. Approximately 70% of the fuel fed to the gasifier (14–15) is converted into a raw gas, and the remaining char follows the bed material back to the boiler where it is combusted together with the fuel fed to the boiler. The produced raw gas is then directed to the center of the furnace freeboard where it is injected and combusted (see Fig. 2). Since the gasifier is intended for research, commercial production of raw gas for further treatment and use is not the intended purpose of this facility. Nonetheless, the composition and level of the gas are investigated to assess gasifier and gas cleaning performance[13-15]. However, this aspect will not be discussed in this paper.

The combustion process can be followed in detail by monitoring the temperature and pressure throughout the furnace body. Gases can be extracted by inserting a gas sampling probe through dedicated ports located throughout the furnace (referred to as H1–H13 in Fig. 2), upstream and downstream of the cyclone, in the convection path, and downstream of the flue gas fan. The gas sampling probe is an electrically heated tube mounted inside a water-cooled jacket. Figure 3 details the setup for sampling, with the gases being further analyzed after probe extraction. The tip of the probe is equipped with a high-temperature filter, to prevent particles entering the gas analysis system. The gases are transported in heated Teflon tubes from the probe to the analysis instruments through an electrically heated pump. After cooling and water condensation, the gases (CO, O_2, NO, and total hydrocarbons [THC]) are analyzed in a series of online instruments. The CO and O_2 contents are analyzed in a Non-Dispersive Infrared (NDIR) analyzer for CO and in a paramagnetic analyzer for O_2. The NO concentration is determined by a chemiluminescence analyzer, and the concentration of THC is analyzed in a Flame Ionization Detector (FID).

The ilmenite used in the experiments was supplied by Titania A/S (Norway). The batch was concentrated from a naturally occurring ore that contained 40% ilmenite, 37% plagioclase, 8.6% ortopyroxene, 6.5% klinopyroxene, 4.2% biotite, and some other minor phases. When the ilmenite is subjected to repetitive redox cycles in the boiler loop, it undergoes an activation process that leads to an increase in particle porosity, which in turn promotes its catalytic properties. Cuadrat et al.[16] conducted CLC experiments in which they activated ilmenite during repeated redox cycles, and they concluded that the porosity of the ilmenite particles increased and that an external Fe-rich shell was formed on the particle. Furthermore, owing to iron migration towards the particle surface, the oxygen-carrying capacity of the activated material was decreased from 5.0% to 3.3% (kg O_2/kg ilmenite)[16]. This material has been extensively utilized in CLC applications that involve particle circulation and without any evidence of attrition or deactivation[17, 18]. However, it should be kept in mind that the activation of ilmenite in a biomass boiler may be different from that in a CLC unit. Most likely, the activation of ilmenite in the present setup proceeds at a slower pace, as the redox cycles are less prominent than in CLC.

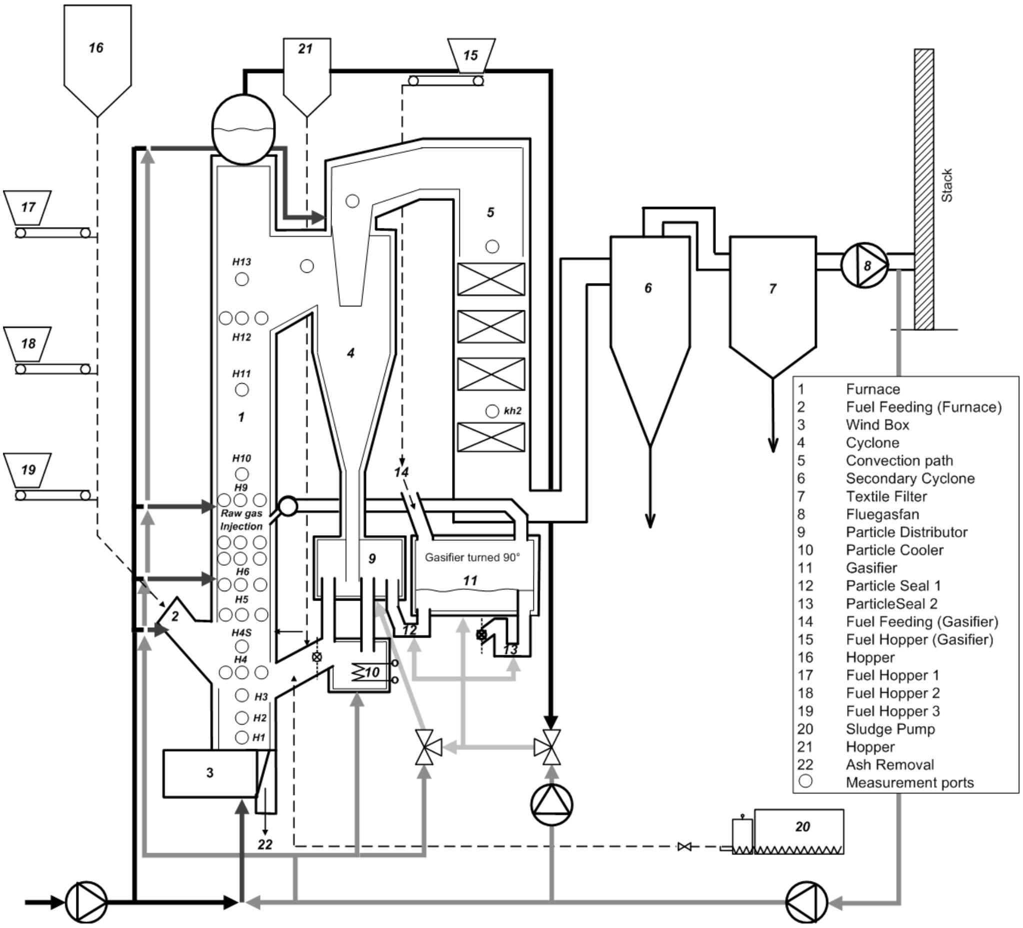

Figure 2. Chalmers boiler/gasifier reactor system.

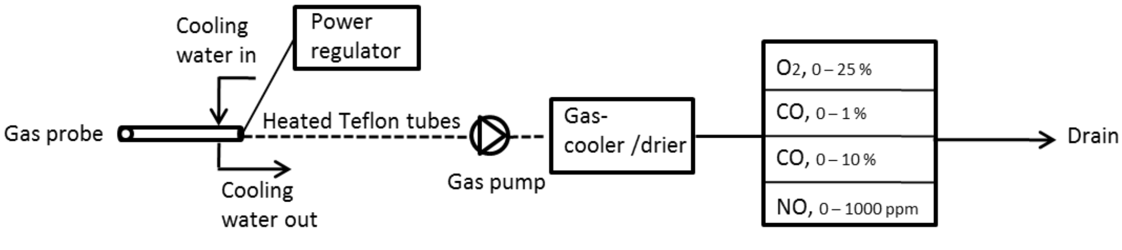

Figure 3. Sampling probe for extraction of gases from the boiler, shown together with the gas cooling/drier and analysis system.

3. Experimental performance and process assessment

Combustion experiments were conducted in two distinct phases. One phase included operation in the boiler, while the other phase involved both the boiler and the gasifier. When running the gasifier in combination with the boiler, a concentrated stream of combustible gases from the gasifier, approximately 1.4 MW of devolatilizing gases and steam, could be forced into one position in the furnace freeboard and the corresponding performance in terms of overall combustion efficiency could be investigated. Furthermore, by operating the boiler/gasifier system initially with silica-sand and subsequently with increasing proportions of ilmenite in the sand, it was possible to determine whether the oxygen-carrier material improves the mixing of the oxidizer and fuel throughout the furnace geometry.

Table 1: Fuel properties[1]

(wt.%)	Pellets	Wood chips
Moisture	7.2–9.8	38.5–45.3
Volatiles	72.9–75.3	43.8–50.1
Ash	0.2–0.4	0.4–0.6

[1] Based on fuel "as-received"

4.1 Boiler experiments

The experiment with ilmenite in the boiler was conducted over three consecutive days. On the first day, the bed inventory consisted of 100% silica sand (2000 kg), which was designated as the *reference case*. The feeds of primary and secondary air to the boiler were kept constant, while the feed of wood chips was varied to achieve four different air-to-fuel ratios, which ranged from 1.04 to 1.17. Each case was operated for about 1 hour. During these experiments, the O_2, CO, and NO concentrations in the flue gases were analyzed online. Gas extraction was achieved using the gas sampling probe, which was inserted in the convection path just before the economizer (kh2; Fig. 2).

On the second day, the boiler was started up with 1600 kg of silica sand as the bed material and with wood chips as the fuel. Table 1 lists the properties of the fuels as received and used in the respective experiments, either in the boiler only or in the combined boiler and gasifier. When the operating conditions were stable, 400 kg of ilmenite (corresponding to around 20 wt.% of the total bed mass) was introduced into the boiler. The ratio of the fed primary air to the fed secondary air was kept constant, while the sum of the primary and secondary air feeds was varied together with the fuel feed, to achieve the specified air-to-fuel ratios.

Three different air-to-fuel ratios were examined, and the O_2, CO, and NO concentrations were sampled online in the same manner as for the reference case. After the experiment, 15 wt.% of the bed material was regenerated. Thus, 300 kg of “sand plus ilmenite” was replaced with 300 kg of silica-sand. The boiler was then operated overnight with the corresponding 17 wt.% ilmenite in the bed inventory.

On the third day, the same experimental method was used, except that additional ilmenite, bringing it up to 40 wt.% of the total bed mass, was introduced into the boiler.

4.2 Boiler and gasifier experiments

Experiments were conducted during the 2-day period in which both the boiler and the gasifier were running. The boiler was operated with wood chips and the gasifier was operated with wood pellets, which had the properties specified in Table 1. During the first day, only silica sand was used as the bed material in the boiler/gasifier loop. In this experiment, the concentrations of CO and THC were measured across the furnace horizontal cross-section at the following heights (Fig. 2): 1) H7, which is located at a height of 7 m; 2) H9, which is located right above the raw gas injection pipe; and H12, which is located in the cyclone inlet. Nine gas measurements were conducted at H7, H9 and H12 according to the subdivision of the cross-section in the freeboard shown in Figure 4. These measurements were performed by stepwise horizontal insertion of the probe. In Figure 4, the term “Front” indicates the wall of the furnace where the fuel is fed, while “Back” refers to the wall opposite the front, and “Center” refers to the position in between these locations.

On the second day, the boiler was started up according to the principle used on the first day, and ilmenite corresponding to 12 wt.% of the total bed inventory was introduced into the system. The measurements at the horizontal wall of the furnace were performed in the same manner as on the first day.

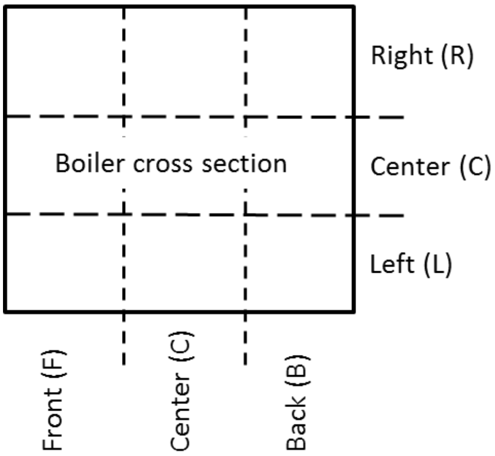

Figure 4. Measurement positions in the furnace cross-section (as viewed from above) for gas extraction *via* the gas sampling probe.

4. Results and Discussion

For clarity, this section is divided into three parts. The first part (5.1) details the results of the experiments that were conducted during operation in the boiler alone, whereas the second part (5.2) details the results from operation that involved both the boiler and gasifier. Section (5.3) discusses the potential commercial operation of a CFB boiler with ilmenite, as well as interesting observations made by the boiler operating staff during the experiments.

5.1 Results of the boiler experiments

The major objective of this investigation was to determine whether ilmenite enhances the conversion of unburned species in a biomass-fired furnace even with a low excess of air. The concentrations of CO were measured at position kh2 (Fig, 2) for all four cases of 0wt.%, 20wt.%, 17wt.%, and 40wt.% ilmenite in the total bed inventory. Three or four experimental points corresponding to air-to-fuel ratios that ranged from 1.04 to 1.17 were considered for each of the cases. Figure 5 shows the corresponding measured concentration of CO, which is expressed in mg/nm^3 at 6% O_2, as a function of the air-to-fuel ratio. As shown in Figure 5, independently of the ilmenite content in the boiler, the CO level decreased as the air-to-fuel ratio increased, which is in line with expectation. Moreover, as more ilmenite was introduced to the boiler, the concentrations of CO decreased, in comparison with the reference case. In particular, an abatement of nearly 75%, i.e., from 54 mg/m$_n^3$ to 13 mg/m$_n^3$, from the reference case to the 40% ilmenite case was detected at the air-to-fuel ratio of 1.12. This trend is even more pronounced at lower air-to-fuel ratios. For instance, at an air-to-fuel ratio of 1.08, an

80% drop in CO concentration was achieved, as compared to the base case without ilmenite. This decrease in CO can most likely be attributed to the oxygen-carrying properties of ilmenite. As explained by *Condition (1)* in the *Introduction*, when an oxygen-carrying material is introduced into the furnace, the amount of fed oxygen is in theory evenly distributed along the entire furnace, which in turn leads to increased conversion of the CO fraction. This can be compared with the higher levels of CO seen in the reference case, where the bed inventory consisted only of silica-sand and the secondary air was injected as a distinct stream into the furnace freeboard, which resulted in poorer mixing of the fuel and the oxygen.

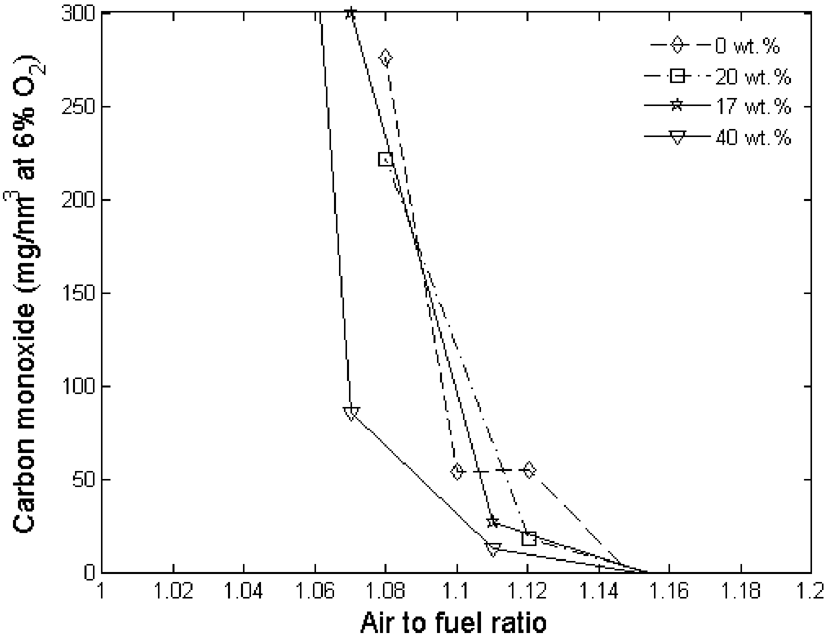

Figure 5. Measured concentrations of CO (mg/nm^3, at 6% O_2) at position kh2 in the convection path as a function of the air-to-fuel ratios for solely silica-sand operation and operation with ilmenite fractions in the range of 17–40wt.% of the total bed inventory.

In addition, to monitor the emission levels in the flue gases, the concentration of NO was evaluated at the same position as the CO, i.e., at position kh2. Figure 6 shows the corresponding measured concentrations of NO, expressed in mg/mn^3 at 6% O_2, as a function of the air-to-fuel ratio. As shown in Figure 6, independently of the ilmenite load in the bed, the concentration of NO increased with increasing air-to-fuel ratio. This outcome was expected, as the more oxygen that is present, the more oxidation of nitrogen species can be expected. It is noteworthy that the concentration of NO decreased when ilmenite was introduced into the furnace. In fact, the concentration of NO decreased by as much as 29% at an air-to-fuel ratio of 1.15, comparing the 40wt.% ilmenite case with the reference case. However, in this investigation, it was not possible to determine whether the actual formation of NO was lower or the reduction of NO was enhanced. However, a lower concentration of NO was observed for the 17wt.% ilmenite case than for the 20wt.% ilmenite case. This may be a reflection of the catalytic activity, which in this case suggests that ilmenite stimulates the reduction of NO. CLC experiments have shown that fresh ilmenite is not fully oxidized and needs to be activated during continuous redox cycles at temperatures >800°C[16]. This activation process further enhances the migration of iron to the outer shell of the particles, thereby creating active sites. Before the measurements were started, the ilmenite in the 17wt.% case was in the boiler-loop for about 20 hours longer than the ilmenite in the 20wt.% case, which most likely led to more properly activated particles in the 17wt.% case.

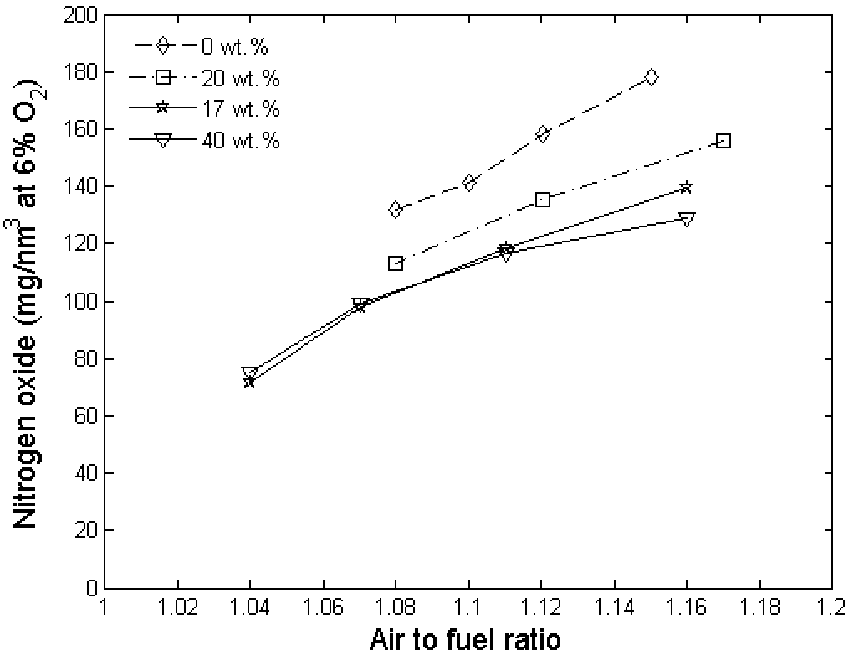

Figure 6. Measured concentrations of NO (mg/nm^3, at 6% O_2) at position kh2 in the convection path as a function of the air-to-fuel ratios for solely silica-sand operation and operation with ilmenite fractions in the range of 17–40wt.% of the total bed inventory.

5.2 Results of the experiments with the boiler and gasifier

Initially, only silica-sand was used as the bed material in the boiler/gasifier loop. This provided a reference case for other operational conditions, such as ilmenite addition. In these tests, measurements of O_2 and CO across the furnace horizontal cross-section were performed at three different heights, as described in section *4.2*. Figure 7 shows the CO concentrations (in mole%) at these heights in the furnace. In Figure 7, on the left-hand side, the CO concentrations are for the reference case, while the right-hand side presents the CO concentrations measured after the addition of 12wt.% ilmenite to the total bed inventory. As previously stated, the raw gas produced in the gasifier is injected at an upper location alongside the “Back-side” of the furnace (see Fig. 2). More precisely, heights H7 and H9 are located respectively up-stream and down-stream of this injection point, which gives a basis for the comparisons. In Figure 7, the location of the injection point is clearly evident, as a substantial increase in CO concentration is measured at height H9. Moreover, the decrease in CO concentration between the two experimental configurations at height H7 is consistent with the oxidation of CO in presence of oxidized ilmenite in and above the furnace bed. In particular, at the “Front” side, where the fuel is fed into the furnace, the CO peaks are less pronounced in the ilmenite case. In general, using ilmenite seems to smooth the CO peaks observed on the left-hand sides in Figure 7. This confirms the tendency for this material to enhance the mixing of available oxygen in the furnace and the combustible compounds. It appears that oxidation reactions are moved to the bed, where fuel devolatilization occurs and, in turn, volatile conversion is favored. This phenomenon also occurs higher up in the furnace, where entrained ilmenite at height H12 continues to oxidize CO (see Fig. 7). Taken together, the experiments involving both boiler and gasifier operation support the notion that ilmenite promotes fuel and oxygen mixing throughout the entire cross-section of the furnace. This corresponds to a beneficial effect of ilmenite with respect to CO concentration, as detailed in Section 5.1.

The sampled gases from the three different heights in the furnace were also assayed for the concentration of THC. Together with the CO measurements, the THC measurements give additional information on the concentration of unreacted HC along the furnace. The resulting concentrations are presented in Figure 8 in the same disposition as the CO concentrations in Figure 7. The level of unreacted HC was maximal at position H9 in both the reference case and the ilmenite case, which is expected, as this position is just above the inlet feed from the gasifier. In this case, and this is also valid for the CO concentrations shown in Figure 7, the amount of oxygen present in the ilmenite is not sufficient to combust the rich stream of unreacted species. However, the levels of hydrocarbon present at the front and the center of the furnace cross-section decreased in comparison to the reference case. This trend was also noted for positions H7 and H12, supporting the idea that ilmenite can be used for the purpose of increasing contact between the oxygen and fuel.

It should also be remembered that the amount of ilmenite constituted only 12wt.% of the total bed inventory in this experiment.

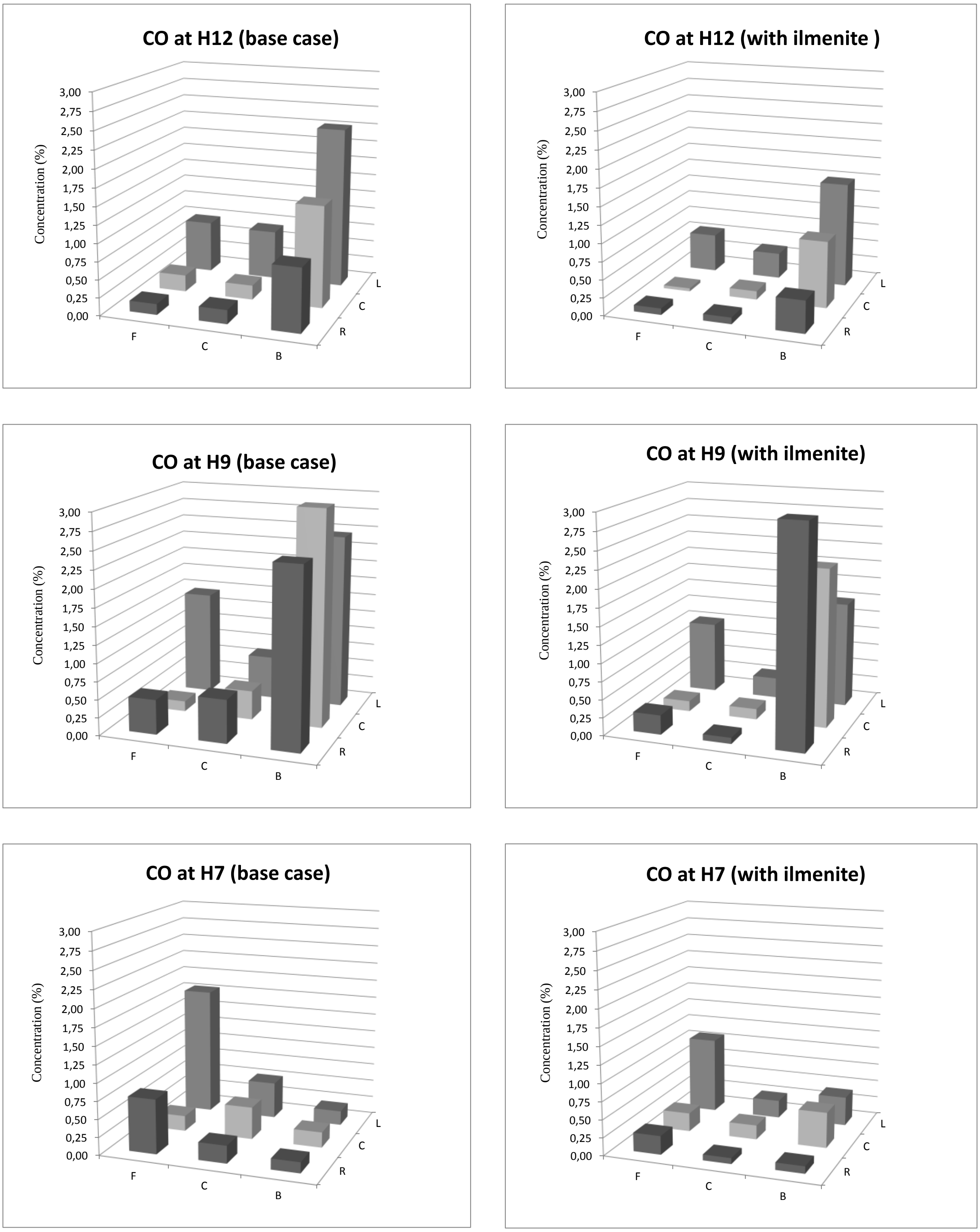
CO at H12 (base case)

CO at H12 (with ilmenite)

CO at H9 (base case)

CO at H9 (with ilmenite)

CO at H7 (base case)

CO at H7 (with ilmenite)

Figure 7. Measured concentrations of CO at three heights (H7, H9 and H12) in the furnace cross-section for the reference case and the ilmenite case.

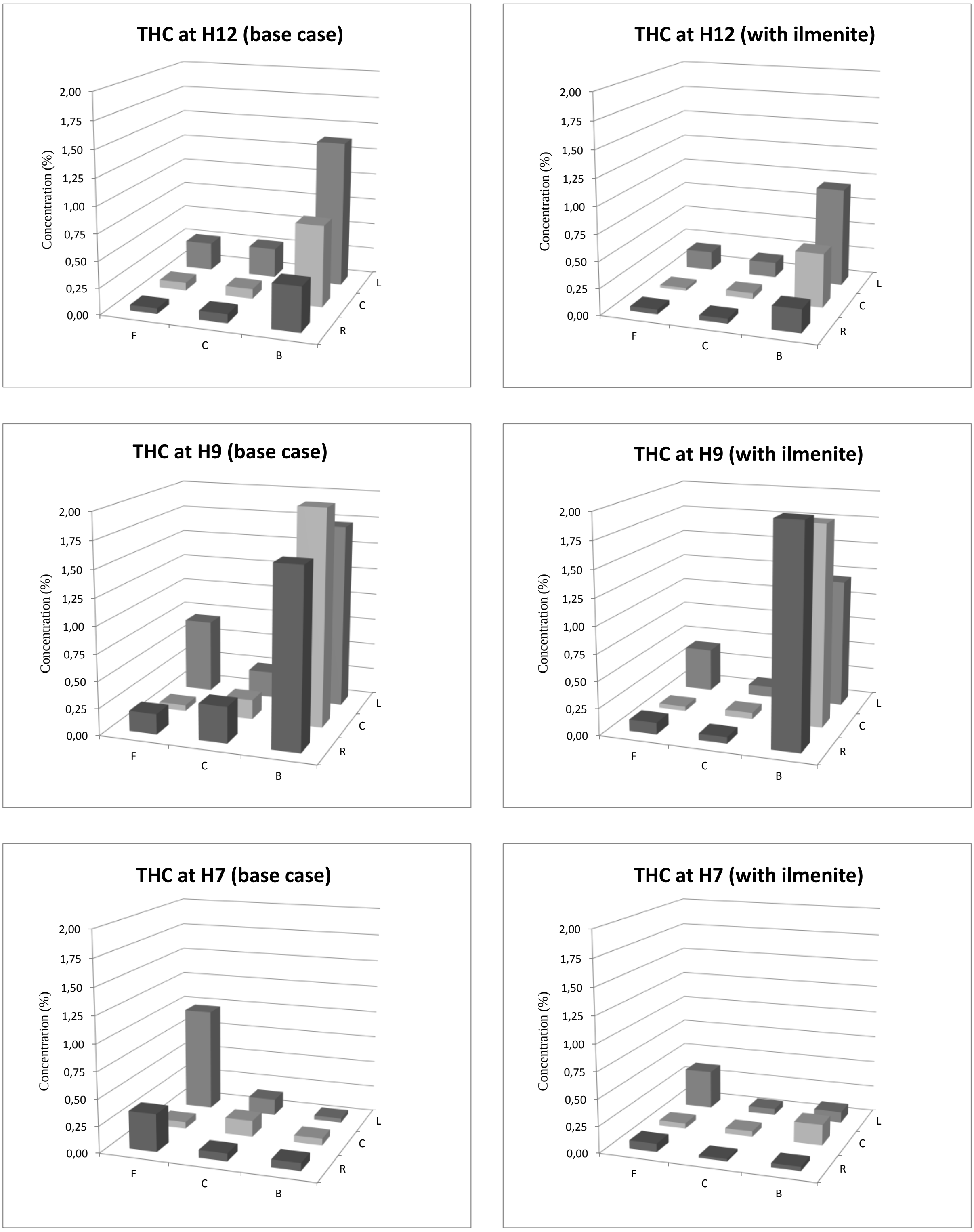

Figure 8. Measured concentrations of total hydrocarbons (THC) at three heights (H7, H9 and H12) in the furnace cross-section, for the reference case and the ilmenite case.

Figure 9 shows the average temperature variation between the inlet and the outlet of the cyclone for the four cases: boiler with silica-sand; boiler/gasifier with silica-sand; boiler with the addition of 12wt.% ilmenite; and boiler/gasifier with the addition of 12wt.% ilmenite. During normal boiler operation with only silica-sand as bed material, i.e., when the gasifier was not in operation and no raw gas was injected into the freeboard of the furnace, the difference in temperature between the inlet and the outlet of the cyclone was usually around 35°C, owing to heat transfer to the surrounding walls (first bar in Fig. 9). When the gasifier was in operation, the concentrated stream of combustibles into the furnace could not realize complete oxidation during its residence time along the freeboard. This was due to the lack of mixing of the available oxygen and unreacted species, as reflected in the concentrations of CO and THC (the first column in Figs. 7 and 8) at height H12. Instead, when the gas entered the well-mixed cyclone, these unreacted species came in contact with the oxygen and were combusted, which means that the cyclone works as an after-burner/post-oxidation volume. The heat of reaction leads to an increase in the temperature of the gas inside the cyclone and therefore, the commonly observed temperature drop in the cyclone during normal boiler operation is clearly diminished during gasifier operation (bar 2 in Fig. 9). Comparing these temperature changes for the cases of boiler and boiler/gasifier operation with the addition of 12wt.% ilmenite (bars 3 and 4 in Fig. 9), it is clear that the temperature drop in the cyclone is augmented by almost 50°C and 20°C, respectively. The reason to this is that less combustion occurs in the cyclone as more of the combustibles are already converted in the furnace. Thus, the oxygen-carrying properties of the ilmenite together with the well-distributed particles inside the furnace increase the mixing of the fuel and oxygen.

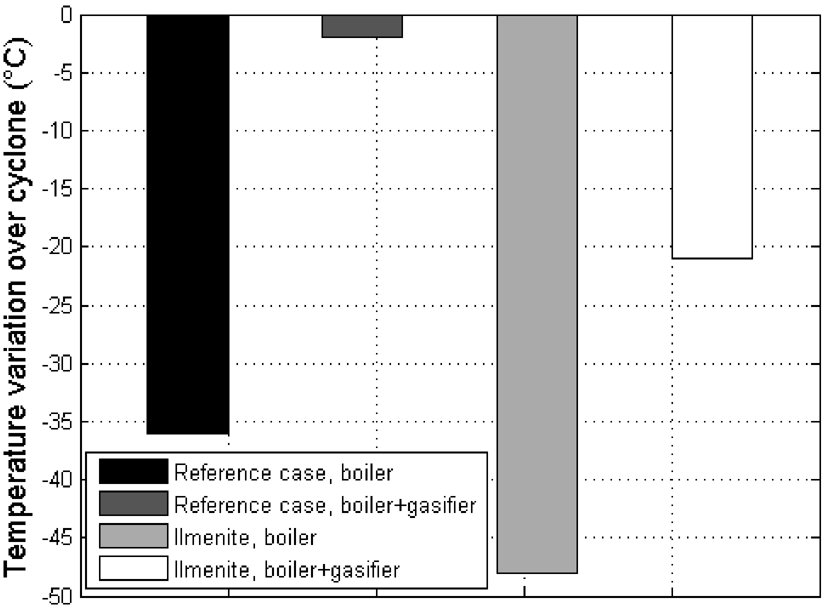

Figure 9: Average temperature differences between the inlet and the outlet of the cyclone for the reference and ilmenite experiments in the boiler/gasifier-system.

5.3 Potential commercial benefits and practical operational findings

As discussed in the *Introduction* of this work, the available measures for increasing the mixing of fuel and oxygen during combustion are usually associated with higher investment costs and operating expenses. Moreover, these costs can be especially high when solid fuels and waste are considered, mainly due to the heterogeneity of the fuel. The idea presented in the present work could theoretically be used to replace these measures or at least reduce their levels of complexity in both existing commercial CFB boilers and even for grass-root designs. The performed experiments reveal several interesting features that could eventually lead to these benefits. However, additional research needs to be carried out to confirm these preliminary observations. One example of such a study would be to operate the boiler with 100wt.% ilmenite. Nevertheless, the potential benefits include:

- The oxygen-buffering effects when ilmenite is used in the boiler-loop, which implies that the system is likely to become less sensitive to bias in the fuel load. Thus, advanced fuel-feeding systems with several fuel-feeding chutes/positions could be simplified.

- Operation with ilmenite suggests that the temperature profile along the furnace and in the cyclone could be evened out, as the combustion of volatiles is close to thermally neutral. Thus, high-temperature zones can be avoided and ash-related problems could be reduced. As the oxygen is more evenly distributed inside the furnace, fewer ash-related problems associated with excess char particle temperatures can be expected.

Finally, during the running the aforementioned experiments, the boiler staff observed some interesting features. After the experiment with ilmenite, less accumulation of deposits on the heat transfer surfaces was observed by the operating technicians, as compared with the reference cases with silica-sand operation only. This meant that fewer sooting measures were required. Furthermore, the ilmenite could readily be separated from the ashes with a simple magnet. This observation suggests the potential to separate the ilmenite from the ashes to avoid the cost associated with disposal.

6. Conclusion

An experimental investigated on how the concentrations of CO and unburned HC in a CFB furnace could be smoothed through addition of the oxygen-carrying material ilmenite to the bed material inventory have been conducted. These experiments were performed in the 12-MW_{th} biomass-fired boiler/gasifier-system at Chalmers University of Technology. The system was operated in different experimental configurations: a reference case in which only silica-sand was used as bed material; and a set of cases in which ilmenite was added so that up to 40 wt.% of the ordinarily used silica-sand was replaced. The air-to-fuel ratio was varied from 1.04 to 1.17, and the concentrations of CO, NO, and HC were measured in the cross-section of the furnace at nine positions and at three different heights, as well as at one position in the convection path. Based on the results of these experiments, the following conclusions are drawn:

- Already when 12 wt. % of ilmenite is mixed in with the ordinary bed material, the spatial variation in concentration of unburned species across the furnace becomes less prominent as compared with operation with only silica-sand. This implies that the ilmenite improves the distribution of the fed oxygen in the furnace.
- The CO concentration in the gas leaving the boiler was decreased by as much as 80% when 40wt.% ilmenite was used, as compared with operation with only silica-sand.

- The concentration of NO was clearly decreased when the system was operated with a mixture of ilmenite and silica-sand. A reduction in the NO concentration of up to 30%, as compared with the reference case, was observed when 40%.wt ilmenite was mixed with the ordinary silica-sand.
- The temperature profiles over the cyclone suggest that combustion is reduced in the cyclone body when using ilmenite in the boiler, as compared with operating solely with silica-sand. Once again, this suggests that the distribution of oxygen in the furnace is improved by the addition of ilmenite.

Acknowledgment

This work has been financially supported by E.On. The operation of the gasifier has been possible through support from Göteborg Energi, Metso, Akademiska Hus, Chalmers Energy Initiative and Svenskt Förgasningscentrum. The authors would also like to acknowledge research engineers Johannes Öhlin, Jessica Bohwalli and Rustan Marberg for their work with the experimental equipment.

Nomenclature

CFB: Circulating Fluidized Bed; (T)HC: (Total) Hydrocarbons; TWC: Three-Way Catalyst; CLC: Chemical-Looping Combustion; FID: Flame Ionization Detector; NDIR: Non-Dispersive Infrared; Me/MeO: Metal Oxide

References

[1] B. Leckner, Prog. Energy Combust. Sci. 24 (1) (1998) 31-61
[2] S. Karlsson; J. Pettersson; L. Johansson; J. Svensson, Oxid. Met. 78 (1) (2012) 83-102
[3] L. L. Baxter; T. R. Miles; T. R. Miles Jr; B. M. Jenkins; T. Milne; D. Dayton; R. W. Bryers; L. L. Oden, Fuel Process. Technol. 54 (1–3) (1998) 47-78
[4] H. P. Nielsen; F. J. Frandsen; K. Dam-Johansen; L. L. Baxter, Prog. Energy Combust. Sci. 26 (3) (2000) 283-298
[5] K. Svoboda; M. Pohořelý; M. Hartman, Energy Fuels 17 (4) (2003) 1091-1099
[6] F. Niklasson; H. Thunman; F. Johnsson; B. Leckner, Ind. Eng. Chem. Res 41 (18) (2002) 4663-4673
[7] M. V. Twigg, Applied Catalysis B: Environmental 70 (1–4) (2007) 2-15
[8] A. Lyngfelt; B. Leckner; T. Mattisson, Chem. Eng. Sci. 56 (10) (2001) 3101-3113

[9] T. Mattisson; A. Lyngfelt; H. Leion, International Journal of Greenhouse Gas Control 3 (1) (2009) 11-19

[10] C. Linderholm; A. Lyngfelt; A. Cuadrat; E. Jerndal, Fuel (0))

[11] P. Hallberg; H. Leion; A. Lyngfelt, Thermochim. Acta 524 (1–2) (2011) 62-67

[12] G. I. Palchonok; C. Breitholtz; H. Thunman; B. Leckner, in: *14th International Conference on Fluidized Bed Combustion*, Vancouver, 1997.

[13] H. Thunman; M. C. Seemann, in: *20th International conference on fluidized bed combustion*, G. Z. Yue, H.; Zhao, C.; Luo, Z., (Ed.) xi´an, China, 2009; pp 659 - 663.

[14] N. Berguerand; F. Lind; M. Seemann; H. Thunman, Biomass Conversion and Biorefinery 2 (3) (2012) 245-252

[15] F. Lind; M. Seemann; H. Thunman, Ind. Eng. Chem. Res 50 (20) (2011) 11553-11562

[16] A. Cuadrat; A. Abad; J. Adánez; L. F. de Diego; F. García-Labiano; P. Gayán, Fuel Process. Technol. 94 (1) (2012) 101-112

[17] N. Berguerand; A. Lyngfelt, Fuel 87 (12) (2008) 2713-2726

[18] N. Berguerand; A. Lyngfelt, International Journal of Greenhouse Gas Control 2 (2) (2008) 169-179